STUDIES ON METAL ACCUMULATION AND SYNTHESIS OF INORGANIC NANOMATERIALS IN PLANTS AND THEIR APPLICATIONS

A THESIS
SUBMITTED TO THE
UNIVERSITY OF PUNE

FOR THE DEGREE OF
DOCTOR OF PHILOSOPHY
IN
BIOTECHNOLOGY

BY
RAJU D.

UNDER THE GUIDANCE OF
DR. ABSAR AHMAD
DIVISION OF BIOCHEMICAL SCIENCES

And

CO- GUIDANCE OF
DR. URMIL J. MEHTA
PLANT TISSUE CULTURE DIVISION
NATIONAL CHEMICAL LABORATORY
PUNE – 411008, INDIA.

June, 2012

CONTENTS

CERTIFICATE OF THE GUIDE

Certified that the work incorporated in the thesis entitled **"Studies on metal accumulation and synthesis of inorganic nanomaterials in plants and their applications"** submitted by Mr. Raju D. was carried out by the candidate under my supervision at the Biochemical Science Division, National Chemical Laboratory, Pune, India. Such material as has been obtained from other sources has been duly acknowledged in the thesis.

Date: **Dr. Absar Ahmad**

Place: **(Research Guide)**

CERTIFICATE OF THE CO-GUIDE

Certified that the work incorporated in the thesis entitled **"Studies on metal accumulation and synthesis of inorganic nanomaterials in plants and their applications"** submitted by Mr. Raju D. was carried out by the candidate under my supervision at the Plant Tissue Culture Division, National Chemical Laboratory, Pune, India. Such material as has been obtained from other sources has been duly acknowledged in the thesis.

Date: **Dr. Urmil J. Mehta**

Place: **(Research Co- Guide)**

DECLARATION BY THE CANDIDATE

I declare that the thesis entitled **"Studies on metal accumulation and synthesis of inorganic nanomaterials in plants and their applications"** submitted by me for the degree of Doctor of Philosophy is the record of work carried out by me under the guidance of **Dr. Absar Ahmad** and co-guidance of **Dr. Urmil J. Mehta** and has not formed the basis for the award of any degree, diploma, associateship, fellowship, titles in this or any other university or other institute of higher learning. I further declare that the material obtained from other sources has been duly acknowledged in the thesis.

Date: Raju D.

Place: Pune   (Research student)

Dedication

I dedicate my thesis to my Parents and Friends. . .

Acknowledgements

First of all I would like to give the full credit of my thesis to my parents and family. This thesis is the result of years of work whereby I have been accompanied and supported by many people. It is a pleasant aspect that I now have the opportunity to express my gratitude towards all of them.

First and foremost with a deep sense of gratitude and indebtedness, I thank my mentor, Dr. Absar Ahmad for his invaluable guidance, encouragement and keen interest. My experience with him has inculcated in me qualities that will always remain ingrained in my heart, mind and soul. His scientific, methodical, focused and positive approach combined with exceptional zeal and dynamism are some of the qualities which I admire most and often yearn for them. His frequent discussions inspired me to go ahead in difficult times and cope up with every little problem during my Ph.D. I learned to believe in my future, my work and myself. I thank him for making me a better person, guiding me and improving my silliest and minutest mistakes.

I deeply thank my co-mentor Dr. Urmil J. Mehta. I could not have managed at any step without her help and sincere efforts, her friendly attitude and soothing words of solace which always helped me to relieve my tensions. I will always remember her motherly care. When life turned its bitter face on me, it was her encouragement and understanding that showed me the lane of confidence. Her positive attitude and motivational abilities guided me to work harder and put in my best. I thank her for being there for me always.

My heartfelt thanks go to Dr. Sulekha Hazra who boosted my research, supported me and guided me towards independent research.

I am extremely grateful to Dr. Vidya Gupta, Chair, Biochemical Science Division for the support and help extended during my Ph.D. work. I also thank Dr. S.K. Rawal previous Head and Dr. B.M. Khan, Chair, Plant Tissue Culture Division for the support and help extended during my Ph.D. work. I also thank all the staff members of PTC Division for their cooperation. I am thankful to Mrs. Anuya Nishal, Polymer Science and Engineering Division for training me for ESEM and ultramicrotome.

This research has been supported by grant from The Council of Scientific and Industrial Research (CSIR), New Delhi who awarded me Senior Research Fellowship for this work. The financial support from CSIR for fellowship and research grant provided in the network program P24-COR0008 and NWP0019, on phytoremediation and ecorestoration is gratefully acknowledged. I would like to thank the Director, National Chemical Laboratory, for allowing me to submit my work in the form of a thesis.

My life in the lab during my Ph.D. tenure was smooth because of my colleagues. My heartfelt thanks to all the help and suggestions rendered by my lab mates. My research life would not have been enjoyable and exciting without the company of my dear lab mates Dr. Sunil, Dr. VSS Prasad, Poonam, Rita, Dr. Sujatha Raman, Dr. Shweta Singh, Dr. Bhuban Mohan Panda, Komal, Rishi, Prashant, Somesh, Parth, Santhosh and Krunal many other friends who helped me during my stay at NCL. I

ABBREVIATIONS

APS: Ammonium Per Sulphate

AAS: Atomic Absorption Spectroscopy

BAP: 6- Benzyl Amino Purine

cDNA: Complementary Deoxyribonucleic Acid

DNA: Deoxyribonucleic Acid

EDS: Energy Dispersive Spectroscopy

FTIR: Fourier Transform Infrared Spectroscopy

FPLC: Fast Protein Liquid Chromatography

GNPs: Gold Nanoparticles

GUS: β-glucuronidase

HRTEM: High Resolution Transmission Electron Microscopy

HCl: Hydrochloric Acid

H_2SO_4: Sulfuric Acid

$HAuCl_4$: Chloroauric Acid

HNO_3: Nitric Acid

$HgCl_2$: Mercuric Chloride

HPLC: High-Performance Liquid Chromatography

hr: Hour(s)

ICP-AES: Inductive Coupled Plasma Atomic Emission Spectroscopy

kDa: kilo Dalton

kb: kilo base pairs

mA: Milli Ampere

MS: Murashige and Skoog's medium

mg: Milligram

mL: Milli litre

nm: Nano meter

NAA: Naphthalene Acetic Acid

BSA: Bovine Serum Albumin

NADPH: Nicotinamide Adenine Dinucleotide Phosphate, reduced

OD: Optical Density

PAGE: Poly Acrylamide Gel Electrophoresis

pDNA: Plasmid DNA

PPM: Parts Per Million

pI: Isoelectric point

rpm: Rotation Per Minute

SEM: Scanning Electron Microcopy

SDS: Sodium Dodecyl Sulphate

SAED: Selected Area Electron Diffraction

TEM: Transmission Electron Microscopy

TEMED: Tetramethylethylenediamine

UV: Ultra-Violet

XRD: X-ray Diffraction

EDS: Energy Dispersive Spectroscopy

ESEM: Environmental Scanning Electron Microscope

XPS: X-ray Photoelectron Spectroscopy

µL: Micro Liter

µg: Microgram

°C: Degree Centigrade

Abstract

Study of metal accumulation by plants growing on mine area will be an easy way to identify the metal accumulating and tolerances in plants as they grow in natural conditions of high metal content in soil. Plant tissue culture technique can be used as a tool for identification of hyperaccumulator plants. Culturing the plants in culture vessels in the laboratory offers a potential technique to screen hyperaccumulator plants. Thus, this technique can be used to generate new information, which can directly or indirectly be used in phytoremediation, phytomining and nanoparticle synthesis by using plants. Various micro-organisms such as bacteria, fungi and yeasts have been suggested as nanofactories for synthesizing metal nanoparticles of silver and gold. But, the use of "plants" for the fabrication of nanoparticles has drawn the attention of researchers as a rapid, low-cost, eco-friendly and a single-step method for the biosynthesis process.

Chapter 1: General Introduction.

This chapter gives a brief introduction to phytoremediation and nanotechnology with emphasis on gold nanoparticles, the various methods of syntheses of nanomaterials and their applications.

Chapter 2: Studies on Cu and Mn accumulation by plants growing on mine areas, leaching of metals from plants and converting to nanoparticles.

Section 1: Natural accumulation of copper and distribution of metals in plants growing in copper mining areas.

This chapter describes the study of *Prosopis juliflora* plants growing in different locations of Khetri mining sites, a single tree of *Ailanthus excelsa* growing at Khetri and *Prosopis* plants seen growing in Kolihan mining area. A study was conducted to generate information on Cu accumulation and distribution of other metals like Mn, Zn and Fe in aerial parts of *Prosopis juliflora* from both mines and *Ailanthus excelsa* from Khetri.

Section 2: Bioleaching of copper from *Prosopis juliflora* leaves and its conversion to copper oxide nanoparticles using the fungus *Fusarium oxysporum*.

In this section we report the bioleaching of copper and its simultaneous biotransformation to copper nanoparticles. Our approach involves the use of *Fusarium oxysporum*, a plant fungus, in the biotransformation of naturally accumulated copper present in the plant leaves (*Prosopis juliflora*).

Section 3: Differential accumulation of manganese in three mature tree species (Holoptelia, Cassia, Neem) growing on a mine dump.

In this section we studied three naturally growing tree species on a manganese mine dump viz. *Cassia siamea* (Cassia), *Azadirachta indica* (Neem) and *Holoptelia integrifolia* (Holoptelia). Experiments were conducted to generate information on Mn accumulation and distribution in these trees. The data was compared with the data generated from the samples collected from the trees growing in natural vegetation in contamination free soil. The dry fallen leaves of the respective trees were collected and analyzed for Mn content.

Section 4: Bioleaching of manganese from *Holoptelia* leaves and its conversion to manganese oxide nanoparticles using the fungus *Fusarium oxysporum*.

In this section, we report the bioleaching of manganese, initially in which we could get 5-7 µM particles and then the same particles were retreated with the same fungus which simultaneously biotransformed them to manganese nanoparticles. Our approach involves the use of *Fusarium oxysporum*, a plant fungus, in the biotransformation of naturally accumulated manganese by the leaves of the plant *Holoptelia integrifolia*.

Chapter 3: Biosynthesis of intra and extracellular nanomaterials by using plants

Section 1: Synthesis of gold nanoparticles by various leaf fractions of *Semecarpus anacardium* L. tree.

In this study, the natural ability of the *S. anacardium* leaf extract and leaf derived biomass to synthesize gold NPs from $HAuCl_4$ was demonstrated. Comparison of

untreated extract, boiled extract and untreated biomass showed that reduction of $HAuCl_4$ was optimum in the reaction mixture with green extract.

Section 2: Synthesis of extra and intra cellular gold nanoparticles by living peanut plant (*Arachis hypogaea* L.).

We report, for the first time, both intra and extracellular synthesis of gold nanoparticles by using living peanut seedlings without any interference of other metal ions and complete characterization of nanoparticles. We have demonstrated the extra- and intra-cellular formation of gold nanoparticles using living peanut seedlings. This result possibly shows the synthesis of intracellular nanoparticles by uptake of Au (III) and converting it to Au (0) by peanut seedling or the up-take of Au (0) from the extracellular nanoparticles solution synthesized by peanut seedling and transporting it to different parts of the plant as was studied in this section.

Section 3: Recovery of intracellular gold nanoparticles from peanut roots.

The recovery of intracellular gold nanoparticles which were synthesized in dry and fresh roots of peanut was made by extraction with ethanol, followed by sonication for 20 min. The recovered particles were further characterized by UV-vis, TEM and ICP-AES as reported in this section.

Section 4: Callus cell mediated synthesis of gold nanoparticles.

Though there are reports on the synthesis of nanoparticles using bacteria, algae, fungi and viruses, there are no reports on the synthesis of GNPs using living plant cells. Here we report for the first time, the synthesis of intra and extracellular GNPs by using living peanut callus cells, which is an environment friendly and cheap method.

Chapter 4: Identification of biomolecules responsible for the biosynthesis of nanomaterials.

In this chapter, we report the isolation of protein from the peanut root and purification of protein which is helping in the formation of GNPs. The isolation of protein from plant sources has not been much studied. The purification of protein was done by FPLC method; different fractions collected were used to check the activity for the formation of gold nanoparticles. The active fractions were checked on the gel

electrophoresis for confirmation of proteins. The formed nanoparticles were characterized by UV-vis, TEM and SAED.

Chapter 5: Applications of nanoparticles.

In this chapter we demonstrate, for the first time, the biosynthesis of cationic gold nanoparticles and their binding with p-DNA. The formation of cationic nanoparticles was noted and confirmed the charge on the surface of nanoparticles. As these particles were not stable for a longer time, the chemical mediated synthesis of cationic gold nanoparticles was carried out. Characterization of these nanoparticles by TEM, UV-vis and EDS analysis was done. The p-DNA bound to these nanoparticles was used as carriers for transformation of p-DNA into plant tissue.

Chapter 6: General discussion and conclusions.

This chapter of the thesis gives summary of the findings and conclusions derived from the present work.

Chapter 1

General Introduction

Summary:

This chapter provides an introduction to the thesis and brief overview about Phytoremediation, nanotechnology and the various routes used to synthesize nanomaterials viz, chemical, physical and biological. Biological synthesis methods have developed the interest of many researchers due to their advantages over other methods and their considerable success in the synthesis of various nanoparticles and applications of nanoparticles are also discussed in brief.

Heavy metals are described as metals having a specific gravity (density) of more than about 5 gm cm^{-3}. Heavy metal pollution is mainly caused due to mining, industrialization, sewage water, agricultural waste and smelting of metalliferous ores, which leads to pollution of soil, air and water. These heavy metals when exposed to living cells often cause toxicity. These include chromium, cadmium, mercury, copper, manganese, lead, etc. These metals at lower concentrations in soil are not toxic to plants; toxicity is caused when the plants are exposed to higher concentrations.

1.1 Phytoremediation:

Phytoremediation is an environmental cleanup strategy in which selected green plants are employed to remove, contain, or render environmentally toxic contaminants harmless. This is an emerging biotechnological application and operates on the principles of biogeochemical cycling [1]. This remediation approach is attracting attention from governments as cost-effective and environmental friendly green technique to clean up heavy metal polluted soil by using hyperaccumulators [2]. However, it is in developing stage, and more knowledge and advanced techniques are needed to study the related mechanisms in plants for phytoremediation.

The schematic representation of the process involved in heavy metal phytoextraction is shown in Figure 1.1. Translocation from the root to the shoot must occur efficiently for the ease of harvesting. After harvesting, a biomass processing step or disposal method that meets regulatory requirements should be implemented.
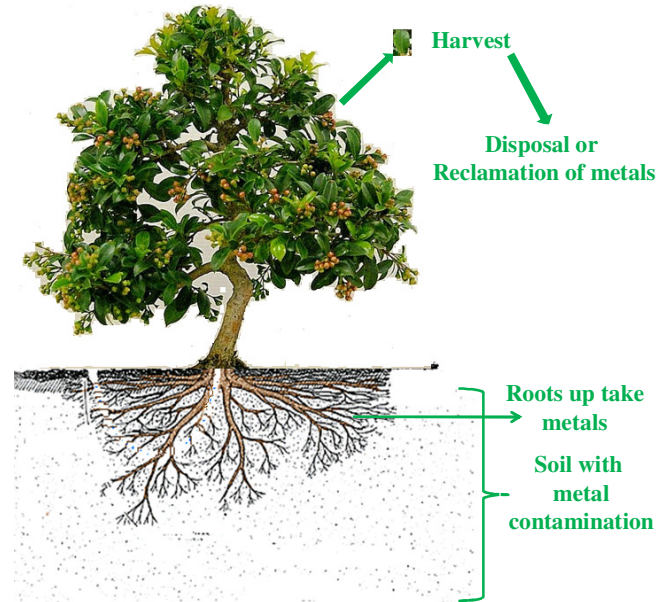
Figure 1.1: The schematic representation describes the processes during phytoextraction of heavy metals.

Phytoremediation consists of four different plant-based technologies each having a different mechanism of action for the remediation of metal-polluted soil, sediment, or water. These include rhizofiltration, phytostabilization, phytovolatilization and phytoextraction.

Rhizofiltration:

Rhizofiltration is absorption, precipitation and accumulation of metals in roots only. The plant must have rapidly ramifying roots to remove toxic metals from water and soil for an extended period of time.

Phytostabilization:

The traditional means by which metal toxicity is reduced at these sites is by in-place inactivation, a remediation technique that employs the use of soil amendments to immobilize or fix metals in soil. Although metal migration is minimized, soils are often subjected to erosion and still pose an exposure risk to humans and other animals.

Phytovolatilization:

The naturally occurring or genetically modified plants that are capable of absorbing elemental forms of the metals such as As, Hg, Se and from the soil, biologically converting them to gaseous form within the plant, and releasing them into the atmosphere.

Phytoextraction:

The use of plants to remove contaminants from the environment and concentrating them in above-ground plant tissue is known as phytoextraction. This is employed to recover heavy metals from soil, however, this technology is now used for other materials in different media. Greenhouse-based hydroponic systems using plants with high contaminant root uptake and poor translocation to the shoots are currently being studied for the removal of heavy metals and radionuclides from water.

A big advantage of phytoremediation over conventional pump and treat systems is the ability of the roots to penetrate the microscopic scale pores in the soil matrix. Contaminants adsorbed or trapped in these micropores are minimally or not impacted by the pump and treat system. In case of phytoremediation, the roots can penetrate these micropores for contaminant removal. As shown in Figure 1.2, the tree has an advantage as it increases in age, for the removal of deeper level of contamination in soil and water bodies.
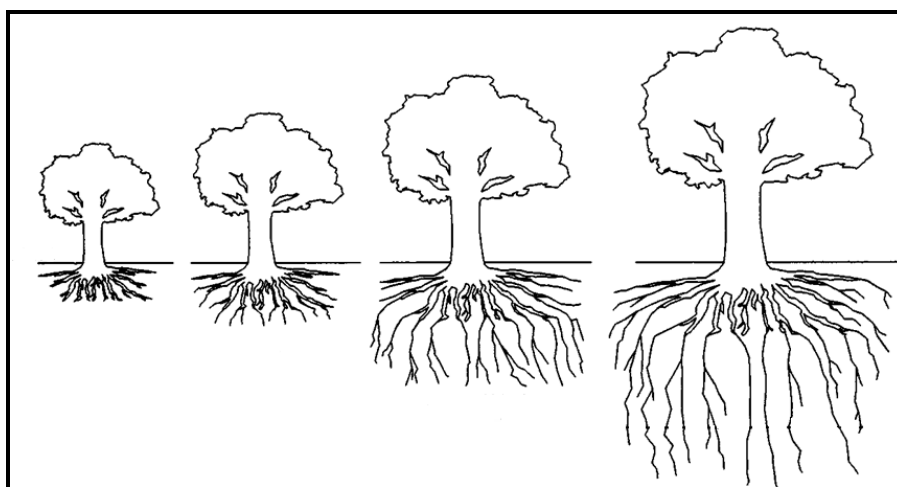
Figure 1.2: The enhancement of roots deeper into the soil with time due to maturation of the tree. Figure courtesy: Reference [3].

Hyperaccumulators are those plants that can accumulate (toxic metals) 100 times more than the plants, which are found in normally growing vegetation. Trees have been suggested as appropriate plants for phytoremediation of heavy metal-contaminated land because they provide a number of beneficial attributes viz.,

Large biomass:

The study of hyperaccumulator plants suggested that the plants can take up large amounts of heavy metals into their aerial tissues and thereby clean up contaminated soil [4, 5]. These plants take up and tolerate very high concentrations of heavy metals. Their main disadvantage is low productivity because of low biomass. Trees, on the other hand, include many high yielding biomass species that would need to accumulate only moderate amounts of metal to be effective.

Genetic variability:

There are species of many fast growing, short-rotation trees, such as *Salix* and *Populus*, which are genetically diverse; this helps to select genotypes with traits for resistance to high metal concentrations, or for high or low metal uptake.

Economic value:

Trees have predominantly been used as biomass fuel by burning the chipped stems. The other uses are for the production of chipboard, paper, charcoal, and for specialist uses such as basket weaving. Progress is also being made towards more efficient conversion of biomass to energy fuels using anaerobic digestion, fermentation, thermo chemical conversion and improved combustion techniques [6].

Site stability:

Trees can protect the soil surface from dispersal by wind or erosion by water. The roots help to stabilize the substrate. Uptake of water and transpiration through the leaves may help to limit the downward migration of heavy metals by leaching and thus help to protect ground and surface waters. The leaf fall contributes a significant amount of organic material to the soil surface.

Metals, such as copper, nickel, chromium and iron, for example, are essential in very low concentrations for the survival of all forms of life. These are described as essential trace elements and can cause toxicity only when they are present in greater quantities. On the other hand, heavy metals such as lead, cadmium and mercury can cause metabolic anomalies even at very low concentrations.

Copper:

Copper (Cu) is an essential redox-active transition metal for plants. The average content of Cu in plant tissue is 10 $\mu g\ g^{-1}$ dry weight [7]. It is an important metal for several enzymes, many of which are involved in electron transfer chain in mitochondria and chloroplast e.g. plastocyanin and cytochrome oxidase. The Cu ions act as cofactors in many enzymes such as Cu/Zn superoxide dismutase (SOD), cytochrome C oxidase, etc.

Copper is a major contaminant which is released into the environment by different anthropogenic activities, like bactericidal, fungicidal and industrial waste [8]. Excess amount of Cu can cause disorders in plant growth and development by adversely affecting important physiological changes in plants. Plants grown in the presence of high amounts of Cu normally show reduced biomass and chlorosis symptoms [9]. A lower content of chlorophyll and alterations of chloroplast structure and thylakoid membrane composition was found in leaves growing under such conditions [10, 11].

Manganese (Mn)

Manganese (Mn) is a trace element that is found in varying amounts in all tissues and is amongst the mostly used elements in industries. It is an essential micronutrient and activator for enzymes involved in tricarboxylic acid cycle. However, Mn is toxic when in excess and consequently represents an important factor in environment contamination and causes various phytotoxic effects [12].

Chloroplasts are the most sensitive of cell organelles to Mn deficiency [13]. As a result, a common symptom of Mn deficiency is interveinal chlorosis in young leaves. Two well known Mn deficiencies in arable crops are grey speck in oats and marsh spot in peas. White streak in wheat and interveinal brown spot in barley are also

symptoms of Mn deficiency [14]. Some of the studies on metal hyperaccumulator plants are enlisted in Table 1.1.

Table 1.1 List of hyperaccumulator plants [Source: McIntyre 2003 **(Cu, Pb, Zn, Ni, Cr, Cd, Hg, Co, As)**; Borovicka 2007 [Ag]

Metals	Plant	English name	Reference
Ag	*Amanita strobiliformis*	European Pine Cone and related sp. of Lepidella	[15]
Cu, Pb, Zn, Ni	*Brassica juncea*	Indian Mustard	[16]
Cr, Cu, Cd	*Bacopa monnieri*	Smooth Water Hyssop	[16]
Cr, Cu, Cd, Pb	*Vallisneria americana*	Tape Grass	[16]
Cd, Hg, Pb	*Eichhornia crassipes*	Water Hyacinth	[16]
Cd, Pb, Hg	*Hydrilla verticillata*	Hydrilla	[16]
Cr, Hg	*Pistia stratiotes*	Water lettuce	[16]
Cr, Ni, Pb	*Salvinia molesta*	Kariba weeds or water ferns	[16]
Cd, Ni ,Pb, Cr	*Spirodela polyrhiza*	Giant Duckweed	[16]
Cd, Co, Ni, Cu, Pb, Zn	*Thlaspi caerulescens*	Alpine pennycress	[16]]
As	*Agrostis castellana*	'Highland Bent Grass	[16]
Cu, Zn, Pb	*Athyrium yokoscense*	Japanese false spleenwort	[16]

Study of metal accumulation by plants growing on mining area will be an easy way to identify the metal accumulating and tolerant plants as they are growing in natural conditions containing high metal content in soil. Plant tissue culture technique can be used as a tool for identification of hyperaccumulating plants. By culturing the plants in culture vessels in laboratory, it offers a potential technique to screen hyperaccumulator plants. Thus, this technique can be used to generate new information, which can directly or indirectly be used in phytoremediation, phytomining and nanoparticle synthesis by using plants. Various micro-organisms such as bacteria, fungi, and yeasts have been suggested as nanofactories for synthesizing metal nanoparticles of silver and gold. But, the use of plants for the fabrication of nanoparticles has drawn the attention of researchers as a rapid, low cost, eco-friendly and a single step method for the biosynthesis process [17].

1.2 Nanotechnology:

Nanotechnology is the designing, characterization, production and application of structures, devices and systems by controlling shape and size at nanometer scale. Nanotechnology, in a very short period of time has emerged as one of the most important areas of research and development and shows considerable promise with regards to biomedical, chemical, electronic, energy and drug delivery applications.

Synthesis of nanomaterials:

Nanomaterials are materials with at least one dimension roughly between 1 and 100 nanometers. 1 nm is 10^{-9} of a meter i.e. the size of a marble compared to the size of the earth! Nanoparticles of metals, metal oxides and semiconductor materials (quantum dots) have attracted attention because of their unique properties. When characteristic structural features are intermediate between isolated atoms and bulk materials, the objects often show behavior substantially different from those displayed by either atoms or bulk materials. The unique chemical, electronic, magnetic, optical, and other properties of nanoparticles have sparked their application in a broad range of fields, including chemistry, physics, biology, materials science, medicine, catalysis, engineering and computer science and so on. The fabrication of nanoparticles can be done by top-down and bottom-up approach using chemical, physical or biological methods as shown in Figure 1.3.
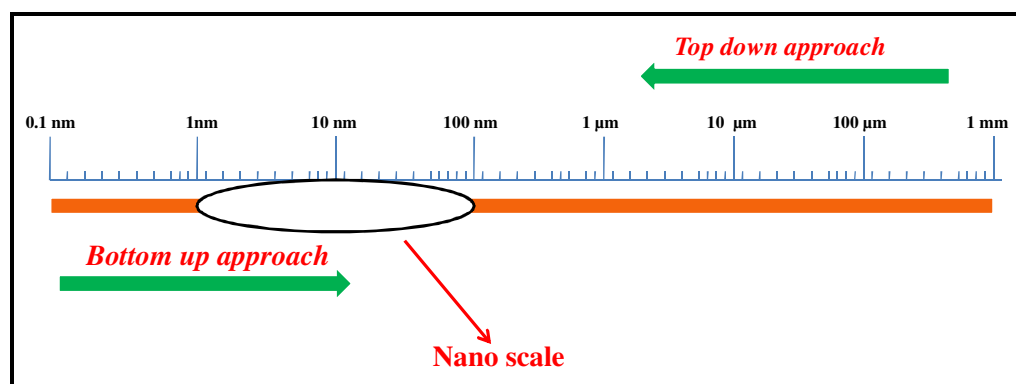
Figure 1.3: Different approaches of nanoparticles synthesis [Modified Figure courtesy: Reference Niemeyer 2001[18].

The syntheses of nanoparticles are mostly done by physical, chemical and recently developed biological methods (Figure 1.4). Most of the physical methods which have been used for the synthesis of various compositions of nanoparticles are spray pyrolysis [19], photoirradiation [20], radiolysis [21], physical vaporization [22], electrochemical [23], ultrasonication [24], solvated metal atom dispersion [25], electrospinning [26], lithography [27], chemical vapor deposition [28], sputtering [29], laser ablation [30], etc.

Chemical methods for synthesis of nanoparticles have attracted attention as these offer control over size and shape of nanoparticles. Chemical reduction methods such as, sol-gel [31], co-precipitation [32], solvothermal [33] and template based methods [34] are generally employed for the synthesis of nanoparticles of various compositions. The nature of precursor ions also determines the kind of reducing agents to be applied. The chemical reduction method is a very common route for the synthesis of metal nanoparticles of different sizes and shapes.

The biological routes for the synthesis of nanoparticles have recently been developed and yield nanoparticles at room temperature and physiological pH, with properties such as high stability, water dispersal, fluorescence, etc. which are very difficult to achieve by chemical and physical routes. Moreover, biologically synthesized nanoparticles are naturally protein capped, which prevents their flocculation, thus eliminating the need of any external capping agents which are usually toxic as is seen in chemical routes. Thus, the biosynthesis of nanoparticles is in complete synchronization with the environment and should be further developed in order to obtain nanoparticles of variable sizes, shapes and chemical compositions which will find major applications in cancer research, treatment of cardiovascular disorders, targeted drug delivery systems, catalysis, advanced materials, biotechnology, etc.
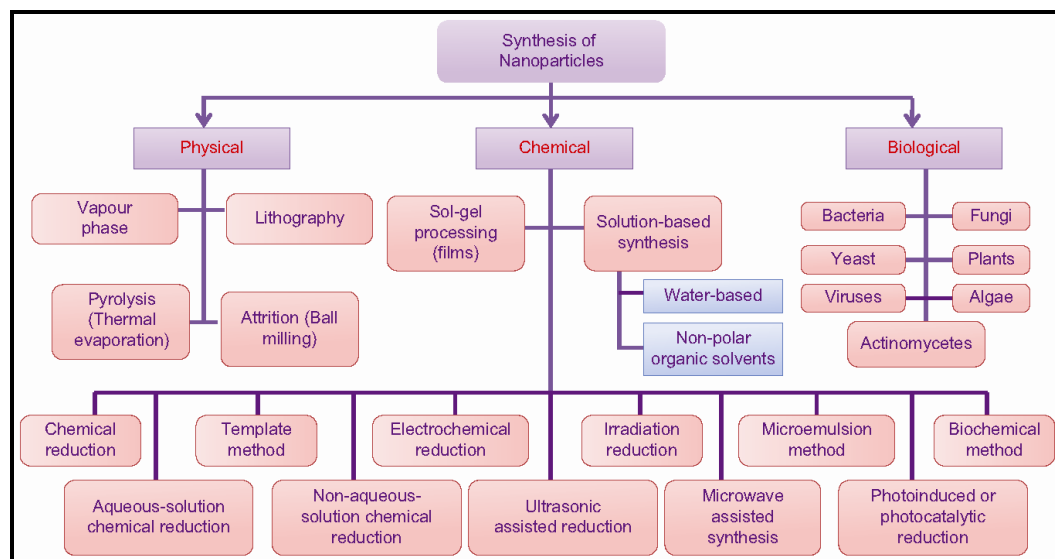
Figure 1.4 Different types of methods for synthesis of nanoparticles (Figure courtesy: Reference [35].

1.2.1 Biosynthesis of nanoparticles:

Synthesis of nanoparticles using biological processes is of great interest due to their unusual optical [36], chemical [37], photo electrochemical [38], and electronic [39] properties. There are different processes of synthesis of nanoparticles such as physical, chemical and biological, some of which are novel while others are quite common. Nature has devised various processes for the synthesis of nano- and micro-length scaled inorganic materials which have contributed to the development of relatively new and largely unexplored areas of research based on the biosynthesis of nanomaterials [40]. The synthesis and assembly of nanoparticles would benefit from the development of clean, non-toxic and environmentally acceptable ''green chemistry'' procedures, probably involving organisms ranging from bacteria to fungi and plants [40, 41]. Hence, both unicellular and multicellular organisms are known to produce inorganic materials either intra- or extracellularly [42].

Use of bacteria for synthesis of nanoparticles:

The synthesis of nanoparticles using bacteria has been shown in Table 1.2. The *Pseudomonas stutzeri* AG259 isolated from silver mines has been used in synthesis of silver nanoparticles [43, 44]. Similarly, in the presence of exogenous electron donor,

sulphate-reducing bacterium *Desulfovibrio desulfuricans* NCIMB 8307 has been shown to be synthesizing palladium nanoparticles [45]. The growth of microscopic gold, silver and gold-silver alloy crystals of well-defined morphology by common *Lactobacillus* strains found in buttermilk has been reported [46]. The supernatant of *Pseudomonas aeruginosa* was used for the reduction of gold ions resulting in extracellular biosynthesis of gold nanoparticles [47]. It has been reported that extracellular synthesis of nanoparticles using cell filtrate could be beneficial over intracellular synthesis. The control over the shape of gold nanoparticles has been achieved by using *Plectonema boryanum* UTEX 485, a filamentous cyanobacterium, when it was reacted with aqueous Au $(S_2O_3)_2^{-3}$ and $AuCl_4^-$ solutions at 25–100ºC for upto 1 month and at 200ºC for 1 day resulting in the formation of cubic gold nanoparticles and octahedral gold platelets, respectively [48]. The mechanisms of gold bioaccumulation by cyanobacteria (*Plectonema boryanum* UTEX 485) from gold (III) chloride solutions have shown that interaction of cyanobacteria with aqueous gold (III)-chloride initially promoted the precipitation of nanoparticles of amorphous gold (I)-sulfide at the cell walls, and finally deposited metallic gold in the form of octahedral (III) platelets near cell surfaces and in solutions [49].

Table 1.2: Different types of bacteria used for synthesis of nanoparticles

Metals	Bacteria	Reference
Au	*Bacillus subtilis*	[50]
Au	*Bacillus cereus*	[51]
Au	*Actinobacter* sp.	[52]
Au	*Pseudomonas aeruginosa*	[47]
Ag	*Pseudomonas stutzeri*	[43, 44]
Ag	*Shewanella oneidensis*	[53]
Ag	*Lactobacillus* sp.	[46]
Ag	*Bacillus megaterium*	[54]
Ag	*Bacillus* sp.	[55]
CdS	*Clostridium thermoaceticum*	[56]
CdS	*Escherichia coli*	[57]
CdS	*Klebsiella pneumoniae*	[58, 59]
		Table 1.2 Contd…..

CdS	*Klebsiella aerogenes*	[60]
CdS	*Glucanobacter xylinus*	[61]
Se	*Klebsiella pneumonia*	[62]
Fe_3SO_4	*Magnetospirillum* sp.	[63]
Fe_3SO_4	*Aquaspirillum* sp.	[64]
Fe_3SO_4	*Thermoanaerobacter ethanolicus*	[63]
Au-Ag alloy	*Lactobacillus*	[46]

Bacteria have also been used for the synthesis of semiconductor nanoparticles such as CdS, ZnS, Se and Te. The use of cysteine-hydrochloride as the sulfide source for the extracellular synthesis of CdS quantum dots with a large size distribution of 20-200 nm by *Clostridium thermoaceticum* has been demonstrated [57]. The formation of CdS crystallites were formed by *Klbesiella pneumoniae* when incubated with Cadmium solution [58, 59]. The formation of Selenium nanoparticles using *Klebsiella pneumonia* has also been reported [61].

Fungal based synthesis of nanoparticles:

Fungi have been extensively studied for the synthesis of nanomaterials of different elemental compositions (Table 1.3), shapes and sizes. They are preferred over other microbes because fungi could be a source for the production of large amounts of nanoparticles as fungi are known to secrete much higher amounts of proteins. It has been shown with an experiment where bioreduction of aqueous $AuCl^{-4}$ ions was carried out using the fungus *Verticillium* sp. that led to the formation of gold nanoparticles with good monodispersity [65]. The *Fusarium oxysporum* was also used in the formation of extremely stable silver hydrosol [66]. The acidophilic fungus *Verticillium* sp. has capability of synthesis of gold as well as silver nanoparticles upon their incubation with Ag^+ and $AuCl^{-4}$ ions [67]. However, a novel biological method for both the intra- and extra-cellular synthesis of silver nanoparticles using the fungi *Verticillium* sp. and *Fusarium oxysporum*, respectively, has been demonstrated. This has opened up an exciting possibility wherein the nanoparticles may be entrapped in the biomass in the form of a film or produced in solution, both having interesting commercial potential [68]. The fungus *Aspergillus flavus* also resulted in the accumulation of silver nanoparticles on the surface of its cell wall when incubated

with silver nitrate solution [69]. The synthesis of zirconia nanoparticles extracellularly by using the fungus *Fusarium oxysporum* was studied [70]. The exciting finding is that the exposure of *F. oxysporum* to the aqueous $CdSO_4$ solution yields CdS quantum dots extracellularly which are monodispersed.

Table 1.3: Different types of fungi used for synthesis of nanoparticles.

Metals	Fungi	Reference
Au	*Verticillium* sp.	[65]
Au	*Fusarium oxysporum*	[71]
Au	*Colletotrichum* sp.	[72]
Au	*Trichothecium* sp.	[73]
Au	*Verticillium. luteoalbum*	[74]
Au	*Helminthosporum solani*	[75]
Au	*Volvariella volvaceae*	[76]
Ag	*Aspergillus fumigatus*	[77]
Ag	*Fusarium oxysporium*	[66]
Ag	*Verticillium* sp.	[68]
Ag	*Aspergillus flavus*	[69]
Ag	*Phaenerochaete chrysosporium*	[78]
Ag	*Trichoderma viride*	[79]
Ag	*Trichoderma asperellum*	[80]
CdS	*Fusarium oxysporum*	[81]
SiO$_2$	*Fusarium oxysporum*	[82]
Ti O$_2$	*Fusarium oxysporum*	[82]
Bi$_2$O$_3$	*Fusarium oxysporum*	[83]
ZrO$_2$	*Fusarium oxysporum*	[84]
Fe$_3$O$_4$	*Fusarium oxysporum*	[85]
CuAlO$_2$	*Humicola* sp.	[86]
Pt	*Fusarium oxysporum.*	[87]
Au-Ag Alloy	*Fusarium oxysporum*	[88]

Nanoparticles synthesis by plants:

The synthesis of nanoparticles using plants has been shown in Table 1.4. The very high rate of nanoparticle synthesis justifies the use of plants over microorganisms in the biosynthesis of metal nanoparticles through greener and safer methods [89]. Control of the size of silver nanoparticles has been shown to be a function of reaction time. Nanoparticles using oat and wheat biomass are used for the formation of nanoparticles of different sizes and shapes. This work shows that the pH of the solution plays an important role in the determination of shape and size of the nanoparticles and by modulating the pH of the aqueous extract, size controlled nanoparticles can be obtained. The biosynthesis of metal nanoparticles using leaf extracts of *Azadirachta indica* [90] and *Geranium,* [72, 89] has been reported. Shankar *et al.* (2004) reported the synthesis of triangular nanoparticles using lemongrass plant extract [91]. Thin, flat and crystalline gold nanotriangles were seen when reacted with aqueous chloroaurate ions. Similar work on the synthesis of gold nanotriangles was performed using tamarind leaf extract as the reducing agent [92]. The formation of gold nanotriangles and silver nanoparticles using leaf extract of *Aloe vera* as the reducing agent was reported by [93].

Huang *et al.* (2007) demonstrated the synthesis of silver and gold nanoparticles using sun-dried leaf extract of *Cinnamomum camphora* [17]. They demonstrated that the sun-dried leaves were better than the aqueous leaf extract used for the biosynthesis. Li *et al.* (2007) synthesised silver nanoparticles by reacting silver ions with *Capsicum annuum* L. extract, at the period of five hours reaction time led to form spherical shaped nanoparticles. As the time prolongs in reaction time from 9 hr to 13 hr, the size of the nanoparticles was increased. The leaf extracts of plants have been used for the synthesis of silver and gold nanoparticles. However, amla (*Emblica officinalis*) fruit extract, showed synthesis of extracellular gold and silver nanoparticles. The formed particles were highly stable [94].

The above plants described the synthesis of nanoparticles by using leaf extracts. In contrast to these, the sweet desert willow (*Chilopsis linearis*) has shown the ability of intracellular gold nanoparticle synthesis. This plant has the capability to take up gold (Au) from gold-enriched media (Au 160 mg L^{-1} in agar) and synthesize average size

of nanoparticles of 8, 35, and 18Å in root, stem, and leaves, respectively [95]. The formation of intracellular nanoparticle has the ability of potential use in phytoextraction applications. This enhancement of gold accumulation and formation of nanoparticles could further be enhanced by providing thiocyanate. However, using this plant, very small size nanoparticles (0.55 nm) could also be synthesized [96]. Similarly, growth of *Sesbania* seedlings in chloroaurate solution resulted in the accumulation of gold with the formation of stable gold nanoparticles in plant tissues [97]. It has been shown that *Alfalfa* plants synthesize silver nanoparticles *in vitro*. The roots were capable of absorbing Ag (0) from the agar medium and transferring it to the shoot. The silver atoms arrange themselves by undergoing nucleation to form nanoparticles inside the plant. The nucleated nanoparticles further join to form larger particles [98]). Haverkamp *et al.* (2007) reported the synthesis of mixed nanoparticles suggesting the possibility to produce nanoparticle catalysts of specific composition [99].

Table 1.4: Different types of plants and their extracts used for the synthesis of nanoparticles.

Metals	Plants	References
Au	*Cymbopogon flexuosus*	[91]
Au	*Coriandrum sativum*	[100]
Au	*Terminalia cattappa*	[101]
Au	*Azadirachta indica*	[90]
Au	*Emblica officinalis*	[94]
Au	*Pelargonium graveolens*	[72]
Au	*Humulus* (Hop biomass) sp.	[102]
Au	*Cicer arietinum*	[103]
Au	*Tamarindus indica*	[92]
Au	*Aloe vera*	[93]
Au	*Triticum aestivum*	[104, 105]
Au	*Sesbania drummondi*	[97]
Au	*Avena sativa*	[106]
Au	*Brassica juncea*	[99]
Au	*Medicago sativa*	[107]
		Table 1.4 Contd….

Au	*Semecarpus anacardium*	[108]
Au	*Coleus amboinicus*	[109]
Au	*Eucalyptus camaldulensis*	[110]
Au	*Pelargonium roseum*	[110]
Au	*Camellia sinensis*	[111]
Au	*Lawsonia inermis*	[112]
Au	*Phyllanthus amarus*	[113]
Au	*Aloe ferox*	[114]
Au	*Hibiscus rosa sinensis*	[115]
Au	*Psidium guajava*	[116]
Au	*Diopyros kaki*	[117]
Au	*Scutellaria barbata*	[118]
Au	*Tanacetum vulgare*	[119]
Au	*Szyygium aromaticum*	[120]
Au	*Mucuna pruriens*	[121]
Au	*Musa paradisiaca*	[122]
Au	*Beta vulgaris*	[123]
Au	*Centella asiatica*	[124]
Au	*Sorbus aucuparia*	[125]
Au	*Rosa rugosa*	[126]
Au	*Chenopodium album*	[127]
Au	*Camellia sinensis*	[128]
Au	*Olea europaea*	[129]
Au	*Callistemon viminalis*	[130]
Au	*Panax ginseng*	[131]
Au	*Ocimum sanctum*	[132]
Au	*Murraya koenigii*	[133]
Au	*Anacardium occidentale*	[134]
Au	*Cicer arietinum*	[135]
Au	*Pyrus sp.*	[136]
Ag	*Medicago sativa*	[137]
Ag	*Tetrapanax papyriferus*	[138]
Ag	*Azadirachta indica*	[90]
Ag	*Emblica officinalis*	[94]
Ag	*Capsicum annuum*	[139]
		Table 1.4 Contd….

Ag	*Pelargonium graveolens*	[89]
Ag	*Aloe vera*	[93]
Ag	*Moringa oleifera*	[140]
Ag	*Coleus amboinicus*	[141]
Ag	*Citrus sinensis*	[142]
Ag	*Vitex negundo*	[143]
Ag	*Allium cepa*	[144]
Ag	*Solanum torvum*	[145]
Ag	*Bacopa monniera*	[146]
Ag	*Brassica juncea*	[147]
Ag	*Magnolia sp.*	[148]
Cu	*Brassica juncea*	[99]
Cu	*Magnolia sp.*	[149]
Pt	*Diopyros kaki*	[150]
Au-Ag alloy	*Azadirachta indica*	[90]

Synthesis of nanoparticles by Actinomycetes:

The actinomycetes are classified as prokaryotes but they share important characteristic features of fungi. They are also known as ray fungi. It has been shown that the extremophilic actinomycete, *Thermomonospora* sp. when exposed to gold ions, synthesized extracellular gold nanoparticles with high polydispersity [151] (Table 1.5). The synthesis of the metal nanoparticles is done by enzymes present on the cell wall and in the cytoplasmic membrane. These metal ions were not toxic to the cells, which are producing them, and continued to multiply even after the biosynthesis of gold nanoparticles [152].

Table 1.5: Different types of actinomycetes used for the synthesis of nanoparticles

Metals	Actinomycetes	References
Au	*Thermomonospora* sp.	[151]
Au	*Rhodococcus* sp.	[152]
Au	*Streptomyces* sp.	[153]

Yeast mediated synthesis of nanoparticles:

The synthesis of nanoparticles using Yeast has been shown in Table 1.2. Among the eukaryotic microorganism, yeast has been exploited mostly for the synthesis of semiconductor nanoparticles. *Candida glubrata* produced intracellularly monodispersed spherically shaped peptide- bound CdS quantum crystallites of 20 Å by neutralizing the toxicity of metal ions by forming metal–thiolate complex with phytochelatins. It has also been reported that *Saccharomyces cerevisiae* biosorbs and reduces Au^{+3} to elemental gold in the peptidoglycan layer of the cell wall *in situ* by the aldehyde group present in reducing sugars [154]. Similarly, yeast *Pichia jadinii* (*Candida utilis*), intracellularly formed gold nanoparticles of spherical, triangular and hexagonal morphologies in 24 hr. These NPs are present throughout the cell mainly in the cytoplasm and are 100 nm in size [155]. Tropical marine yeast, *Yarrowia lipolytica* NCIM 3589, also synthesized gold nanoparticles associated with cell wall. The reduction of gold ions occurred in pH dependent manner. When cells were incubated at pH 2.0, it produced hexagonal and triangular gold crystals due to the nucleation on the cell surfaces giving rise to golden color in the visible region at 540 nm. At pH 7.0 and pH 9.0, NPs with pink and purple colors were synthesized with an average size of 15 nm [156].

The method for synthesis of large quantities of silver nanoparticles by using silver-tolerant yeast strain MKY3 has been standardized. The procedure for separation of these silver particles has also been documented that was based on differential thawing of the samples [157]. Recently, yeast strains have been identified for their ability to produce gold nanoparticles. The synthesis of PbS nanocrystallites exhibiting quantum semiconductor properties by yeast, *Torulopsis* sp. has been reported, which produces intracellular, spherical nanoparticles of 2–5 nm in size when incubated with Pb^{2+} [158].

 The synthesis of spherical shaped antimony oxide (Sb_2O_3) nanoparticles of 2–10 nm size was carried out at room temperature by *S. cerevisiae*. These particles exhibit semiconductor properties. The formation was possibly due to the radial tautomerization of membrane-bound quinines or by membrane bound or cytosolic pH-dependent oxidoreductases [159].

Table 1.6: Different types of yeast used for the synthesis of nanoparticles.

Metals	Yeast	Reference
Au	*Saccharomyces cerevisiae*	[154]
Au	*Pichia jadinii*	[155]
Ag	*Yarrowia lipolytica NCIM 3589*	[156]
Ag	*Yeast strain MKY3*	[157]
PbS	*Torulopsis* sp.	[158]
Sb_2O_3	*Saccharomyces cerevisiae*	[159]
CdS	*Saccharomyces pombe*	[160]
CdS	*Candida glubrata*	[161]

Algae mediated synthesis of nanoparticles:

The synthesis of nanomaterials using algae has been studied in the biosynthesis of extracellular gold nanoparticles (Table 1.7) using marine alga, *Sargassum wightii* [162]. Recently synthesis of intracellular gold nanoparticles by using *Tetraselmis kochinensis* was reported [163]. The Palladium nanoparticles of different sizes and shape were synthesized by cyanobacteria, *Plectonema boryanum* UTEX 485, when reacted with palladium (II) chloride complex [164]. In addition to the synthesis of metal nanoparticles, algae have also been used for synthesis of nanobiomaterials by coccoliths and diatoms [165].

Table 1.7: Different types of algae used for the synthesis of nanoparticles

Metals	Algae	Reference
Au	*Sargassum wightii*	[162]
Au	*Tetraselmis kochinensis*	[163]
Pd	*Plectonema boryanum*	[164]
CdS	*Phaeodactylum tricornutum*	[166]

1.2.2 Role of biomolecules in synthesis of nanoparticles:

The physical and chemical methods for NPs synthesis lead an effect on the environment which can be relatively high. Therefore it is necessary to develop environmentally sustainable ("green chemistry") alternatives to the existing methods [167]. The selection of an environmentally acceptable solvent system, an eco-friendly

reducing agent and particle-stabilizing capping agent are the qualifying criteria for a totally green nanoparticles synthesis protocol.

The synthesis of nanoparticles using biomolecules has been shown in Table 1.8. The protein as biomolecules plays an important role which provides the dual function of Au III reduction and the size- and shape-controlled synthesis of the nanogold particles. A protein with a molecular weight of approximately 28 kDa was isolated and purified by reverse-phase HPLC. This protein tested positive for the reduction of chloroauric acid in aqueous solution [168]. The bioreduction of Au^{+3} to Au^0 on the plasma membrane, extracellularly by the carotenoids and NADPH-dependent enzymes which are embedded in plasma membrane were involved in the formation of nanoparticles [169].

A novel extremophilic actinomycete, *Thermomonospora* sp. was found to synthesize extracellular monodispersed spherical gold nanoparticles. These nanoparticles particles were stable for a longer period. The gel electrophoresis analysis showed that the proteins of molecular weight ranging from 80-10kDa were involved in stabilization of nanoparticles [151]. In addition to this, baker's yeast, *S. cerevisiae* was reported to biosorb and reduce Au^{+3} to gold nanoparticles in the peptidoglycan layer of the cell wall *in situ* by the aldehyde group present in reducing sugars [154]. It has been shown the α-NADPH-dependent sulfite reductase (35.6 kDa) and phytochelatin helped in the gold nanoparticle formation [170].

The culture supernatants of Enterobacteriaceae (*Klebsiella pneumonia*, *E. coli* and *Enterobacter cloacae*) also rapidly synthesized silver nanoparticles by reducing Ag^+ to Ag^0. The silver ion reduction was partially inhibited, which showed the involvement of nitroreductase enzymes in the reduction process [171]. The *Aspergillus niger* isolated from soil produced spherical silver nanoparticles of size 20 nm in diameter. Elemental spectroscopy demonstrated the presence of fungal protein for the stabilization of the nanoparticles. The *in vitro* synthesis of silver hydrosol nanoparticles by enzymatic route by using α-NADPH-dependent nitrate reductase (44kDa) from *F. oxysporum* with capping peptide, phytochelatin was demonstrated recently [172]. The reduction of Ag^+ ions has occurred by the action of nitrate reductase enzyme and quinine in extracellular electron transfer [173]. The Compactin

isolated from fungus *P. brevicompactum* WA2315 was involved in the biosynthesis of silver nanoparticles in 72 hr [174].

It was believed that under aerobic conditions, a 90 kDa bacterial protein present in the cell-free extract was responsible for the bioreduction of selenite to elemental red selenium by *Tetrathiobacter kashmirensis* [175]. The synthesis of Zirconia nanoparticles which were produced by cationic proteins secreted by *F. oxysporum* when reacted with ZrF_6^{-2} anions, the protein of molecular weight 24–28 kDa was found to be responsible for the formation of zirconia nanoparticles [70]. A passively reduced H_2PtCl_6 to platinum nanoparticles by dimeric hydrogenase enzyme (44.5 and 39.4 kDa) of *F. oxysporum* showed the reduction with optimum activity at pH 7.5 and 38°C [176]. The *S. cerevisiae* was found to produce spherical shaped antimony oxide (Sb_2O_3) nanoparticles in the size of 2–10 nm at room temperature exhibiting semiconductor properties. This was possibly due to the radial tautomerization of membrane-bound quinines or by membrane bound or cytosolic pH-dependent oxidoreductases [159].

Table 1.8: Different types of biomolecules involved for the synthesis of nanoparticles

Metals	Biomolecules	Reference
Au	28 kDa protein	[168]
Au	Carotenoids and NADPH-dependent enzymes	[169]
Au	Au 66 and 10 kDa protein	[71]
Au	α-NADPH-dependent sulfite reductase (35.6 kDa) and phytochelatin	[170]
Au	Glutathiones	[72]
Au	80–10 kDa protein	[151]
Au	Peptidoglycan reducing sugars	[154]
Ag	Nitroreductase	[171]
Ag	α-NADPH-dependent nitrate reductase (44 kDa) and phytochelatin	.[172]
Ag	Nitrate reductase	[173]
Ag	Compactin	[174]
Zr	24–28 kDa protein	[70]
		Table 1.8 Contd….

Se	90-kDa	[175]
Pt	Dimeric hydrogenase (44.5 and 39.4 kDa)	[176]
Sb$_2$O$_3$	Membrane-bound quinine or membrane-bound/cytosolic pH dependent oxidoreductase	[159]

1.2.3 Applications of nanoparticles:

The development of nano-devices by using biological materials and their use in wide range of applications on living organisms has recently attracted the attention of biologists towards nanobiotechnology. The applications of this technology will help in understanding the use of different living organisms in nano-devices production and also in the use of these nano products in various applications.

Bioremediation of radioactive wastes which is released from the nuclear power plants and nuclear weapon production such as Uranium (a long-lived radionuclide hazardous for both flora and fauna) have been achieved by using nanoparticles. The *Bacillus sphaericus* JG-A12 cells and S-layer proteins have capabilities for the clean-up of uranium contaminated waste waters. The effluents derived from such sources can be bioremediated by treating with *Chromobacterium violaceum* [177].

Recently, nanoparticles have found applications in antibacterial effects. It has been shown that extracellularly produced silver or gold nanoparticles using *Fusarium oxysporum*, can be incorporated in several kinds of materials such as cloth. These cloth with silver nanoparticles are sterile and can be useful in hospitals to prevent or to reduce the infection with pathogenic bacteria such as *Staphylococcus aureus* [177]. Silver nanoparticles also have large number of applications such as in non-linear optics, spectrally selective coating for solar energy absorption, biolabelling and intercalation materials for electrical batteries, as optical receptors, catalyst in chemical reactions and as antibacterial capacities [178].

Magnetite (Fe$_3$O$_4$)/greigite (Fe$_3$S$_4$) and siliceous materials produced from magnetotactic bacteria and diatoms, respectively, are used in optical coatings for solar energy applications and as ion insertion materials for electrical battery applications [179]. Nanoparticles can be used as labels for optical biodetection, as substrates for

multiplexed aqueous bioassays, as probes for cellular imaging or as carriers for therapeutic delivery [180-183].

In medical applications, gold nanoparticles have been used in treating B-chronic lymphocytic leukemia (CLL). CLL is an incurable disease predominantly characterized by apoptosis resistance. VEGF antibody (AbVF) was used to treat CLL; however VEGF antibody attached to the gold nanoparticles, was found to be more effective. Apoptosis with gold–AbVF was higher than with the CLL cells exposed only to VEGF antibody or gold nanoparticles. Non-coated gold nanoparticles alone were able to induce some level of apoptosis in CLL B-cells. Thus gold nanoparticles could be used for treating CLL [184].

Gold nanoparticles have also been used in the Carter-Wallace home pregnancy test 'First Response'. This uses conventional micrometer-sized latex particles in conjunction with gold nanoparticles (<50 nm diameter), which make them pink. The nanoparticles are derivatized with antibodies to human chorionic gonadotrophin, a hormone released by pregnant women. When mixed with a urine sample containing this hormone, the micro- and nanoparticles are co-agglutinated and the resulting clumps are colored pink [185].

Small interfering RNA (siRNA) delivery can be monitored by a novel method based on nanodevice that combines unmodified siRNA with semiconductor quantum dots (QDs) as multicolor biological probes. Co-transfection of siRNA with QDs using standard transfection techniques has led to the formation of photostable fluorescent nanoparticles that help in tracking the delivery of nucleic acid, the degree of transfection in cells and also in purifying homogeneously silenced subpopulations [186].

The HIV-1 virus can be inhibited by nanoparticles ranging in size from 1 to 10 nm when they readily interact and bind to gp120 glycoprotein knobs. This interaction of silver nanoparticles inhibits the virus from binding to host cells which was demonstrated by *in vitro* study. Hence, silver nanoparticles could find application in preventing as well as controlling HIV infection [187]. These nanoparticles can also be

used in topical ointments and creams used to prevent infection of burns and open wounds [188].

The honeycomb mesoporous silica nanoparticle (MSN) system with 3 nm pores can be used to transport DNA and chemicals into isolated plant cells and intact leaves. The MSN is loaded with the gene and its chemical inducer and is capped at the ends with gold nanoparticles to keep the molecules from leaching out. Uncapping the gold nanoparticles releases the chemicals and triggers gene expression in the plants under controlled release conditions [189]. The potential use of nanodevices as delivery systems to specific targets in living organisms was explored for medical uses. The same principle can also be applied in plant systems for a broad range of uses, in particular to tackle infections. Nanoparticles tagged to agrochemicals or other substances could reduce the damage to other plant tissues and the amount of chemicals released into the environment. The penetration and translocation of magnetic nanoparticles in whole living plants and into plant cells were determined. The magnetic character allowed nanoparticles to be positioned in the desired plant tissue by applying a magnetic field [190].

The aim of the present research was to study the accumulation of copper and manganese by the plants *Prosopis juliflora* and *Holoptelia integrifolia* respectively growing on mining areas; bioleaching of the above metals and their conversion to oxide nanoparticles using the fungus *Fusarium oxysporum*. Secondly, the plant *Arachis hypogea* was used for the biosynthesis of highly monodispersed gold nanoparticles for use in biomedical applications, with properties such as bio-compatibility, high stability, non-toxicity, etc. which would further aid in their efficacy in treatment of various disorders. Moreover, we attempted to obtain these nanoparticles in the size range of 10-50 nm so that these inorganic particles may not block the kidneys. The protein responsible for the formation of nanoparticles was purified and characterized. Also, successful gene delivery into peanut leaves was carried out using cationic gold nanoparticles and transformation was confirmed using GUS assay method.

References

[1] Prasad, M. N. V. Phytoremediation of metals in the environment for sustainable development. *Proc. Indian Natn. Sci. Acad*. 2004, B70, 1, 71-98.

[2] Raskin, I., Ensley, B. D. (eds), Phytoremediation of toxic metals: *Using Plants to Clean up the Environment*, John Wiley and Sons Inc., New York, 2000.

[3] Suthersan, S. S. Phytoremediation. In: Suthan S. S. (eds). *Remediation engineering design concepts*. Boca Raton, CRC Press LLC, 1999.

[4] Chaney, R. L., Malik, M., Li, Y. M., Brown, S. L., E.P., B., Angle, J. S., Baker, A. J. M. Phytoremediation of soil metals. *Curr. Opin. Biotechnol*. 1997, 8, 279.

[5] Brooks, R. R. *Plants that Hyperaccumulate Heavy Metals*, CAB International, Wallingford, MA, 1998, p 380.

[6] Raiko, M. O., Gronfors, T. H. A., Haukka, P. Development and optimization of power plant concepts for local wet fuels, *Biomass Bioenerg*. 2003, 24, 27-37.

[7] Baker, D. E., Senef, J. P. 1995. Copper. In: Alloway, B. J. (eds), Heavy metals in soils, Blackie Academic and Professional, London, pp.179-205.

[8] Ducic, T., Polle, A. Transport and detoxification of manganese and copper in plants. *Brazilian J. Plant Physiol*. 2005, 17, 1, 103-112.

[9] Simova-Stoilova, L., Stoyanova, Z., Demirevska-Kepova, K., Smilova, E. Effect of Cu and Mn toxicity on growth parameters and photosynthetic pigments of young barley plants. *Compt. Rend. Acad. Bulg. Sci*. 2002, 55, 83-88.

[10] Ciscato, M., Valcke, R., Van, L. K., Clijsters, H., Navari-Izzo, F. Effects of *in vivo* copper treatment on the photosynthetic apparatus of two *Triticum durum* cultivars with different stress sensitivity. *Physiol. Plant*. 1997, 100, 901-908.

[11] Quartacci, M. F., Pinzino, C., Sgherri, C. L. M., Vecchia, F. D., Navari-Izzo, F. Growth in excess copper induces changes in the lipid composition and fluidity of PSII-enriched membranes in wheat. *Physiol. Plant*. 2000, 108, 87-93.

[12] Pittman, J. K. Manganese molecular mechanisms of manganese transport and homeostasis. *New Phytol*. 167, 2005, 733-742.

[13] Mengel, K., Kirkby, E. A. Principles of plant nutrition. Netherlands. Kluwer Academic Publishers. 2001, p. 849

[14] Jacobsen, J. S., Jasper. C. D. Diagnosis of nutrient deficiencies in *Alfalfa* and wheat. EB 43, February 1991. Bozeman, M. T. Montana State University extension.

[15] Borovicka, J., Randa, Z., Jelinek, E., Kotrba, P., Dunn, C. E. Hyperaccumulation of silver by *Amanita strobiliformis* and related species of the section Lepidella. *Mycol. Res.* 2007, 111 (Pt 11), 1339-1344.

[16] McIntyre T. C, Data bases and protocol for plant and microorganism selection: Hydrocarbons and metals *In*: McCutcheon, S. C., and Schnoor, J. L. (eds) *Phytoremediation: Transformation and control of contaminants.* New Jersey, John Wiley & Sons, 2003, pp. 887-904.

[17] Huang, J., Chen, C., He, N., Hong, J., Lu, Y., Qingbiao, L., Shao, W., Sun, D., Wang, X. H., Wang, Y., Yiang, X. Biosynthesis of silver and gold nanoparticles by novel sundried *Cinnamomum camphora* leaf. *Nanotechnology*, 2007, 18, 105–106.

[18] Niemeyer C. M. Nanoparticles, proteins, and nucleic acids biotechnology meets materials science. Angew. Chem. Int. Ed. 2001, 40, 4128 – 4158.

[19] Brennan, J. G., Seigrist, T., Carroll, P. J., Stuczynski, S. M., Brus, L. E., Steigerwalk, M. L. The preparation of large semiconductor clusters via the pyrolysis of a molecular precursor *J. Am. Chem. Soc.* 1989, 111, 4141-4143.

[20] Henglein, A., Mulvaney, P., Holtzworth, A., Sosebee, T. E., Fojitik, A. *Ber. Bunsenges. Phys. Chem.* 1992, 96, 754.

[21] Henglein, A. Radiolytic preparation of ultrafine colloidal gold particles in aqueous solution: optical spectrum, controlled growth, and some chemical reactions. *Langmuir,* 1999, 15, 6738-6744.

[22] El-Shall, M. S. Laser vaporization for the synthesis of nanoparticles and polymers containing metal particulates *Appl. Surf. Sci.* 1996, 106, 347-355.

[23] Reetz, M. T., Helbig, W. Size-Selective Synthesis of Nanostructured transition metal clusters *J. Am. Chem. Soc.* 1994, 116, 7401-7402.

[24] Salkar, R. A., Jeevanandam, P., Kataby, G., Aruna, S. T., Koltypin,Y., Palchik, O., Gedanken, A. Elongated copper nanoparticles coated with a zwitterionic surfactant *J. Phys. Chem. B.* 2000, 104, 893-897.

[25] Davis, S. C., Klabunde, K. J. Unsupported small metal particles: preparation, reactivity, and characterization *Chem. Rev.* 1982, 82, 153-208.

[26] Frenot, A., Chronakis, H. S. Polymer nanofibers assembled by electrospinning *Current opin. Colloids Interf. Sci.* 2003, 8, 64-75.

[27] Ginger, D. S., Zhang, H., Mirkin, C. A. The evolution of dip-pen nanolithography. *Angew. Chem. Int. Ed.* 2004, 43, 30-45.

[28] Choy, K. L. Chemical vapour deposition of coatings *Prog. Mater. Sci.* 2003, 48, 57-170.

[29] Wagener, M., Gunther, B. Sputtering on liquids- a versatile process for the production of magnetic suspensions. *J. Magnet. Mag. Mater.* 1999, 201, 41-44.

[30] Fojtik, A., Henglein, A. *Ber. Bunsen-Ges.* Laser ablation of films and suspended particles in a solvent. Formation of cluster and colloid solutions. *Phys. Chem.* 1993, 97, 252-256.

[31] Cannas, C., Musinu, A., Peddis, D., Piccaluga, G. Synthesis and characterization of $CoFe_2O_4$ nanoparticles dispersed in a silica matrix by a sol–gel autocombustion method *Chem. Mater.* 2006, 18, 3835-3842.

[32] Jayakumar, O. D., Salunke, H. G., Kadam, R. M., Mohapatra, M., Yaswant, G., Kulshresshtha, S. K. Magnetism in Mn-doped ZnO nanoparticles prepared by a co-precipitation method *Nanotechnology,* 2006, 17, 1278-1285.

[33] Li, M., Liu, X. L., Cui, D. L., Xu, H.Y., Jiang, M. H. Preparation of ZnO bulk porous nanosolids of different pore diameters by a novel solvothermal hot press (STHP) method *Mater. Res. Bull.* 2006, 41, 1259-1265

[34] Qu, L., Shi, G., Wu, X., Fan, B. Facile route to silver nano tubes *Adv. Mater.* 2004, *16*, 1200-1203.

[35] Singh D. G., Kaur, B. S., Surinder, K., Mausam, V. Green approach for nanoparticle biosynthesis by fungi: current trends and applications. *Crit .Rev. Biotechnol*, 2012, 32, 49-73.

[36] Krolikowska, A., Kudelski, A., Michota, A., Bukowska, J. SERS studies on the structure of thioglycolic acid monolayers on silver and gold. *Surf. Sci.* 2003, 532, 227–232.

[37] Kumar, A., Mandal, S., Selvakannan, P. R., Parischa, R., Mandale, A. B., Sastry, M. Investigation into the interaction between surface-bound alkylamines and gold nanoparticles. *Langmuir,* 2003, 19, 6277–6282.

[38] Chandrasekharan, N., Kamat, P. V. Improving the photo electrochemical performance of nanostructured TiO$_2$ films by adsorption of gold nanoparticles. *J. Phys. Chem. B.* 2000, 104, 10851–10857.

[39] Peto, G., Molnar, G. L., Paszti, Z., Geszti, O., Beck, A., Guczi, L. Electronic structure of gold nanoparticles deposited on SiOx/Si. *Mater. Sci. Eng. C.* 2002, 19, 95–99.

[40] Sastry, M., Ahmad, A., Khan, M. I., Kumar, R. 2004. Microbial nanoparticle production. In: Niemeyer C. M., Mirkin C. A. (eds) Nanobiotechnology. Wiley-VCH, Weinheim, Germany, pp. 126–135.

[41] Bhattacharya, D., Rajinder, G. Nanotechnology and potential of microorganisms. *Crit. Rev. Biotechnol.* 2005, 25, 199– 204.

[42] Mann, S. (eds) Biomimetic materials chemistry. VCH Publishers, New York 1996.

[43] Joerger, R., Klaus, T., Granqvist, C. G. Biologically produced silver-carbon composite materials for optically functional thin film coatings. *Adv. Mater.* 2000, 12, 407–409.

[44] Klaus, T., Joerger, R., Olsson, E., Granqvist, C. G. Silver based crystalline nanoparticles, microbially fabricated. *Proc. Natl. Acad. Sci. USA*. 1999, 96, 13611–13614.

[45] Yong, P., Rowsen, N. A., Farr, J. P. G., Harris, I. R., Macaskie, L. E. Bioreduction and biocrystallization of palladium by *Desulfovibrio desulfuricans* NCIMB 8307. *Biotechnol. Bioeng*. 2002, 80, 369–379.

[46] Nair, B., Pradeep, T. Coalescence of nanoclusters and formation of submicron crystallites assisted by *Lactobacillus* strains. *Crystal Growth Design.* 2002, 4, 293–298.

[47] Husseiny, M. I., El-Aziz, M. A, Badr, Y., Mahmoud, M. A. Biosynthesis of gold nanoparticles using *Pseudomonas aeruginosa. Spectrochim. Acta A Mol. Biomol. Spectrosc*. 2007, 67, 1003–1006.

[48] Lengke, M., Fleet, M. E., Southam, G. Morphology of gold nanoparticles synthesized by filamentous cyanobacteria from gold (I)-thiosulfate and gold (III) -chloride complexes. *Langmuir,* 2006, 22, 2780–2787.

[49] Lengke, M., Ravel, B., Fleet, M. E., Wanger, G., Gordon, R. A., Southam, G. Mechanisms of gold bioaccumulation by filamentous cyanobacteria from gold (III)-chloride complex. *Environ. Sci. Technol*. 2006, 40, 6304–6309.

[50] Konishi, Y., Nomura, T., Tskukiyama, T., Saitoh, N. Microbial preparation of gold particles by anaerobic bacterium. *Trans. Mater. Res. Soc. Jpn.* 2004, 29, 2341-2343.

[51] Slocik, J. M., Knecht, M. R., Wright, D. W. In: *Encylopedia Nanosci. Nanotechnol.* Nalwa, H. S., Ed., 2004 Vol. 1, pp 293-308.

[52] Bharde, A., Kulkarni, A., Rao, M., Prabhune, A., Sastry, M Bacterial enzyme mediated biosynthesis of gold nanoparticles *J. Nanosci. Nanotechnol*. 7, (12), 2007, 4369-4377.

[53] Kumar, S. A., Wang, W., Pelletier, D., Gu, B., Moon, J., Mortensen, N., Allison, D., Joy, D., Phelps, T., Doktycz, M. Silver nanocrystallites: Biofabrication using *Shewanella oneidensis,* and an evaluation of their comparative toxicity on gram-

negative and gram-positive bacteria. *J. Environ. Sci. Technol*. 2010, 44, 5210-5215.

[54] Prakash, A., Sharma, S., Ahmad, N., Ghosh, A., Sinha, P. Bacteria mediated extracellular synthesis of metallic nanoparticles. *Int. Res. J. Biotechnol*. 2010, 1(5), 71–77.

[55] Pugazhenthiran, N., Anandan, S., Kathiravan, G., Prakash, N. K. U., Crawford, S., Ashokkumar, M. Microbial synthesis of silver nanoparticles by *Bacillus* sp. *J. Nanopart. Res*. 2009, 11, 1811-1815

[56] Cunningham, D. P., Lundie, L. L. Precipitation of cadmium by *Clostridium thermoaceticum. Appl. Environ. Microbiol*. 1993, 59, 7–14.

[57] Sweeney, R. Y., Mao, C., Gao, X., Burt, J. L., Belcher, A. M., Georgiou, G., Iverson, B. L. Bacterial biosynthesis of cadmium sulfide nanocrystals. *Chem. Biol*. 2004, 11, 1553–1559.

[58] Smith, P. R., Holmes, J. D., Richardson, D. J., Russell, D. A., Sodeau, J. R. Phyto physiological and phytochemical characterization of bacterial semi conductors sulphide nanoparticles. *J. Chem. Soc. Faraday Trans*. 1998, 94, 1235-1241.

[59] Holmes, J. D., Richardson, D. J., Saed, S., Evans Gowing, R., Russell, D. A., Sodeau, J. R. Cadmium-specific formation of metal sulfide Q-particles 'by *Klebsiella pneumoniae. Microbiology,* 1997, 143, 2521-2530.

[60] Holmes, J. D., Smith, P. R., Evans-Gowing, R., Richardson, D. J., Russell, D. A., Sodeau, J. R. Energy-dispersive X-ray analysis of the extracellular cadmium sulfide crystallites of *Klebsiella aerogenes. Arch. Microbiol*. 1995, 163, 143-147.

[61] Li, X., Chen, S., Hu, W., Shi, S., Shen, W., Zhang, X., Wang, H. *In situ* synthesis of CdS nanoparticles on bacterial cellulose nanofibers. *Carbohyd. Poly*. 2009, 76, 509-512.

[62] Fesharaki, P. J., Nazari, P., Shakibaie, M., Rezaie, S; Banoee, M., Abdollahi, M., Shahverdi, A. R. Biosynthesis of selenium nanoparticles using *Klebsiella*

pneumoniae and their recovery by a simple sterilization process. *Braz. J. Microbiol.* 2010, 41, 461-466.

[63] Roh, Y., Lauf, R. J., McMillan, A. D., Zhang, C., Rawn, C. J., Bai, J., Phelps, T. J. Microbial synthesis and the characterization of metal-substituted magnetites. *Solid State Commun*. 2001, 118, 529–534.

[64] Philipse, A., Maas, D. Magetic colloids from magnetotactic bacteria: chain formation and colloidal stability. *Langmuir,* 2002, 18, 9977-9984.

[65] Mukherjee, P., Ahmad, A., Mandal, D., Senapati, S., Sainkar, S. R, Khan, M. I, Ramani, R., Parischa, R., Kumar, P. A. V., Alam, M., Sastry, M., Kumar, R. Bioreduction of $AuCl_4^-$ ions by the fungus, *Verticillium* sp. and surface trapping of the gold nanoparticles formed. *Angew. Chem. Int. Ed*. 2001, 40, 3585– 3588.

[66] Ahmad, A., Mukherjee, P., Senapati, S., Mandal, D., Khan, M. I., Kumar, R., Sastry, M. Extracellular biosynthesis of silver nanoparticles using the fungus *Fusarium oxysporum*. *Colloids Surf. B,* 2003, 28, 313–318.

[67] Sastry, M., Ahmad, A., Khan, M. I., Kumar, R. Biosynthesis of metal nanoparticles using fungi and *actinomycete*. *Curr. Sci*. 85, 2, 2003, 162-170.

[68] Senapati, S., Mandal, D., Ahmad, A., Khan, M. I., Sastry, M., Kumar, R. Fungus mediated synthesis of silver nanoparticles: a novel biological approach. *Indian J. Phys*. 2004, 78A, 101–105.

[69] Vigneshwaran, N., Ashtaputre, N. M., Varadarajan, P. V., Nachane, R. P., Paralikar, K. M., Balasubramanya, R. H. Biological synthesis of silver nanoparticles using the fungus *Aspergillus flavus*. *Mat. Lett*. 2007, 61, 1413–1418.

[70] Bansal, V., Rautaray, D., Ahmad, A., Sastry, M. J. Biosynthesis of zirconia nanoparticles using the fungus *Fusarium oxysporum. Mater. Chem*. 2004, 14, 3303.

[71] Mukherjee, P., Senapati, S., Mandal, D., Ahmad, A., Khan, M. I., Kumar, R., Sastry, M. Extracellular synthesis of gold nanoparticles by the fungus *Fusarium oxysporum*. *Chem. Bio. Chem*. 2002, 3, 461–463.

[72] Shankar, S. S., Ahmad, A., Pasricha, R., Sastry, M. Bioreduction of chloroaurate ions by geranium leaves and its endophytic fungus yields gold nanoparticles of different shapes. *J. Mater. Chem.* 2003, 13, 1822–1826.

[73] Ahmad, A., Senapati, S., Khan, M. I., Kumar, R., Sastry, M. Extra-/intracellular, biosynthesis of gold nanoparticles by an alkalotolerant fungus, *Trichothecium* sp. *J. Biomed. Nanotechnol*. 2005, 1, 47–53.

[74] Gericke, M., Pinches, A. Microbial production of gold nanoparticles. *Gold Bull.* 2006, 39, 22-28.

[75] Kumar, S. A., Peter. Y., Nadeau, J. Facile Bio-synthesis, separation and conjugation of gold nanopar-ticles to Doxorubicin. *Nanotechnology,* 2008, 19, 39, 22–28.

[76] Philip, D. V. Biosynthesis of Au, Ag and Au–Ag nanoparticles using edible mushroom extract. *Spectrochim Acta Part A Mol. Biomol. Spectrosc.* 2009, 73, 374-381.

[77] Bhainsa, K. C., Dsouza, S. F. Extracellular biosynthesis of silver nanoparticles using the fungus *Aspergillus fumigatus. Colloids Surf. B,* 2006, 47, 160–164.

[78] Vigneshwaran, N., Kathe, A. A., Varadarajan, P. V., Nachane, R. P., Balasubramanya, R. H. Biomimetics of silver nanoparticles by white rot fungus, *Phaenero-chaete chrysosporium. Colloids Surf. B,* 2006, 53, 55-59.

[79] Fayaza, A. M., Balaji, K., Kalaichelvana, P. T., Venkatesan, R. Fungal based synthesis of silver nanoparticles—An effect of temperature on the size of particles. *Colloids Surf. B,* 2009, 74, 123–126.

[80] Southam, G., Beveridge, T. J. The *in vitro* formation of placer gold by bacteria. *Geochim. Cosmochim. Acta*. 1994, 58, 4527-4530.

[81] Ahmad, A., Mukherjee, P., Mandal, D., Senapati, S., Khan, M. I, Kumar, R., Sastry, M. Enzyme mediated extracellular synthesis of CdS nanoparticles by the fungus *Fusarium oxysporum. J. Am. Chem. Soc*. 2002, 124, 12108–12109.

[82] Bansal, V., Rautaray, D., Bharde, A., Ahire, K., Sanyal, A., Ahmad, A., Sastry, M. Fungus-mediated biosynthesis of silica and titania particles. *J. Mater. Chem.* 2005, 15, 2583–2589.

[83] Uddin, I., Adyanthaya, S., Syed, A., Selvaraj, K., Ahmad, A., Poddar, P. Structure and microbial synthesis of sub-10 nm Bi_2O_3 nanocrystals. *J. Nanosci. Nanotechnol.* 2008, 8, 3909-3913.

[84] Bansal, V., Rautaray, D., Ahmad, A., Sastry, M. Biosynthesis of Zirconia nanoparticles using the fungus *Fusarium oxysporum*. *J. Mater. Chem.* 2004, 14, 3303-3305.

[85] Bharde, A., Rautaray, D., Bansal, V., Ahmad, A., Sarkar, I., Yusuf, S. M., Sanyal, M., Sastry, M. Extracellular biosynthesis of magnetite using fungi. *Small*, 2006, 2, 135- 141.

[86] Ahmad, A., Jagdale., T, Dhas, V., Khan, S., Patil, S., Pasricha., R, Ravi, V., Oagle, S. Fungus based synthesis of chemically difficult to synthesize multifunctional nanoparticles of $CuAlO_2$. *Adv. Mater.* 2007, 19, 3295-3299.

[87] Syed, A., Ahmad, A. Extracellular biosynthesis of platinum nanoparticles using the fungus *Fusarium oxysporum*. *Colloids Surf. B,* 2012, 97, 27–31.

[88] Senapati, S., Ahmad, A., Khan, M. I, Sastry, M., Kumar, R. Extracellular biosynthesis of bimetallic Au–Ag alloy nanoparticles. *Small*, 2005, 1, 517–520.

[89] Shankar, S. S., Ahmad, A., Sastry, M. Geranium leaf assisted biosynthesis of silver nanoparticles. *Biotechnol. Prog*. 2003, 19, 1627–1631.

[90] Shankar, S. S., Rai, A., Ahmad, A., Sastry, M. Rapid synthesis of Au, Ag, and bimetallic Au core–Ag shell nanoparticles using neem (*Azadirachta indica*) leaf broth. *J. Colloid Interf. Sci*. 2004, 275, 496–502.

[91] Shankar, S. S., Rai, A., Ankamwar, B., Singh, A., Ahmad, A., Sastry, M. Biological synthesis of triangular gold nanoprisms *Nat. Mater.* 2004, 3, 482-488.

[92] Ankamwar, B., Chaudhary, M., Sastry, M. Gold nanotriangles biologically synthesized using tamarind leaf extract and potential application in vapor sensing. *Synth. React. Inorg. Metal-Org. Nano- Metal Chem*. 2005, 35, 19–26.

[93] Chandran, S. P., Chaudhary, M., Pasricha, R., Ahmad, A., Sastry, M. Synthesis of gold nanotriangles and silver nanoparticles using *Aloe vera* plant extract. *Biotechnol. Prog*. 2006, 22, 577–583.

[94] Ankamwar, B., Damle, C., Ahmad, A., Sastry, M. Biosynthesis of gold and silver nanoparticles using *Emblica officinalis* fruit extract, their phase transfer and transmetallation in an organic solution. *J. Nanosci. Nanotechnol*. 2005, 5, 1665–1671.

[95] Rodriguez, E., Parsons, J. G., Peralta-Videa, J. R, Cruz-Jimenez, G., Romero-Gonzalez, J., Sanchez-Salcido, B. E. Potential of *Chilopsis linearis* for gold phytomining: using XAS to determine gold reduction and nanoparticle formation within plant tissues. *Int. J. Phytoremed*. 2007, 9, 133–147.

[96] Gardea-Torresdey, J. L., Rodriguez, E., Parsons, J. G., Peralta-Videa, J. R., Meitzner, G., Cruz-Jimenez, G. Use of ICP and XAS to determine the enhancement of gold phytoextraction by *Chilopsis linearis* using thiocyanate as a complexing agent. *Anal. Bioanal. Chem*. 2005, 382, 347–352.

[97] Sharma, N. C., Sahi, S. V., Nath, S., Parsons, J. G., Gardea-Torresdey, J. L., Pal, T. Synthesis of plant-mediated gold nanoparticles and catalytic role of biomatrix-embedded nanomaterials. *Environ. Sci. Technol*. 2007, 41, 5137–5142.

[98] Gardea-Torresdey, J. L., Gomez, E., Peralta-Videa, J. R., Parsons, J. G., Troiani, H., Jose-Yacaman, M. *Alfalfa* sprouts: a natural source for the synthesis of silver nanoparticles. *Langmuir,* 2003, 19, 1357–1361.

[99] Haverkamp, R. G., Marshall, A. T., van Agterveld, D. Pick your carats: nanoparticles of gold-silver-copper alloy produced *in vivo*. *J. Nanoparticle Res.* 2007, 9, 697–700.

[100] Narayanan, K. B., Sakthivel, N. Coriander leaf mediated biosynthesis of gold nanoparticles. *Mater. Lett*. 2008, 62, 4588-4590.

[101] Ankamwar, B. Biosynthesis of gold nanoparticles (Green-Gold) using leaf extract of *Terminalia catappa*. *E- J. Chem.* 2010, 7, 1334-1339.

[102] Lopeza, M. L., Parsonsb, J. G., Peralta Videab, J. R., Gardea-Torresdey, T. L. An XAS study of the binding and reduction of Au(III) by hop biomass. *Microchem. J.* 2005, 81, 50–56.

[103] Ghule, K., Ghule, A. V., Liu, J. Y., Ling, Y. C. Microscale size triangular gold prisms synthesized using Bengal gram beans (*Cicer arietinum* L.) extract and $HAuCl_4 \times 3H_2O$: a green biogenic approach. *J. Nanosci. Nanotechnol*. 2006, 6, 3746–3751.

[104] Armendariz, V., Gardea-Torresdey, J. L., Jose-Yacaman, M., Gonzalez, J., Herrera, I., Parsons, J. G. Gold nanoparticles formation by oat and wheat biomasses, in *Proceedings –Waste Research Technology* Conference at the Kansas City, Mariott-Country Club Plaza July30–Aug1 (2002).

[105] Gardea-Torresdey, J. L., Tiemann, K. J., Gamez, G., Dokken, K., Tehuacanero, S., Jose-Yacaman, M. Gold nanoparticles obtained by bioprecipitation from gold (III) solutions. *J. Nanopart. Res*. 1999, 1, 397–404.

[106] Armendariz, V., Herrera, I., Peralta-Videa, J., Jose-Yacaman, M., Troiani, H., Santiago, P., Size controlled gold nanoparticle formation by *Avena sativa* biomass: use of plants in nanobiotechnology. *J. Nanopart. Res*. 2004, 6, 377–382.

[107] Gardea-Torresdey, J. L., Parsons, J. G., Gomez, E., Peralta-Videa J. R., Troiani H. E., Santiago, P., Jose-Yacaman, M. Formation and growth of Au nanoparticles inside live alfalfa plants. *Nano Lett*. 2002, 2, 397–401.

[108] Raju, D., Mehta, U. J., Hazra, S. Synthesis of gold nanoparticles by various leaf fractions of *Semecarpus anacardium* L. tree. *Trees- Strut. Funct.* 2011, 25, 145-151.

[109] Narayanan, K. B., Sakthivel, N. Phytosynthesis of gold nanoparticles using leaf extract of *Coleus amboinicus* Lour. *Mater. Charact*. 2010, 61, 1232-1238.

[110] Ramezani, N., Ehsanfar, Z., Shamsa, F., Amin, G., Shahverdi H. R., Esfahani, H. R. M., Shamsaiea, A., Bazazb, R. D., Shahverdia, A. R. Screening of medicinal plant methanol extracts for the synthesis of gold nanoparticles by their reducing potential. *J. Chem. Sci.* 2008, 63, 903-908.

[111] Vilchis-Nestor, A. R., Sanchez-Mendieta, V., Camacho-Lopez M. A., Gomez-Espinosa, R. M., Camacho-Lopez, M. A, Arenas-Alatorre, J. A. Solvent less synthesis and optical properties of Au and Ag nanoparticles using *Camellia sinensis* extract *Mater. Lett.* 2008, 62, 3, 103-105.

[112] Kasthuri, J., Veerapandian, S., Rajendiran, N. Biological synthesis of silver and gold nanoparticles using apiin as reducing agent. *Colloids Surf. B,* 2009, 68, 55-65.

[113] Kasthuri, J., Kathiravan, K, Rajendiran, N. Phyllanthin-assisted biosynthesis of silver and gold nanoparticles: a novel biological approach. *J. Nanopart. Res.* 2009, 11, 1075- 1085.

[114] Krpetic, Z., Scari, G., Caneva, E., Speranza, G., Porta, F. Gold nanoparticles prepared using cape aloe active components. *Langmuir*, 2009, 25, 7217-7221

[115] Philip, D. Green synthesis of gold and silver nanoparticles using *Hibiscus rosa sinensis. Physica E.* 2009, 42, 1417-1424.

[116] Raghunandan, D., Basavaraja, S., Mahesh, B., Balaji, S., Manjunath, S. Y, Venkataraman, A. Biosynthesis of stable polyshaped gold nanoparticles from microwave-exposed aqueous extracellular anti-malignant guava (*Psidium guajava*) leaf extract. *Nanobiotechnology,* 2009, 5, 34-41.

[117] Song, J. Y., Jang, H. K., Kim, B. S. Biological synthesis of gold nanoparticles using *Magnolia kobus* and *Diopyros kaki* leaf extracts. *Process. Biochem.* 2009, 44, 10, 1133–1138.

[118] Wang, Y., He, X., Wang, K., Zhang, X., Tan, W. Barbated skullcup herb extract-mediated biosynthesis of gold nanoparticles and its primary application in electrochemistry. *Colloids Surf. B,* 2009, 73, 75-79.

[119] Dubey, S. P., Lahtinen, M., Sillanpaa, M. Tansy fruit mediated greener synthesis of silver and gold nanoparticles. *Proc. Biochem.* 2010, 45, 1065-1071.

[120] Singh, A. K., Talat, M., Singh, D. P., Srivastava, O. N. Biosynthesis of gold and silver nanoparticles by natural precursor clove and their functionalization with amine group. *J. Nanopart. Res.* 2010, 12, 1667-1675.

[121] Arulkumar, S., Sabesan, M. Biosynthesis and characterization of gold nanoparticle using antiparkinsonian drug *Mucuna pruriens* plant extract. *Int. J. Res. Pharm. Sci.* 2010, 1, 417-420.

[122] Banka, R. A., Joshi, B., Kumar, A. R., Zinjarde, S. Banana peel extract mediated novel route for the synthesis of silver nanoparticles. *Colloids Surf. A: Physico. Chem. Eng. Asp.* 2010, 80, 58-63.

[123] Castro, L., Blazquez, M. L., Gonzalez, F., Munoz, J. A., Ballester, *A.* Extracellular biosynthesis of gold nanoparticles using sugar beet pulp. *Chem. Eng. J.* 2010, 164, 92-97.

[124] Das, R. K., Borthakur, B. B., Boram, U. Green synthesis of gold nanoparticles using ethanolic leaf extract of *Centella asiatica Mater. Lett.* 2010, 64, 1445-1447.

[125] Dubey, S. P., Lahtinen, M., Sarkka, H., Sillanpaa, M. Bioprospective of *Sorbus aucuparia* leaf extract in development of silver and gold nanocolloids. *Colloids Surf. B,* 2010, 80, 26-33.

[126] Dubey, S. P., Lahtinen, M., Sillanpaa, M. Green synthesis and characterizations of silver and gold nanoparticles using leaf extract of *Rosa rugosa. Colloids Surf. A Physicochem. Eng. Asp.* 2010, 364, 34-41.

[127] Dwivedi, A. D., Gopal, K. Plant-mediated biosynthesis of silver and gold nanoparticles. *J. Biomed. Nanotechnol.* 2011, 7, 163-167.

[128] Gupta, N., Singh, H. P., Sharma, R. K. Single-pot synthesis: Plant mediated gold nanoparticles catalyzed reduction of methylene blue in presence of

stannous chloride. *Colloids Surf. A Physicochem. Eng. Asp*. 2010, 367, 102-107.

[129] Khalil, M. M. H., Ismail, E. H., El-Magdoub, F. Biosynthesis of Au nanoparticles using olive leaf extract *Arab J. Chem.*, in press, doi:10.1016/j.arabjc.2010.11.011

[130] Kumar, P., Singh, P., Kumari, K., Mozumdar, S., Chandra, R. A green approach for the synthesis of gold nanotriangles using aqueous leaf extract of *Callistemon viminalis*. *Mater. Lett*. 2011, 65, 595.

[131] Leonard, K., Ahmmad, B., Okamura, H., Kurawaki. *In situ* green synthesis of biocompatible ginseng capped gold nanoparticles with remarkable stability. J. *Colloids Surf. B*, 2011, 82, 391-396.

[132] Philip, D., Unni, C. Extracellular biosynthesis of gold and silver nanoparticles using *Krishna tulsi* (*Ocimum sanctum*) leaf. *Physica E*. 2011, 43, 1318-1322.

[133] Philip, D., Unni, C., Aromal, S. A, Vidhu, V. K. *Murraya koenigii* leaf-assisted rapid green synthesis of silver and gold nanoparticles *Spectrochim Acta A Mol. Biomol. Spectrosc.* 2011, 78, 899-904.

[134] Sheny, D. S., Mathew, J., Philip, D. Phytosynthesis of Au, Ag and Au-Ag bimetallic nanoparticles using aqueous extract and dried leaf of *Anacardium occidentale. Spectrochim Acta A Mol. Biomol. Spectrosc.* 2011, 79, 254-262.

[135] Ghule, K., Ghule, A. V., Liu, J. Y., Ling, Y. C. Microscale size triangular gold prisms synthesized using Bengal gram beans (*Cicer arietinum* L.) extract and HAuCl$_4$x3H$_2$0: a green biogenic approach. *J. Nanosci. Nanotechnol*. 2006, 6, 3, 746-751.

[136] Ghodake, G. S., Deshpande, N. G., Lee, Y. P., Jin, E. S. Pear fruit extract-assisted room-temperature biosynthesis of gold nanoplates. *Colloids Surf. B,* 2010, 75, 584-589.

[137] Gardea-Torresdey, J. L., Gomez, E., Peralta-Videa J. R., Parsons, J. G., Troiani, H., Jose-Yacaman M. *Alfalfa* sprouts: a natural source for the synthesis of silver nanoparticles. *Langmuir,* 2003, 19, 1357–1361.

[138] Zeng, F., Hou, C., Wu, S., Liu, X., Tong, Z., Yu, S. Silver nanoparticles directly formed on natural macroporous matrix and their antimicrobial activities. *Nanotechnology,* 2007, 18, 1–8.

[139] Li, S., Shen, Y., Xie, A., Yu, X., Qiu, L., Zhang, L., Zhang, Q. Green synthesis of silver nanoparticles using *Capsicum annuum* L. extract. *Green Chem.* 2007, 9, 852–858.

[140] Sathyavathi, R., Krishna, M. B. M., Rao, D. N. Biosynthesis of silver nanoparticles using *Moringa oleifera* leaf extract and its application to optical limiting. *J. Nanosci. Nanotechnol.* 2011, 11, 2031-2035.

[141] Narayanan, K. B., Sakthivel, N. Extracellular synthesis of silver nanoparticles using the leaf extract of *Coleus amboinicus* Lour. *Mater. Res. Bull.* 2011, 46, 1708-1731.

[142] Kaviya, S., Santhanalakshmi, J., Viswanathan, B., Muthumary, J., Srinivasan, K. Biosynthesis of silver nanoparticles using *Citrus sinensis* peel extract and its antibacterial activity *Spectrochim. Acta A Mol. Biomol. Spectrosc.* 2011, 79, 594-598

[143] Prabhu, N., Divya, R. T., Yamuna, G. K., Ayisha, S. S. Joseph, P. I. D. Synthesis of silver phyto nanoparticles and their antibacterial efficacy *Digest J. Nanomater. Bionanostruct.* 2010, 5, 185-189.

[144] Saxena, A., Tripathi, R. M., Singh, R. P. Biological synthesis of silver nanoparticles by using onion *Allium cepa* extract and their antibacterial activity. *Digest J. Nanomater. Bionanostruct.* 2010, 5, 427-432.

[145] Govindaraju, K., Tamilselvan, S., Kiruthiga, V., Singaravelu, G. Biogenic silver nanoparticles by *Solanum torvum* and their promising antimicrobial activity *J. Biopesticides* 2010, 3, 394-399.

[146] Mahitha, B., Raju, D. P., Dillip, G. R., Reddy, C. M., Mallikarjuna, K., Manoj, L. Biosynthesis, characterization and antimicrobial studies of AgNPs extract from *Bacopa monniera* whole plant. *Digest J. Nanomater. Biostruct.* 2011, 6, 135-142.

[147] Ray, S., Nath, S. K., Kumar, A., Agarwala, R. C., Agarwala, V., Chaudhari, G. P., Daniel, B. S. S. Biological synthesis of Ag nanoparticles through i*n vitro* cultures of *Brassica juncea* C. zern. *Adv. Mat. Res*. 2009, 67, 295-299.

[148] Song, J. Y., Kim, B. S. Rapid biological synthesis of silver nanoparticles using plant leaf extracts. *Bioprocess Biosyst. Eng*. 2009, 32, 79.

[149] Maensiri, S., Laokul, P., Klinkaewnarong, J., Phokha, S., Promarak, V., Seraphin, S. Indium oxide (In_2O_3) nanoparticles using *Aloe vera* plant extract: Synthesis and optical properties. *J. Optoelec. Adv. Mater*. 2008, 10, 161-165.

[150] Song, J. Y., Kwon, E, Y., Kim, B. S. Biological synthesis of platinum nanoparticles using *Diopyros kaki* leaf extract. *Bioprocess Biosyst. Eng*. 2010, 33, 159–164.

[151] Ahmad, A., Senapati, S., Khan, M. I., Kumar, R., Sastry, M. Extracellular biosynthesis of monodisperse gold nanoparticles by a novel extremophilic actinomycete, *Thermomonospora* sp. *Langmuir,* 2003, 19, 3550-3553.

[152] Ahmad, A., Senapati, S., Khan, M. I., Ramani, R., Srinivas, V., Sastry, M. Intracellular synthesis of gold nanoparticles by a novel alkalotolerant actinomycete *Rhodococcus* species. *Nanotechnology,* 2003, 14, 824–828.

[153] Usha, R., Prabu, E., Palaniswamy, M., Venil, C. K., Rajendran, R., Synthesis of metal oxide nano particles by *Streptomyces s*p. for development of antimicrobial textiles. *Global. J. Biotech. Biochem.* 2010, 5, 153-160.

[154] Lin, Z., Wu, J., Xue, R., Yang, Y. Spectroscopic characterization of Au^{3+} biosorption by waste biomass of *Saccharomyces cerevisiae Spectrochim. Acta A Mol. Biomol. Spectrosc.* 2005, 61, 761-766.

[155] Gericke, M., Pinches, A. Biological synthesis of metal nanoparticles. *Hydrometallurgy,* 2006, 83, 132–140.

[156] Agnihotri, M., Joshi, S., Kumar, A. R., Zinjarde S., Kulkarni, S. Biosynthesis of gold nanoparticles by the tropical marine yeast *Yarrowia lipolytica* NCIM 3589 *Mat. Lett*. 2009, 63, 1231-1234.

[157] Kowshik, M., Ashtaputre, S., Kharrazi, S., Vogel, W., Urban, J., Kulkarni, S. K., Paknikar, K. M. Extracellular synthesis of silver nanoparticles by a silver-tolerant yeast strain MKY3. *Nanotechnology,* 2003, 14, 95-100.

[158] Kowshik, M., Vogel, W., Urban, J., Kulkarni, S. K., Paknikar, K. M. Microbial Synthesis of Semiconductor PbS Nanocrystallites. *Adv. Mater.* 2002 14, 815-818.

[159] Jha, A. K., Prasad, K., Prasad, K. A green low-cost biosynthesis of Sb_2O_3 nanoparticles. *Biochem. Eng. J.* 2009, 43, 303-306.

[160] Kowshik, M., Deshmukh, N., Vogel, W., Urban, J., Kulkarni, S. K., Paknikar, K. M. Microbial synthesis of semiconductor CdS nanoparticles, their characterization, and their use in the fabrication of an ideal diode *Biotechnol. Bioeng.* 2002, 78, 583-588.

[161] Dameron, C. T., Reese, R. N., Mehra, R. K., Kortan, A. R., Carroll, P. J., Steigerwald, M. L., Brusl, L., Winge, E. D. R. Biosynthesis of cadmium sulphide quantum semiconductor crystallites. *Nature,* 1989, 338, 596-597.

[162] Singaravelu, G., Arockiamary, J. S., Kumar, V. G., Govindaraju, K., A novel extracellular synthesis of monodisperse gold nanoparticles using marine alga, *Sargassum wightii Greville. Colloids Surf. B,* 2007, 57, 97-101.

[163] Senapati, S., Syed, A., Moeez, S., Kumar, A., Ahmad, A. Intracellular synthesis of gold nanoparticles using alga *Tetraselmis kochinensis. Mat. Let.* 79, 15, 2012, 116–118

[164] Lengke, M. F., Fleet, M. E., Southam, G., Synthesis of palladium nanoparticles by reaction of filamentous cyanobacterial biomass with a palladium (II) chloride complex. *Langmuir,* 2007, 23, 8982-8987.

[165] Slocik, J. M., Knecht, M. R., Wright, D. W. Biogenic nanoparticles. In: Nalwa, H.S. (eds) *The Encyclopedia of Nanosci. Nanotechnol.* American Scientific Publishers, Stevenson Ranch, CA, 2004, pp 293-308.

[166] Scarano, G., Morelli, E. Properties of phytochelatin-coated CdS nanocrystallites formed in a marine phytoplanktonic alga (*Phaeodactylum tricornutum*, Bohlin) in response to Cd. *Plant Sci*. 2003, 165, 803–810.

[167] Raveendran, P., Fu, J., Wallen, S. L, Completely "green" synthesis and stabilization of metal nanoparticles. *J. Am. Chem. Soc*. 2003, 125, 13940–13941.

[168] Xie, J., Lee, J. Y., Wang, D. I. C., Ting, Y. P. Identification of active biomolecules in the high-yield synthesis of single-crystalline gold nanoplates in algal solutions. *Small,* 2007, 3, 4, 672 – 682.

[169] Feng, Y., Yu, Y., Wang, Y., Lin, X. Biosorption and bioreduction of trivalent aurum by photosynthetic bacteria *Rhodobacter capsulatus. Curr. Microbiol.* 2007, 55, 402-408.

[170] Kumar, S. A., Abyanehm M. K., Gosavi. S. W., Kulkarni, S. K., Ahmad, A., Khan, M. I. Sulfite reductase-mediated synthesis of gold nanoparticles capped with phytochelatin *Biotechnol. Appl. Biochem.* 2007, 47, 191-195.

[171] Shahverdi, A. R., Minaeian, S., Shahverdi, H. R., Jamalifar, H., Nohi, A .A. Rapid synthesis of silver nanoparticles using culture supernatants of Enterobacteria: a novel biological approach. *Proc. Biochem.* 2007, 42, 919-923.

[172] Kumar, A. S., Abyaneh, M. K., Gosavi, S. W., Kulkarni, S. K., Pasricha, R., Ahmad, A. Nitrate reductase-mediated synthesis of silver nanoparticles from AgNO$_3$. *Biotechnol. Lett*. 2007, 29, 439-445.

[173] Gade, A. K., Bonde, P. P., Ingle, A. P., Marcato, P., Duran, N., Rai, M. K. Exploitation of *Aspergillus niger* for synthesis of silver nanoparticles. *J. Biobased Mater. Bioenergy.* 2008, 2, 243-247.

[174] Shaligram, N. S., Bule, M., Bhambure, R., Singhal, R. S., Singh, S. K., Szakacs, G., Pandey, A. Biosynthesis of silver nanoparticles using aqueous extract from the compactin producing fungal strain *Proc. Biochem.* 2009, 44, 939- 943.

[175] Hunter, W., Manterm, D. Bio-Reduction of Selenite to Elemental Red Selenium by *Tetrathiobacter kashmirensis. Curr. Microbiol*. 2008, 57, 83-88.

[176] Govender, Y., Riddin, T. L., Gericke, M., Whiteley, C. G. On the enzymatic formation of platinum nanoparticles. *J. Nanopart. Res*. 2010, 12, 261-271.

[177] Duran, N., Marcato, D. P., De Souza, H. I., Alves, L. O., Espsito, E. Antibacterial effect of silver nanoparticles produced by fungal process on textile fabrics and their effluent treatment. *J. Biomed. Nanotechnol.* 2007, 3, 203-208.

[178] Klaus, T., Joerger, R., Olsson, E., Granqvist, C. G. Bacteria as workers in the living factory: metal-accumulating bacteria and their potential for materials science. *Trends Biotechnol.* 2001, 19, 15–20.

[179] Joerger, R., Klaus, T., Olsson, E., Granqvist, C. G. Spectrally selective solar absorber coatings prepared by a biomimetic technique. *Proc. Soc. Photo-Opt Instrum. Eng*. 1999, 3789, 2–7.

[180] Schultz, S. Single-target molecule detection with nonbleaching multicolor optical immunolabels. *Proc. Natl. Acad. Sci. U. S. A*. 2000. 97, 3, p. 996-1001.

[181] Tkachenko, A. G. Multifunctional gold nanoparticle-peptide complexes for nuclear targeting. *J. Am. Chem. Soc.* 2003. 125, 4700-4701.

[182] Cao, Y. W., Jin, R., Mirkin, C. A. DNA-modified core-shell Ag/Au nanoparticles. *J. Am. Chem. Soc*. 2001. 123, 32, 7961-7962.

[183] Feldherr, C. M., Lanford, R. E., Akin, D. Signal-mediated nuclear transport in simian-virus 40- transformed cells is regulated by large tumor-antigen. *Proc. Natl. Acad. Sci. U. S. A*. 1992. 89, 11002-11005.

[184] Mukherjee, P., Bhattacharya, R., Bone, N., Lee, Y.K., Patra, C. R. Wang, S. Potential therapeutic application of gold nanoparticles in B-chronic lymphocytic leukemia (BCLL): enhancing apoptosis. *J. Nanobiotechnol*. 2007, 5(4), 1-13.

[185] Bangs, L. B. New developments in particle-based immunoassays: introduction. *Pure. Appl. Chem*. 1996, 68, 1873–1879.

[186] Chen, A. A., Derfus, A. M., Khetani, S. R, Bhatia, S. N. Quantum dots to monitor RNAi delivery and improve gene silencing. *Nucleic Acids Res*. 2005, 33, 190.

[187] Torney, F., Trewyn, B. G, Lin V. Y Wang, K. Mesoporous silica nanoparticles deliver DNA and chemicals into plants. *Nat. Nanotechnol*. 2, 2007-295-300.

[188] Gonzalez-melendi, P., Fernandez-pacheco, R., Coronado, M. J., Corredor, E., Testillano, P. S., Risueno, M. C., Marquina, C., Ibarra, M. R., Rubiales, D., Pe rez-de-luque, D. Nanoparticles as smart treatment-delivery systems in plants: assessment of different techniques of microscopy for their visualization in plant tissues. *Ann. Bot*. 2008, 101, 187–195.

[189] Elechiguerra, J. L., Burt, J. L., Morones, J. R., Camacho-Bragado, A., Gao, X. Lara, H. H. Interaction of silver nanoparticles with HIV-1. *J. Nanobiotechnol*. 2005, 3, 6.

[190] Becker, R. O. Silver ions in the treatment of local infections. *Met. Based Drugs*. 1999, 6,311-314

Chapter 2

Studies on Cu and Mn accumulation by plants growing on mine areas, leaching of metals from plants and converting to nanoparticles.

Summary:

This chapter describes the metal accumulation studies by plants growing at different mines (copper and manganese) and different locations alongwith accumulation of metals in different parts of the plants. *Prosopis juliflora* and *Ailanthus excelsa* plants growing at Khetri mine showed higher accumulation of Cu in leaves which was 42 times more than that shown by the control plant grown in normal land. *Holoptelia integrifolia* plant growing in Gumgaon (Maharashtra, India) mine area accumulated 19 times more Mn than control plant. These metals (Cu / Mn) were leached from the leaves of the plants which accumulated high amounts of metal by using *Fusarium oxysporum* and were converted to nanoparticles. The leached Cu nanoparticles were of 5-10 nm and Mn particles were 200-300 nm in size.

Section 1 & 2
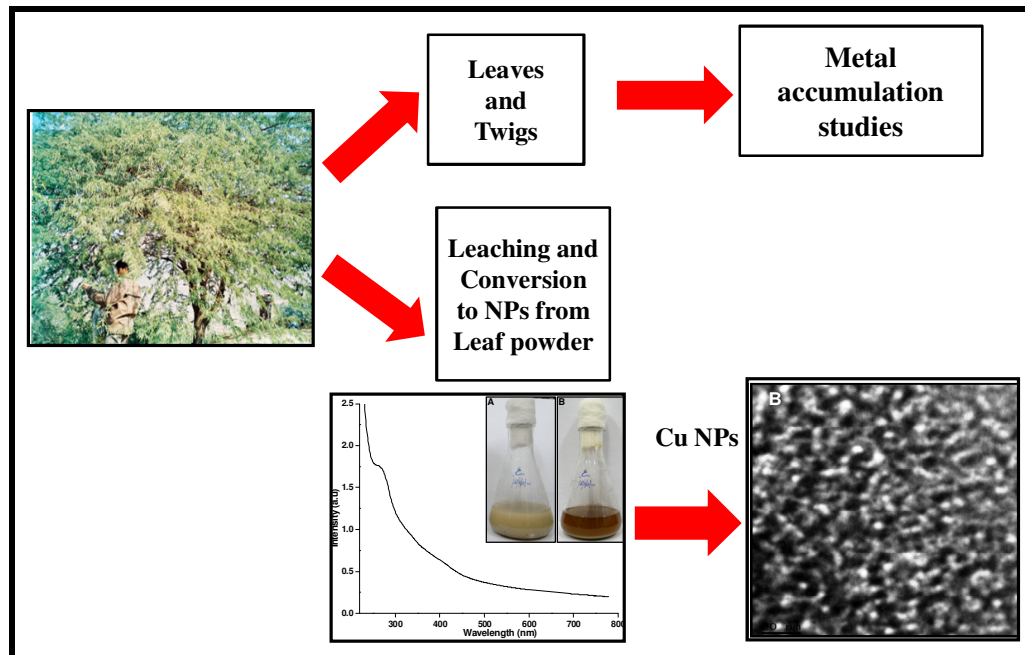
Section 1

2.1 Natural accumulation of copper and distribution of metals in plants growing in copper mining areas.

2.1.1 Introduction

The term heavy metals include those elements having its density above 5 gm cm^{-3}. Metals which are released into the environment with an increasing rate through processes like mining, industrialization, agriculture, etc. cause serious problems to the environment and health [1]. Mining, in particular the metal ore extraction is the second source of heavy metal contamination in soil after sewage sludge in India [2].

Phytoremediation is a sustainable technology for removal of metals from soil by using plants, which is relatively inexpensive [3, 4]. Phytoremediation strategies for metals are stabilization and accumulation [4]. Phytostabilization of metals may employ plants to reduce leaching, runoff and erosion via stabilization of soil by plant roots, or metals may be transferred to less toxic forms [5]. Accumulation of metal in shoot tissue, followed by harvesting shoot biomass is called phytoextraction [6]. The harvested plant tissue can be used for non-food purposes, they can be ashed and used by recycling the metals or disposal in land fill [7].

Most experimental studies of heavy metal tolerance confirm that populations growing in metal contaminated habitats are different from population growing from clean sites of the same species by possessing genetically based tolerance [8]. Some plants that grow on naturally metal contaminated soils may adapt and develop to survive and accumulate greater concentration of heavy metals in their shoots than other plant species [9].

Over the past 10 years, woody plants have shown to be excellent candidates for the purpose of phytoremediation, due to rapid growth, high biomass, profuse root apparatus and low impact on food chain and human health [4, 10]. Majority of such work concerns accumulation capacity and biomass production of woody plants as a response to high concentration of pollutants [11]. Phytoremediation using trees provides a potential opportunity to extract or stabilize metals. It involves the use of trees that readily transport targeted metals from soil to plant organs, which allows

removal of metal by harvesting the plant part. This process takes a long time but simultaneously helps in greening of land and reducing pollution [12]. However, there is need to identify trees having the ability to uptake and translocate the metal to the aerial parts. This ability of translocation from the polluted soil to their above ground tissues was studied in five woody species including *Alnus, Fraxinus, Sorbus, Salix* and *Betula* [13]. In a recent study [14], interaction of calcium with copper and cadmium accumulation in roots and stem of Norway spruce (*Picea abies* L.) has been demonstrated.

There are evidences that plants such as *Silene armeria* [15], *Typha latifolia* [16], *Salix viminalis* [13], *Juncus conglomerates* [17] grown on metal enriched soil can accumulate high amount of heavy metals in their tissues. In Rakha mine area, Jharkhand, (India) there are several abandoned Cu-tailing ponds that causing severe metal pollution to the nearby areas. The concentration of Cu, Ni, Mn, Zn, Pb and Cd was examined in the above and underground tissues of 5 naturally growing plant species [18]. The study on differential accumulation of Mn in three mature tree species (Holoptelia, Cassia and Neem) growing on mine tailing of Gumgaon, Nagpur showed that Holoptelia accumulates high amount of Mn in its leaves [19]. It has been shown that *Prosopis* plants accumulated higher amounts of Fe, Mn, Cu, Zn and Cr in various fly ash amendments than in garden soil. This shows the potential of *P. juliflora* to grow in plantations on fly ash landfills and also to reduce the metal contents of fly ash by bioaccumulation in its tissues [20]. The use of *P. juliflora* for the biorecovery of aluminium from urban industrial sites of Coimbatore was reported by Thangaval *et al.* (2000) [21]. Senthilkumar *et al.* (2005) [22] suggested the use of *P. juliflora* to decontaminate heavy metal polluted soil in view of its ability to accumulate various heavy metals such as Cd, Cu, Ni, Cr and Al. Recently, Varun *et al.* (2011) [23] have also shown that *Prosopis juliflora* has a good phytoextraction potential demonstrated by the accumulation of Cd and Pb under natural conditions.

Copper (Cu) is a major contaminant which is released into the environment by different anthropogenic activities, e.g. from bactericidal, fungicidal and industrial waste [24]. Cu is both, a micronutrient for plants as well as a heavy metal capable of stress induction [25]. This trace element plays important role in CO_2 assimilation, ATP synthesis and is a component of various proteins, particularly those involved in both, the photosynthetic (plastocyanin) and the respiratory (cytochromeoxidase)

electron transport chain [26]. The uptake of Cu from soil by plant depends on the ability of the plants to transfer the metal across the soil–root interface and the total amount of Cu present in the soil [27]. Excessive amount of Cu in soil plays cytotoxic role induces stress and can cause damage and symptoms in plants including growth retardation and leaf chlorosis [28, 29, 30].

The present study was carried out on *Prosopis juliflora* plants growing in different locations of Khetri mining sites, a single tree of *Ailanthus excelsa* growing at Khetri and *Prosopis* plants seen growing in Kolihan mining area. A study was conducted to generate information on Cu accumulation and distribution of other metals like Mn, Zn and Fe, in aerial parts of *Prosopis juliflora* from both the mines and *Ailanthus excelsa* from Khetri mine.

2.1.2 Experimental Details

2.1.2.1 Sample collection:

The Khetri and Kolihan underground mines of Khetri Copper Complex (KCC) which come under Hindustan Copper Limited are located in Rajasthan. KCC is in the cradle of Aravelly hills in district Jhunjhunu, Rajasthan which is about 190 km southwest of Delhi and 180 km north Jaipur (27°59′N 75°48′E). KCC has two well developed townships at Khetri- Nagar and Kolihan. Plants, including *Prosopis juliflora* and *Ailanthus excelsa* growing naturally at Khetri mine and *Prosopis juliflora* at Kolihan mine, Rajasthan, India were identified based upon morphology, etc. (Fig. 2.1).
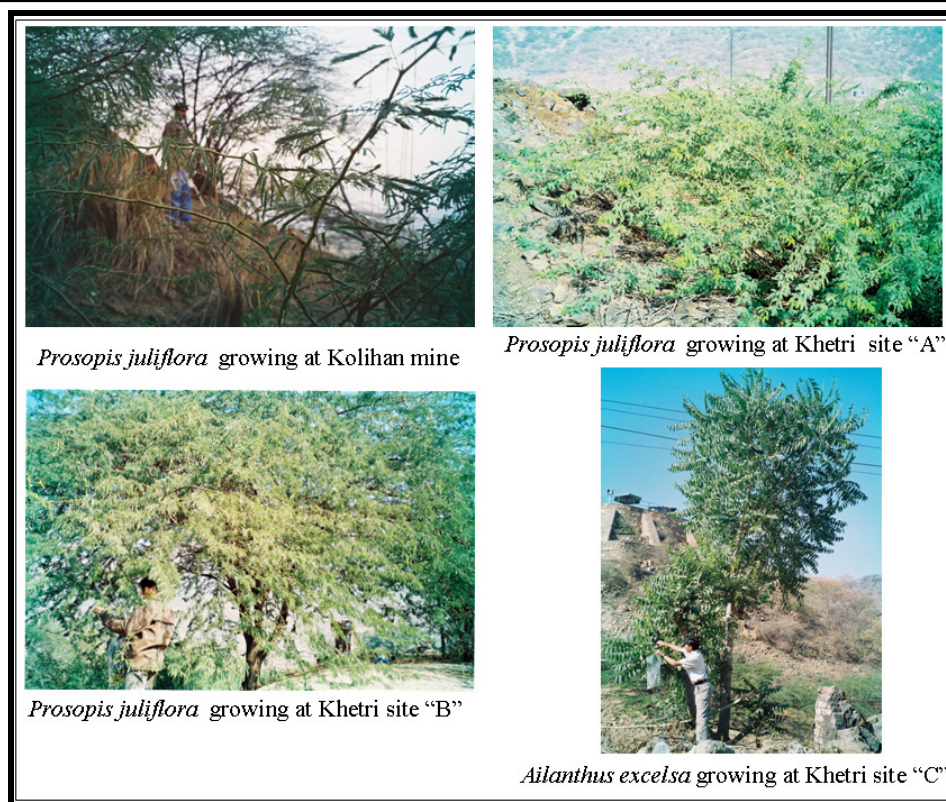
Figure 2.1: Plants growing at Kolihan and different locations of Khetri Copper mines.

A single *Ailanthus excelsa* tree was seen growing at Khetri mining area, whereas several plants of *Prosopis juliflora* could be seen growing naturally at both the mining areas. The leaf and twig samples of *Prosopis juliflora* were collected from different locations of Khetri mine. The area near the temple "Mata mandir" was named as "A" and the place where the explosive waste material was dumped was named as "B". In another area near Mata mandir, the only tree growing was *Ailanthus excelsa* near trolley used for carrying crude ore for smelting and refining purpose. This was named as site "C". These samples were compared with the samples obtained from *Prosopis juliflora* and *Ailanthus* sp. growing in metal contamination-free soil (control), near National Chemical Laboratory (NCL), Pune. We collected soil samples from the different sites at a depth of 10 cm where plants were growing and compared them with the soil where *Prosopis juliflora* and *Ailanthus* sp. were growing. Assessment of metal content in natural vegetation in mining areas and in contamination-free soil was done. Sampling was carried out in a randomized design. *Ailanthus excelsa* at Khetri site "C" was seen growing on heaps of waste dumps left after the metal extraction from ore. Due to difficulty in obtaining soil sample from there, the data of soil from

the nearest site "A" was taken for further studies. Copper tailings were disposed in slurry impoundments. At this place no habitat was observed.

2.1.2.2 Soil and plant analysis:

Soil samples were collected from both mines from different places and for control soil; sample was taken from NCL, (Pune, India). The soil samples were dried at 100°C for two days and ground to a fine powder with mortar and pestle. Dust accumulated on the surface of the leaves and twigs was removed by washing thoroughly with tap water. This was followed by thorough washing of the samples with deionized water. The samples were then dried on a filter paper to eliminate adhering moisture from the surface. The same process was repeated for the control leaves and twigs of all plants. Fresh leaves and twigs were taken (1–3 g) in pre-weighed glass beakers of 50 mL volume. Fresh weights of the tissues were determined from the difference in the weights. Samples were dried in an oven at 100°C and weighed intermittently until constant weight was observed. Dried plant materials were ground in mortar and pestle to a fine powder for metal analysis.

An amount of 150 mg of finely powdered plant tissues and soil was taken separately in Borosil vials. This was digested with 3 mL of Nitric acid and 1 mL of 70% perchloric acid on a hot plate under the hood. The volume of digested sample solution was made to 10 mL with deionized water. Metal content in analytes was determined using Atomic Absorption Spectroscopy (Perkin Elmer 1100B). Metal content was calculated and expressed in $\mu g\ g^{-1}$ of dry tissue [31]. The values were expressed as mean ± standard deviation (SD) of three replicates. The data was subjected to ANOVA (Analysis of Variance) at a significance level of P<0.01 and P<0.05.

Metal accumulation by plants can be evaluated using a simple index termed, Transfer Coefficient (TC). The Transfer Coefficient is calculated by dividing the concentration of a metal in the plant by the total metal concentration in the soil [32].

2.1.3 Results and discussion

2.1.3.1 Cu accumulation study:

Among the soil samples collected, high amount of Cu was found at Khetri tailing dam (Table 1) where the waste leftover after recovery of Cu from the ore was dumped. Absence of vegetation was noted at this site. The next high amount of Cu metal was found at site "A" followed by "B" where *Prosopis juliflora* plants were growing. When compared with the control soil, the ratio of Cu was 1:9 in tailing dam, 1:8 at site "A" and 1:3 at site "B" of Khetri mine. In the soil of Kolihan mine the ratio of Cu content was 1:3. The plants of *Prosopis* at Kolihan mine, *Prosopis* and *Ailanthus* at Khetri mine were growing in soil containing high Cu content. The permissible limit of Cu in India is 135 to 270 mg kg^{-1} [33]. The Cu content in mine area soil shows that it is above the permissible limit (Table 2.1).

Table 2.1: Analysis of metals in soils of different mine sites as compared to control.

Metal	NCL (Control) (µg g^{-1}) (Mean ± SD)	Kolihan Mine (µg g^{-1}) (Mean ± SD)	Khetri Tailing Dam (µg g^{-1}) (Mean ± SD)	Khetri Site "A" (µg g^{-1}) (Mean ± SD)	Khetri Site "B" (µg g^{-1}) (Mean ± SD)
Cu	216.95 ± 83.67	594.31 ± 9.70[*]	2059.05 ± 169.75[*]	1840.95 ± 120.45[*]	715.27 ± 40.48[*]
Mn	66.59 ± 10.47	172.63 ± 22.6[*]	404.45 ± 45.2[*]	133.17 ± 14.8[**]	611.58 ± 47.59[*]
Zn	160.99 ± 27.8	164.92 ± 7.86[†]	445.03 ± 32.7[*]	83.77 ± 4.53[†]	212.04 ± 28.3[†]
Fe	14721.57±233.6	23855.23 ± 586.12[**]	26980.66 ± 236.5[†]	31420.22 ± 228.3[†]	17207.09 ± 609.7[†]

ANOVA carried out using 3 replicates of samples.
SD Standard Deviation
[*] Significant at P<0.01
[**] Significant at P<0.05
[†] Non-significant

In the present study, Cu content in the leaves collected from all the mine sites was higher than that collected from the control sites (Fig. 2.2). The leaf samples collected from Khetri mines particularly showed maximum Cu accumulation, among which the leaf samples collected from location "A" and "B" accumulated significantly higher amount of Cu. However, in Kolihan mines, the plants displayed low Cu accumulation in leaf tissues, probably due to the plants growing in less Cu containing soil. The Cu content was less in the soil of Kolihan mine area than Khetri, hence the metal uptake by plant was also low.
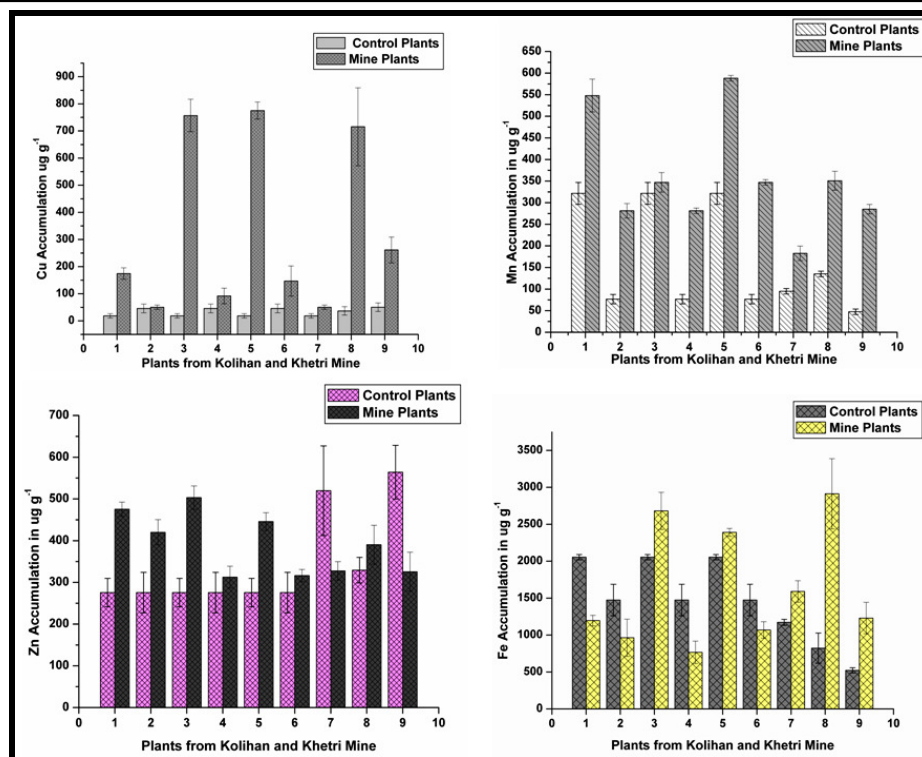
Figure 2.2: Accumulation of Cu and distribution of other metals (Mn, Zn, Fe) in plants growing at Kolihan, Khetri mine and controls. (**1**) Kolihan *Prosopis julifera* leaf, (**2**) Kolihan *Prosopis* twigs, (**3**) Khetri Site "A" Prosopis leaf, (**4**) Khetri Site "A" *Prosopis* twigs, (**5**) Khetri Site "B" *Prosopis* leaf, (**6**) Khetri Site "B" Prosopis twigs, (**7**) Khetri "B" site *Prosopis* Green Pods, (**8**) Khetri Site "C" *Ailanthus excelsa* leaf, (**9**) Khetri Site "C" *Ailanthus* twigs.

Twigs also showed a similar pattern of higher Cu accumulation in samples collected from the mine dumps when compared to controls, although the capacity for Cu accumulation was lower than the respective leaf samples. Variable contents of Cu have been noticed among the twigs with respect to mine locations. However, in *Ailanthus* tree species grown in Khetri mine site "C" the twigs contained significantly higher amount of Cu when compared to those from control and *Prosopis* growing at different mine sites. The maximum accumulation of Cu (775.29 μg g^{-1}) with respect to leaf tissue was observed in "B" site. The least accumulation of Cu was in green pod of *Prosopis juliflora* growing at site "B" (50.46 μg g^{-1}). When compared with controls, the leaves of *Prosopis juliflora* accumulated more Cu (1: 42.2 times) at site "B", 1: 41.2 times at site "A and leaves of *Ailanthus* growing at site "C" accumulated 1: 19.5 times more. In *Prosopis* leaves at Kolihan mine the ratio of Cu content was 9.5 times. The green pods from *Prosopis* growing at site "B" accumulated 1: 2.75 times higher Cu content.

In case of twigs, highest amount of Cu was noticed in *Ailanthus*. The leaves of *Prosopis juliflora* were found to be highly efficient in Cu accumulation, as compared to twigs (8 and 5 times, respectively in site "A" and "B"), 3.45 times higher in leaves than twigs of *Prosopis* plant growing at Kolihan mines. Leaves of *Ailanthus* accumulated 2.73 times higher amount of Cu than the twigs. The Cu accumulation was found to be higher in leaf tissues when compared to that in twigs in all the mine sites studied. In Kolihan mine, the accumulation rate was less than at Khetri mine.

In literature, the highest concentration of Cu was found in the leaves of *Rumex acetosa* ranging from 340 to 1102 mg kg^{-1} and averaging 601 mg kg^{-1}. Kelepertsis and Andrulakis (1983) [34] have reported a maximum of 800 mg kg^{-1} Cu in *Rumex acetosella*. Most of the samples in literature have Cu concentrations ranging from 230 to 400 mg kg^{-1} in the species. It is to be noted that Cu, a component of enzymes, is an essential element for plant growth but causes toxicity when shoots or leaves accumulate more than 20 mg kg^{-1} [35]. The plant samples collected in the present study, from different mines and locations, accumulated more than 20 mg kg^{-1}. The Cu concentration ranged from 50.46 to 775.29 μg g^{-1} in samples from the mine areas, whereas in control it was 18.35 to 50.46 μg g^{-1}. The highest amount of Cu was 775.29 μg g^{-1}. The high amount of Cu found in leaf samples of mining sites suggests the uptake of metal by plant through roots and transportation to leaves. The twig samples from mining sites showed less amount of Cu. It was not more than 3.2 times than its control. In case of control sample of all the plants, Cu content was higher in twigs than the leaves. The amount of Cu is mostly utilized in leaves as it is used by plastocyanin in photosynthesis, Cytochrome *c* oxidase in respiration [36]. This could be the possible reason for less amount of Cu in leaves than twigs of control plants.

2.1.3.2 Distribution of other metals (Mn, Zn and Fe):

The distribution of other metals (Mn, Zn and Fe) was also studied in the soil of Cu mining areas. Manganese (Mn) is an essential micronutrient and an activator for enzymes involved in tricarboxylic acid cycle [37]. Mn content in the soil of Khetri at different sites and Kolihan mine is shown in Table 2.1. In control soil, the Mn content was 66.59 μg g^{-1}. When compared with the control soil, the ratio was 1: 6 in tailing dam, 1: 2 in Khetri site "A", and 1:9 in site "B". In Kolihan mine, the ratio of Mn content was 1: 2. The permissible limit of Mn was not available but, the range in

uncontaminated soil of India is between 100 to 4000 mg kg^{-1} [38]. Content of Mn in Khetri Cu mine area soil shows that it is within permissible limits.

The amount of Mn present in leaves and twigs of *Prosopis juliflora* growing in the surrounding areas of NCL is shown in (Fig. 2.2). The control leaves accumulated more amount of Mn than the twig samples of *Prosopis* and *Ailanthus*. Significant content of Mn was observed in leaves of *Prosopis* plants growing at both the mines, highest being at Khetri site "B" and Kolihan mine, followed by Khetri site "A" but it was less than the Cu content. In twigs, the amount of Mn was less than the leaves. The green pods of *Prosopis* at site "B" accumulated 182.68 μg g^{-1} whereas in control it was 94.99 μg g^{-1}, this shows the transl;ocation of Mn to other parts of the plant.

Twigs accumulated more Mn than leaves when compared with their respective controls. Twigs of *Ailanthus* growing in Khetri site "C" accumulated 6 times higher Mn than the controls followed by the twigs of *Prosopis* growing in Khetri site "B" (4.52 times) and site "A" (3.66 times) and also to those plants growing in Kolihan mine (3.6 times). The content of Mn was more in leaves, but when compared with control, the twigs had more amount of Mn. In comparison to the controls, higher amount of Mn was found in *Ailanthus excelsa* twigs than in *Prosopis*.

Mn concentration in the range of 20-300 mg kg^{-1} in plant is considered as normal by Kabata-Pendias and Pendias (1992) [39]. The Mn concentration ranged from 182.68 to 588.25 μg g^{-1} in plant samples from mine areas, whereas in control it was 47.49 to 321.53 μg g^{-1}. Mn content was found to be more in leaves than in twigs. The leaves of all the plants of Cu mines showed higher accumulation of Mn than the normal range. In other parts it is in normal range whereas the *Prosopis* twigs of Khetri site "B" and control leaves of *Prosopis* are slightly higher than normal limits.

More amount of Zinc (Zn) was found in the soil of tailing dam (Table 2.1) followed by that at Khetri site "B" and Kolihan mine. Site "A" of Khetri mine has least amount of Zn content. The ratio of Zn content when compared with the control soil was 1: 2.8 in tailing dam, 1: 0.5 at site "A", 1:1.3 at site "B" of Khetri mine. In Kolihan mine, Zn content was almost same as that of the control. The permissible limit of Zn in India is 300 to 600 mg kg^{-1} [33]. The Zn metal concentration of all the soils of both mines fall in the normal limit.

The amount of Zn present in *Prosopis juliflora* growing in the area around NCL and plants growing at Cu dump site were compared (Fig. 2.2). The amount of Zn was more in leaves than twigs. In green pods of *Prosopis juliflora*, Zn content was less than its control. The amount of metal in *Prosopis* twigs of dump site was more than its control. It was more in Kolihan mine followed by almost similar amount in twigs of plants growing at site "A" and "B". In green pods of *Prosopis*, Zn content was less in dump site than control while it was similar to that in case of *Ailanthus* twigs. When compared with control, the ratios of Zn content in *Prosopis juliflora* leaves was 1.8 and 1.6 times more at site "A" and "B, respectively. The Zn content in the twigs of *Prosopis* growing at Khetri site "A" and "B" was similar to that of control. In *Ailanthus excelsa* leaves of Khetri site "C", Zn accumulation was 1.18 times while *Ailanthus* twigs did not accumulate more Zn than the control. In Kolihan mine, Zn content was 1.7 times more in the *Prosopis* leaves than its control while in twigs it was 1.52 time high. In the dump samples, the Zn content of leaves was more than twigs in both *Prosopis* and *Ailanthus*, while in control samples twigs had more Zn content than the leaves of *Ailanthus*.

Zinc is an essential element which is divalent cation and acts as co-factor of enzymes in plants [40]. The normal level of Zn is 20-400 mg kg^{-1} as reported by Reeves and Baker (2000) [41]. The highest content of Zn in plants growing at Cu mine site was 312.61 to 475.40 $\mu g\ g^{-1}$. In all the plants, content of Zn was within normal range except leaf samples of *Prosopis* of Kolihan and Site "A" of Khetri mine which were slightly higher. In control samples, the Zn content in plants was in normal limits except the pods of *Prosopis* and twigs of *Ailanthus*.

High amount of Iron (Fe) was present in soil of Khetri site "A" (31420.22 $\mu g\ g^{-1}$), followed by Khetri tailing dam, Kolihan mine and Khetri site "B" (Table 2.1). When compared with the control soil, the ratio of Fe content was 1: 2.1 in Khetri site "A", 1: 1.83 in tailing dam, 1:1.6 in Kolihan mine and 1:1.1 in Khetri site "B". Regarding Fe, there is lack of specific criteria for its toxicity. The form of Fe, the growth stage, the nutrient status and environmental factors, all affect the toxicity level [42]. However, the safe limits of Fe are not available in Indian standard [43].

The amount of Fe present in leaves and twigs collected from both the mines and control plants are shown in (Fig. 2.2) Irrespective of the plant species and sites, all the

leaves had more Fe content as compared to twigs. Leaves of the plants at all other locations were accumulating high amount of Fe except in Kolihan mine which has less amount of Fe when compared with control. All the twigs of *Prosopis juliflora* plants growing in mine area accumulated less amount of Fe than the control plant. In case of *Ailanthus* tree, the twigs had high amount of Fe than its control. *Ailanthus* leaves of the Khetri site "C" had 3.3 times more Fe when compared with control. *Prosopis* leaves from Khetri site "A" and "B" showed 1.3 and 1.16 times more Fe. Green pods showed 1.3 times more Fe content than their controls. The accumulation of Fe in *Prosopis* twigs was not higher than its control, while the twigs of *Ailanthus* growing at Khetri site "C" had 2.3 times more Fe than control.

Fe is an essential nutrient for plants. It functions to accept and donate electrons and plays important role in the electron-transport chains of photosynthesis and respiration [44]. Leaf tissues of all Cu mining sites accumulated high amount of Fe except in Kolihan mine which had less amount of Fe when compared with control. All the twigs of *Prosopis juliflora* plants growing in mine area accumulated less amount of Fe than the controls. This could possibly be the effect of Cu on these plants. Further study needs to be conducted to know the exact mechanism of metal uptake.

2.1.3.3 Transfer Coefficient (TC):

The TC quantifies the relative differences in the bioavailability of metals to plants and is a function of both soil and plant properties. In the present study, the coefficient is calculated by dividing the concentration of a metal in the plant matter dry weight (DW) by the total metal concentration in the soil. TC was studied in vegetables [32] and in plant parts growing in municipal solid waste composts [45].

The TC for Cu of control leaves and twigs was 0.08 and 0.21, respectively. The TC of all the samples ranged from a minimum of 0.05 in the *Prosopis* twigs of Khetri site "A" to a maximum of 1.08 in leaves of Khetri site "B" (Fig. 2.3). It was noted that the uptake of metal from soil and accumulation in leaves was more than twigs. The TC of Cu was different in same plant species from different sites. In *Prosopis* growing at Khetri site "A" it was 0.41 but in site "B" it was 1.08. In control plants of *Ailanthus*, the TC of leaves and twigs was 0.16 and 0.23, respectively. In *Ailanthus* growing at Khetri site "C" the TC was 0.38 and in twigs it was 0.14, showing metal transport from soil and its increased accumulation in leaves than twigs.

In control plants of *Prosopis*, the TC for Mn was 4.28 in leaves and 1.15 in twigs. The TC factor of Mn ranged from 3.17 (Kolihan mine *Prosopis* leaves) to 0.29 (Khetri site "B" *Prosopis* green pods). Maximum transport of Mn from soil to leaves of *Prosopis julifera* was observed at Kolihan mine and minimum transport in *Prosopis* green pods of Khetri mine. In control leaves and twigs the TC of Zn was 1.72 whereas in mining area plants the TC of Zn ranged from 6 (Khetri site "A" *Prosopis* leaves) to 1.49 (Khetri site "B" *Prosopis* twigs). In case of Fe, it was 0.13 and 0.02 at site "A" leaves and site "B" twigs respectively. Among the TC of Mn, Zn and Fe in *Ailanthus*, Zn was highest followed by Mn and then Fe.
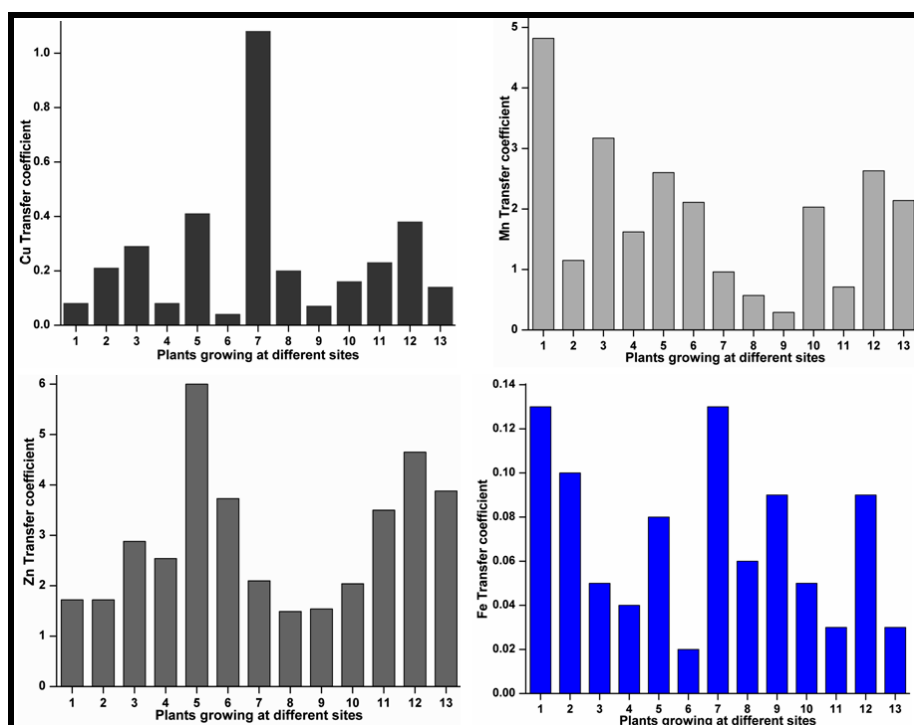
Figure 2.3: Transfer Coefficient of different metals (Cu, Mn, Zn, Fe) in leaf and twigs of plants growing on both mines and its controls. (**1**) Control *Prosopis julifera* leaf, (**2**) Control *Prosopis julifera* twigs, (**3**) Kolihan *Prosopis julifera* leaf, (**4**) Kolihan *Prosopis* twigs, (**5**) Khetri Site "A" Prosopis Leaf, (**6**) Khetri Site "A" Prosopis twigs, (**7**) Khetri Site "B" Prosopis leaf, (**8**) Khetri Site "B" *Prosopis* twigs, (**9**) Khetri Site "B" *Prosopis* green pods, (**10**) Control *Ailanthus excelsa* leaf, (**11**) Control *Ailanthus excelsa* twigs, (**12**) Khetri Site "C" *Ailanthus* leaf, (**13**) Khetri Site "C" *Ailanthus* twigs.

Maximum transport of Zn from soil was noted in *Prosopis* leaves of Khetri site "A".

Among all the metals studied, TC of Fe was the least. The soil had high concentration of Fe but it was not taken up by the plants growing there.

2.1.4 Conclusions

This study reveals that the plants studied here, can tolerate excess amount of Cu. They accumulated higher amount of Cu in aerial parts of plants. Higher content of the metals than the toxic level, prove that these plants have mechanism for stress tolerance, defense and detoxification of Cu, which has to be elucidated.

The present results prove that Cu accumulation was higher in leaves than twigs of both the plants of Khetri mine. Both *Prosopis juliflora* and *Ailanthus excelsa* accumulate high amount of metal in leaves, of which *Prosopis juliflora* accumulates at a higher-fold than *Ailanthus* when compared to their respective controls. This reveals that these plants could be hyperaccumulators. Further studies need to be carried out to determine whether they can accumulate higher amount of metal. This field study suggests that these plants can be used for phytoextraction of Cu from contaminated sites.

Among the distribution of other metals in plant samples, Mn content was found to be more. The content of Mn in the soil of Cu mining area was higher than the control soil which may have led to higher uptake of Mn by the plants growing there. The less amount of Zn in green pods of *Prosopis juliflora* and twigs of *Ailanthus excelsa* in the sample from dumpsite than the control could be the effect of Cu on these tissues. In case of Fe, all the leaves had more amount of metal than its control except those from Kolihan mines. Dumpsite leaf and twig samples of *Ailanthus excelsa* had higher Fe content than *Prosopis* tissues, respectively. This indicates that distribution of metals differs from one part to another and also between the two different plant species. Highest TC was observed in *Prosopis* leaves of Khetri site "A" for Zn.

Section 2

2.2 Bioleaching of copper from *Prosopis juliflora* leaves and its conversion to copper oxide nanoparticles using the fungus *Fusarium oxysporum.*

2.2.1 Introduction

Bioleaching is a new technique used by the mining industry to extract minerals and metals with the use of microorganisms. The process involves removing a soluble substance from a solid structure by making it into a liquid form, thus easy for extraction. In this process, low concentration of metals does not pose a problem for the microorganisms as they just ignore the waste which surrounds the metals, whereas with traditional extraction processes of roasting and smelting require sufficient concentration of elements in the ores for leaching. Copper is one of the most widely used materials in the world. It has great significance in all industries, particularly in the electrical one.

Bioleaching is a biological process where metals and microorganisms interact with each other. In this process, insoluble metals are recovered by transforming them into soluble form with the help of several microorganisms [46, 47]. In recent years, it has been shown that bioleaching is a novel and promising technology for recovering some minerals from municipal and industrial wastes [48, 49, 50, 51].

In recent years, increase in environment awareness and need for cost effective processes have led to the consideration of biohydrometallurgical approaches. The advantages of microorganisms include the absence of noxious gases or toxic effluents, simple operation and maintenance, easy process and economic recovery, and which are applicable to various metals [52, 53, 54, 55].

Fungal-mediated solubilization of a variety of metals has been demonstrated for metal ores, coal, kaolinite clay, quartz sand, fly ash and tannery sludges [56, 57]. Leaching experiments with synthetic solutions containing organic acids similar to those produced by fungi have also confirmed the ability of these chelating agents to solubilize metals in complex matrices, including preservative-treated wood [58, 59].

Fungal activity has been reported to release metallic and silicate ions from minerals and rocks [60]. The heterotrophic fungi such as *Aspergillus niger* and various *Penicillium* species have also been found to be amongst the most effective microorganisms for metal recovery [61, 62]

The feasibility of the fungus *Aspergillus niger* for bioleaching of copper and other metals from low-grade ore has been explored. Large quantities of the metals which are present in the low grade ores and mining residues can be recovered. The currently available techniques (pyrometallurgical and hydrometallurgical) are expensive or may have a negative impact on the environment [61]. Inorganic materials commercially produced by microorganisms via bioleaching include various metals like copper, iron and gold [63].

Copper nanoparticles have been synthesized and characterized by different methods [64, 65, 66, 67]. Our group in the past has demonstrated that the fungus *Fusarium oxysporum* could be used for selective bioleaching of crystalline silica nanoparticles from white sand and zircon sand. [63, 68] In another experiment carried out by our group, it has been shown that *F. oxysporum* when exposed to rice husk is not only capable of leaching out huge amounts of amorphous silica present in the rice husk in the form of flat, porous silica nanostructures; but more interestingly, the fungus also biotransforms this amorphous silica into crystalline silica particles at room temperature [69]. We in the past have also obtained silicate nanoparticles using the fungus *Humicola* sp. at 50°C by bioleaching of glass with the accompanied modification of the glass surface. [70]

Bioleaching has become a potential tool for eco-friendly, low-cost synthesis of various metals from their precursors. Inorganic materials produced by organisms via bioleaching at commercial level include various metals like copper, iron and gold. To our knowledge, there have been no attempts made to recover the copper present in the plant leaves which accumulated high amount of copper and conversion to nanoparticles. In this chapter, we report the bioleaching of copper and simultaneously its biotransformation to copper nanoparticles. Our approach involves the use of

Fusarium oxysporum, a fungus, in the biotransformation of naturally accumulating copper by plant leaves (*Prosopis juliflora*).

In this chapter, we have extended this issue of fungal bioleaching and described our efforts to set up a biological model system for the extracellular bioleaching of copper and simultaneous conversion to copper oxide nanoparticles from leaves of *Prosopis juliflora* obtained from copper mining area. This process is completely biogenic, economical and eco-friendly. Here we show that the fungus *Fusarium oxysporum* selectively bioleaches the high concentrations of copper accumulated in the leaves of *Prosopis juliflora* plant and then biotransforms this copper into copper oxide nanoparticles of irregular morphology after 7 days of reaction at ambient conditions. Since the synthesized nanoparticles are extracellular, water soluble and protein capped, they may find significant use in several commercial applications.

2.2.2 Experimental Details

The copper accumulated leaves of *Prosopis juliflora* used in this study were obtained from Khetri mine, Rajasthan, India. The processing of the sample, metal accumulation and estimation has been described in the Section 2.1.2.

The mesophilic fungus *Fusarium oxysporum* was isolated from plant material and maintained on MGYP (malt extract, glucose, yeast extract and peptone) agar slants. Stock cultures were maintained by sub culturing at monthly intervals. After growing the fungus for 96 hr, the slants were preserved at 15°C. From an actively growing stock culture, subcultures were made on fresh slants and after 96 hr of incubation were used as the starting material for fermentation experiments. For the bioleaching of copper present in *Prosopis juliflora* leaves and subsequent production of copper oxide nanoparticles, the fungus was grown in 500 ml Erlenmeyer flasks containing 100 ml of MGYP medium which is composed of malt extract (0.3%), glucose (1%), yeast extract (0.3%) and peptone (0.5%). The culture was grown with continuous shaking on a rotary shaker (200 rpm) at 25°C for 96 hr. After 96 hr of fermentation, mycelial mass were separated from the culture broth by centrifugation (5000 rpm) at 20°C for 20 min and then the mycelia were washed thrice with sterile distilled water under sterile conditions. The harvested mycelial mass (20 g of wet mycelia) was then

resuspended in 400 mg of dried leaf powder of *Prosopis juliflora* sterilized by keeping the leaf powder under UV for a period of 30 min, which was then added to 100 mL of distilled water. The whole mixture was put onto a shaker at 25°C (200 rpm) and maintained in the dark. The reaction between the fungal biomass and *Prosopis juliflora* leaves was carried out on a shaker (200 rpm) at 27°C for a period of one week. The bioleaching of copper and conversion of nanoparticles in the solution was monitored after a period of one week. The aqueous component was used for further characterization.

2.2.3 Results and Discussion

2.2.3.1 UV-vis analysis:

The UV-vis data of bioleached copper and conversion to copper oxide nanoparticles shows a broad hump at 380-420 nm which could be attributed to copper oxide nanoparticles (Fig. 2.4). In previous reports it has been shown that the peak at 420 could be due to copper oxide nanoparticles [67]. Another broad hump can be seen in curve 2 in the region of 280 nm which is due to the presence of proteins capped over nanoparticles. The inset image A shows leaf powder of *Prosopis juliflora* added to fungus at '0' hr forming an off-white colored solution which turns dark brown in color within a period of one week indicating the leaching of copper as is seen in inset image B.
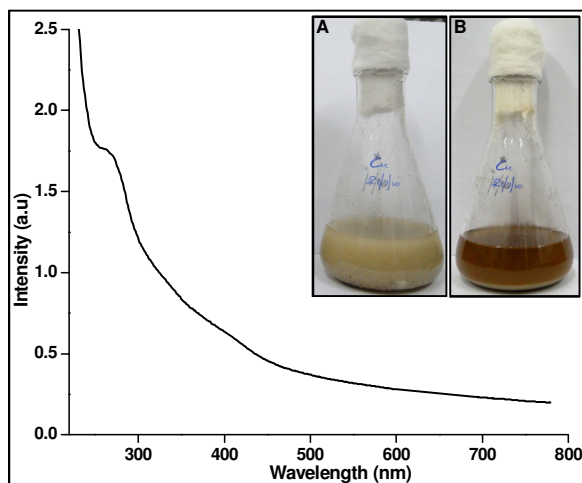
Figure 2.4: UV-Vis analysis of copper nanoparticles synthesized by using *Fusarium oxysporum*. The inset image **(A)** shows the '0' hr sample where there is no change in color of the solution, and **(B)** after a period of one week of incubation whereby a noticeable change in color can clearly be seen.

2.2.3.2 TEM and XRD analysis:

The TEM visualization of NPs which were bioleached from *Prosopis juliflora* leaves showed different shapes and sizes (Fig. 2.5A, B). The particles were polydispersed and spherical in morphology and were well separated with no agglomeration. The selected area electron diffraction (SAED) pattern (Fig. 2.5C) confirms the crystalline nature of these particles. The average particle diameter approximately ranged from 10-15 nm. The XRD analysis exhibits the presence of CuO_2 and CuO nanoparticles (Fig. 2.5 D). The peaks at 29.71, 36.8 and 41.9 correspond to the plane (110), (111) and (200) respectively of CuO_2 nanoparticles, whereas the peaks 35.4, 46.5, 48.7 and 53.7 respectively correspond to the plane (002), (112), (202) and (020) of CuO nanoparticles. This shows that the Cu nanoparticles leached by the fungus *Fusarium oxysporum* were of CuO_2 and CuO nanoparticles.
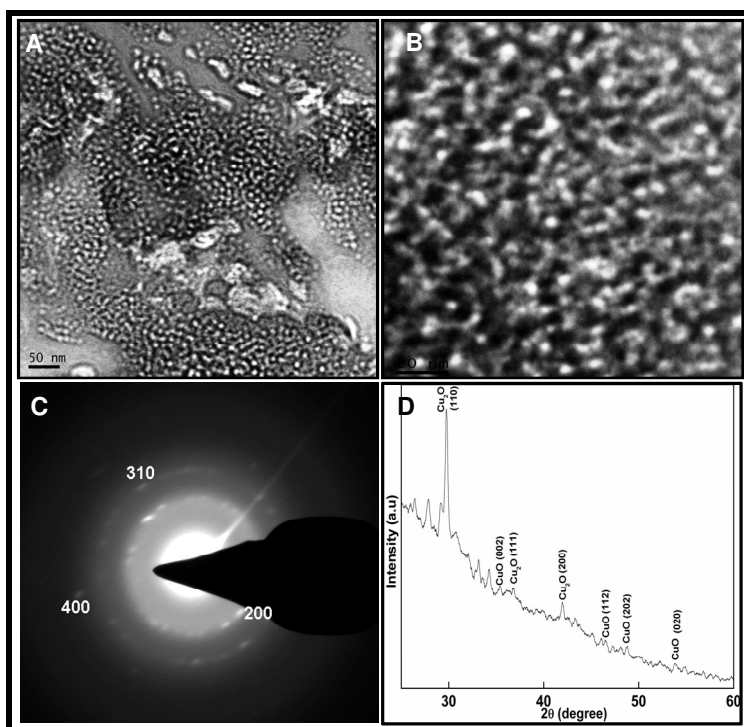

Figure 2.5: (A, B) TEM images of nanoparticles at different magnifications, **(C)** SAED of Cu oxide nanoparticles, **(D)** XRD of Cu oxide nanoparticles which were bioleached by *Fusarium oxysporum* from the leaves of *Prosopis juliflora* plant.

2.2.3.3 ESEM Chemical mapping and EDS analysis:

The ESEM (Environmental Scanning Electron Microscope) images of copper oxide (CuO_2 and CuO) nanoparticles show that these nanoparticles are in aggregates and the

particles are irregular in shape (Fig. 2.6A). EDS (Energy Dispersive Spectroscopy) analysis shows a peak corresponding to copper which has leached from the *Prosopis juliflora* leaves (Fig. 2.6B). The presence of other molecules such as carbon and oxygen can also be seen. Carbon is due to the proteins bound to the nanoparticles. The highest peak corresponds to silica which is used as a template for analyzing the sample. The inset image shows the elemental analysis in which the presence of Cu is 1% in the solution with respect to silica, carbon and oxygen. Presence of Cu is in small amount, since biosynthesis protocols of nanoparticles account for a low yield. Overall chemical mapping confirms the presence of carbon, oxygen and copper in the solution (Fig. 2.6C). The EDS chemical mapping of the sample (Fig. 2.6D) shows homogeneous dispersion of blue colored spots which indicate the presence of Cu oxide nanoparticles. The presence of metal nanoparticles by chemical mapping has also been confirmed by other researchers [71, 72].
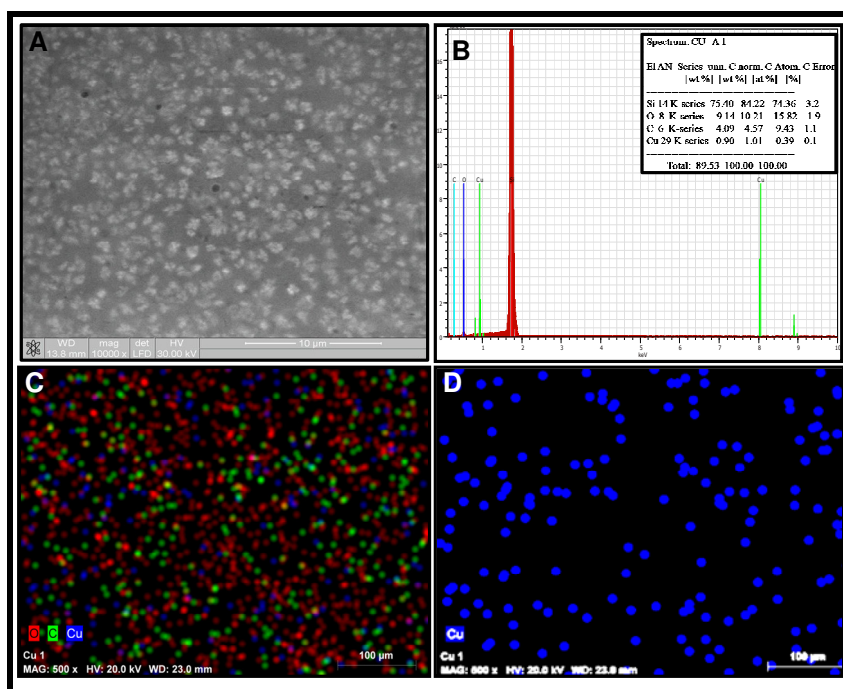

Figure 2.6: (A) ESEM images of Cu oxide nanoparticles, **(B)** Elemental analysis of Cu oxide nanoparticles by EDS, **(C)** The Overall chemical mapping, **(D)** EDS chemical mapping for Cu which was bioleached by *Fusarium oxysporum* from the leaves of *Prosopis juliflora*.

2.2.3.4 XPS Analysis:

XPS is an important tool for surface-sensitive analytical studies. It is useful for the identification of elements present in the sample along with their oxidation states. The

C1s core level spectrum could be decomposed into three chemically distinct components centered at 282.8eV, 285.01eV, 287.69eV (Fig. 2.7A). The lower binding energy peak at 282.8 is due to the presence of aromatic carbon present in amino acids from protein bound onto the surface of copper nanoparticles. The C1s which is centered at 285.01 is due to the electron emission from adventitious carbon or due to core levels originating from hydrocarbon chains present in the sample. The high binding energy peak at 287.69eV could be due to COOH groups and α carbon bound to COOH and –NH$_2$ groups of the protein which is bound to surface of nanoparticles. [73]. The O1s core level with the binding energy about 531.4eV which attributes to the OH groups and/or C=O groups present in capping proteins present on the surface of copper oxide nanoparticles (Fig. 2.7B) [74]. The (Fig. 2.7C) N1s core levels spectra with binding energy at 401.6eV correspond to –NH amide linkage or amidic (peptidic) nitrogen [75]. The high resolution narrow scan of the Cu 2p region (Fig. 2.7D) shows two copper bands 2p3/2 and 2p1/2 which occur at 933.2eV and 952.2eV, respectively[75, 76]. These results show that copper present in copper oxide is metallic in form.
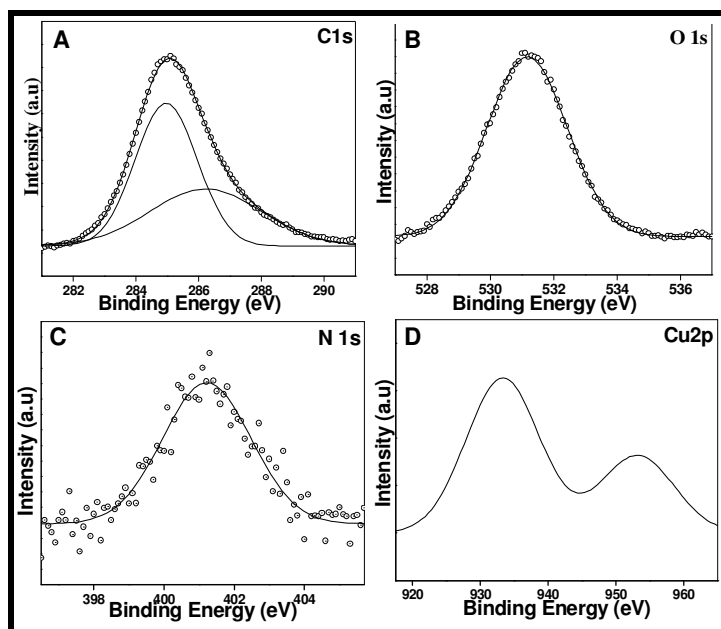

Figure 2.7: XPS characterization of copper oxide nanoparticles leached from *Prosopis juliflora* leaves by *Fusarium oxysporum.* **(A)** Spectrum of carbon 1s, **(B)** oxygen 1s, **(C)** nitrogen 1s and **(D)** copper 2p.

2.2.4 Conclusions

In conclusion, we have demonstrated that the fungus *Fusarium oxysporum* may be used for bioleaching of Cu present in the *Prosopis juliflora* leaves and simultaneous conversion to crystalline copper oxide nanoparticles. The copper oxide nanoparticles synthesized in this manner may possibly be capped by stabilizing proteins. The nanoparticles are released into the solution, which is an advantage of this process with significant application for leaching of copper from the leaves of plants accumulating high amounts of metals. The synthesis of oxide nanomaterials using microorganisms from potential waste of leaves accumulating high amount of copper is an exciting possibility and could lead to recovery of Cu from plants and economically viable green approach toward the large-scale synthesis of oxide nanomaterials. We believe that this non-hazardous approach can also be extended towards identification of plants which accumulate high concentrations of chromium, nickel, iron, zinc, cobalt, etc. alongwith bioleaching and simultaneous conversion to technologically challenging oxide nanoparticles which will be highly stable, water dispersible, protein capped and cost-effective.

Section 3 & 4
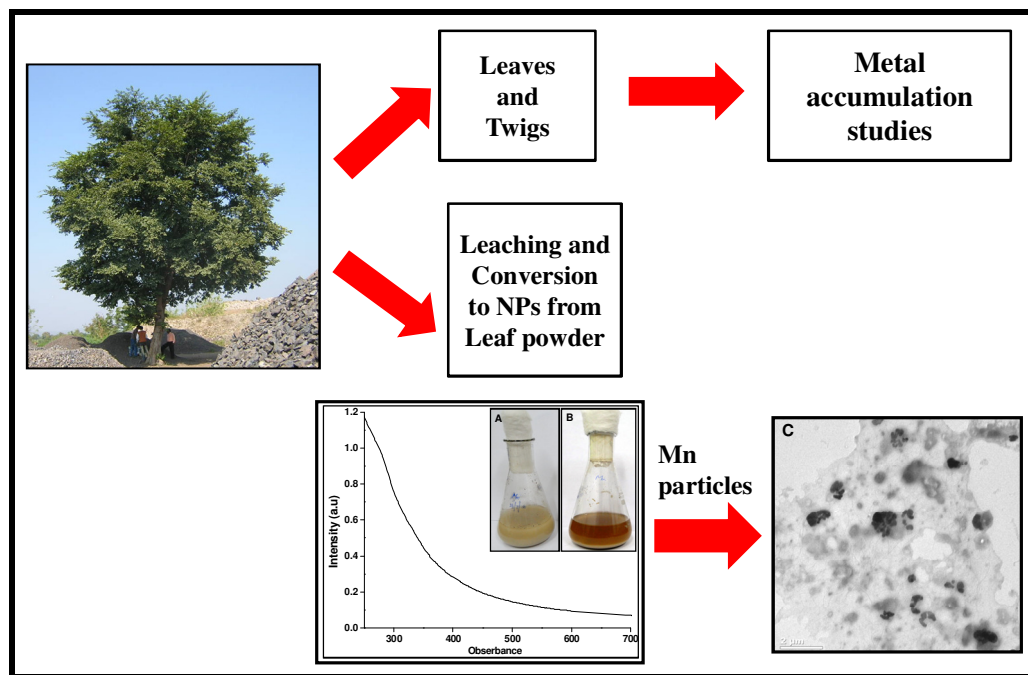
Section 3

2.3 Differential accumulation of manganese in three mature tree species (Holoptelia, Cassia, Neem) growing on a mine dump.

2.3.1 Introduction

Manganese (Mn) is a trace element that is found in varying amounts in all tissues and is amongst the mostly used elements in industries. It is an essential micronutrient and activator for enzymes involved in tricarboxylic acid cycle. However, Mn is toxic when present in excess and consequently it represents an important factor in environment contamination and can produce various phytotoxic effects [1]. The excess Mn concentrations in plant tissues can alter various processes such as enzyme activity, absorption, translocation and utilization of other mineral elements (Ca, Mg, Fe and P), causing oxidative stress [24, 77]. The threshold of Mn injury as well as the tolerance to an excess of this metal is highly dependent on the plant species and cultivars or genotypes within a species [78, 79]

When Mn is present in excessive amounts, it is extremely toxic to plant cells [80]. The injury extent of Mn toxicity is approximately proportionate to the concentration of Mn accumulated in excess. However, there is considerable inter- and intra- specific variation among Mn levels that induce toxicity as well as the symptoms of this toxicity in plant species [78].

There are only few reports on restoration of Mn-contaminated mine lands [81-83]. Mn toxicity thresholds have been established for six grasses commonly used for restoration [84]. Currently there were twelve Mn hyperaccumulators reported, including 9 species listed by [41]. The other Mn hyperaccumulators include *Eugenia* species [85], the newly found tree species *Austromyrtus bidwillii* from Australia [86] and a perennial herb *Phytolacca acinosa* Roxb. from China [87, 88]. Hyperaccumulators have great potential for phytoremediation of light to moderate metal-contaminated soils [89]. The high accumulation of manganese uptake in roots, stem and leaves of *Phytolaccia acinosa* populations has been shown. [88]. However,

little is known about uptake, accumulation and detoxification of heavy metals, especially about Mn in woody plants [77].

In the present investigation, three naturally growing tree species including *Cassia siamea* (Cassia), *Azadirachta indica* (Neem), *Holoptelia integrifolia* (Holoptelia) have been identified on a manganese mine dump. Experiment was conducted to generate information on Mn accumulation and distribution in these trees. The data was compared with the data generated from the samples collected from the trees growing in natural vegetation in contamination free soil. The dry fallen leaves of the respective tree were collected from the ground under the trees and were analyzed for Mn content.

2.3.2 Experimental Details

The manganese mine is located in Gumgaon in Maharashtra State of India. We identified three plants including Holoptelia (A), Cassia (B) and Neem (C) growing naturally in the mine dump where sorting of the ore is being carried out (Fig. 2.8A, B, C). This was the only Holoptelia tree growing in that mining area whereas several plants of Cassia and Neem could be seen growing naturally in the dump area. The three plants identified for our study, are growing within an area of 400 (approx.) square meters. The Fig. 2.8D, E shows the soils from NCL (control) and from mining area, respectively.
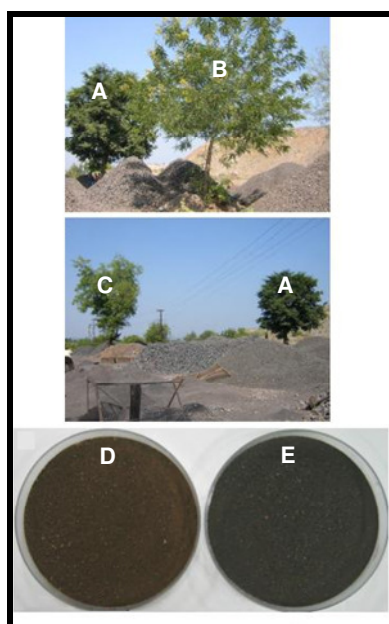
Figure 2.8: The trees growing on the manganese mine dump. **(A)** *Holoptelia integrifolia*, **(B)** *Cassia siamea*, **(C)** *Azadirachta indica*, **(D)** Sample of normal soil, **(E)** Sample of soil from Mn mine dump.

2.3.2.1 Soil analysis:

The pH of the soil samples was determined following the method described by Sparks et al. [90]. In brief, soil samples collected from dump site (Gumgaon) and local vegetation (NCL) (Fig. 2.8D, E) were air dried at room temperature. Soil samples were taken in glass beaker and on adding distilled water were kept on shaker for 1 hr. On removing from shaker, it was kept stationary for a period of 1hr for the suspended particles to settle. The pH of the solution was measured using pH meter (Model 420A, ORION).

Manganese content in the soil sample was determined using the method described in Lab Procedures [91]. Moisture free samples were ground with mortar and pestle to make fine powder and the powder was sieved. In brief, 1 g of sieved soil was taken in test tube and 4 mL of each extracting solutions (0.05N HCL and 0.025N H_2SO_4) was added and kept on shaker for 15min. The solution was filtered through Whatman filter paper and the volume was made to 10 mL with extracting solutions. Mn content was determined by Atomic Absorption Spectroscopy. The procedure of metal estimation from different plant parts has been described in Section 2.1.2.2.

2.3.3 Results and discussion

The aim of the present study was to characterize some of the tree species that have naturally colonized in Mn mine tailings. The objective was to assess these plants for their ability to uptake and accumulate Mn in the different organs. The tree species including Holoptelia, Cassia and Neem do not appear in the list of the known hyper accumulators. The Mn hyperaccumulators (>10,000 $\mu g\ g^{-1}$) are from the families Apocynaceae, Celastraceae, Clusiaceae, Myrtaceae and Proteaceae [45] [85 [92]. In addition, mention may be made of *Eleuherococcus* (formerly *Acanthopanax*) *sciadophylloides* (Araliaceae) from Japan [93], which can accumulate Mn up to 7900 $\mu g\ g^{-1}$ in leaf dry matter. Some plants that grow on naturally metal contaminated soils may adapt and develop to survive and accumulate much greater concentrations of heavy metals in their shoots than other plant species [9]. Accumulation of manganese

in leaf mesophyll of four tree species namely *Gossia bidwillii, Virotia neurophylla, Macadamisa integrifolia* and *Macadamia tetraphylla* has been reported [94].

The pH of the dump soil was 8.84 as compared to 7.37 of control soil and the Mn content in the soil of tailing dump was 1296.33 µg g$^{-1.}$ This is approximately 44 times higher than the control soil (Table 2.2). The color of the soil from the contaminated site and normal site varied distinctly (Fig. 2.8D, E). Comparison of Mn content (Table 2.2) in the organs of three tree species of local vegetation of Pune and samples from the trees growing on Mn tailing dump, revealed following information,

Table 2.2: Manganese Content and pH in Soil of Dump site and normal vegetation

Soil	Mn in µg g^{-1}*	pH
NCL (Control)	29.27 ± 1.55	7.37
Mn tailing Dump	1296.33 ± 102.89	8.84
Mn dump: NCL	Ratio is 1:44	
t-test	S1%	

* Mean of three repeats

i) Manganese content in the samples of leaves and twigs collected from the tailing dump was higher than in control. This indicates accumulation of Mn in all the plants growing on the tailing dump. Although all the three plants are growing under identical conditions, the Mn content in their organs varied. This suggests that mechanisms of Mn uptake and sequestration in these three plants may be different.

ii) In the leaf tissues Mn content was significantly higher compared to the twigs irrespective of location of the plant thereby maintaining a gradient between these two organs. This is possibly due to deposition of Mn in leaves. The three trees under study are growing in the high Mn containing medium for several years. Still, Mn is not evenly distributed in the organs. There is need to conduct detailed studies to understand the process of transfer of Mn from twigs to the leaves to maintain the gradient.

iii) Among the samples collected from normal vegetation, Mn content varied in the three species (Table 2.3). Mn content in this soil was 29.27 ± 1.55 µg g^{-1}. Cassia

showed highest Mn content followed by Neem and Holoptelia in the leaves and twigs, respectively. The values are several folds higher than the concentration of the metal in soil. It needs further studies to determine if these are the required concentrations in the organs for their normal functioning. The varying amounts of Mn in organs of the three plants under normal and identical condition indicate that the ability of a plant to uptake and accumulate Mn differs from species to species.

Table 2.3: Distribution of Manganese ($\mu g\ g^{-1}$) in leaf and stem of Holoptelia, Cassia and Neem.

Tree		Leaf* (A)	Stem* (B)	t test (A&B)	Dry Fallen* leaves
Holoptelia	Control (a)	168.59± 57.20 (11)	98.78± 41.70 (6)	S-5%	143.12 ± 8.50 (6)
	Dump (b)	1744.06±539.46 (11)	1248.15± 268.3 (9)	S-5%	2682.19 ± 94.11 (6)
	t test (a & b)	S-1%	S-1%		S-1%
Cassia	Control (a)	437.56± 144.9 (9)	248.88± 13.34 (3)	S-1%	185.58 ± 32.1 (6)
	Dump (b)	1199.35± 296.9 (9)	642.96±123.52 (3)	S-1%	2852.50 ± 131.7 (6)
	t test (a & b)	S-1%	S-5%		S-1%
Neem	Control (a)	286.86±122.6 (9)	174.78±20.04 (3)	NS	139.36 ± 15.2 (6)
	Dump (b)	726.60±177.1(9)	626.66±113.40 (3)	NS	2513.30 ± 127.7 (6)
	t test (a & b)	S-1%	S-5%		S-1%

*Figures in parenthesis indicate number of replicates.

iv) Among the three trees of the dump site, Mn content was highest in the tissues of Holoptelia (Table 2.3). This was followed by Cassia and Neem. In Holoptelia the ratio of Mn in leaf samples of control and mine dump respectively is approximately 1: 8. In twigs the ratio is 1:13. It appears that under Mn stress condition, Holoptelia can uptake more amount of Mn. The optimum capacity of this plant to uptake and accumulate Mn needs to be determined by designing appropriate experiments.

v) Cassia in dumpsite did uptake more Mn (1199.35$\mu g\ g^{-1}$) in addition to its level of Mn in control (437.56$\mu g\ g^{-1}$) but it was not as high as in Holoptelia. However the ratio of Mn content between the control and dump site soil sample is 1: 44 (Table 2.1) whereas the ratio between the control and dump site samples of both leaves and twigs of Cassia were only 1: 3. Thus the amount of Mn accumulated in the two organs of

Cassia may be the optimum for this plant. The mechanism of Mn tolerance in this plant is possibly different from the mechanism in Holoptelia.

vi) In Neem leaf and twig samples from control soil, Mn content was higher (Table 2.3) than in Holoptelia, whereas its amount in the organs of the plants in dump site was less than in Holoptelia. We presume that the amount of Mn detected in the organs of the plants of normal soil is the amount required for their normal functioning and growth. In Mn rich soil, each plant uptakes the metal as per its own specific ability.

vii) Comparison of the data generated from the three trees growing on the dump site (Table 2.3) suggests that Holoptelia has special ability to accumulate high amounts of Mn under stress condition. Till date there is no literature on metal accumulation in this species. Further studies will reveal more information on its optimum ability to accumulate Mn and possibly other metals too.

viii) The metal content in the mature fallen leaves of all three trees were estimated (Table 2.3). In the fallen leaves collected from the trees growing in normal soil, Mn content was less than in their green counterparts. This observation cannot be explained with the present state of knowledge. It is assumed that the amount of Mn required by the plant organ for its normal function is taken up by the plants and is maintained. The cellular activities diminish gradually with aging prior to abscission. Presumably, demand of Mn as co factor for cellular processes is reduced in the maturing tissues causing mobilization and transfer of the metal to the more active organs thereby resulting in reduction of Mn in the dry fallen leaves. Foliar Mn sequestration in *Gossia bidwillii* (Myrtaceae), a species discovered relatively recently to be Mn-hyperaccumulating [95] has been shown to occur in the photosynthetic tissues [94]. A possible association of reduction in Mn in aging leaves with reduction in photosynthetic activity requires further investigation. The pattern of Mn content in dry leaves of the three species was similar as in green leaves; cassia showing highest amount followed by Holoptelia and Neem, respectively.

ix) Unlike the dry leaves of plants from normal soil, in dry fallen leaves of dump site, Mn content were higher than in their green counterparts. In view of our assumption regarding reduced Mn in matured leaves of control plant, in the dump site there is unlimited supply of Mn from soil. Thus, Mn from the aging leaves need not move to

the more active parts leaving the Mn content unaltered in dry leaves. Due to optimum accumulation of Mn in leaves prior to abscission, Mn content is higher in the dry leaves than in the green leaves. Abscission of the leaves with high Mn may be the mechanism of these plants to eliminate excess Mn from the system. In fallen leaf of Cassia, (Table 2.3) the ratio of Mn content between control and dump site leaf is approximately 1:15 times. In Holoptelia the Mn content (Table 2.3) was approximately 1:19 times in fallen leaf samples. In Neem, Mn is approximately 1:18 times more than control. But when all the three fallen leaves are compared they are almost similar.

2.3.4 Conclusions

All plants uptake metals to varying degrees from the substrates in which they are rooted [96]. The flora of metal contaminated sites is typically impoverished by comparison with that of surrounding vegetation and populations of plants growing there are often genetically distant from populations of the same species in the adjacent location with soil of low heavy-metal content [97]. Moreover, the level of tolerance developed can often be related to the amount of metal in the soil [78].

There are plenty of evidences from natural establishment of trees on contaminated sites that some types of trees can survive under such adverse conditions e.g. *Salix* (Willow), *Betula* (Birch), *Populus* (poplar), *Alnus* (Alder) and *Acer* (Sycamore). The main characteristic of trees that make them suitable for phytoremediation is their large biomass, both above and below the ground level. Physical phytostabilization can be readily achieved, and is often the main benefit of using trees on such sites. Vegetation of tree species helps in decreasing the risk of soil, water and wind erosion. Phytoremediation and especially the use of trees is an emerging and developing technology and its use has grown rapidly in recent years [98]. From the present study it may be concluded that accumulation of manganese in the three tree species and in their different parts, vary. This could be due to differences in mechanisms of uptake and sequestration of this metal in different plant systems [99]. These three trees are from different families. However, all three plants have the ability to thrive on Mn rich dump. This common characteristic makes these plants suitable for restoration of Mn contaminated sites but all three may not be suitable for phytoremediation. The aim in a phytoremediation program is to reduce the toxic metal from soil. From the three

trees tested, *Holoptelia* has the ability to uptake more metal. Thus this plant is more suitable for removal of Mn from the soil. Further studies using higher concentrations of Mn needs to be conducted to determine if *Holoptelia* is a hyperaccumulator. The differential accumulation of Mn in the three tree species demands close studies to determine the mechanism of Mn tolerance in each.

Section 4

2.4 Bioleaching of manganese from *Holoptelia* leaves and its conversion to manganese oxide nanoparticles using the fungus *Fusarium oxysporum.*

2.4.1 Introduction

Manganese (Mn) has been widely used in various industries. Mn is industrially important because it aids in desulfuring, deoxidation as well as an alloying element in manufacturing of steel and iron cast [100] Most of the biotechnical processes for leaching of metals have been developed using aerobic microorganisms [46, 54, 55]

Bioleaching is a process in which metal ions are extracted from low-grade ores by microorganisms. The conventional methods for the recovery of metal form of Mn from low grade ores involve physicochemical processes. The recovery of Au (III) as Au (0) from test solutions and from waste electronic scrap leachate was studied. Au (0) was precipitated extracellularly by a different mechanism from the biodeposition of Pd (0) where *Desulfovibrio desulfuricans* was used for recovery [101].

The first report of microbial Mn reduction was of Mn oxides to $MnCO_3$ by microorganisms in sewage [102]. A wide range of microorganisms, including bacteria, algae, yeast and fungi, can reduce Mn (III) or Mn (IV) oxides. Under aerobic conditions, metabolically excreted end products such as formate, malate, oxalate, citrate and other organic acids are presumed to be involved indirectly in the microbial Mn reduction process [103].

The principle involves the non-enzymatic reduction of pyrolusite [Mn (IV) oxides] to +2 oxidation state by fungi with the production of metabolites such as oxalic acid and citric acid. The study on *in-situ* fungal (*Penicillium citrinum*) leaching of manganese from the low grade ores was done with the effect of various parameters such as particle size, pulp density, sucrose concentration, inoculum size and duration of leaching [104]. It was proposed that the enzymatic method of leaching silica from sand to silica nanoparticles was done in two steps involving the leaching of silica to silicic acid with the help of protein present in fungal biomass and second step

involving conversion of silicate complexes to silica nanoparticles [63]. The fungus *Fusarium oxysporum* when reacted with zircon sand leads to selective extracellular bioleaching of silica nanoparticles. Since this reaction does not result in zirconia being leached out from the sand, there is a consequent enrichment of the zirconia component in zircon sand [68].

To the best of our knowledge, there have been no attempts made so far to recover the manganese present in the plant leaves accumulating high amount of Mn and its conversion to nanoparticles. In this chapter, we report the bioleaching of manganese, initially in which we could get 5-7 µM particles and then the same particles were retreated with the same fungus and simultaneously biotransformed to manganese nanoparticles. Our approach involves the use of *Fusarium oxysporum*, a plant fungus, in the biotransformation of naturally accumulating manganese by plant *Holoptelia* (leaves).

2.4.2 Experimental Details

The manganese accumulated leaves of *Holoptelia* used in this study were obtained from Gumgaon mine, Nagpur, Maharashtra, India. The process of the samples, metal accumulation and estimation has been described in the Section 2.1.2.2. The Mn bioleaching process by using the fungus *Fusarium oxysporum* was same as that described in Section 2.2.2. (copper bioleaching)

2.4.3 Results and Discussion

2.4.3.1 UV -vis analysis:

The UV-Vis data of bioleached manganese and conversion to manganese oxide particles shows a broad hump at 330-340 nm (Fig. 2.9) which could be attributed to Mn oxide nanoparticles. In previous report it has been shown that the peak at 330 could be manganese nanoparticles [105]. Another broad hump can be seen in curve 2 in the region of 280 nm which is due to the presence of proteins capped over nanoparticles. The inset Fig. 2.9 image A shows leaf powder of *Holoptelia integrifolia* added to fungus at '0' hr forming an off-white colored solution which

turns dark brown in color within a period of one week indicating the leaching of manganese as is seen in inset image B.
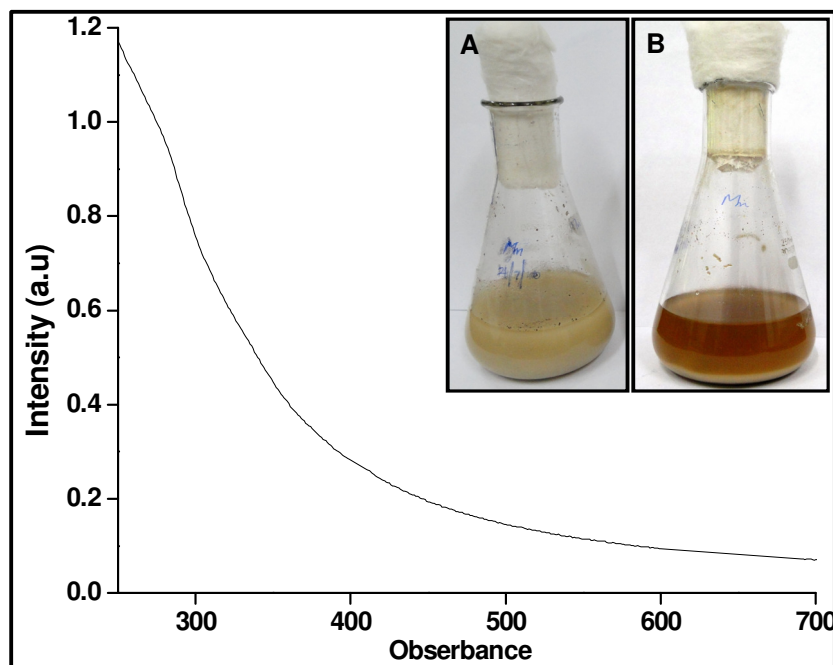

Figure 2.9: UV image analysis of the manganese nanoparticles synthesized by using *Fusarium oxysporum.* The inset image **(A)** shows 0 hr sample where no change in colour of the solution, **(B)** after a period of one week of incubation where by a noticeable change in colour can clearly be seen.

2.4.3.2 ESEM and Chemical Mapping study:

The ESEM images of manganese oxide particles show that these particles are well separated and circular in shape. The particles are large sized, being 5-7µm in size (Fig. 2.10A). EDS analysis shows a peak corresponding to the manganese which has leached from the *Holoptelia integrifolia* leaves (Fig. 2.10B). The presence of other molecules such as carbon, nitrogen, oxygen, magnesium, potassium, chlorine, phosphorous and sodium is observed. The carbon is due to the protein bound onto the particles. The oxygen could be from the air in the chamber; the highest peak corresponds to silica which is used as a template for analyzing the sample and the other elements are from the plant material. The presence of Mn is in small amount, since biosynthesis protocols of nanoparticles account for a low yield. The overall chemical mapping of the sample shows the presence of carbon, oxygen, nitrogen,

magnesium, potassium, chlorine, phosphorous, sodium and manganese in solution (Fig. 2.10C) The EDS chemical mapping of the sample (Fig. 2.10D), shows homogeneous dispersion of dark red colored spots which indicate the presence of Mn particles. The previous studies also confirmed the presence of metal by chemical mapping [71, 72].
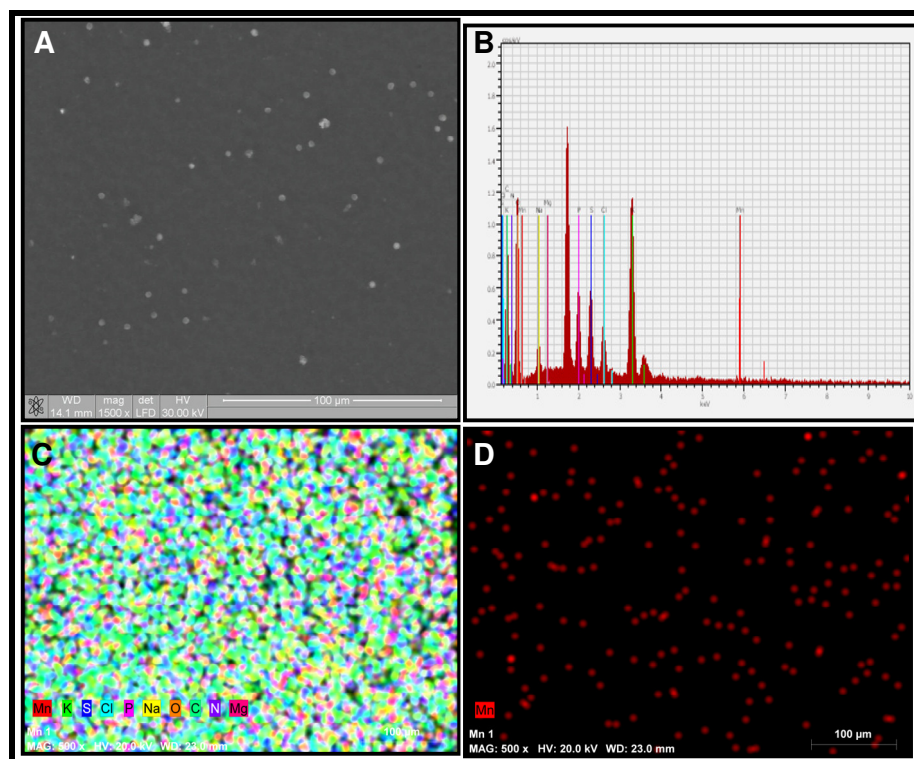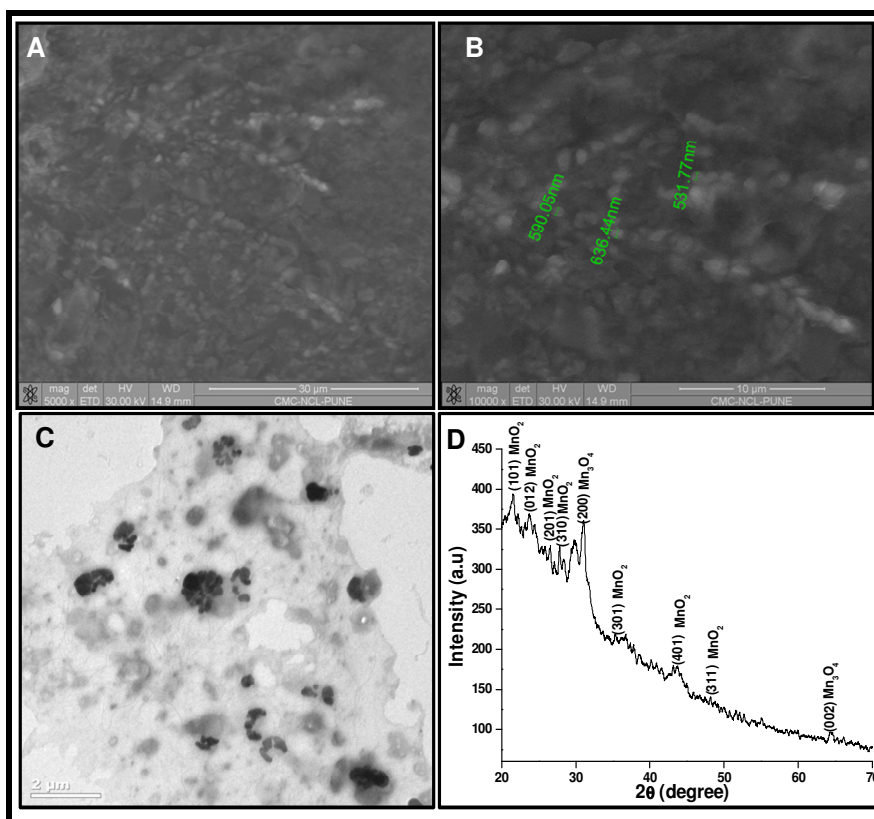

Figure 2.10: (A) ESEM images of particles, **(B)** EDS analysis of Mn particles, **(C)** overall chemical mapping by EDS, **(D)** EDS chemical mapping for Mn which was bioleached by *Fusarium oxysporum* from *Holoptelia integrifolia* leaves.

2.4.3.3 Breakdown of Mn particles:

The particles initially released were 5-7 µm in size. The particles were challenged to the same fungus for the breakdown of the larger particles to nano size. The ESEM images of the Mn oxide particles at different magnification shows that the particles were of 500- 650 nm (Fig. 2.11A, B). The breaking down of the particles was also confirmed by TEM analysis and the particles were of 300-400 nm in size (Fig. 2.11C). The XRD (Fig. 2.11.D) confirms MnO_2 and Mn_3O_4 particles. The peaks 21.6, 23.8, 27.2, 35.3, 36.8, 43.4 and 48.2 correspond to (101), (012), (201), (310), (301), (401), and (311) planes of MnO_2 particles respectively, whereas the peaks 28.4 and 64.6 correspond to (112) and (400) planes of Mn_3O_4 particles. This showed that the

leached nanoparticles by *Fusarium oxysporum* were of MnO_2 and Mn_3O_4 nanoparticles.


Figure 2.11: **(A, B)** ESEM images of Mn particles at different magnifications, **(C)** TEM of Mn particles, **(D)** XRD of Mn particles which were re-treated by *Fusarium oxysporum.*

2.4.3.4 XPS Analysis:

The C1s core level spectrum that could be decomposed into three chemically distinct components centered at 282.8eV, 285.01eV, 287.69eV (Fig. 2.12A). The lower binding energy peak at 282.8 is due to the presence of aromatic carbon present in amino acids from protein bound on the surface of manganese particles. The C1s which is centered at 285.01 is due to the electron emission from adventitious carbon or due to core levels originating from hydrocarbon chains present in the sample. The high binding energy peak at 287.69eV could be due to COOH groups and α carbon bound to COOH and –NH$_2$ groups of the protein which are bound to nanoparticles surface [73]. The Fig. 2.12B shows the O1s core level with the binding energy about 531.4eV is attributed to the OH groups and/or C=O groups present in capping proteins present on the surface of manganese oxide particles [74]. The (Fig. 2.12C)

N1s core levels spectra with binding energy at 401.6eV which corresponds to –NH amide linkage or amidic (peptidic) nitrogen [75]. The high resolution narrow scan of the Mn 2p region (Fig. 2.12D) shows two manganese bands 2p3/2 and 2p1/2 which occur at 641.4eV and 651.2eV, respectively. This was also reported earlier [106,107]. These results show that Mn present in manganese oxide is metallic in form.
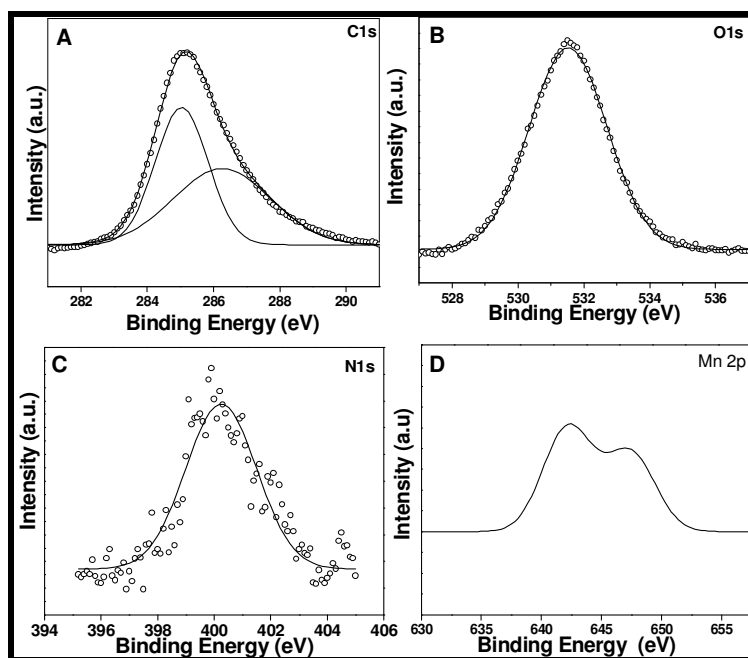
Figure 2.12: XPS Characterization of Mn oxide particles leached from *Holoptelia integrifolia* leaves by *Fusarium oxysporum.* **(A)** Spectrum of carbon 1s, **(B)** oxygen 1s, **(C)** nitrogen 1s, **(D)** manganese 2p.

2.4.4 Conclusions

In conclusion, we have demonstrated that the fungus *Fusarium oxysporum* may be used for bioleaching of Mn present in the *Holoptelia* leaves and its conversion into crystalline Mn oxide nanoparticles. The Mn oxide nanoparticles are, possibly capped by stabilizing proteins. The nanoparticles are released into the solution, which is an advantage of this process with significant application for leaching of Mn from the leaves of plants accumulating high amounts of metal.

The synthesis of oxide nanomaterials using microorganisms from potential waste of leaves accumulating high amount of Mn is an exciting possibility and could lead to

recovery of Mn from plants and economically viable green approach toward the large-scale synthesis of oxide nanomaterials.

References

[1] Ross, S. M. 1994. Toxic metals in soil-plant systems. John Wiley & Sons, Chichester, UK.

[2] Singh, A. N., Zeng, D. H., Chen, F. S. Heavy metal concentrations in redeveloping soil of mine spoil under plantations of certain native woody species in dry tropical environment, *Indian J. Environ Sci*. 2005, 1, 168-174.

[3] Salt, D. E., Blaylock, M., Kumar, N. P. B. A., Dushenkov, V., Ensley, B. D., Chet, I., Raskin, I. Phytoremediation: A novel strategy for the removal of toxic metals from the environment using plants. *Biotechnology*, 1995, 13, 468–474.

[4] Salt, D. E., Smith, R. D., Raskin, I. Phytoremediation. *Annual Review of Plant Physiol. Plant Mol. Biol.* 1998, 49, 643–668.

[5] Berti, W. R., Cunningham, S. D. Phytostabilization of metals. *In*: Raskin, I., Ensley, B.D., (eds). *Phytoremediation of toxic metals: Using plants to clean up the environment.* John Wiley & Sons, New York, pp. 2000, 71–88.

[6] Blaylock, M. J., Huang, J. W. Phytoextraction of metals. *In*: Raskin, I., Ensley, B.D., (eds). *Phytoremediation of toxic metals: Using plants to clean up the environment*. John Wiley & Sons, New York, pp. 2000, 53–70.

[7] Chaney, R. L., Li, Y. M., Brown, S. L., Homer, F. A., Malik, M., Angle, J. S., Baker, A. J. M., Reeves, R. D., Chin, M. Improving metal hyperaccumulator wild plants to develop commercial phytoextraction systems: Approaches and progress. *In*: Terry, N., Banuelos, G. (eds). *Phytoremediation of contaminated soil and water.* Lewis Publ, Boca Raton, FL, pp. 2000, 129-158.

[8] Antonovics, J., Bradshaw, A. D., Turner, R. G. Heavy metal tolerance in plants. *In*: Cragg, J. B. (eds). *Advances in Ecological Research*. Academic Press, New York, Vol.**7**, pp. 1971, 1-85.

[9] Long, X., Yang, X., Ye, Z., Ni, W., Shi, W. Difference of uptake and accumulation of Zinc in four species of Sedum. *Acta. Bot. Sin*. 2002, 44, 152-157.

[10] Pilon- Smits, E., Phytoremediation. Annual Review *Plant Biol*. 56, 2005, 15-39.

[11] Pulford, I. D., Watson, C. Phytoremediation of heavy metal contaminated land by trees – a review. *Environ. Int*. 2003, 29, 529-540.

[12] Pulford, I. D., Dickinson, N. M. Phytoremediation Technologies using Trees. *In:* Prasad, M. N. V., Sajwan, K. S., Naidu R. (eds). *Trace elements in the environment: Biogeochemistry, Biotechnology and Bioremediation*. CRC Press, Boca Raton, Taylor and Francis Group, 2006, pp.375-395.

[13] Rosseli, W., Keller, C., Boschi, K. Phytoextraction capacity of trees growing on a metal contaminated soil. *Plant and Soil*, 2003, 256, 265-272.

[14] Osteras, A. H., Greger, M. Interactions between calcium and copper or cadmium in Norway spruce. *Biol. Plant.* 2006, 50, 4, 647-652.

[15] Dinelli, E., Lombini, L. Metal distribution in plants growing on copper mine spoils in Northern Apennies, Italy: the evaluation of seasonal variations. *Appl. Geochem*. 1996, 11, 375-385.

[16] Ye, Z. H., Whiting, S. N., Lin, Z. Q., Lytle, C. M., Qian, J. H., Terry, N. Removal and distribution of iron, manganese, cobalt and nickel with in a Pennsylvania constructed wetland treating coal combustion by-product leachate. *J. Environ. Qual*. 2001, 30, 1464-1473.

[17] Freitas, H., Prasad, M. N. V., Pratas, J. Plant community tolerant to trace elements growing on the degraded soils of Sao Domingos mine in the south east of Portugal: environmental implications. *Environ. Intl*. 2004, 30, 65-72.

[18] Das, M., Maiti, S. K. Metal accumulation in 5 native plants growing on abandoned Cu-tailings ponds. *App. Ecol. Environ. Res*. 2007, 5, 1, 27-35.

[19] Raju, D., Kumar, S., Mehta, U. J., Hazra, S. Differential accumulation of manganese in three mature tree species (Holoptelia, Cassia, Neem) growing on a mine dump. *Curr. Sci*. 2008, 94, 5, 639-643.

[20] Rai, U. N., Pandey, K., Sinha, S., Singh, A., Saxena, R., Gupta, D, K. Revegetating fly ash landfills with *Prosopis juliflora* L.: Impact of different amendments and Rhizobium inoculation. *Environ. Int*. 2004, 30, 293–300.

[21] Thangavel, P., Subburam, V., Shanmughavel, P., Muthukumar, T. 2000. *Prosopis juliflora* - a metallophyte for the biorecovery of aluminium from urban industrial enclaves. XII IUFRO World Congress 2000, Kula Lumpur, Malaysia.

[22] Senthilkumar, P., Prince, W. S., Sivakumar, S., Subbhuraam, C.V. *Prosopis juliflora*-a green solution to decontaminate heavy metal (Cu and Cd) contaminated soils. *Chemosphere,* 2005, 60, 1493–1496.

[23] Varun, M., Souza, R. D., Pratas, J., Paul, M. S. Phytoextraction potential of *Prosopis juliflora* (Sw.) DC. with specific reference to lead and cadmium. *Bull. Enviro.n Contam. Toxicol*. 2011, 87, 45–49.

[24] Ducic, T., Polle, A. Transport and detoxification of manganese and copper in plants. *Brazilian J. Plant. Physiol.* 2005, 17, 1, 103-112.

[25] Thomas, F., Malick, C., Endreszl, E. C., Davies, K. S. Distinct responses to copper stress in the halophyte, *Mesembryan-themum crystallium. Physiol. Plant.* 1998, 102, 360–368.

[26] Demirevska-Kepova, K., Simova-Stoilova L., Stoyanova, Z., Holzer, R., Feller, U. Biochemical changes in barely plants after excessive supply of copper and manganese. *Environ. Exp. Bot*. 2004, 52, 253–266.

[27] Fargasova, A., Beinrohr., E. Metal–metal interactions in accumulation of V^{5+}, Ni^{2+}, Mo^{6+}, Mn^{2+} and Cu^{2+} in under and above ground parts of *Sinapis alba*. *Chemosphere*, 1998, 36, 1305–1317.

[28] Baker, A. J. M., Proctor, J. The influence of cadmium, copper, leads, and zinc on the distribution and evolution of metallophytes in British Island. *Plant. Systematics Evol*. 1990. 173, 91–108.

[29] Waldermar, M., Ryszard, R., Teresa, U. Effect of excess Cu on the photosynthetic apparatus of runner bean leaves treated at two different growth stages. *Physiol. Plant*. 1994, 91, 715–721.

[30] Lewis, S., Donkin, M. E., Depledge, M. H. Hsp70 expression in *Enteromorpha intestinalis* (Chlorophyta) exposed to environmental stressors. *Aquat. Toxicol.* 2001, 51, 277–291.

[31] Kashem, M. A., Singh, B. R., Kondo, T., Imamul, Huq S.M., Kawai, S. Comparison of extractability of Cd, Cu, Pb and Zn with sequential extraction in contaminated and non-contaminated soils. *Int. J. Environ. Sci. Tech*. 2007, 4, 2, 169-176.

[32] Yan, S., Ling, Q. C., Bao, Z. Y. Metals contamination in soils and vegetables in metal smelter contaminated sites in Huangshi. *Bull. Environ. Contam. Toxicol.* 2007, 79, 361–366.

[33] Awashthi, S. K. 2000. Prevention of Food Adultration Act No. 37 of 1954. Central and State rules as Amended for 1999. 3rd edn., Ashoka Law House, New Delhi.

[34] Kelepertsis, A. E., Andrulakis, J. Geobotany biogeochemistry for mineral exploration of sulphide deposits in Northern Greece - heavy metal accumulation by *Rumex acetosella* L. and *Minuarita verna* (L.) *Hiern. J. Geochem. Explo.* 1983, 18, 267–274.

[35] Borkert, C. M., Cox, F. R., Tucker, M. R. Zinc and Copper toxicity in peanut, soyabean, rice and corn in soil mixtures. *Commun. Soil. Sci. Plant. Anal*. 1998, 29, 2991-3005.

[36] Rodriguez, F. I., Esch, J. J., Hall, A. E., Binder, B. M., Schaller, G. E., Bleecker A. B. A. copper cofactor for the ethylene receptor ETRI from Arabidopsis. *Science*, 1999, 283, 996-998.

[37] Pittman, J. K. Manganese molecular mechanisms of manganese transport and homeostasis. *New Phytol*. 2005, 167, 733–742.

[38] Bowen, H. J. M. 1966. Trace elements in biochemistry. 1st edn. Academic Press, New York, ISBN-13: 9780003686463.

[39] Kabata-Pendias A., Pendias K. 1992. Trace elements in Soils and Plants, 2nd Ed., CRC Press, Boca Raton, FL.

[40] Alloway B. J. 1990. Heavy metals in soils. Blackie Academic & Professional, Glasgow, UK.

[41] Reeves, R. D., Baker, A. J. M.. Metal accumulating plants. *In*: Raskin, I., Ensley, B. D. (eds). *Phytoremediation of toxic metals: Using plants to clean up the environment.* John Wiley & Sons, New York, 2000, pp. 193-230.

[42] (http://www.agnet.org/library/bc/51008/).

[43] Islam, M. M., Halim, M. A., Safiullah, S., Waliul Hoque, S. A. M., Saiful Islam M. Heavy metal (Pb, Cd, Zn, Cu, Cr, Fe, and Mn) Content in textile sludge in Gazipur, Bangladesh. *Res. J. Environ. Sci.* 2009, 3, 3, 311-315.

[44] Connolly, E. L., Guerinot, M. L. Iron stress in plants. *Geno. Biol.* 2002, 3, 8, reviews 1024.1–1024.

[45] Ayari, F., Hamdi, H., Jedidi, N., Gharbi, N., Kossai, R. Heavy metal distribution in soil and plant in municipal solid waste compost amended plots. *Intl. J. Environ. Sci. Technol.* 2010, 7, 3, 465-472.

[46] Bosecker, K. Bioleaching solubilization by microorganisms. *FEMS Microbiol. Rev.* 1997, 20, 591-604.

[47] Krebs, W., Brombacher, C., Bosshard, P. P., Bachofen, R., Brand, I. H. Microbial recovery of metals from solids. *FEMS Microbiol. Rev*. 1997, 20, 605 - 617.

[48] Bojinova, D. Y., Velkova, R. G. Bioleaching of metals from mineral waste product. *Acta Biotechnol.* 2001, 21, 275- 282.

[49] Solisio, C., Lodi, A., Veglio, F. Bioleaching of zinc and aluminium from industrial waste sludges by means of *Thiobacillus ferrooxidans. Waste Manag*. 2002, 22, 667-675.

[50] Aung, K. M., Ting, Y. P. Bioleaching of spent fluid catalytic cracking catalyst using *Aspergillus niger. J. Biotechnol.* 2005, 116, 159-170.

[51] Santhiya, D., Yen-Peng, T. Bioleaching of spent refinery processing catalyst using *Aspergillus niger* with high-yield oxalic acid. *J. Biotechnol.* 2005, 116, 171-184.

[52] Haines, A. K., Van Aswegen, P. C. Process and engineering challenges in the treatment of refractory gold ores. International deep mining conference: innovations in metallurgical plant. SAIMM, Johhanesburg, South Africa. P.103-110 (1990)

[53] Bosecker, K. Bioleaching metal solubilization by microorganisms. *FEMS Microbiol Rev.* 1997, 20, 591-604.

[54] Rawlings, D. E. Industrial practices and the biology of leaching metals from ores. *J. Industrial Microbiol. Biotechnol.* 1998, 20, 268-274.

[55] Agate, A. D. Recent advance in microbial mining. *World J. Microbial Biotechnol.*1996, 12, 487-495.

[56] Torma, A. E. Use of biotechnology in mining and metallurgy. *Biotechnol. Adv.* 1988, 6, 1–8.

[57] Burgstaller, W., Schinner, F. Leaching of metals with fungi. *J. Biotechnol.* 1993, 27, 91–116.

[58] Clausen, C. A., Smith, R. L. Removal of CCA from treated wood by oxalic acid extraction, steam explosion, and bacterial fermentation. *J. Ind. Microbiol. Biotechnol.* 1998, 20, 25, 1–7.

[59] Kartal, S. N., Kose, C. Remediation of CCA-C treated wood using chelating agents. *Holz Roh Werkst.* 2003, 61, 382–387.

[60] Moira, E. K., Henderson, K., Duffy, R. B. J. The release of metallic and silicate ions from minerals rocks and soils by fungal activity. *Soil Sci.* 1963, 14, 23-246.

[61] Mulligan, C. N., Kamali, M. Bioleaching of copper and other metals from low-grade oxidized mining ores by *Aspergillus niger. J. Chem. Technol. Biotechnol.* 2003, 78, 497–503.

[62] Valix, M., Usai, F., Malik, R. Fungal bio-leaching of low grade laterite ores. M*ater. Eng*. 2001, 14, 197-203.

[63] Bansal, V., Sanyal, A., Rautaray, D., Ahmad, A., Sastry, M. Bioleaching of sand by the fungus *Fusarium oxysporum* as a means of producing extracellular silica nanoparticles. *Adv. Mater.* 2005, 17, 889-892.

[64] Savinova, E. R., Chuvilin, A. L., Parmon, V. N. J. Copper colloids stabilized by water-soluble polymers: Part I. Preparation and properties. *Mol. Catal.* 1988, 48, 217-219.

[65] Ershova, B. G., Janata, E., Michaelis, M., Henglein, A. Reduction of aqueous copper (2+) by carbon dioxide (1): first steps and the formation of colloidal copper. *J. Phys. Chem.* 1991, 95, 8996-8999

[66] Tanori, J., Duxin, N., Petit, C., Lisiecki, I., Veillet, P., Pileni, M. P. Synthesis of nanosize metallic and alloyed particles in ordered phases. *Colloid Polym. Sci*. 1995, 273, 886-892.

[67] Guo, L., Wu, Z. H., Ibrahim, K., Liu, T., Tao, Y., Ju, X. Research of nonlinear optical properties of copper nanoparticles. *Eur. Phys. J*. 1999, D9, 591- 594.

[68] Bansal, V., Syed, A., Bhargava, S. K., Ahmad, A., Sastry, M. Zirconia enrichment in zircon sand by selective fungus-mediated bioleaching of silica. *Langmuir,* 2007, 23, 4993-4998.

[69] Bansal, V., Ahmad, A., Sastry, M. Fungus-mediated biotransformation of amorphous silica in rice husk to nanocrystalline silica. *J. Am. Chem. Soc*. 2006, 128, 14059-14066.

[70] Kulkarni, S., Syed, A., Singh, S., Gaikwad, A., Patil, K., Vijayamohanan, K., Ahmad, A. Silicate nanoparticles by bioleaching of glass and modification of the glass surface. *J. Non-Cryst. Solids*. 2008, 354, 3433–3437.

[71] Martinez, L., Romero, R., Lopez, J. C., Romero, A., Mendieta, V.S., Natividad, R. Preparation and characterization of CaO nanoparticles/NaX Zeolite catalysts for the transesterification of sunflower oil sandra. *Ind. Eng. Chem. Res*. 2011, 50, 2665–2670.

[72] Zielinska-Jurek, A., Walicka, M., Tadajewska, A., Lacka, I., Gazda, M., Zaleska, A physicochemical problems of preparation Ag/Cu-doprd titanium (IV) oxide nanoparticles in W/O microemulsion. *Miner. Process*. 45, 2010, 113-126.

[73] Seo, K. I., McIntyre, P. C., Kim, H., Saraswat, K. C. Formation of an interfacial Zr-silicate layer between ZrO_2 and Si through *in situ* vacuum annealing. *Appl. Phys. Lett.* 2005, 86, 082904.-082907.

[74] Margalit, R., Vasquez, R. P, J. Determination of protein orientation on surfaces with X-ray photoelectron spectroscopy. *Protein Chem.* 1990, 9, 1, 105-108.

[75] Wagner, C. D., Riggs, W. M., Davis, L. E., Mouler, J. F. *Handbook of X-Ray Photoelectron Spectroscopy*; Muilenberg, G. E., (Ed) Perkin Elmer Corporation, Physical Electronics Division: Eden Prairie, MN, 1979.

[76] Chusuei, C. C., Brookshier, M. A., Goodman, D. W. Correlation of Relative X-ray Photoelectron Spectroscopy Shake-up Intensity with CuO Particle Size. *Langmuir,* 1999, 15, 2806-2808.

[77] Lei, Y., Korpelainen, H., Li, C. Physiological and biochemical response to high Mn concentrations in two contrasting *Populus cathayana* populations. *Chemosphere,* 2007, 68, 686-694.

[78] Foy, C. D., Chaney, R. L., White, M. C. The physiology of metal toxicity in plants. *Ann. Rev. Plant Physiol.* 1978, 511-566.

[79] Horst, W. J. The physiology of manganese toxicity. *In*: Graham, R.D. Hannam. R. J, Uren, N. J. (eds). *Manganese in Soil and Plants.* Kluwer Academic Publishers, Dordrecht, the Netherlands, 1988, pp. 175–188.

[80] Migocka, M., Klobus, G. The properties of the Mn, Ni and Pb transport operating at plasma membranes of cucumber roots. *Physiol. Plant*. 2007, 129, 578-587.

[81] Xue, S. G. 2002. Ecological restoration experiment on Xiangtan Manganese Tailings in Southern China. Master's degree thesis, Central-South Forestry University, China (in Chinese).

[82] Yang, S. X., Li, M. S., Li, Y., Huang, H. R. Study on heavy metal pollution in soil and plants in Pingle Manganese Mine, Guangxi and implications for ecological restoration. *Min. Saf. Environ. Protect.* 2006, 1, 21- 23 (in Chinese)

[83] Zhang, H. Z., Liu, Y. G., Huang, B. R., Li, X. A survey of heavy metal content in plants growing on the soil polluted by manganese mine tailings. *Chin. J. Ecol.* 2004, 1, 111-113.

[84] Paschke, M. W., Valdecantos, A., Redente, E. F. Manganese toxicity thresholds for restoration grass species. *Environ. Pollut.* 2005, 135, 313-322.

[85] Proctor, J., Phillips, C., Duff, G. K., Heaney, A., Robertson, F. M. Ecological studies in Gunung Silam, a small ultra basic mountain in Sabah, Malaysia II. Some forest processes. *J. Ecol.* 1989, 77, 317-331.

[86] Bidwell, S. D. 2000, Hyperaccumulator of metal in Australian native plants. Ph.D. Thesis, University of Melbourne, Australia.

[87] Xue, S. G., Chen, Y. X., Lin, Q., Xu, S. Y., Wang, Y. P. *Phytolacca acinosa* Roxb: a new manganese hyperaccumulator plant from south China. *Acta. Ecologica. Sinica.* 2003, 5, 935- 937 (in Chinese with English abstract).

[88] Xue, S. G., Chen, Y. X., Reeves, R. D., Baker, A. J. M., Lin, Q., Fernando, D. Manganese uptake and accumulation by the hyperaccumulator plant *Phytolacca acinosa* Roxb. (Phytolaccaceae). *Environ. Pollut.* 2004, 131, 393-399.

[89] Wong, M. H. Ecological restoration of mine degraded soils, with emphasis on mental contaminated soils. *Chemospere,* 2003, 50, 775-780.

[90] Sparks, D. L., Page, A. L., Helmke, P. A., Leoeppert, R. H., Soltanpour, P.N, Tabatabai, M.A, Johnston, C. T., Sumner, M. E. *Methods of Soil Analysis. Part 3. In.* Madison W.I., (eds). *Chemical Methods. Soil Science Society of America*, 1996, pp. 487- 489.

[91] Lab Procedures 1970, Soil testing and Plant Analysis Laboratory, Cooperative Extension Service, Athens, G.A.

[92] Bidwell, S. D. Hyperaccumulator of metal in Australian native plants. Ph.D. thesis, University of Melbourne, Australia, 2000.

[93] Memon, A. R., Chino, M., Takeoka, Y., Hara, K, Yatazawa. M. Distribution of Manganese in leaf tissue of the manganese accumulator. *Acanthopanax sciadophylloides* as revealed by electronprob X-ray microanalysis. *J. Plant Nutr*. 1980, 2, 457-47.

[94] Fernando, D. R., Bakkaus E, J., Perrier, N., Baker, A. J. M., Woodrow, I. E., Batianoff, G. N., Collins, R. N. Manganese accumulation in the leaf mesophyll of four tree species, a PIXE/EDAX localization study. *New Phytol*. 2006, 171, 751-758.

[95] Bidwell, S. D., Woodrow, I. E., Batianoff, G. N., Sommer-Knusden, J. Hyperaccumulation of manganese in the rainforest tree *Austromyrtus bidwillii* (Myrtaceae) from Queensland, Australia. *Funct. Plant. Biol*. 2002, 29, 899-905.

[96] Baker, A. J. M., McGrath, S. P., Reeves, R. D., Smith, J. A. C. Metal hyperaccumulator plants: A review of the ecology and physiology of a biological resource for phytoremediation of metal-polluted soils. *In:* Terry N., Banuelos G. (eds). *Phytoremediation of Contaminated Soil and Water,* Lewis Publishers, Florida, 2000, pp. 85-107.

[97] Ye, Z. H., Baker, A. J. M., Wong, M. H., Willis, A. J. Copper tolerance, uptake and accumulation by *Phragites australis*. *Chemosphere*, 2003, 50, 795-800.

[98] Van der Lelie, D., Schwitzguébel, J. P., Glass, D. J., Vangronsveld, J., Baker, A., Assessing phytoremediation's progress in the United States and Europe. *Environ. Sci. Technol*. 2001, 35, 446A–452A

[99] Clemens, S. Molecular mechanisms of plant metal tolerance and homeostasis. *Planta*. 2001, 212, 475-486. .

[100] Rossi, G., Ehrlich, H. L. Other bioleaching processes *In*: Ehrlich, H. L., Brierley, C. L. (eds). *Microbial mineral leaching*. Mc Graw-Hill Inc., New York, 1990, pp. 149-170.

[101] Creamer, N. J., Baxter-plant, V. S., Henderson, J., Potter, M., Macaskie, L. E. Palladium and gold removal and recovery from precious metal solutions and electronic scrap leachates by *Desulfovibrio desulfuricans*. *Plant Biotechnol. Lett*. 2006, 28, 1475–1484.

[102] Pak, K. R., Lim, O. Y., Lee, H. K., Choi, S. C. Aerobic reduction of manganese oxide by *Salmonella sp*. strain MR4. *Biotechnol. Lett*. 2002, 24, 1181–1184.

[103] Bang, S. W., Clark, D. S., Keasling, J. D. Cadmium, lead, and zinc removal by expression of the thiosulfate reductase gene from *Salmonella typhimurium* in *Escherichia coli*. *Biotechnol. Lett*. 2000, 22, 1331–1335.

[104] Acharya, C., Kar, R. N., Sukla L. B., Misra V. N. Fungal leaching of manganese ore *Trans. Indian Inst. Met*. 2004, 57, 5, pp. 501-508.

[105] Taira, S., Kitajima, K., Katayanagi, H., Ichiishi, E., Chiyanagi, Y. Manganese oxide nanoparticle-assisted laser desorption/ionization mass spectrometry for medical applications. *Sci. Technol*. *Adv. Mater*. 10, 2009, 034602.

[106] Tan, B. J., Klabunde, K. J., Sherwood, P. M. A. XPS studies of solvated metal atom dispersed (SMAD) catalysts. Evidence for layered cobalt-manganese particles on alumina and silica. *J. Am. Chem. Soc*. 1991, 113, 855–861.

[107] Strohmeier, B. R., Hercules, D. M. J. Surface spectroscopic characterization of. Mn/Al$_2$O$_3$ catalysts. *Phys. Chem. B,* 1984, 88, 4922–4929.

Chapter 3

Biosynthesis of intra and extracellular nanomaterials by using plants.

Summary:

Inorganic nanomaterials of different chemical compositions are conventionally synthesized under harsh environments like extremes of temperatures, pressure and pH. Moreover, these methods are eco-unfriendly, cumbersome, yield bigger particles and agglomerate due to not being capped by capping agents. In contrast, biological synthesis of inorganic nanomaterials occurs under ambient conditions viz., room temperature, atmospheric pressure and physiological pH. These methods are reliable, eco-friendly and cost-effective.

In this chapter we report the synthesis of GNPs which was studied using different fractions of *Semecarpus* leaves. The extracts of green, boiled and biomass of *Semecarpus anacardium* L. leaves were used for the synthesis of GNPs. The formation of particles was observed in all the three conditions. The synthesis of GNPs was more in green extract. Synthesis of intracellular and extracellular gold nanoparticles (GNPs) by using living seedlings and callus cells induced from the leaves of *Arachis hypogaea* (Peanut) was studied. Living seedlings and callus cells exposed to $HAuCl_4$ solution led to the formation of stable GNPs. The intracellular GNPs from dried and fresh root tissue of peanut were recovered by crushing the root tissue in ethanol. The recovered particles were characterized and confirmed.

Section 1

Synthesis of gold nanoparticles by various leaf fractions of *Semecarpus anacardium* L. tree.

Semecarpus leaves

Green extract   Boil extract   Biomass

GNPs formed

TEM images
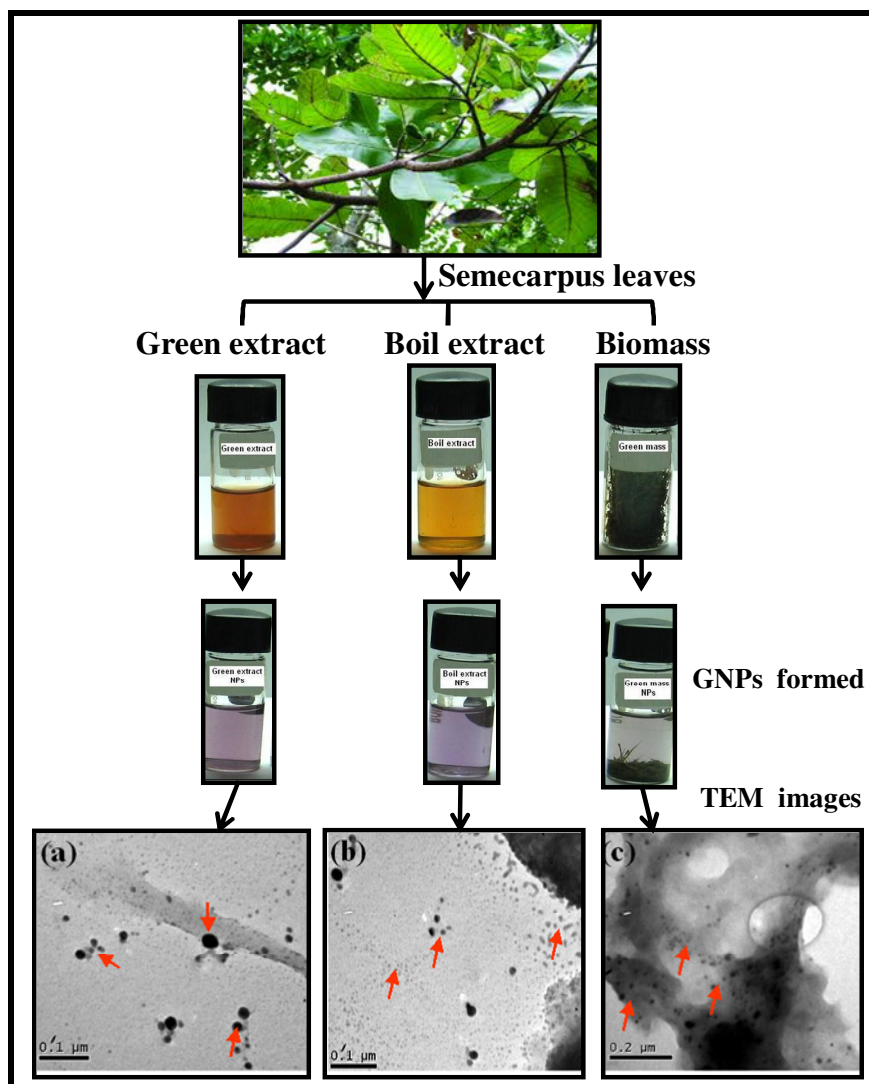
<div align="center">**Section 1**</div>

3.1 Synthesis of gold nanoparticles by various leaf fractions of *Semecarpus anacardium* L. tree.

3.1.1 Introduction

Nanotechnology is one of the upcoming areas of modern science. Nanoparticles find various applications in drug formulations and therapeutic medicine [1, 2]. Utilization of biological systems has emerged as a novel route for the synthesis of nanoparticles (NPs) and nano wires. The advantages of using plant materials for the synthesis of nano materials against the use of microorganisms are emphasized [3]. Microorganisms need maintenance of cultures and controlled conditions such as temperature, pH and other factors for growth. Plant extracts are continuously explored for the production of metal NPs [4, 5]. Use of freshly prepared untreated extracts, parts or whole plants in NPs synthesis is under-explored [6]. *Medicago sativa* (*A*lfalfa) seedlings germinated on gold rich medium reduced the ionic form of gold and silver into NPs in leaf, stem and roots [7, 8].

However, reports on synthesis of NPs by tissues of tree species are rather scarce. Production of NPs using tree tissues has additional advantages. The trees can serve as the perennial source of material for production of NPs from metal rich soil thereby supporting the concept of nanoparticles farming [7, 8]. Although there are a few reports [3] on production of NPs using boiled extract of leaves from tree species (*Azadirachta indica*), there is no report on the synthesis of gold NPs using water extracts of green leaves or green leaf-derived biomass of trees growing in a natural environment. Here we demonstrate the natural ability of a tree species for rapid synthesis of gold NPs using water extracts of *Semecarpus anacardium* leaves and leaf derived biomass to synthesize gold NPs from $HAuCl_4$. Both Alfalfa [7] and *Brassica juncea* [9] plants, in which synthesis of NPs has been demonstrated, are herbaceous species and are annual crops.

Similar work is not done in tree species to demonstrate intracellular NP synthesis. There are few reports on tree species *Boswellia ovalifoliolata* [10], *Jatropha curcas* L. [11] and *Azadirachta indica* [3] describing the synthesis of NPs using boiled extracts

of bark and leaves. In *Syzygium cumini*, extracts of dry powders of leaf and seeds were used for the synthesis of silver NPs [12]. Some microorganisms [4] have been identified for their ability to synthesize NPs isolated from plants.

There are reports [4, 3, 13-16] describing methods for production of NPs using boiled leaf extracts of *Pelargonium* sp., *Aloe vera, Pinus* sp., *Persimmon* sp., *Ginkgo* sp., *Mangnolia* sp., *Platanus* sp., *Magnolia kobus and Diopyros kaki.* The *Pelargonium* and *Aloe vera* leaves were boiled and used for reduction of NPs. The leaves of other plants were dried at room temperature and then were boiled and used for the reduction of NPs. In the present investigation, the boiled leaf extract of *S. anacardium* was tested as a control.

3.1.2 Experimental details

3.1.2.1 UV-vis analysis:

The reaction mixtures incubated at room temperature were scanned at 0 hr from 300 to 800 nm wave lengths with UV-vis Spectrophotometer (Perkin Elmer) using a dual beam operated at 1 nm resolution. The reaction mixtures were scanned under the same wavelengths at different time intervals.

3.1.2.2 Quantification of extracellular gold by inductive coupled plasma atomic emission spectrometry (ICP-AES):

Gold nanoparticles were separated from unreacted ions by centrifuging 3 mL each of green extract, boiled extract and biomass nanoparticle solutions at 15,000 rpm for 30 min. These separated gold nanoparticles were redispersed in 20 mL of deionized water, subsequently digested with 6 mL of aqua regia (3:1 v/v concentrated HCl and concentrated HNO_3) and the volume was made to 30 mL [17]. Gold nanoparticles in each reaction mixture were quantified using ICP-AES Spectro Arcos at 267.59 nm.

In case of peanut seedlings, intracellular GNPs were analyzed by separating leaf, stem and root from the seedling which was exposed to $HAuCl_4$ and dried in oven at 70°C till it achieved constant weight. 100 mg of dried power was taken in borosil vials and digested with 3 mL of nitric and 1 mL of perchloric acid in 3:1 ratio and heated on hot plate till a clear solution was formed, the volume was then made to 30 mL. The quantification of gold was done using ICP-AES Spectro Arcos at 267.59 nm.

3.1.2.3 Transmission electron microscopy (TEM):

The images of Au NPs were recorded with TEM for determination of the shape, size of the particles along with their SAED. Two to three drops of the sample solutions and the control were placed individually on carbon coated copper grids and the moisture was allowed to evaporate. TEM measurements were performed on JOEL model 1200EX instrument operated at an accelerating voltage of 120 kV. The measurements of particles sizes were determined using Gatan software.

3.1.2.4 Scanning electron microscopy (SEM):

One mL of Au NPs formed by green extract, green biomass and boiled extract were coated on the stub by placing small drops of nanoparticle suspension every time and eliminating the moisture before adding another drop. The intracellular EDS were done by adding approximately 1 mL of methanol to the peanut plant's root powder and ground finely. The slurry was coated on the stub. The presence of Au was analyzed with SEM, attached with phoenix EDS to identify the elemental composition.

3.1.2.5 X-ray diffraction analysis (XRD):

The particles were isolated by centrifuging 20 mL of the suspension in deionized water containing Au NPs for 20 min at 10,000 rpm. These were washed three times to remove the unbound proteins and other metabolites. The pellet of NPs was re-suspended in deionized water and coated on a glass plate. This was dried in the oven at 50°C for removing water content and used for XRD studies. The intra cellular gold nanoparticles in peanut root sample were dried at 70°C and the root sample powder was used for XRD analysis.

3.1.2.6 Fourier Transform Infrared Spectroscopy:

An attempt to understand the responsible factor for NPs formation was carried out. The suspension was centrifuged at 10,000 rpm for 10 min. The supernatant was discarded and the pellet was washed with deionized water to remove the excess amount of reducing agents and other compounds which were not bound to NPs. The process of centrifugation and re-dispersion in deionized water was repeated three times to ensure better separation of free entities from the metal nanoparticles. The purified pellets were then dried and the powders were subjected to FTIR spectroscopy

measurement. These measurements were carried out in KBr pellets on a Perkin–Elmer instrument in the diffuse reflectance mode at a resolution of 4 cm^{-1} in KBr pellets.

3.1.2.7 Light microscopy:

After the harvest of peanut plant from NPs solution, the control roots and Gold chloride solution exposed roots were excised. Cross sections of the roots were taken with a hand held razor blade and observed under light microscope.

3.1.2.8 High Resolution Transmission Electron Microscopy (HRTEM):

For the HRTEM analysis, the plant root samples were fixed in 2.5% glutaraldehyde and caodylate buffer pH 7.2 for overnight, the peanut root was washed 3 times with 0.1M caodylate buffer pH 7.2 for 5 min, dehydrated in different grades of ethanol, washed 3 times with acetonitrile for 10 min and then embedded in a synthetic resin and dried in a furnace at 60°C for 48 hr. The blocks were prepared and thin sections (50-100 nm) were cut using an ultra microtome with diamond knife and put on Cu grids and placed on the sample holder of the TEM. The samples were not stained for the TEM analysis. As a consequence, the only possible sources of contrast are mass thickness differences.

3.1.2.9 X-Ray Photoemission Spectroscopy (XPS):

The XPS analysis of the gold nanoparticles was done by casting them on to a Si substrate and analyzed in a VG MicroTech ESCA 3000 instrument.

3.1.2.10 Preparation of water extracts and biomass:

Intact leaves of *Semecarpus* were washed thoroughly with distilled water for few minutes and the water adhering to the tissue was air dried. The loss of biomolecules and soluble components was avoided using the intact leaves (with petioles). Thirty gm of leaves was weighed and homogenized in 100 mL of sterile deionized water and transferred to centrifuge tubes. These were centrifuged at 10,000 rpm for 15 min. The supernatant and the pellet were separated. Hereafter, the liquid fraction is identified as ''green extract'' and the solid fraction as ''green biomass''.

Boiled extract of *Semecarpus* leaves was prepared by cutting 30 gm of leaves into small pieces and boiled in 100 mL of sterile deionized water for 30 min. This extract

was used as a control. The solution was cooled and filtered using filter paper. The extract prepared by boiling the leaves was identified as ''boiled extract''. Boiled leaf extracts have been used for the synthesis of nanoparticles by other researchers [14]. The green extract, green biomass and boiled extract were used for the reduction experiments. The pH of the green extract was 5.37 whereas the boiled extract was 5.35. Both the liquid extracts were straw colored and the green extract was darker than the boiled extract.

In four graduated test tubes, 5 mL of 10^{-4} M solution of $HAuCl_4$ was taken. In two of these tubes 200μl of green extract or boiled extract was added. In the third tube 500 mg of green mass was added. The volumes were made to 10 mL with 10^{-4} M $HAuCl_4$ solution. After 4 hr the mixture was filtered using Whatman filter paper and the filtrate was used for the detection, quantification and characterization of the NPs. In the fourth tube, the solution of 10^{-4} M $HAuCl_4$ was taken as control. The yield of particle synthesis was determined by UV and inductive coupled plasma atomic emission spectroscopy (ICP-AES). The particles were characterized using transmission electron microscopy (TEM), scanning electron microscopy (SEM), energy dispersive spectroscopy (EDAX), and X-ray diffraction (XRD). Distribution of the particles of various sizes was determined using the Gatan software. An attempt was made to identify the critical factors responsible for the reduction of Au using Fourier transform infrared spectroscopy (FT-IR) and the crystalline nature was confirmed by XRD and TEM.

3.1.3 Results and Discussion

3.1.3.1 UV-vis and ICP-AES analyses:

The UV-vis scan at 0 hr reaction did not show peak formation at 530–550 nm in the reaction mixtures containing green extract, boiled extract or green biomass (Fig. 3.1A). After a period of 15–20 min of the reaction at room temperature, there was a change in color of the reaction mixture to pink due to the reduction of $HAuCl_4$ to metallic Au (0) NPs (Fig. 3.2). There was no change in the color of the control mixture without extracts or green biomass.
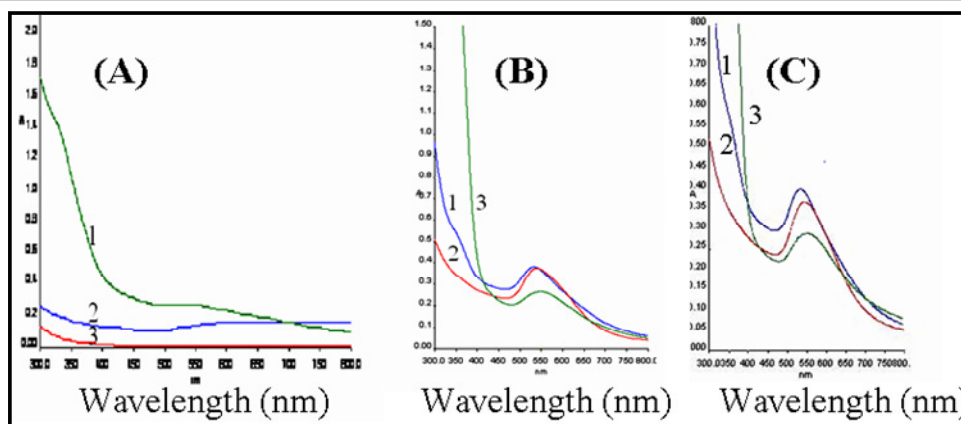
Figure 3.1 UV-vis spectra in ranges from 300 – 800 nm of 10^{-4} M HAuCl$_4$ solution with, **(1)** green extract. **(2)** boiled extract and **(3)** green mass. **(A)**. 0 hr reaction. **(B)**.1 hr reaction. **(C)** 4 hr reaction.
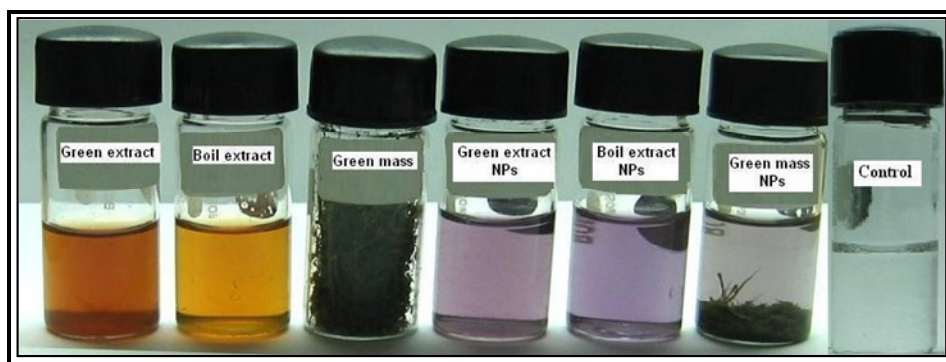

Figure 3.2: Appearances of the green extract, boiled extract and green biomass used for reduction of 10^{-4} M HAuCl$_4$, the change in color after the reaction and formation of gold NPs. No change in color in control with 10^{-4} M HAuCl$_4$.

After 1 hr these solutions were subjected to UV–vis spectroscopy scanning from 300 to 800 nm wavelength. The maximum intensity of the peaks for all leaf derived samples was noted at 530–550 nm (Fig. 3.1B, C) indicating the presence of gold particles [18]. The peak intensities were different for each leaf derived sample. Most intense peak was noted in the mixture with green extract. This was followed by the boiled extract and the green biomass. Peak with higher intensity suggests increased gold NP concentration (Fig. 3.1). UV–vis spectra ranged from 300 to 800 nm of 10^{-4} M HAuCl$_4$ solution with, 1- green extract, 2- boiled extract and 3- green mass at 0 ,1 and 4 hr reaction (Fig. 3.1).

Appearances of the green extract, boiled extract and green biomass used for reduction of 10^{-4} M $HAuCl_4$ and the change in color after the reaction and formation of gold NPs was noted. No change in color was noted in control with 10^{-4} M $HAuCl_4$ in accordance with other researchers [19]. NPs synthesized were quantified using ICP-AES spectro Arcos at 267.59 nm. The amount of GNPs in green extract, boiled extract and green biomass were 20.82, 17.99, and 8.29 ppm, respectively. The concentration was showing similar pattern as noted in UV spectroscopy. It is not clear if the increased response in the presence of the green extract could be due to the existence of active proteins and other bioactive molecules as the extract was prepared at room temperature. Due to the mutilation of the cells the proteins and other active biomolecules leached in the extract. Presumably these proteins or other molecules enhanced the reduction of $HAuCl_4$. Production of NPs due to the presence of proteins was reported earlier [4, 15, 16]. Alternately, the increased production of NPs by the unboiled extracts could be due to the presence of co-existing microorganisms in the leaves which enhanced the process of reduction and the yield of NPs. The microorganisms harbor the plants in the natural stands and there are reports on production of NPs by microorganisms [4]. Boiling of the extract may destroy the microorganisms or denaturize the proteins and other biomolecules causing reduced reduction of $HAuCl_4$. The kinetics was studied to determine if the reaction has stopped or continued.

The reaction mixtures were scanned with UV spectrophotometer at 0, 1 and 4 hr. There was an increase in the intensity of peaks in UV absorbance (Fig.3.1B, C), with the period of the reaction. With the extension of the reaction period the intensity of the peaks increased in all three reaction mixtures with *S. anacardium* leaf derived components suggesting the increase in gold NP concentration. The optimum reduction of $HAuCl_4$ in the presence of untreated water extract followed by boiled extract and minimum reduction by the untreated biomass indicates that (1) the factors responsible for the production of NPs by the *S. anacardium* leaves have possibly moved out in the soluble fraction and (2) some of these factors are heat labile.

3.1.3.2 TEM analysis:

TEM images of particles formed with green extract, boiled extract and green biomass showed that the particles were of different shapes and sizes according to the results of surface plasmon absorption. The particle sizes ranged from 13 to 55 nm (Fig. 3.3A–C) and were polydispersed. In green extract, more number of particles were of 15 and 16 nm. In boiled extract, more number of particles ranged between 16 and 18 nm. In green biomass, 14 and 21 nm size particles were more (inserts in Fig. 3.3A–C). The average diameter of nanoparticles in green extract was 18.63 nm, in boiled extract 19.22 nm and in biomass was 18.12 nm. The particles of green extract, boiled extract and green biomass were in crystalline form as shown in SAED (Fig. 3.3D–F) and XRD (Fig. 3A–C).
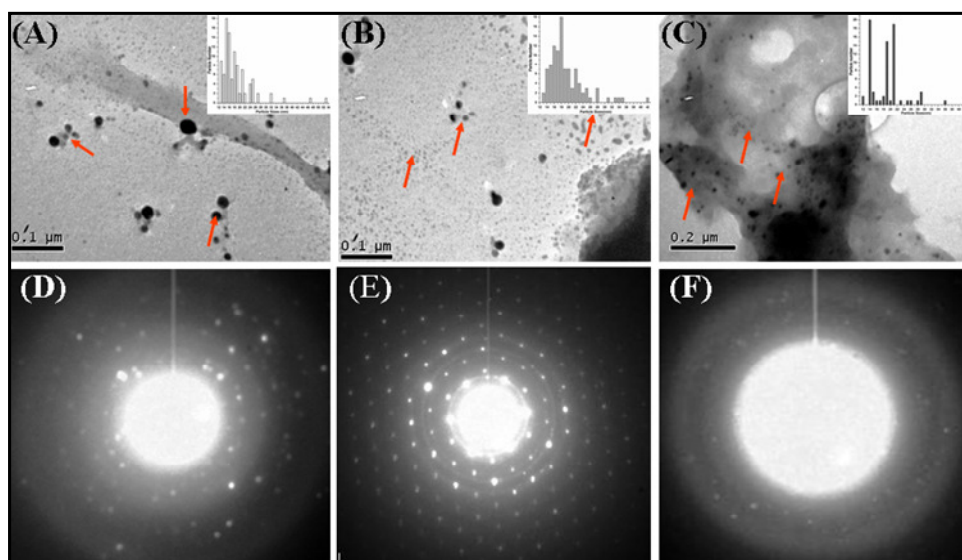
Figure. 3.3: TEM images of gold NPs synthesized by reducing 10^{-4} M HAuCl$_4$ ions using **(A)** Green extract. **(B)** Boiled extract. **(C)** Green biomass of Semecarpus leaf and SAED **(D- F)** of corresponding NPs. Insert images shows the particles size distribution.

3.1.3.3 EDS analysis:

EDS analysis of the samples (Fig. 3.4A–C) shows a strong peak of Au in all the three reactions. Other peaks of Cu and Zn were from the stub used for EDAX analysis. The stubs were made up of the alloys of metals. The weaker carbon peaks were possibly due to the biomolecules that are bound to the particles [14]. The intensity of Au NPs

peaks was stronger in green extract, followed by boiled extract and green biomass. The trend was similar to the pattern noted in UV spectroscopy where equal volume of NPs solution was used for EDS study.
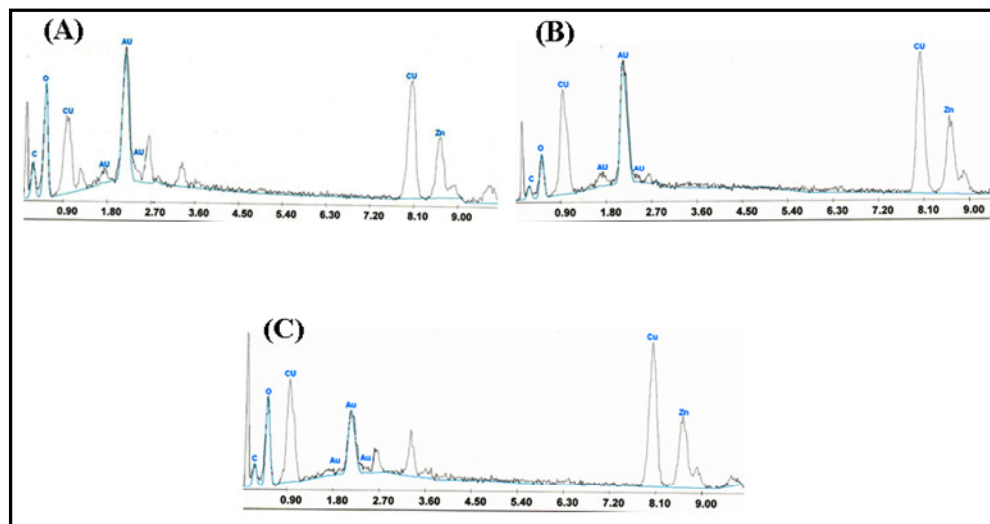
Figure 3.4: EDS analysis of gold NPs. **(A)** Green extract. **(B)** Boiled extract. **(C)** Green biomass.

3.3.3.4 FT-IR analysis:

The FT-IR spectra (Fig. 3.5A, 1, 2) show peaks at 771, 1,027, 1,377, 1,628 and 2,919 cm^{-1}. The peaks 1,027 and 1,377 cm^{-1} could be due to the bending vibration of C–O–C groups and the antisymmetric stretching bands of COH groups of polysaccharides or chlorophylls [5]. The peak at 1,628 cm^{-1} could be due to the amide-I protein. Similar peak at 1,658 cm-1 identified for amide-I protein was previously reported [4]. The peaks at 2,919 cm^{-1} could be due to the stretching vibrations of methylene groups [6]. Methylene compounds and Amide-I protein thus detected possibly support the reduction of particles. The only extra peak in green extract is at 3,278 cm^{-1}. This could be due to the hydrogen bonded NH group [20]. The spectrum for green biomass reduced reaction (Fig.3.5B) shows peaks at 1,216, 1,425, 1,521, 2,401 and 3,020 cm^{-1}. The peak 1,425 cm^{-1} indicates bending vibration of COH groups and a strong peak at 1,216 cm^{-1} could be due to the amide III protein [4]. This indicates that some proteins had played a role in reduction of $HAuCl_4$ to generate particles. Peak at 1,521 cm^{-1} is a characteristic of stretching vibration of the NH groups [5]. The peak 3,020 cm^{-1} is O–H group of alcohols or phenols indicating phenols have also played a role in the reduction of NPs content [20].
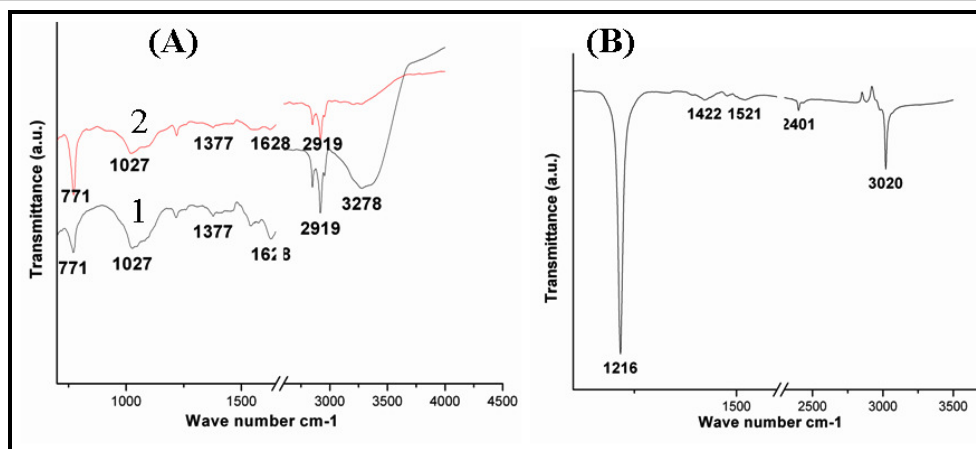
Figure 3.5: FT-IR spectra recorded from gold NPs solution. **(A) 1**. Green extract. **2.** Boiled extract and **(B)** Green biomass.

3.3.3.5 XRD analysis:

X-Ray diffraction (XRD) of particles of green extract, boiled extract and green biomass were carried out after coating on a glass substrate. The prominent Bragg reflection could be seen. The reflections were assigned to diffraction from (111), (200), (220), (311) and planes of face center cubic (fcc) at the 2 theta of 38.109, 44.36, 64.17, and 77.26. All diffraction patterns of NPs of the substrate used in the reduction showed similar patterns despite different intensity of the peaks as illustrated in Fig. 3.6A–C.
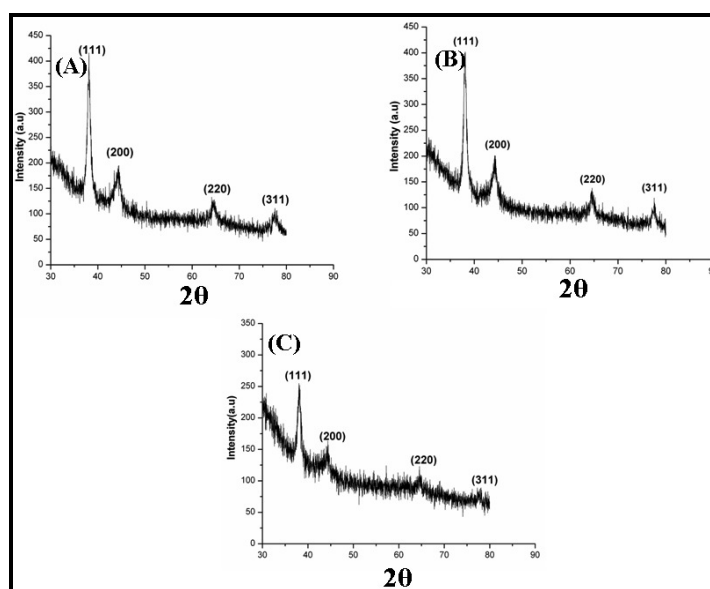
Figure 3.6: XRD patterns of gold NPs synthesized by the reaction of 10^{-4} M HAuCl$_4$ solution with **(A)** Green extract, **(B)** Boiled extract and **(C)** Green biomass.

3.1.4 Conclusions

In this study, the natural ability of the *S. anacardium* leaf extract and leaf derived biomass to synthesize gold NPs from $HAuCl_4$ was demonstrated. Comparison of untreated extract, boiled extract and untreated biomass showed that the reduction of $HAuCl_4$ was optimum in the reaction mixture with green extract. This suggests that the mechanism responsible for the reduction of $HAuCl_4$ to make NPs is naturally present in S. *anacardium* leaves and some of these factors are heat labile. Further experiments will demonstrate if the leaves or the *S. anacardium* plants have the ability to reduce other metal ions and produce NPs. The present method for testing the green leaves of *S. anacardium* is simple and fast. This method can possibly be applied for testing the NP producing capability of other naturally growing plants.

Section 2

Synthesis of intra and extracellular gold nanoparticles by living peanut plant (*Arachis hypogaea* L.)

Protein

Gold Nanoparticles

Gold ions
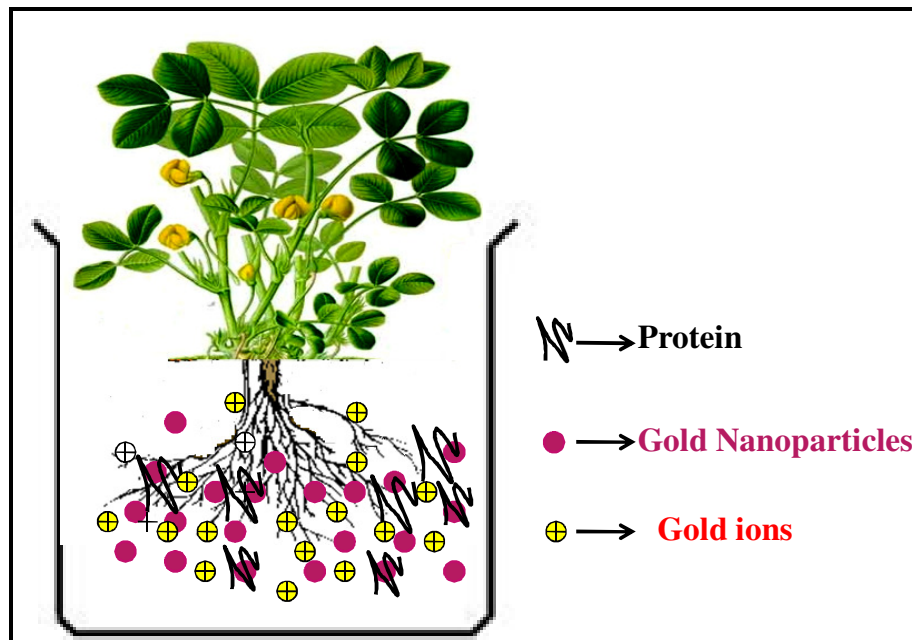
Section 2

3.2 Synthesis of extra and intra cellular gold nanoparticles by live peanut plant (*Arachis hypogaea* **L.**)

3.2.1 Introduction

An important area of research in nanotechnology is the synthesis of nanoparticles of different chemical compositions, sizes, shapes and controlled dispersities. Currently, there is a growing need to develop environmentally benign nanoparticle synthesis processes which do not use toxic chemicals in their synthesis protocols. As a result, researchers in the field of nanoparticle synthesis and assembly have turned to biological systems for inspiration [21].

Understanding biochemical processes which led to the formation of nanoscale inorganic materials is therefore potentially appealing as environmentally friendly alternatives to chemical methods for nanoparticle synthesis. Although biotechnological applications such as, remediation of toxic metals have used microorganisms such as bacteria and yeast, the use of microorganisms as possible eco-friendly nano factories has now been realized [21- 28].

The other green processes for the synthesis of nanoparticles by various plant extracts have been well studied such as Diopyros, Magnolia, Ginkgo, Platanus, Pinus *Azadirachta indica*, Lemongrass plants, *Boswellia ovalifoliolata, Jatropha curcas Azadirachta indica* extracts [15, 16, 3, 13, 10, 11]. In *Syzygium cumini*, extracts of dry powders of leaf and seeds were used for the synthesis of silver NPs [12]. In our earlier report [29], synthesis of gold nanoparticles by using various leaf fractions of *Semecarpus anacardium* L. was demonstrated.

While microorganisms such as bacteria, actinomycetes, and fungi are used in metal nanoparticles synthesis, the use of parts of whole plants in nanoparticles synthesis methodologies is an exciting possibility that is relatively unexplored and underexploited. Using plants for synthesis of nanoparticles could be advantageous over other environmentally benign biological processes by eliminating the elaborate process of maintaining cell cultures.

Although it is well-known that inactivated biological systems interact with metal ions, the connection between metal ions and biological systems is more in depth. Many elements at trace concentrations are essential for the plant's growth and propagation. The same elements at higher concentrations are toxic to some plants. More specifically it has been shown that many bacteria and plants can uptake and bio reduce metal ions from soils and solutions [7].

The uptake of Au (0) and Ag (0) from the agar medium by alfalfa roots from the medium and then transfer to the shoot of the plant in the same oxidation state has been shown by Gardea-Torresdey et al [7, 8]. It was reported by [30] that the growth of *Sesbania* seedlings in chloroaurate solution resulted in the accumulation of gold with the formation of stable gold nanoparticles in plant tissues. The synthesis of mixed metal nanoparticles by plants suggests the possibility of using plants to produce catalysts of specific composition which are difficult to synthesize by traditional methods. The nanoparticles contain Au, Ag and Cu as an alloy in the plant tissue. Using plants to synthesize large quantities of metallic nanoparticles is feasible, the large uptake and reduction of silver ions and distribution as silver nanoparticles within the cellular structure by both *Medicago sativa* and *Brassica juncea* was reported by [31].

There are few reports on use of living plants (*Medicago sativa, Brassica juncea* and *Sesbania*) explored for the synthesis of intracellular nanoparticles. The synthesis of gold nanoparticles (GNPs) intracellularly and extracellularly by using living plant *Arachis hypogaea* (Peanut) without any interference of other metal ions has been carried out by us. To the best of our knowledge, there is no literature on synthesis of both intra and extracellular gold nanoparticles by the same living plant.

3.2.2 Experimental Details

Mature pods of *Arachis hypogaea* (Peanut cultivar SB-11) were collected from the local market. The seeds were washed in running tap water for 10 min followed by repeated washing with deionized water. Thereafter, the seeds were treated with1% bavistin for a period of 30 min and later with 4% savlon (v/v) for 12 min. On removing traces of savlon by repeated washing with sterile water, these seeds were disinfected by 0.1% $HgCl_2$ (w/v) treatment for 10 min. Adhering $HgCl_2$ was

eliminated by rinsing the seeds with sterile deionized water. The testa of these seeds was removed aseptically, and the seeds were cultured on Whatman filter paper support in deionised water in test tubes. The seed cultures were incubated using a 16 hr photoperiod at 25±2°C. The pH of the deionised water was adjusted to 5.8 prior to autoclaving.

After a period of 15 days, well grown seedlings were used for the synthesis of nanoparticles. Gold chloride solution was prepared under sterile conditions. 10 mL of 10^{-4}M HAuCl$_4$ solution was added to the sterile tubes. Under sterile conditions, the seedlings were transferred to autoclaved test tube containing 10^{-4}M HAuCl$_4$ solution.

The NPs were characterized by UV-vis, Intracellular NPs were quantified by ICP-AES, TEM, HRTEM, SEM, EDS and XRD. Distribution of the particles of various sizes was determined using the Gatan software. An attempt was made to identify the critical factors responsible for the reduction of Au using FT-IR and the crystalline nature was verified by XRD.

3.2.3 Results and Discussion

3.2.3.1 Characterization of Extracellular gold NPs

3.2.3.1.1 Visible and UV-vis spectroscopic analysis:

Peanut seedlings were exposed to 10^{-4} M HAuCl$_4$ solutions under sterile conditions. After a period of 20-30 min, there was change in the colour of the 10^{-4} M HAuCl$_4$ solution from colour less to purple at room temperature, thus indicating the formation of nanoparticles while there was no change in colour in control solution (Fig. 3.7). The appearance of purple colour was due to the excitation of surface plasmon vibrations of Au NPs [32]. The purple colour of the nanoparticles intensified with time.
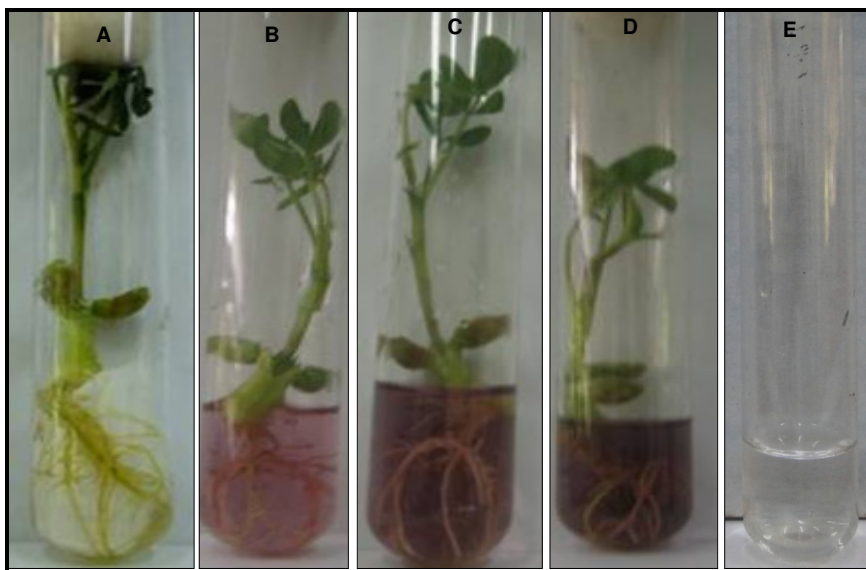
Figure 3.7: (A) plant growing on filter paper, **(B)** 24 hr, **(C)** 48 hr, **(D)** 72 hr exposed seedlings, **(E)** 10^{-4} HAuCl$_4$ solution.

After a period of 2 hr, 1 mL of the coloured solution was taken under aseptic conditions and scanned in UV-vis spectroscope from 300 nm to 800 nm. There was a peak at 520 to 540 nm which shows the formation of nanoparticles also noted [18]. Intensity of the peak increased with an increase in time. The samples were scanned at 0 hr to 72 hr (Fig. 3.8) which indicates an increase in the formation of NPs. In earlier reports [3, 5, and 16], an increase in the intensity of UV peak has been noted with an increase in time. In the present work also, the peanut plant synthesised nanoparticles increased with time. Similarly in our earlier report [29], the increased formation of nanoparticles by *Semecarpus* leaves was studied with respect to time scale.
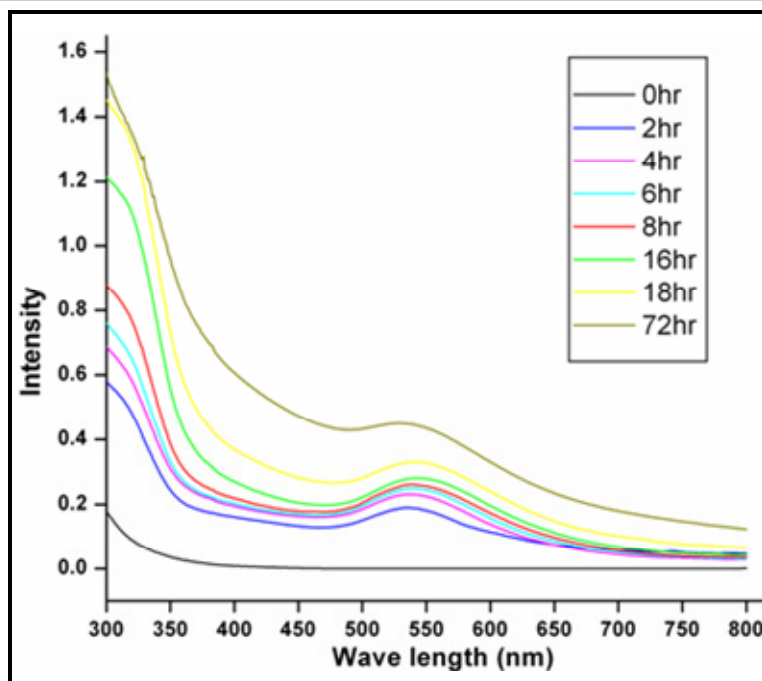
Figure 3.8: UV-vis spectra showing time dependent reaction of gold NPs synthesized by peanut seedling.

3.2.3.1.2 High Resolution Transmission Electron Microscopy:

The HRTEM visualization provides the sizes and shapes of nanoparticles synthesized by peanut plant. The HRTEM images are shown at different magnifications (Fig. 3.9A, B). The particles are polydispersed and highly spherical in morphology. All the particles are well separated with no agglomeration. Selected area electron diffraction (SAED) pattern obtained from gold nanoparticles is shown. The Scherrer ring pattern characteristic of face centered cubic (fcc) gold is observed, showing that the structures seen in TEM images are nanocrystalline in nature. The nanoparticle diameter ranges from 5-9 nm, most of which where 5–6 nm in size (Fig. 3.9C). The nanoparticle diameter ranges from 5 - 9 nm of which most were 5 – 6 nm in size (Fig. 3.9D). NPs with smaller size have wide range of medical application as these particles can easily pass through the kidneys.
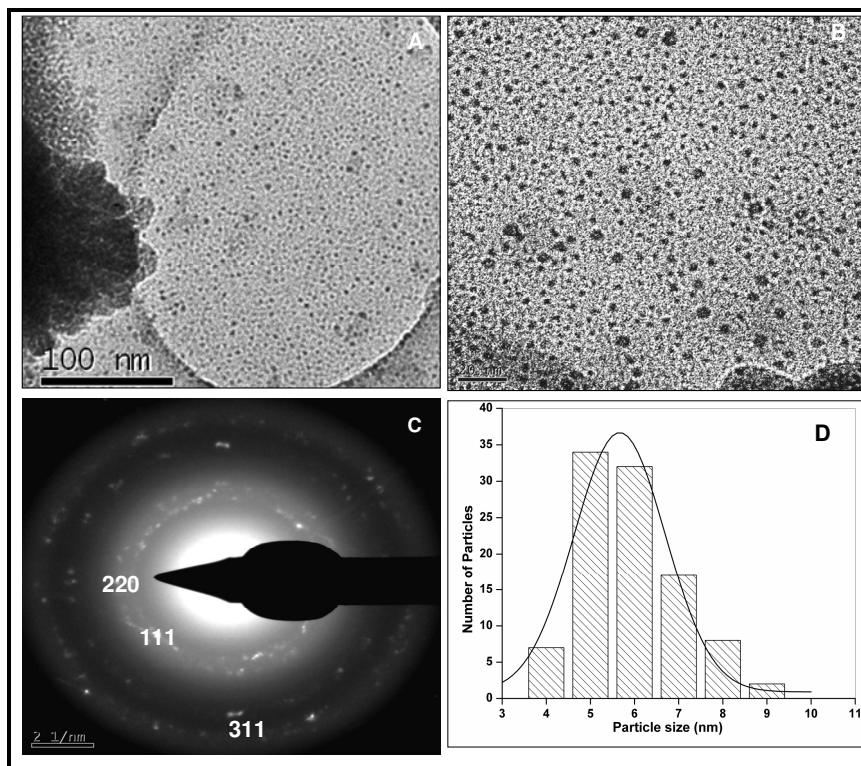
Figure 3.9: (A, B). TEM images of nanoparticles at different magnifications, **(C)** SAED. **(D)** Particle size distribution.

3.2.3.1.3 EDS Analysis:

The EDS analysis of the extra cellular nanoparticles sample (Fig. 3.10) shows the presence of gold and other peaks of oxygen, carbon and copper. The oxygen is due to the air present in the chamber, carbon is from the bio molecules capped to nanoparticles, copper from the substrate used for EDAX analysis. This shows the presence of gold in the sample. This EDS analysis proves the presence of gold in the sample.
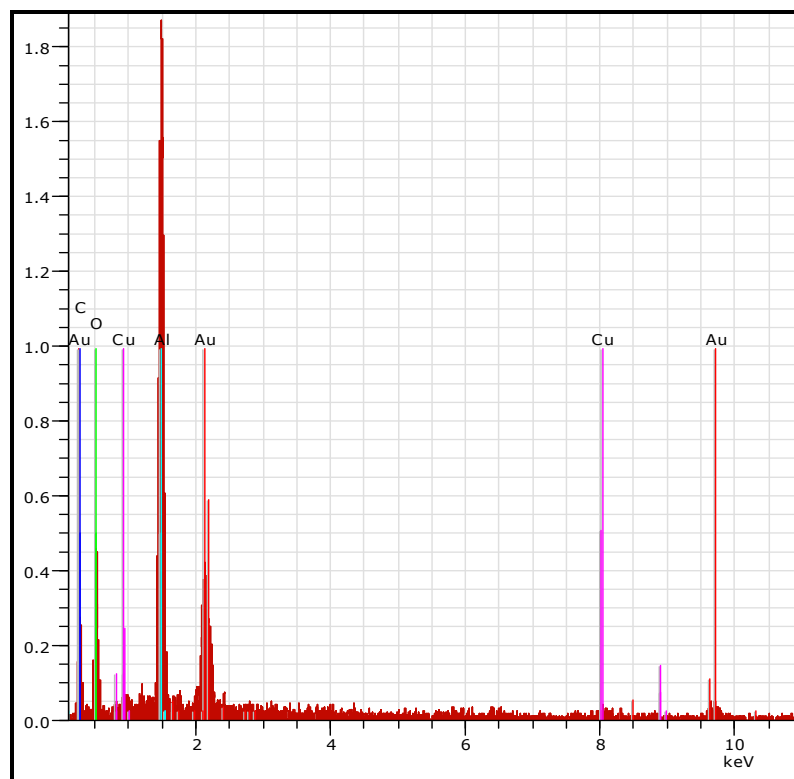
Figure 3.10: Elemental analysis of extracellular gold nanoparticles synthesized by peanut seedling.

3.2.3.1.4 Fourier Transform Infrared Spectroscopy:

The FT-IR spectra (Fig. 3.11) shows peaks at 1018 cm^{-1}, 1460 cm^{-1}, 1549 cm^{-1}, 1635 cm^{-1}, 2854 cm^{-1}, 2921 cm^{-1}, and 3437 cm^{-1} . The peak at 1018 cm^{-1} could be due to C-O-C groups [5], the peak of 1460 cm^{-1} is due to C-H stretching [20]. The peaks 1549 cm^{-1} and 1635 cm^{-1} are possible from amide II and amide I [5, 4] and peak of 2254 cm^{-1} are from methylene groups [5], peak 2921cm^{-1} are from stretching vibration of methylene compound [6]. The peak 3437 cm^{-1} is possibly from O-H group of phenols or alcohols. The FT-IR result showed that some of the proteins and phenolics leached from the roots helped in the formation of GNPs.
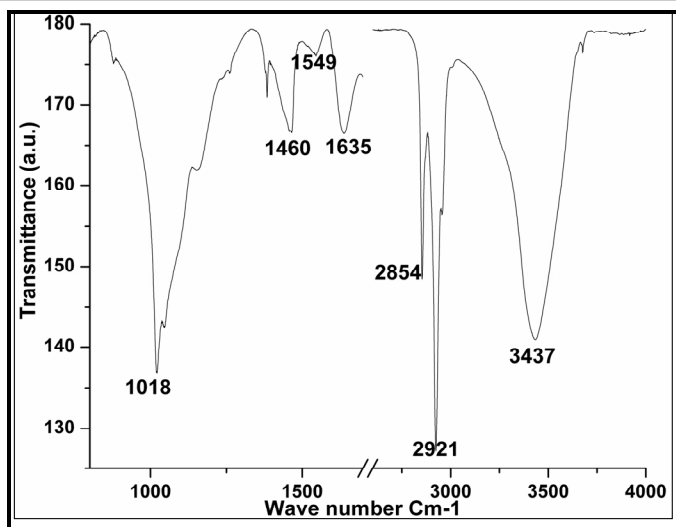
Figure 3.11: FTIR spectra of gold nanoparticles of peanut seedling synthesized nanoparticles

### 3.2.3.1.5 X-ray Diffraction:

XRD analysis can provide information of the crystalline nature of the particles (Fig. 3.12). Shows the presence of four prominent Bragg reflections corresponding to the (111), (200), (220) and (311) orientations agree with those reported for gold nanoparticles. The peak positions and 2θ (38.109, 44.36, 64.17, 77.26) values agree with those reported for gold nanoparticles. These reflections are broad which indicates that the formed nanoparticles are in the nanoscale dimensions.
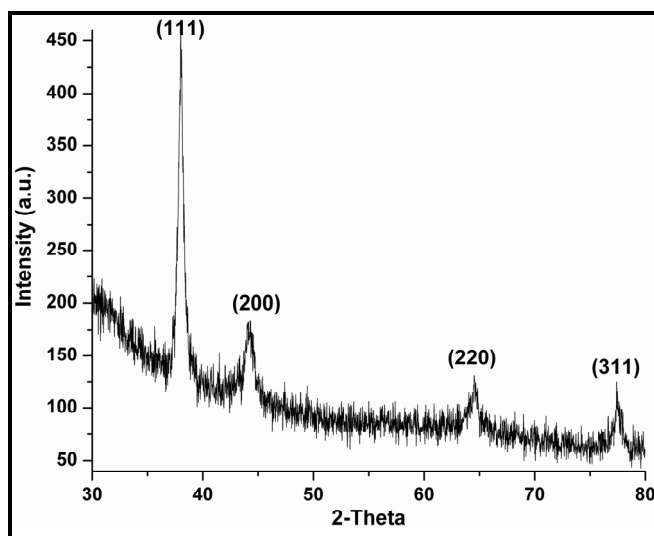
Figure 3.12: XRD of peanut synthesized extra cellular gold nanoparticles.

3.2.3.1.6 X-Ray Photon Spectroscopy Analysis:

XPS is an important tool for sensitive analysis. It is useful for the identification of elements present and also used to know the oxidation state of each element. High resolution of narrow scan of Au 4f (Fig. 3.13A) shows the binding peaks at 84.10 and 87.47 respectively which is a characteristic of Au metallic form [16]. The C1s core level spectrum could be decomposed into three chemically distinct components centered at 282.8eV, 285.01eV, 287.69 (Fig. 3.13B). The lower binding energy peak at 282.8 could be due to the presence of aromatic carbon present in amino acids from protein bound on the surface of gold nanoparticles. The C 1s which is centered at 285.01 is due to the electron emission from adventitious carbon or due to core levels originating from hydrocarbon chains present in the sample. The high binding energy peak at 287.69eV could be COOH groups and α carbon bound to COOH and –NH$_2$ groups of the protein bound to nanoparticles surface [33]. The Fig. 3.13C shows the O1s core level with the binding energy about 531.4eV which attributes from the OH groups and C=O groups present in capping proteins present on the surface of the GNPs [34]. The Fig. 3.13D shows the N1s core levels spectra with binding energy at 401.6eV which corresponds to –NH amide linkage or amidic (peptidic) nitrogen [35].
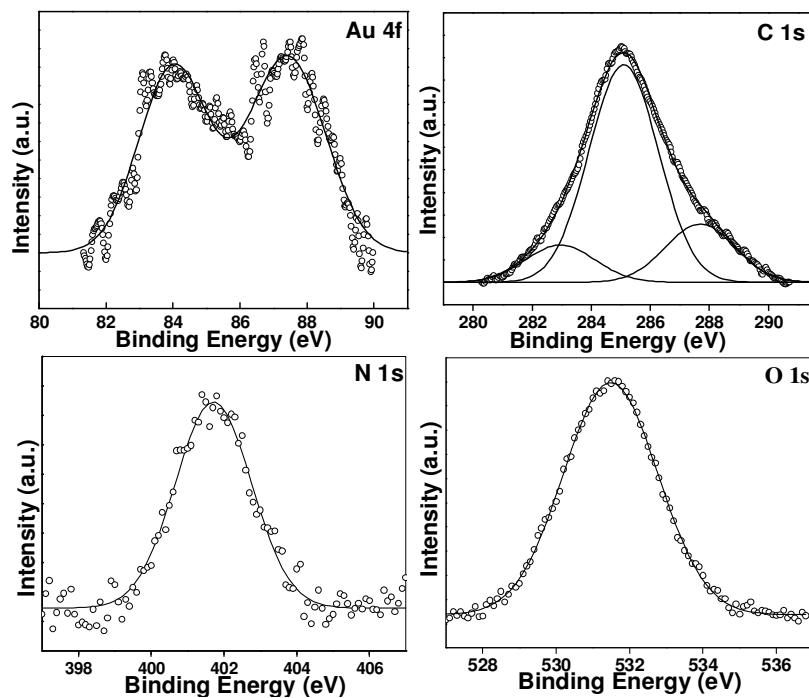

Figure 3.13: XPS characterization of gold nanoparticles synthesized by peanut seedlings. **(A)**. Spectrum of Au 4f. **(B)**. Carbon 1s. **(C)**. Oxygen 1s. **(D)**. Nitrogen 1s.

3.2.3.2 Characterization of Intracellular gold NPs:

The 15 day old peanut seedlings were exposed to 10^{-4}M HAuCl$_4$ solution under sterile conditions. There was no change in colour of the control root sample (Fig. 3.14A), but the roots which were exposed to 10^{-4}M HAuCl$_4$ solution turned to light pink after a period of 24 hr (Fig. 3.14C). The colour shift in itself is an indication of nanoparticle distribution on the root surface. In an earlier report too, the change in colour of the *Sesbania* root was noted after a period of 10 days [30].

3.2.3.2.1 Light Microscopy:

The peanut seedlings were removed after 72 hr and roots were washed with distilled water. As there was a change in the colour of the root (Fig. 3.14C), attempts were made to see the colour formation at the tissue level inside the root. Thin hand cut sections of control sample (Fig. 3.14A) and seedling exposed to HAuCl$_4$ (Fig. 3.14C) were taken with a razor blade to observe under light microscope. There was pinkish colour in cells approximately 5-7 layers inside the root (Fig. 3.14D). This indicates the nanoparticle formation inside the epidermal and cortex cells of the roots. There was no change in the colour of cells of control root sample (Fig. 3.14B) which was not exposed to HAuCl$_4$.
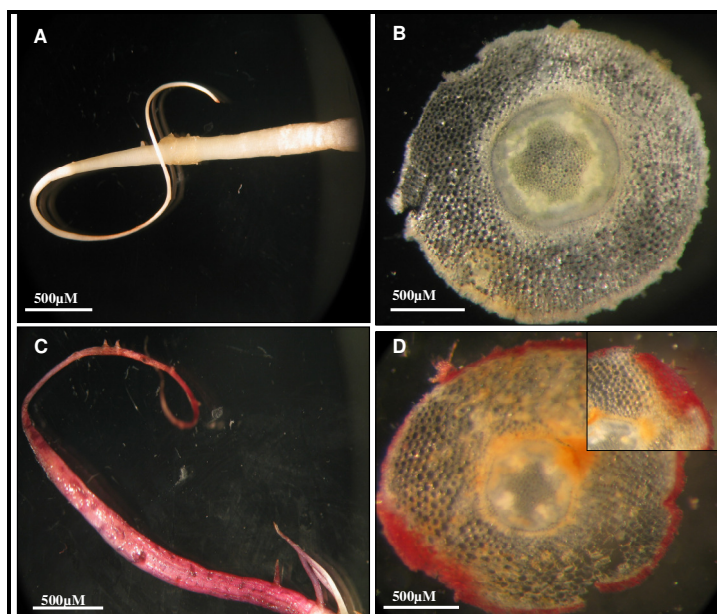

Figure 3.14: Hand cut sections of peanut root **(A)**. Control root, **(B)**. Hand cut section of control root, **(C)**. Root exposed to gold chloride solution, **(D)**. Hand cut section of root exposed to HAuCl$_4$ solution.

3.2.3.2.2 High Resolution Transmission Electron Microscopy:

High Resolution Transmission electron microscopy revealed an interesting pattern of distribution of gold particles inside plant cells at different magnifications (Fig. 3.15 A-C). Particles were of different shapes, spherical and oval. The spherical particles were of 5-8 nm in size and oval shapes particles ranged between 30-50 nm in size. This could be possible due to smaller nanoparticles merging to form larger NPs. The Fig. 3.15C shows de-spacing of gold nanoparticles at 0.23 nm which corresponds to (111) plane as was also observed in Gatan graph (Fig 3.15D).

The roots of peanut plant trap gold from the solution as a result of the affinity between carboxylic acid moieties present in the cell wall and Au (III) as reported in other living systems too [24]. Once the gold enters the root cells, it is transported symplastically to the conducting tissues and aerial parts of the plants in a manner similar to that of Pb [30]. Synthesis of nanoparticles could occur in the cell wall (external boundary) or cytoplasmic membrane (inner boundary), demonstrated as the possible site in *Verticillium* sp. [24]. The periplasmic space was the site for the silver nanoparticles assembly in silver-resistant bacteria [36]. As gold is not an essential element for the plants, the cell undergoes stress upon its entry and release some stress biomolecules which break down the chloroauric acid and possibly help in the synthesis/generation of GNPs.
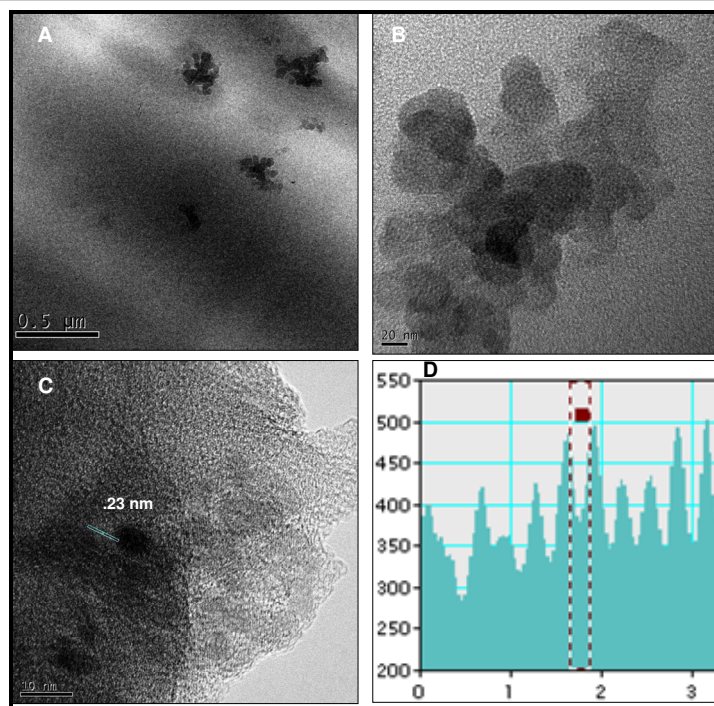
Figure 3.15: (A–C) HRTEM images at different scale of intra cellular gold nanoparticles synthesized by peanut seedling. **(D)**. Gatan graph.

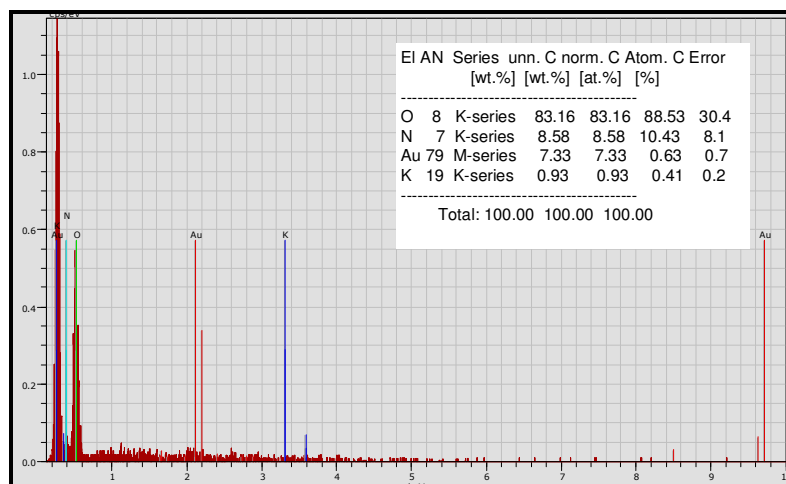### *3.2.3.2.3 Quantification of intra cellular gold by Inductive Coupled Plasma Spectrometry:*

The presence of gold in the root of the peanut plants was confirmed by HRTEM. An attempt was made to know the presence of gold in the parts of the peanut seedlings. Presence of gold was noted in the root, stem and leaves of the seedlings. The amount of gold in root, stem and leaf was 53.31, 2.75 and 1.33 ppm respectively (Fig**.** 3.16). This shows that more amount of gold was found in the root, than in stem, followed by leaf. This shows that the gold nanoparticles had been transported from the roots to the aerial parts of the peanut seedlings. The presence of metallic gold NPs in root was confirmed by HRTEM. Earlier reports of *Alfalfa* and *Sesbania* [8, 30, 37] showed the presence of metallic gold in leaf, stem and root by X-ray absorption near edge structure (XANES). The ICP-AES results of the peanut seedlings too confirm the presence of gold in roots, stem and leaves.
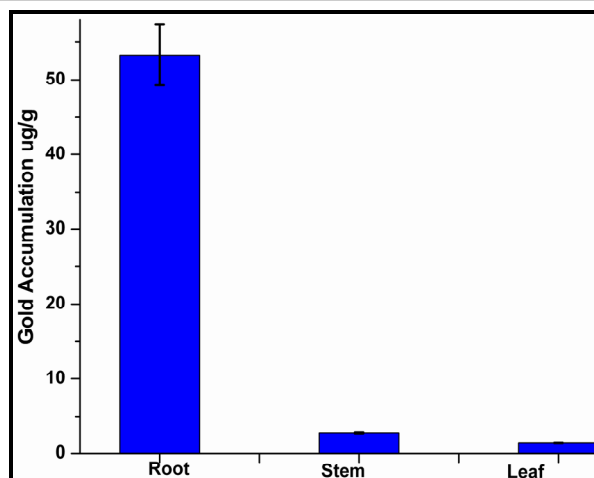
Figure 3.16: Shows the quantification of gold nanoparticles in root, stem and leaf of peanut seedling.

3.2.3.2.4 EDS Analysis:

The EDS analysis of the root sample (Fig 3.17) showed the presence of gold, oxygen, nitrogen, carbon and potassium. The oxygen could be due to the air present in the chamber and the other elements viz., nitrogen and potassium could be possibly from the plant root powder sample. This confirms the presence of Au in the root sample.


El	AN	Series	unn. C [wt.%]	norm. C [wt.%]	Atom. C [at.%]	C Error [%]
O	8	K-series	83.16	83.16	88.53	30.4
N	7	K-series	8.58	8.58	10.43	8.1
Au	79	M-series	7.33	7.33	0.63	0.7
K	19	K-series	0.93	0.93	0.41	0.2
		Total:	100.00	100.00	100.00	

Figure 3.17: EDAX analysis of intracellular peanut root powder.

3.2.3.2.5 X-ray Diffraction:

XRD analysis can provide information of the crystalline nature of the particles. Fig. 3.18 shows the presence of four prominent Bragg reflections corresponding to the (111), (200), (220) and (311) orientations, which agree with those reported for gold

nanoparticles. The peak positions and 2θ (38.109, 44.36, 64.17, 77.26) values agree with those reported for gold nanoparticles. These reflections are broad which indicates that the formed nanoparticles are in the nanoscale dimensions.
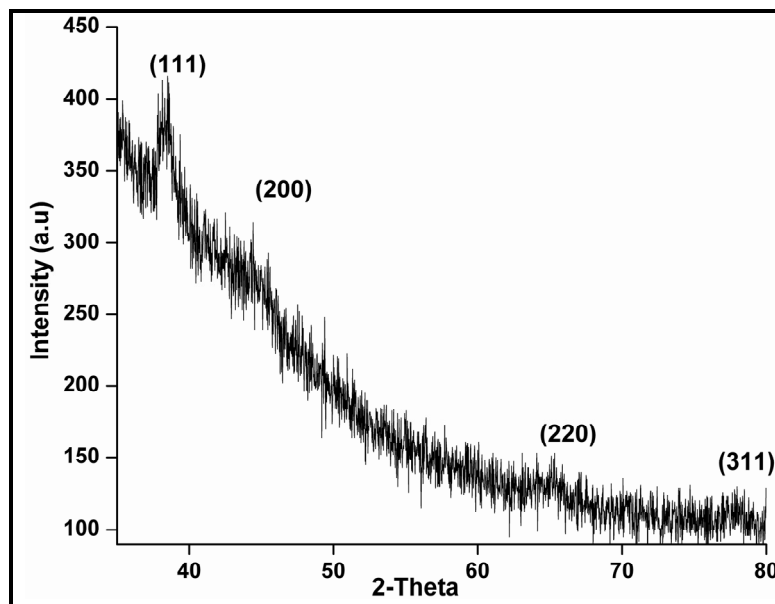
Figure 3.18: XRD analysis of peanut root powder exposed to HAuCl$_4$ solution.

3.2.4 Conclusions

In conclusion, we have demonstrated the extra- and intra-cellular formation of gold nanoparticles using living peanut seedlings. This result possibly shows the synthesis of intracellular nanoparticles by uptake of Au (III) and converting it to Au (0) by peanut seedling or the uptake of Au (0) from the extracellular nanoparticles solution synthesized by peanut seedling and transporting it to different parts of the plant. In the case of intracellular synthesis, reduction of metal ions may occur by the enzyme/protein and secondary metabolites present on the surface of the plant cell or on the cytoplasmic membrane as these surface bound nanoparticles (intracellular) maybe used in catalysis and as precursors for the synthesis of coatings for electronic applications. The extracellular synthesis of nanoparticles is exciting as these may be immobilized in different matrices or in thin-film form for optoelectronic applications as well as in drug delivery. This plant based environment friendly "green synthesis"

approach of nanoparticles synthesis has many advantages, such as the ease with which the process can be scaled up, its economic viability, etc.

We report, for the first time, both intra and extracellular synthesis of gold nanoparticles by using living peanut seedlings without any interference of other metal ions, alongwith complete characterization of nanoparticles. Further studies are required to know the exact mechanisms for intra and extracellular nanoparticles formation and interaction of the Au ions and Au (0) metallic form at cellular level.

Section 3

Recovery of intracellular gold nanoparticles from peanut roots.
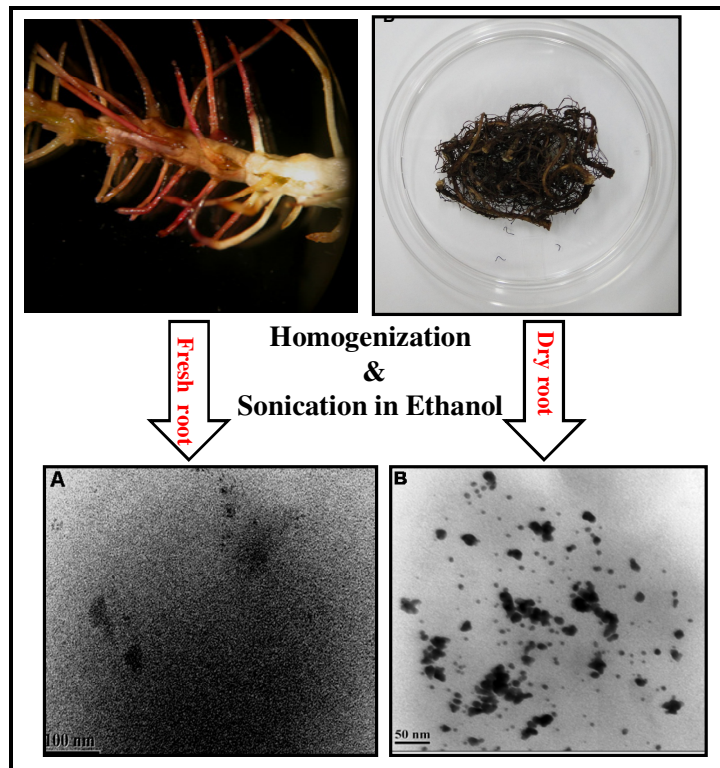
Section 3

3.3 Recovery of intracellular gold nanoparticles from peanut roots.

3.3.1 Introduction

The recovery of gold from aqueous systems has been studied from the industrial sources, such as electronics parts and plating materials. Existing methods of gold recovery, such as, hydrometallurgical and chemical routes [38, 39] can be applied to various wastes but are often energy demanding (e.g., electrolytic refining) or are not eco-friendly (e.g., cyanidation and chlorination). Metal recovery techniques using microorganisms will be cost effective and have few disposal problems; hence the development of these techniques will be worthwhile to study [40]. Biorecovery of metals has recently emerged as a potentially attractive and environment friendly alternative to traditional reclaiming treatments [41].

Gold precipitation has also been successfully achieved using fungi [24, 42, 43] plants and plant extracts (3, 4, 6, 7, 29) in addition to bacteria (44- 46). Application of fungi and actinomycetes in gold recovery has the disadvantage that the reduction is very slow, with complete reduction occurring in 48–120 hr [47].

However, the nanoparticles produced by Oat and wheat biomasses are physically trapped to the biomass after extraction of nanoparticles by cetyltrimethylammonium bromide (CTAB), sodium citrate, washing and centrifugation. Thus a procedure to recover biomass trapped nanoparticles needs to be developed to make this environment friendly synthesis technique a reality [48].

The surfactants such as (CTAB) and sodium citrate are used in the preparation of gold nanoparticles. These chemicals act as capping agents for the stabilization of gold nanoparticles in aqueous solutions and transfer nanoparticles from water phase to liquid organic phase [49- 51].

The recovery of gold from the jewellery waste and conversion to GNPs was studied by using *Escherichia coli* and *Desulfovibrio desulfuricans* [41]. The recovery of gold nanoparticles from *Canola* and *Alfalfa* after growing in ½ strength MS culture

medium was extracted by ethanol followed by sonication. The recovery of gold nanoparticles was confirmed by TEM and EDAX [52].

Harvesting the gold from plants and its economic importance was studied in *Brassica juncea, Chicory* sp., *Impatiens* sp. and *Arrhenatherum elatius* from different mines. The induced hyperaccumulation of gold appears to be relatively independent of plant species, so it should be possible to use plants (such as chicory) that might be easy to grow on mine tailings [53].

There are few reports of using living plants (*Medicago sativa, Brassica juncea* and *Sesbania*) for the synthesis of intracellular nanoparticles, but the recovery of gold nanoparticles from them was not much explored. The other reports in recovery of gold by using *Escherichia coli* and *Desulfovibrio desulfuricans* [41], *Shewanella* algae [47], recovery of Palladium and gold from electronic scrap leachates by *Desulfovibrio desulfuricans* [54] are also known. Here we report the recovery of gold nanoparticles which were synthesised intracellularly from the dry and fresh roots of peanut by extracting with ethanol, followed by sonication for 20 min. The recovered particles were further characterized by UV, TEM and ICP-AES.

3.3.2 Experimental Details

Mature pods of *Arachis hypogaea* (Peanut cultivar SB-11) were collected from the local market. The seeds were washed under running tap water for 10 min followed by repeated washing with deionized water. Thereafter, the seeds were treated with 1% bavistin for a period of 30 min and later with 4% savlon (v/v) for 12 min. On removing traces of savlon with sterile water, these seeds were disinfected by 0.1% $HgCl_2$ (w/v) treatment for 10 min. Adhering $HgCl_2$ was eliminated by rinsing the seeds with sterile deionized water. The testa of these seeds was removed aseptically and the seeds were cultured on Whatman filter paper support in deionised water in test tubes. The seed cultures were incubated in 16 hr photoperiod at $25\pm2°C$. The pH of the deionized water was adjusted to 5.8 prior to autoclaving.

After a period of 15 days, well grown seedlings were used in synthesis of nanoparticles. Solution of $10^{-4}M$ $HAuCl_4$ was prepared under sterile conditions. An amount of 10 mL of $10^{-4}M$ $HAuCl_4$ solution was added to sterile tubes. Under sterile

conditions, the seedlings were transferred to autoclaved test tube containing 10^{-4} M HAuCl$_4$ solution. After a period of 72 hr the roots were harvested. The harvested dry and fresh root tissue were used for recovery of GNPs. The harvested roots were allowed to dry in oven at 70°C till they achieve constant weight.

2 gm of dry tissue and fresh roots which were exposed to 10^{-4}M HAuCl$_4$ solution and its controls were taken in triplicates, crushed in 5 mL of ethanol in mortar and pestle, sonicated for a period of 20 min. The root tissue was allowed to settle down. The supernatant was taken and characterized by UV-vis, TEM and particles were quantified by ICP-AES.

3.3.3 Results and Discussion

3.3.3.1 Particles recovery from dry roots

##### 3.3.3.1.1 Morphology of dry root:

After the exposure of peanut seedlings to 10^{-4}M HAuCl$_4$ solution, the roots were dried along with control samples. There was change in the colour of the roots of control samples and exposed roots. The dry roots of control samples were light brown in colour whereas roots exposed to 10^{-4}M HAuCl$_4$ solution were dark brown in colour indicating the presence of GNPs in the root (Fig.3.19 A, B).
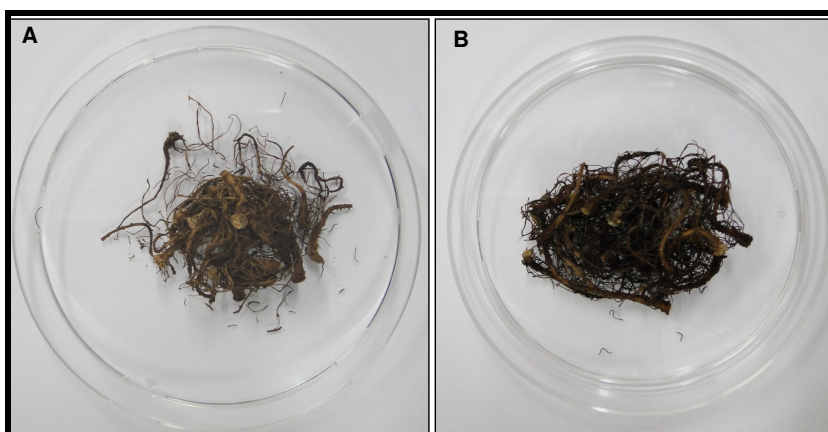
Figure 3.19: (**A**) Morphological difference of peanut dry roots. (**B**). Control Root exposed to HAuCl$_4$.

3.3.3.1.2 UV-vis Analysis:

Dried peanut roots which were exposed to $HAuCl_4$ solution and the ones without exposure (control) were taken, crushed in ethanol and sonicated for a period of 20 min. The supernatant was taken after allowing the sample to settle. The supernatant was scanned from 400 to 900 nm. There was no peak at 520-540 nm in control root samples extracted in ethanol (Fig. 3.20A). In samples of roots exposed to $HAuCl_4$ solution the peak was noted, indicating the presence of nanoparticles (Fig 3.20B). A peak at 610-620 nm was also noted, which could be of some different shape of particles or the UV of some organic molecule which was extractable in ethanol. There was an extra peak which was observed at 650 – 670 nm which was observed in both control and roots exposed to $HAuCl_4$ solution (Fig.3.20A, B).
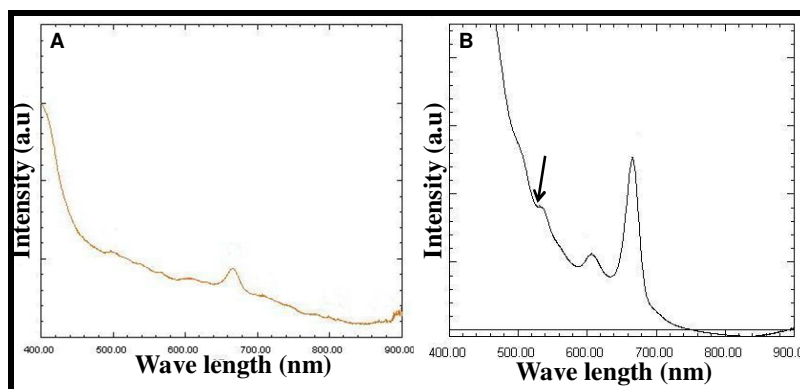

Figure 3.20: Shows **(A)**. UV analysis of peanut root extracted in ethanol Control root exposed to $HAuCl_4$ **(B)**.

3.3.3.1.3 Characterization of GNPs by TEM and EDS

The TEM visualization shows the measurements of NPs sizes and shapes which were recovered from the dry peanut root. TEM images (Fig. 3. 21A, B) show that the particles are polydispersed and of morphologically different shapes. The image shows some of the particles are well separated and few particles were in clusters. The clusters could be possibly due to the root being dried in oven or during the process of recovery. The particles size ranged from12-21 nm, most of them being 14 to 16 nm in size (Fig. 3.21C). The particles which were recovered from the dry root tissue were of nano size. Further confirmation was done by EDS analysis to prove that the recovered particles were of gold. Peak of Au shows the presence of gold and other peaks of oxygen, carbon and copper (Fig. 3.21D). The oxygen is due to the air present in the

chamber, carbon from the bio molecules capped to nanoparticles and copper from the substrate used for EDS analysis in dry root. This confirms that the particles recovered from peanut root were of gold. The inset image of SAED shows the particles are crystalline in nature (Fig. 3.21D). The particles size was more than those obtained from the extraction of the fresh root samples. This may be possible due to the drying of the roots in oven at 70°C which may have increased the size of the particles.
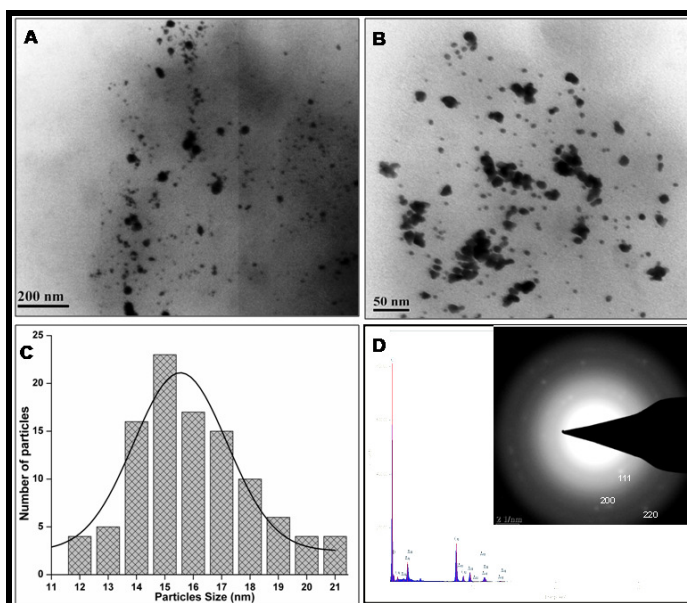

Figure 3.21: The images **(A** and **B)** at different magnifications show the GNPs recovered   in ethanol from peanut dry root, **(C)**. Particles size distribution, **(D)**. Elemental analysis by EDS and insert image shows the SAED of particles.

3.3.3.2 Particles recovery from fresh roots

3.3.3.2.1 Morphology of fresh roots

An attempt was also made to recover the nanoparticles from the fresh root tissue. The control fresh root tissue was white in colour, whereas roots exposed to $HAuCl_4$ solution were purple in colour (Fig. 3.22 A, B). This indicates the possible presence of intracellular GNPs in root. The presence of GNPs inside the root was carried out and confirmed in the Section 2 of this Chapter. In earlier report, change of colour in *Sesbania* root was noted after a period of 10 days [30].
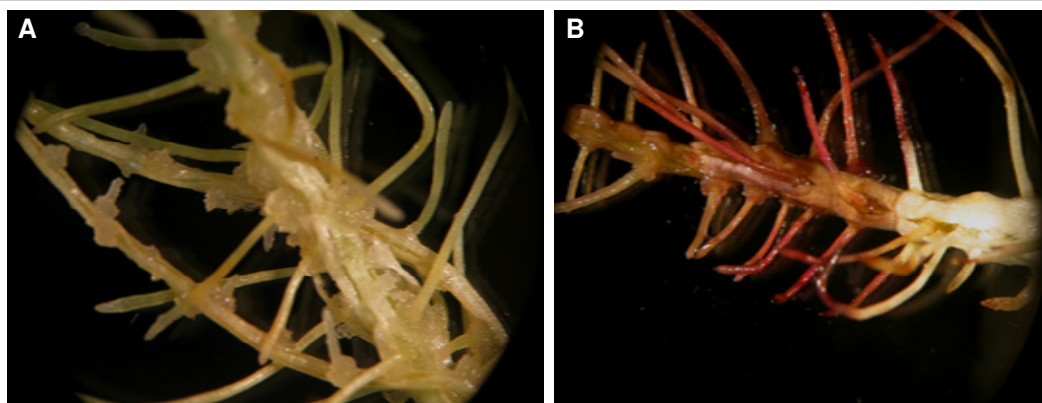
Figure 3.22: Morphological differences of peanut fresh roots. Control **(A)** root exposed to HAuCl$_4$ solution **(B)**.

3.3.3.2.2 UV-vis Analysis:

The fresh root tissue exposed to HAuCl$_4$ solution was extracted in ethanol, sonicated for 20 min and then allowed to settle. The supernatant was taken for UV-vis analysis which was scanned from 400 nm to 800 nm. The presence of peak at 520-530 nm indicates the recovered nanoparticles. There was no peak observed in control root extract. Peak at 650–670 nm which was observed in both control and roots exposed to HAuCl$_4$ solution in fresh root tissue (Fig.3.23 A, B), was also observed in dry extract.
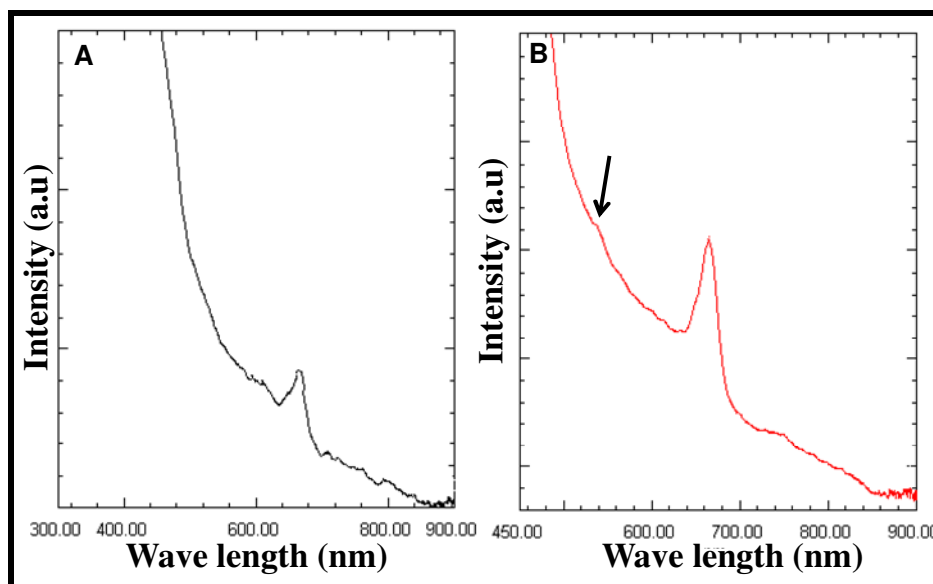
Figure 3.23: **(A)** UV analysis of peanut fresh root extracted in ethanol. (B). Control root exposed to HAuCl$_4$.

3.3.3.2.3 TEM Analysis:

The TEM image analysis (Fig. 3.24A, B) at different magnifications shows the recovery of GNPs from fresh root of peanut. Particles were of approximately 5-8 nm in size well separated and polydispersed. Further confirmation was done by EDS analysis showing the presence of gold. The other peaks of oxygen, carbon and copper were also observed. The oxygen is due to the air present in the chamber, carbon from the biomolecules capped to nanoparticles and copper peak from the grid used for EDS analysis for fresh root recovered particles. The extra element peaks such as potassium and phosphorous were possibly from the fresh root tissue extract (Fig. 3.24C). The SAED image shows that the recovered particles were crystalline in nature (Fig. 3.24D).
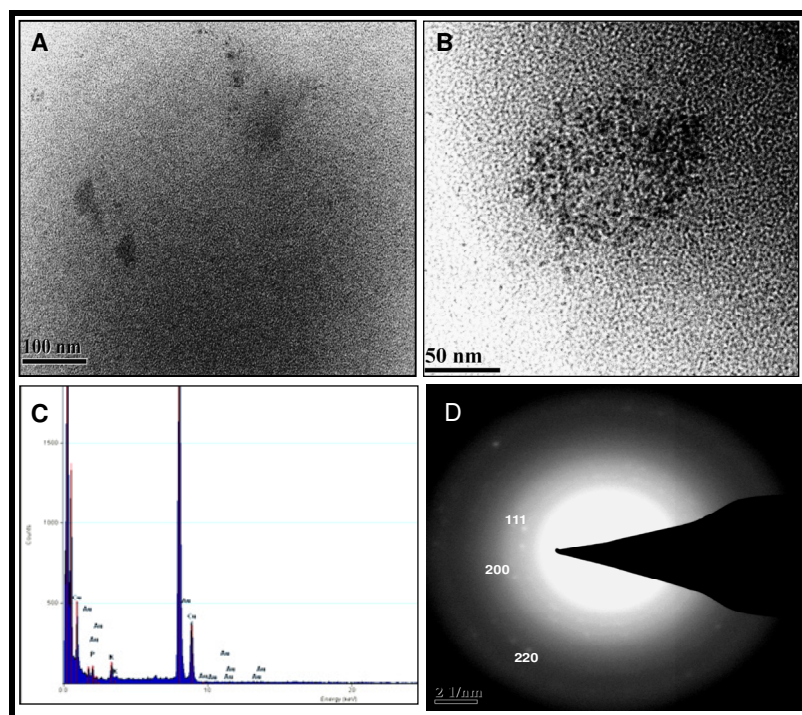
Figure 3.24: The images (**A** and **B**) at different magnifications show the GNPs recovered in ethanol from peanut fresh root, (**C**).Elemental analysis by EDS (**D**). SAED pattern of nanoparticles.

3.3.4 Conclusions

The extraction and recovery of gold nanoparticles synthesized in biological materials (Peanut roots) is possible using the ethanol extraction from fresh and dry roots. The dry root tissue recovered GNPs in more quantity than the fresh tissue. The

intracellular recovery of gold is potentially attractive as an environmentally friendly alternative to conventional methods.

Section 4

Callus cell mediated synthesis of gold nanoparticles.
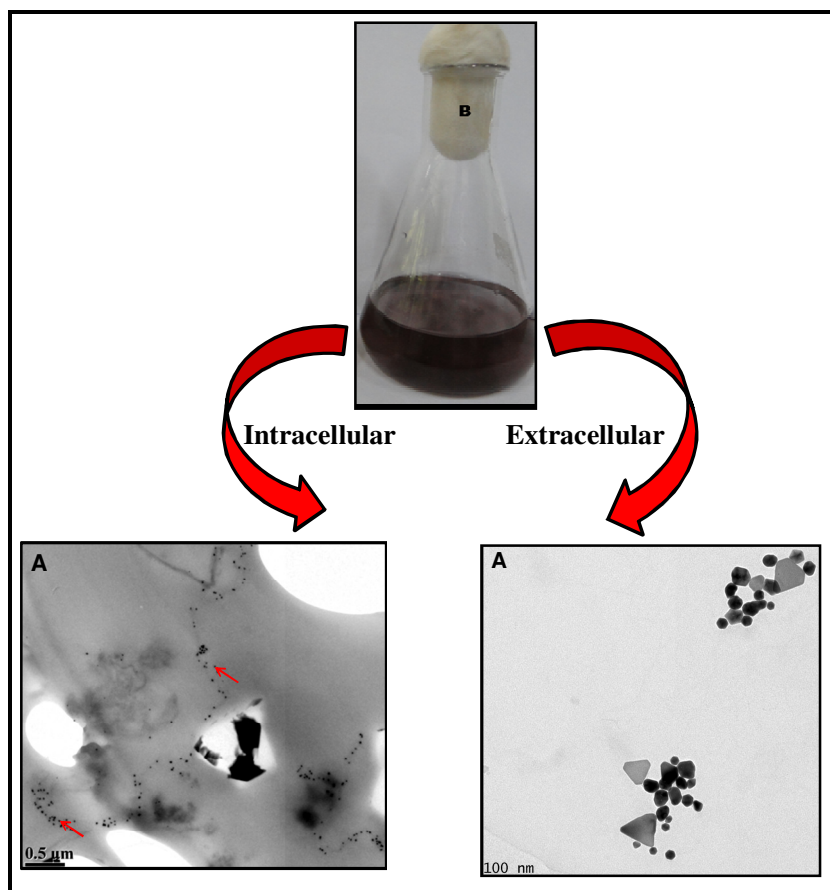
Section 4

3.4. Callus cell mediated synthesis of gold nanoparticles.

3.4.1 Introduction

In recent years, synthesis of inorganic nanoparticles has been the focus of intense interest because of their emerging applications in areas such as bio-imaging, biosensors, biolabels and biomedicines. [55-58]. The chemical synthesis of nanomaterials takes place by reducing a metal salt with sodium citrate or sodium borohydride followed by surface modification with suitable capping ligands, occasionally organic solvents, which causes environmental problems [59-61]. The physical methods of nanomaterial synthesis are very expensive. Therefore, researchers are now concentrating on the "biosynthesis" of metal nanoparticles using both uni- and multicellular organisms [22, 24, 25, 62].

Among the microorganisms, prokaryotic bacteria have been used in the area of biosynthesis of nanoparticles. The early studies show that *Bacillus subtilis* is able to reduce Au^{3+} ions to produce octahedral gold particles of nanoscale dimensions (5–25 nm) within bacterial cells by incubating the cells with gold chloride [63, 46, 64] under ambient temperature and pressure conditions.

The synthesis of GNPs from fungi is seen relatively more in recent years. The use of fungi is potentially exciting since they secrete large amounts of enzymes and are simpler to deal within the laboratory. When challenged with aqueous metal ions such as $AuCl^{-4}$ and Ag^+, fungi yields large quantities of metal nanoparticles either extracellularly [40, 65] or intracellularly [24, 66]. The appearance of purple color in the biomass of *Verticillium* sp. after exposure to 10^{-4} M $HAuCl_4$ solution indicates the formation of gold nanoparticles intracellularly [24]. The Algae too have been used for the synthesis of metallic nanoparticles. Recently, systematic approach has been adapted to study the synthesis of metallic nanoparticles by *Sargassum wightii*. This marine alga has been used to synthesize highly stable extracellular gold nanoparticles [67].

The other green process of synthesis of nanoparticles by using plant extracts has been studied in plants [3, 4, 10-13, 15, 16, 29]. The uptake of Au (0) from agar medium by

the roots of *Alfalfa* and then transferring it to the shoot of the plant in the same oxidation state has been shown Gardea-Torresdey *et al.* [7, 8]. It was reported [30] that the growth of *Sesbania* seedlings in chloroaurate solution resulted in the accumulation of gold with the formation of stable gold nanoparticles in plant tissues. There are a few reports on the synthesis of nanoparticles from plant callus cell extracts. The only two reports available for the synthesis of extracellular silver nanoparticles using callus cell extracts include *Citrullus colocynthis* (L.) and *Carica papaya* [68, 69]. Though there are reports on the synthesis of nanoparticles using bacteria, algae, fungi and virus, there are no reports on the synthesis of GNPs using living plant cells. Here we report for the first time, the synthesis of intra and extracellular GNPs by using living peanut callus cells, which is an environment friendly and cheap method.

3.4.2 Experimental Details

The seedlings germination procedure was explained in this chapter under Section 2. Leaves from the 15 d old well grown peanut seedlings were taken as explant for callus induction on media containing major elements of MS basal medium with minor nutrients and vitamins of B5 basal medium. The media was supplemented with BAP (6-Benzyl Amino Purine) 1 ppm and (Naphthalene Acetic Acid) NAA 1 ppm with 3% sucrose. The media was solidified with 0.7% agar.

Table 3.1: Murashige and Skoog basal medium (Murashige and Skoog, 1962).

Ingredients	Amount (mg L^{-1})	Stock solution
Macronutrients		**(20 X) in 500 mL**
KNO_3	1900	19 gm
NH_4NO_3	1650	16.5 gm
$CaCl_2.2H_2O$	440	4.4 gm
$MgSO_4.7H_2O$	370	3.7 gm
KH_2PO_4	170	1.7 gm
Micro-nutrients		**(100 X) in 100 mL**
$MnSO_4.4H_2O$	22.3	62 mg
$ZnSO_4.7H_2O$	8.6	223 mg
H_3BO_3	6.2	86 mg
		Table contd…

KI	0.83	2.5 mg
$CuSO_4.5H_2O$	0.025	0.25 mg
$Na_2MoO_4.2H_2O$	0.25	8.3 mg
$CoCl_2.6H_2O$	0.025	0.25 mg
$FeSO_4.7H2O$	27.8	278 mg
$Na_2EDTA.2H_2O$	37.3	373 mg
Vitamins		**(100 X) in 100 mL**
Myo-inositol	100	1 gm
Thiamine-HCl	0.1	5 mg
Nicotinic acid	0.5	20 mg
Pyridoxine-HCl	0.5	1 mg
Glycine	2	5 mg

After a period of 1 month incubation in dark, 500 mg of the induced callus was suspended in 20 mL of liquid media of the same media composition for 15 days for the multiplication of callus cells.

20 mL of cell suspension was harvested by centrifugation at 5000 rpm for 10 min at 4°C. The supernatant was discarded and the pellet of callus cells was washed for 3-4 times with sterile distilled water under aseptic conditions. After washing the cells were added to 100 mL of 10^{-4}M $HAuCl_4$ solution under aseptic conditions. Then the flask was then kept on shaker for 24 hr period in dark condition at 25±2°C.

The callus cells which were grown in 10^{-4}M $HAuCl_4$ solution were centrifuged at 5000 rpm for 10 min. The pellet of callus cells was washed 2 to 3 times with sterile deionized water by centrifugation. The pellet was then fixed in 2.5% glutaraldehyde and caodylate buffer (pH 7.2) for overnight. The cells were washed 3 times with 0.1M caodylate buffer (pH 7.2) for 5 min. The samples were stained with 2% uranyl acetate for 2-3 hr, dehydrated in different grades of ethanol and then washed with acetonitrile 3 times for 10 min. The cells were then embedded in a synthetic resin and dried in a furnace at 60°C for 48 hr. Blocks were prepared and thin sections (50-100 nm thick) were cut using ultra microtome with diamond knife and put on Cu grids and placed on the sample holder for TEM analysis. The EDS analysis was done by the EDS attached to the TEM.

3.4.3 Results and Discussion:

3.4.3.1 Extracellular gold nanoparticles

3.4.3.1.1 Visible Analysis:

After the addition of peanut callus cells to 10^{-4}M $HAuCl_4$ solution under sterile conditions, there was a change in colour of the solution to dark purple after a period of 24 hr which indicates the formation of extracellular gold nanoparticles [19] (Fig. 3. 25A). There was no change in colour in the control cells, whereas the cells exposed to 10^{-4}M $HAuCl_4$ solutions changed to purple in colour (Fig. 3.25B). The extracellular nanoparticles were stable over a period of time and no agglomeration was noted.
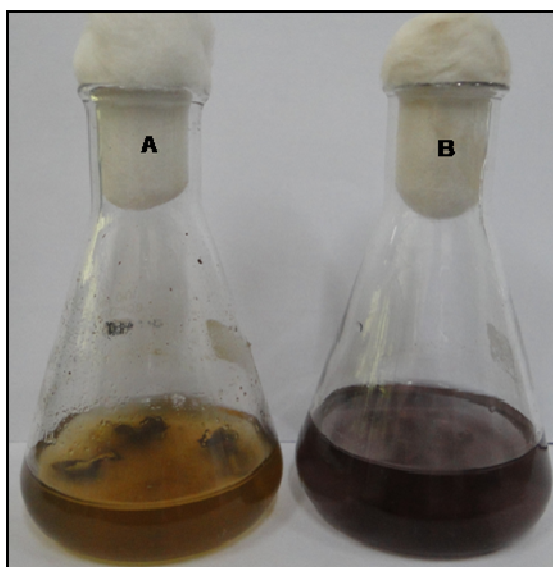
Figure 3.25: **(A)** Control callus cell suspension. **(B)** Callus cells exposed to $HAuCl_4$ solution showing purple colour.

3.4.3.1.2 UV-vis analysis:

The callus cells and extracellular GNPs were separated by filtering with Whatman filter paper. The extracellular particles were subjected to UV analysis and scanned from 300 nm to 800 nm. (Fig. 3.26) A peak at 520 to 540 nm indicates the formation of nanoparticles was noted. In control sample, there was no peak observed between 520 to 540 nm [18].
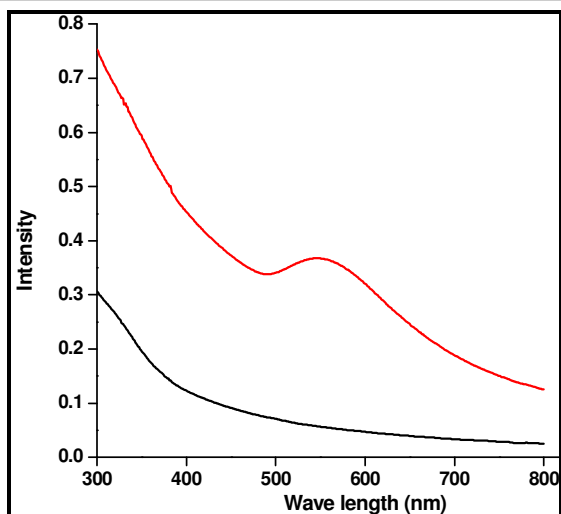
**Figure 3.26:** UV spectra of peanut callus cells synthesized GNPs when exposed to HAuCl₄ solution

3.4.3.1.3 TEM Analysis:

The TEM visualization shows the measurements of sizes and shapes of NPs synthesized extracellularly by peanut callus cells. TEM images at different magnifications (Fig. 3.27A, B) showed that the particles are polydispersed and have different shapes and morphology. Most of the particles are circular and few prism shaped particles were also observed. The selected area electron diffraction pattern confirms that the particles which were synthesized by peanut callus cells were crystalline in nature (Fig. 3.27C). The average particle diameter was calculated by Gatan software. The particle size ranged from 42 nm to 63 nm. The particle size distribution shows that the average particle size is 50 nm (Fig. 3.27D).

The bio-organic components released into the solution may play a possible role in reduction and may act as capping agent. In addition, it is also difficult to prove the role of specific protein/enzyme in the reduction process of metal ions in nanoparticle synthesis at this stage. Further study is under progress to identify the exact biomolecules. In earlier report, due to the presence of chloroaurate and silver ions [70], the induction of new proteins for the reduction process of Au^{3+} and Ag^+ was observed. The new proteins of molecular weights ranging between 25 and 66 kDa could be responsible for the reduction of chloroaurate ions. There are reports showing the formation of nanoparticles by protein. A protein with a molecular weight of

approximately 28 kDa was isolated and purified by reverse- phase HPLC and this protein tested positive for the reduction of chloroauric acid in aqueous solution [71].

It is known that the presence of metal ions can cause induction of new proteins in the bacterial cells. It was demonstrated by the synthesis of gold nanotriangles and silver nanoparticles using *Aloe vera* plant extracts [14], in which only biomolecules of MWs lower than 3 kDa caused reduction of the chloroaurate ions leading to the formation of gold nanotriangles. It was also reported that polyol components and water-soluble heterocyclic components were mainly responsible for the reduction of silver or chloroaurate ions and the stabilization of nanoparticles, respectively [72, 14].
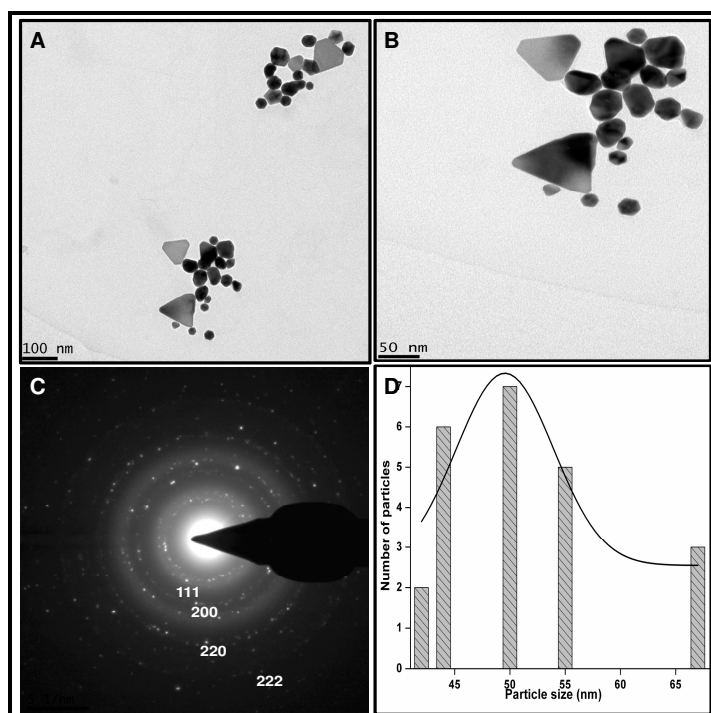

Figure 3.27: TEM analysis **(A, B)** at different magnifications, **(C)** shows the SAED of nanoparticles **(D)** particles size distribution of GNPs synthesized by peanut callus cells.

3.4.3.1.4 XRD Analysis

XRD analysis also provides information about the crystalline nature of the particles. The (Fig. 3.28.A) shows the XRD of extracellular nanoparticles. The presence of four Bragg reflections corresponding to the (111), (200), (220) and (311) orientations agree with those reported for gold nanoparticles. The peak positions and 2θ (38.04,

44.44, 64.45, 77.75) values agree with those reported for gold nanoparticles [65]. These reflections are broad which indicates that the formed nanoparticles are in the nanoscale dimensions.
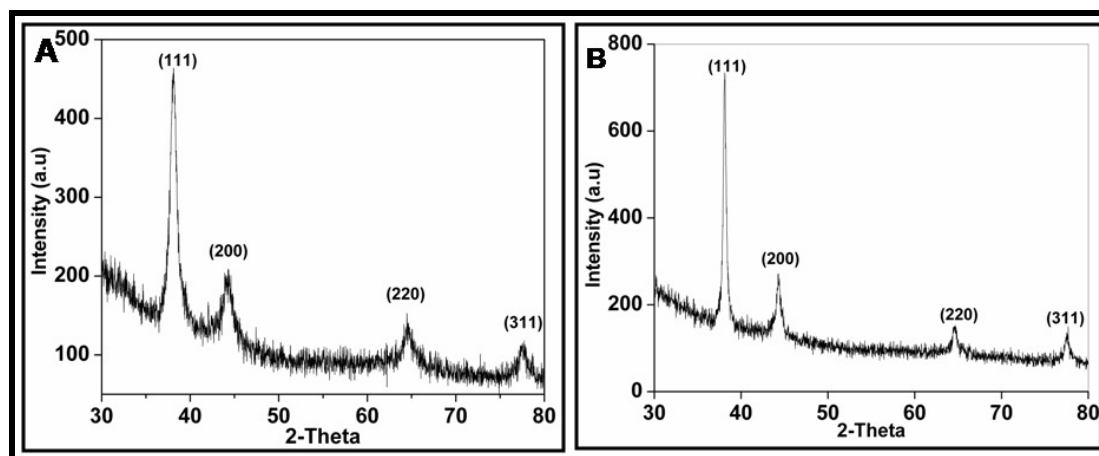

Figure 3.28. XRD of extra and intracellular gold nanoparticles synthesized by peanut callus cells. **(A)** Extracellular. **(B)** Intracellular.

3.4.3.2 Intra cellular gold nanoparticles:

3.4.3.2.1 Microscopy analysis:

An amount of 100 µL of well shaken callus cell suspension culture of control sample and 10^{-4} M $HAuCl_4$ solution exposed cells was removed after 24 hr and drop casted on glass slide to observe under microscope for the colour difference of the cells. In control cells, there was no formation of purple colour (Fig. 3.29A) while the cells exposed to 10^{-4}M $HAuCl_4$ solution turned purple in colour indicating the synthesis of nanoparticles by callus cells (Fig. 3.29B). In earlier reports, purple colour of the actinomycetes and bacterial cells was observed which indicates the formation of intracellular Au nanoparticles by the cells [66, 70]. This shows that peanut callus cells had synthesized GNPs intracellularly.
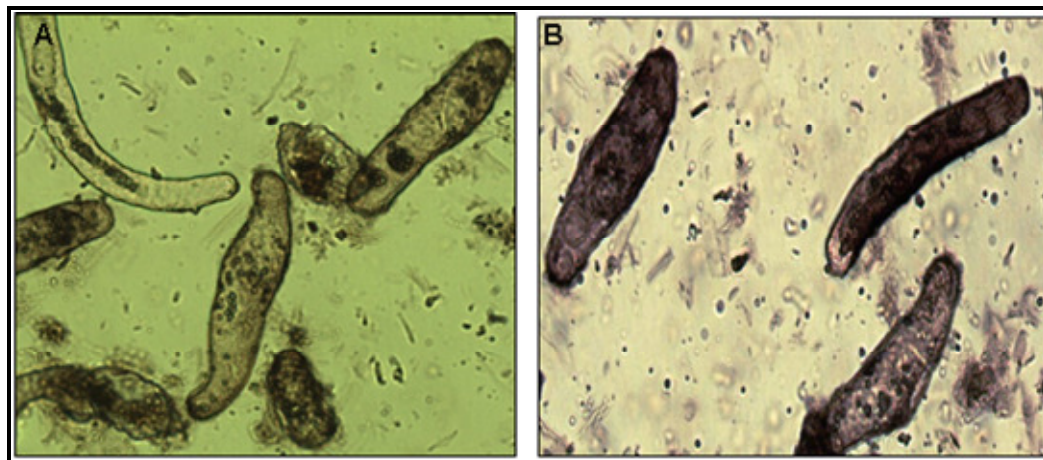
Figure 3.29: Microscopy images of peanut callus cell. **(A)**. Control cells **(B)**. Cells exposed to gold chloride solution.

3.4.3.2.2 TEM Analysis:

The TEM micrographs (Fig. 3.30A-C) reveal the formation of spherical gold nanoparticles inside and along the cell wall (intracellular). Careful observation of TEM images revealed that highly spherical and uniform nanoparticles were synthesized. The GNPs are well-separated without noticeable aggregation. The (Fig. 3.30D) shows the SAED of intracellular nanoparticles which are crystalline in nature. The particles are well separated without any aggregation indicating that some of the molecules that stabilized the nanoparticles are inside the peanut callus cells. The TEM results also indicate the presence of some GNPs on the cytoplasmic membrane as well as within the cytoplasm. It is possible that some Au ions diffuse through the cell wall and are reduced by enzymes present on the cytoplasmic membrane and within the cytoplasm. It may also be possible that some of the smaller GNPs diffuse across the cell wall to be trapped within the cytoplasm.

It has been shown that the role of NADH or NADH-dependent reductase has also been proposed for GNP synthesis using the bacteria *Rhodopseudomonas capsulate* [73]. The presence of GNPs within the cell wall of cyanobacteria is due to the presence of carboxyl groups, polyphosphates and polysaccharides in the cyanobacterial cell membrane which can help in the reduction of the gold ions to GNPs [74]. Similarly, in the present study, the possible involvement of

enzymes/proteins molecules which are helping in nanoparticle formation by peanut callus cells is suggested.
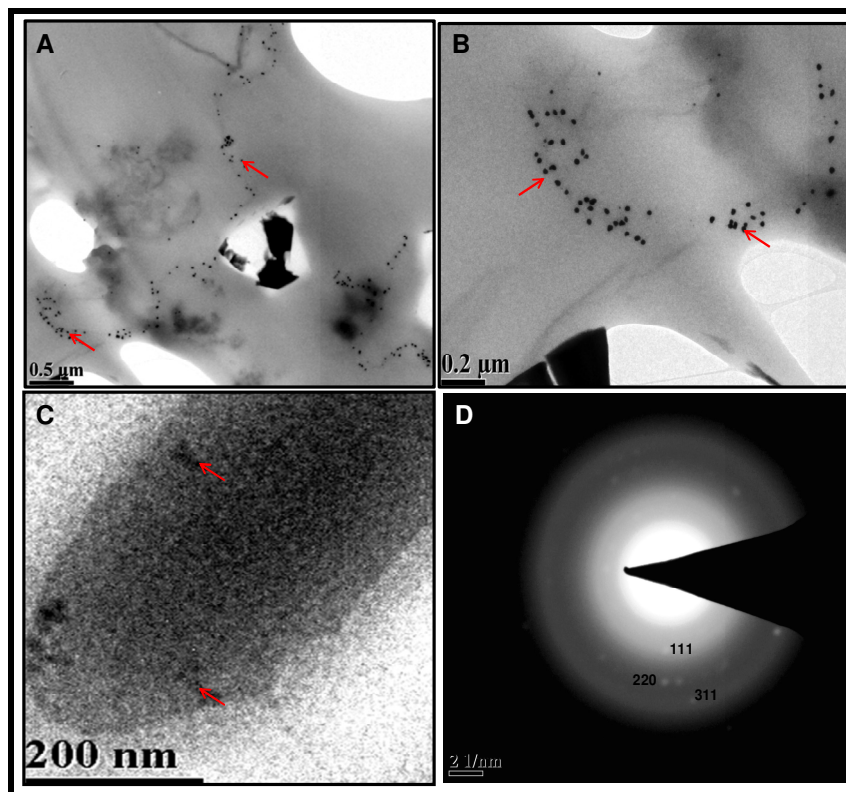
Figure 3.30: TEM images **(A-C)** at different magnifications of intracellular GNPs synthesis by callus cells **(D)**. Shows the SAED

3.4.3.2.3 EDS Analysis:

The EDS analysis of the intracellular nanoparticles of callus cells (Fig. 3.31A) shows the presence of gold and other peaks of oxygen, carbon and copper. The oxygen is due to the air present in the chamber, carbon from the biomolecules capped to nanoparticles and copper from the substrate used for EDS analysis. This confirms the presence of intracellular gold nanoparticles. The particles size distribution analysis (Fig. 3.31B) shows the size of particles ranged from 15 to 35 nm and most of the particles were of 31 nm in size.
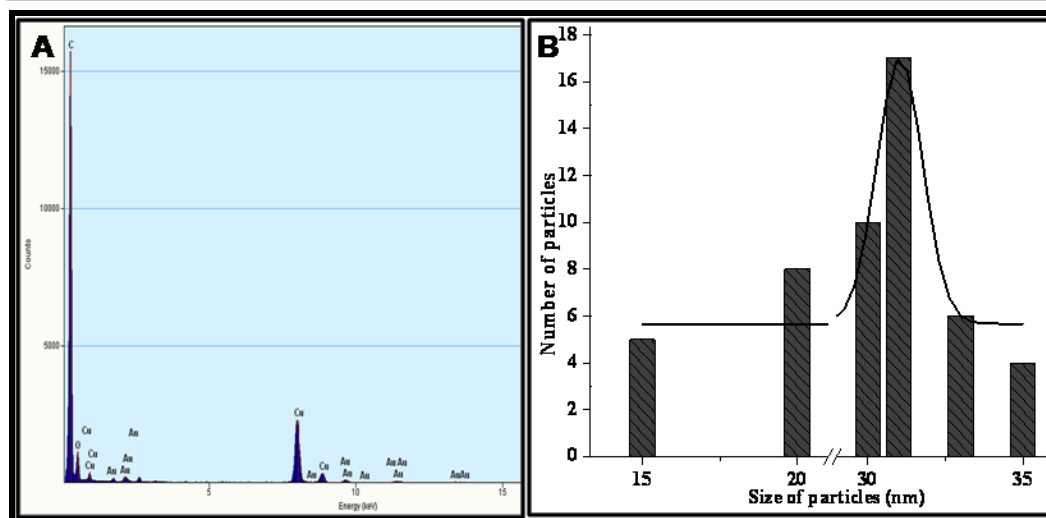
Figure 3.31: (A) EDS analysis. **(B)** Particles size distribution of gold nanoparticles synthesized by peanut callus cells.

3.4.3.2.4 **XRD Analysis:**

XRD analysis can provide information of the crystalline nature of the particles. The Fig. 3.28.B shows the XRD of intracellular nanoparticles. The presence of four Bragg reflections corresponding to the (111), (200), (220) and (311) orientations agree with those reported for gold nanoparticles. The peak positions and 2θ (38.14, 44.35, 64.74, 77.56) values agree with those reported for gold nanoparticles [65]. These reflections are broad which indicates that the formed nanoparticles are in the nanoscale dimensions.

3.4.4 Conclusions

In conclusion the intra- and extra-cellular synthesis of gold nanoparticles by reaction of aqueous $HAuCl_4$ ions with the live peanut callus cells has been demonstrated. The extracellular nanoparticles formed are of different shapes and sizes whereas the intracellular nanoparticles are highly monodispersed. In the case of extracellular synthesis, reduction of gold ions and subsequent formation of highly stable GNPs of different sizes and shapes may occur by the reductases enzymes secreted by the callus cells into the solution. These nanoparticles may be immobilized in different matrices or in thin-film form for several electronic and biomedical applications. The synthesis of highly monodispersed and stable intracellular gold nanoparticles may occur by the above enzymes present on the plant cells or on the cytoplasmic membrane and these

nanoparticles may be used in catalysis and as precursors for synthesis of coatings for electronic applications.

Further investigations are in progress for the identification of the biomolecules released by peanut callus cells when exposed to gold solution leading to the formation of gold nanoparticles both intra- and extra-cellularly. This opens up a new area for environment friendly methods for the synthesis of nanoparticles, which can possibly be extended to other metals.

References

[1] Kumari, A., Yadava, S. K., Pakadeb, Y. B., Singh, B., Yadava, S. C. Development of biodegradable nanoparticles for delivery of quercetin. *Colloids Surf. B.* 2010, 80, 184–192.

[2] Kumari, A., Yadava, S. K, Yadava, S. C. Biodegradable polymeric nanoparticles based drug delivery systems. *Colloids Surf. B.* 2010, 75, 1–18.

[3] Shankar, S. S., Rai, A., Ahmad, A., Sastry, M. Rapid synthesis of Au, Ag, and bimetallic Au core–Ag shell Nanoparticles using Neem (*Azadirachta indica*) leaf broth. *Colloids Surf. B.* 2004, 275, 496–502.

[4] Shankar, S. S., Ahmad, A., Pasricha, R., Sastry, M. Bio reduction of chloroaurate ions by geranium leaves and its endophytic fungus yields gold nanoparticles of different shapes. *J. Mater. Chem.* 2003, 13, 1822–1826.

[5] Li, S., Shen Y., Xie, A., Yu, X, Qiu, L., Zhang, L., Zhang, Q. Green synthesis of silver nanoparticles using *Capsicum annuum* L. extract. *Green Chem.* 2007, 9, 852–858.

[6] Ankamwar, B., Damle, C., Ahmad, A., Sastry, M. Biosynthesis of gold and silver nanoparticles using *Emblica officinalis* fruit extract, their phase transfer and transmetallation in an organic solution. *J. Nanosci. Nanotechnol.* 2005, 5, 16, 5–1671.

[7] Gardea-Torresdey, J. L., Parsons, J. G., Gomez, E., Peralta-Videa, J. R., Troiani, H. E, Santiago, P., Jose-Yacaman, M. Formation and growth of Au nanoparticles inside live *Alfalfa* plants. *Nano Lett.* 2002, 2, 397–401.

[8] Gardea-Torresdey, J. L., Gomez, E., Peralta-Videa J. R., Parsons, J. G., Troiani, H., Jose Yacaman, M. *Alfalfa* sprouts: a natural source for the synthesis of silver nanoparticles. *Langmuir*, 2003, 19, 1357–1361.

[9] Marshall, A. T., Haverkamp, R. G., Davies, C. E., Parsons, J. G., Gardea-Torresdey, J. L., van Agterveld, D. Accumulation of gold nanoparticles in *Brassica juncea. Int. J. Phytorem.* 2007, 9, 197–206.

[10] Ankanna, S., Prasad, T. N. V. K. V., Elumalai, E. K., Savithramma, N. Production of biogenic silver nanoparticles using *Boswellia ovalifoliolata* stem bark. *Digest J. Nanomater. Biostruct*. 2010, 5, 369–372.

[11] Rajasekharreddy, P., Rani, P. U., Sreedhar, B. Qualitative assessment of silver and gold nanoparticle synthesis in various plants: a photobiological approach. *J. Nanopart. Res*. 2010, 12, 1711–1721.

[12] Kumar, V., Yadav, S. C., Yadav, S. K. *Syzygium cumini* leaf and seed extract mediated biosynthesis of silver nanoparticles and their characterization. *J. Chem. Technol. Biotechnol*. 85, 10, 1301–1309.

[13] Shankar, S. S., Rai, A., Ankamwar, B., Singh, A., Ahmad, A., Sastry, M. Biological synthesis of triangular gold nanoprisms. *Nat. Mater*. 2004, 3, 482–488.

[14] Chandran, S. P., Chaudhary, M., Pasricha, R., Ahmad, A., Sastry, M. Synthesis of gold nanotriangles and silver nanoparticles using *Aloe vera* plant extracts. *Biotechnol. Prog*. 2006, 22, 577–583.

[15] Song, J. Y., Kim, B. S. Rapid biological synthesis of silver nanoparticles using plant leaf extracts. *Bioprocess. Biosyst. Eng*. 2009, 32, 79–84.

[16] Song, J. Y., Jang, H. K., Kim, B. S. Biological synthesis of gold nanoparticles using *Magnolia kobus and Diopyros kaki* leaf extracts. *Process Biochem*. 2009, 44, 10, 1133–1138.

[17] Orendorff, C. J., Murphy, C. J. Quantitation of metal in silver assisted growth of gold nanorods. *J. Phys. Chem. B*. 2006, 110, 3990–3994.

[18] Henglein, A. Physicochemical properties of small metal particles in solution, microelectrode reactions, chemisorption, composite metal particles, and the atom-to-metal transition. *J. Phys. Chem*. 1993, 97, 5457–5471.

[19] Wang, X., Egan, C. E., Zhou, M., Prince, K., Mitchell, D. R. G., Caruso, R. A. Effective gel for gold nanoparticle formation, support and metal oxide templating. *Chem. Commun*. 2007, 29, 3060–3062.

[20] http://www.chem.csustan.edu/Tutorials/INFRARED.HTM.

[21] Ahmad, A., Senapati, S., Khan, M. I., Kumar, R., Sastry, M. Extra-cellular biosynthesis of monodisperse gold nanoparticles by a novel extremophilic actinomycete, *Thermomonospora* sp. *Langmuir*, 2003, 19, 3550–3553.

[22] Klaus, T., Joerger, R., Olsson, E., Granqvist, C. G. Silver-based crystalline nanoparticles, microbially fabricated. *Proc. Natl. Acad. Sci.* U.S.A. 1999, 96, 13611–13614.

[23] Hosea, M., Greene, B., Mcpherson, R., Henzl, M., Alexander, M. D., Darnall, D. W. Accumulation of elemental gold on the alga *Chlorella vulgaris. Inorg. Chim. Acta*. 1986, 123,161–165.

[24] Mukherjee, P., Ahmad, A., Mandal, D., Senapati, S., Sainkar, S. R., Khan, M. I., Ramani, R., Parischa, R., Ajayakumar, P. V., Alam, M., Sastry, M., Kumar, R. Bioreduction of AuCl$_4$- ions by the fungus, *Verticillium* sp. and surface trapping of the gold nanoparticles formed. *Angew. Chem. Intl. Edn. Eng.* 2001, 40, 3585–3588.

[25] Brown, S., Sarikaya, M., Johnson, E. A genetic analysis of crystal growth. *J. Mol. Biol.* 2000, 299, 725–735.

[26] Dameron, C. T., Reese, R. N., Mehra, R. K., Kortan, A. R., Carroll P. J., Steigerwald, M. L., Brus, L. E., Winge, D. R. Biosynthesis of cadmium sulphide quantum semiconductor crystallites. *Nature,* 1989, 338, 596–597.

[27] Labrenz, M., Druschel, G. K., Thomsen-Ebert, T., Gilbert, B., Welch, S. A., Kemner, K. M., Logan, G. A., Summons, R. E., Stasio, G. D., Bond, P. L., Lai, B., Kelly, S. D., Banfield, J. F. Formation of sphalerite (ZnS) deposits in natural biofilms of sulfate-reducing bacteria. *Science*, 2000, 290, 1744–1747.

[28] Ahmad, A., Mukherjee, P., Mandal, D., Senapati, S, Khan, M. I., Kumar, R., Sastry, M. Enzyme mediated extracellular synthesis of CdS nanoparticles by the fungus, *Fusarium oxysporum. J. Am. Chem. Soc.* 2002, 124**,** 12108–12109.

[29] Raju, D., Mehta, U. J., Hazra, S. Synthesis of gold nanoparticles by various leaf fractions of *Semecarpus anacardium* L. tree. *Trees- Struct. Funct.* 2011, 25, 145–151.

[30] Sharma, N. C., Nath, S. V., Parsons, J. G., Gardea-Torresdey, J., Pal, T. Synthesis of plant-mediated gold nanoparticles and catalytic role of biomatrix-embedded nanomaterials. *Environ. Sci. Technol.* 2007, 41, 5137-5142.

[31] Harris, A. T., Bali, R. On the formation and extent of uptake of silver nanoparticles by live plants. *Nanopart. Res.* 2008, 10:691–695.

[32] Mulvaney, P. Surface plasmon spectroscopy of nanosized metal particles *Langmuir*, 1996, 12, (3), 788–800.

[33] Seo, K. I., McIntyre, P. C., Kim, H., Saraswat, K. C. Formation of an interfacial Zr-silicate layer between ZrO_2 and Si through *in situ* vacuum annealing. *Appl. Phys. Lett.* 2005, 86, 082904.

[34] Margalit, R., Vasquez, R. P. J. Determination of protein orientation on surfaces with X-ray photoelectron spectroscopy. *Protein. Chem.* 1990, 9, 1, 105.

[35] Wagner, C. D., Riggs, W. M., Davis, L. E., Mouler, J. F. *Handbook of X-Ray Photoelectron Spectroscopy*; Muilenberg, G. E., Ed.; Perkin Elmer Corporation, Physical Electronics Division: Eden Prairie, M. N, 1979.

[36] Joerger, R., Klaus, T., Granqvist C-G. Biologically produced silver–carbon composite materials for optically functional thin film coatings. *Adv. Mater.* 2000, 12, 407–409.

[37] Haverkamp, R. G., Marshall, A. T., Agterveld, D. V. Pick your carats: nanoparticles of gold–silver–copper alloy produced *in vivo*. *J. Nanopart. Res.* 2007, 9, 697–700.

[38] Jones, D. A., Lelyveld, T. P., Mavrofidis, S. D. Microwave heating applications in environmental engineering- A review. *Res. Conserv. Recycl.* 2002, 34, 75–90.

[39] Kozin, L. F., Melekhin, V. T. Extraction of gold from ores and concentrates by leaching with the use of cyanides and alternative reagents. *Russ. J. Appl. Chem.* 2004, 77, 1573–1592.

[40] Volesky, B. Biosorption for the next century. In bio hydrometallurgy and the environment toward the mining of the 21st century. Part B. Molecular Biology, Biosorption, Bioremediation. Chapt. 4, Biosorption. 1999, pp. 161–170.

[41] Deplanche, K., Macaskie, L. E. Biorecovery of gold by *Escherichia coli* and *Desulfovibrio desulfuricans*. *Biotechnol. Bioeng*. 2008, 99, 5, 1055-1064.

[42] Ahmad, A., Senapati, S., Khan, M. I., Kumar, R., Sastry, M. Extra/intracellular biosynthesis of gold nanoparticles by an alkalotolerant fungus, *Trichothecium* sp. *J. Biomed. Nanotechnol*. 2005, 1, 47–53.

[43] Mukherjee, P., Senapati, S., Mandal, D., Ahmad, A., Khan, M. I., Kumar, R., Sastry, M. Extracellular synthesis of gold nanoparticles by the fungus *Fusarium oxysporum*. *Chem. Biochem*. 2002, 5, 461–463.

[44] Kashefi, K., Tor, J. M., Nevin, K. P., Lovley, D. R. Reductive precipitation of gold by dissimilatory Fe (III)-reducing bacteria and Archaea. *Appl. Environ. Microbiol*. 2001, 67, 3275–3279.

[45] Karthikeyan, S., Beveridge, T. J. *Pseudomonas aeruginosa* biofilms react with and precipitate toxic soluble gold. *Environ. Microbiol*. 2002, 4, 667–675.

[46] Southam, G., Beveridge, T. J. The *in-vitro* formation of placer gold by bacteria. *Geochim. Cosmochim. Acta*. 1994, 58, 4527–4530.

[47] Konishi, Y., Tsukiyama, T., Ohno, K., Saitoh, N., Nomura, T., Nagamine, S. Intracellular recovery of gold by microbial reduction of $AuCl^{-4}$ ions using the anaerobic bacterium *Shewanella* alga. *Hydrometallurgy*, 2006, 81, 24–29.

[48] Armendariz, V., Parsons, J. G., Lopez, M. L., Peralta-Videa, J. R., Jose-Yacaman, M., Gardea-Torresdey, J. L. The extraction of gold nanoparticles from oat and wheat biomasses using sodium citrate and cetyltrimethylammonium bromide, studied by x-ray absorption spectroscopy, high-resolution transmission electron microscopy, and UV–visible spectroscopy. *Nanotechnology*, 2009, 20, 105607-105615.

[49] Cheng, W., Wang, E. Size-dependent phase transfer of gold nanoparticles from water into toluene by tetraoctylammonium cations: a wholly electrostatic interaction *J. Phys. Chem*. B. 2004, 108, 24–26.

[50] Selvakannan, P. R., Mandal, S., Phadtare, S., Gole, A., Pasricha, R., Adyanthaya, S. D, Sastry, M. Water-dispersible tryptophan-protected gold nanoparticles

prepared by the spontaneous reduction of aqueous chloroaurate ions by theamino acid *J. Colloid Interface Sci.* 2004, 269, 97–102.

[51] Chen, F., Xu, G. Q., Hor, T. S. A. Preparation and assembly of colloidal gold nanoparticles in CTAB-stabilized reverse microemulsion. *Mater. Lett.* 2003, 57, 3282–3288.

[52] Rostami, H., Haghnazari, A., Kavei, G., Ghareyazie, B., Hesari, F. Phytobiosynthesies of gold nanoparticles and comparision of two plant species (Canola and alfalfa). *Indian J. Biotechnol.* 10, 2011, 245-247.

[53] Anderson, C. W. N., Brooks, R. R., Stewart, R. B., Simcock, R. Harvesting a crop of gold in plants. *Nature*, 1998, 395, 553-554.

[54] Creamer, N. J., Baxter-plant, V. S., Henderson, J., Potter, M., Macaskie, L. E, Palladium and gold removal and recovery from precious metal solutions and electronic scrap leachates by *Desulfovibrio desulfuricans*. *Plant. Biotechnol. Lett*. 2006, 28, 1475–1484.

[55] Mirkin, C. A., Letsinger, R. L., Mucic, R. C., Storhoff, J. J. A DNA-based method for rationally assembling nanoparticles into macroscopic materials. *Nature*, 1996, 382, 607–609.

[56] Han, M., Gao, X., Su, J. Z., Nie, S. *In vivo* cancer targeting and imaging with semiconductor quantum dots. *Nat. Biotechnol.* 2001, 19, 631–635.

[57] Salem, A. K., Searson, P. C., Leong, K. W. Multifunctional nanorods for gene delivery. *Nat. Mater.* 2003, 2, 668–671.

[58] Huang, X., El-Sayed, I. H., Qian, W., El-Sayed, M. A. J. Cancer cell imaging and photothermal therapy in the near-infrared region by using gold nanorods, *J. Am. Chem. Soc.* 2006, 128, 2115–2120.

[59] Masala, O., Seshadri, R. Synthesis routes for large volumes of nanoparticles *Annu. Rev. Mater. Res.* 2004, 34, 41–81.

[60] Hao, E., Bailey, R. C., Schatz, G. C., Hupp, J. T., Li, S. Synthesis and optical properties of "branched" gold nano crystals, *Nano Lett*. 2004, 4, 327–330.

[61] Levy, R., Thanh, N. T. K. Doty, R. C., Hussaiy, I., Nichols, R. J., Schiffrin, D. J., Brust, M., Ferning, D. G. Rational and combinatorial design of peptide capping ligands for gold nanoparticles. *J. Am. Chem. Soc*. 2004, 126, 10076–10084.

[62] Xie, J., Lee, J. Y., Wang, D. I. C., Ting, Y. High-yield synthesis of complex gold nanostructures in a fungal system. *J. Phys. Chem. C*, 2007, 111, 16858–16865.

[63] Beveridge, T. J., Murray, R. G. E. Site of metal deposition in the cell wall of *Bacillus subtilis*. *J. Bacteriol*. 1980, 14, 1876–887.

[64] Fortin, D., Beveridge, T. J. From biology to biotechnology and medical applications. In: Baeuerien E (ed) Biomineralization, Wiley-VCH, Weinheim, 2000, pp 7–22.

[65] Ahmad, A., Senapati S., Khan, M. I., Kumar, R., Ramani, R., Srinivas, V., Sastry, M. Intracellular synthesis of gold nanoparticles by a novel alkalotolerant actinomycete, *Rhodococcus* species*, Nanotechnology*, 2003, 14, 824–827.

[66] Mukherjee, P., Ahmad, A., Mandal, D., Senapati, S., Sainkar, S. R., Khan, M. I, Parischa, R., Ajayakumar, P. V, Alam, M., Kumar, R., Sastry, M. Fungus mediated synthesis of silver nanoparticles and their immobilization in the mycelial matrix: a novel biological approach to nanoparticle synthesis. *Nano Lett*. 2001, 1, 515–519.

[67] Singaravelu, G., Arockiamary, J., Ganesh, K., Govindaraju, K. A novel extracellular synthesis of monodisperse gold nanoparticles using marine alga, *Sargassum wightii* Greville. *Colloids Surf. B*. 2007, 57, 97-101.

[68] Satyavani, K., Ramanathan, T., Gurudeeban, S. Green synthesis of sliver nanoparticles by using stem derived callus extract of bitter apple (*Citrullus colocynthis*) *Digest J. Nanomater. Biostruct*. 2011. 1019 -1024.

[69] Mude, N., Ingle, A., Gade, A., Rai, M. Synthesis of silver nanoparticles by the callus extract of *Carica papaya*: A first report. *J. Plant Biochem. Biotechnol*. 2009, *18,* 83-86.

[70] Reddy, A. S., Chen, C. Y., Chen, C. C., Jean, J. S., Chen, H. R., Tseng, M. J., Fan, C. W., Wang, J. C. Biological synthesis of gold and silver nanoparticles

mediated by the bacteria *Bacillus subtilis. J. Nanosci. Nanotechnol*. 2010, 10, 6567–6574.

[71] Xie, J., Lee, J. Y., Wang, D. I. C., Ting, Y. P. Identification of active biomolecules in the high-yield synthesis of single-crystalline gold nanoplates in algal solutions. *Small,* 2007, 3, 4, 672 – 682.

[72] Shankar, S. S., Ahmad, A., Sastry, M. Geranium Leaf Assisted Biosynthesis of Silver Nanoparticles *Biotechnol. Prog*. 2003, 19, 1627-1631.

[73] He, S., Guo, Z., Zhang, Y., Zhang, S., Wang, J., Gu, N. Biosynthesis of gold nanoparticles using the bacteria *Rhodopseudomonas capsulata. Mater. Lett.* 2007, 61 3984–3987.

[74] Focsan, M., Ardelean, I. I., Craciun, C., Astilean, S. Interplay between gold nanoparticle biosynthesis and metabolic activity of cyanobacterium *Synechocystis* sp. PCC 6803. *Nanotechnology*, 2011, 22, 485101-485109.

Chapter 4

**Identification of biomolecules responsible for
the biosynthesis of nanomaterials.**

| Protein | Gold Ions | GNPs Formation by Protein |
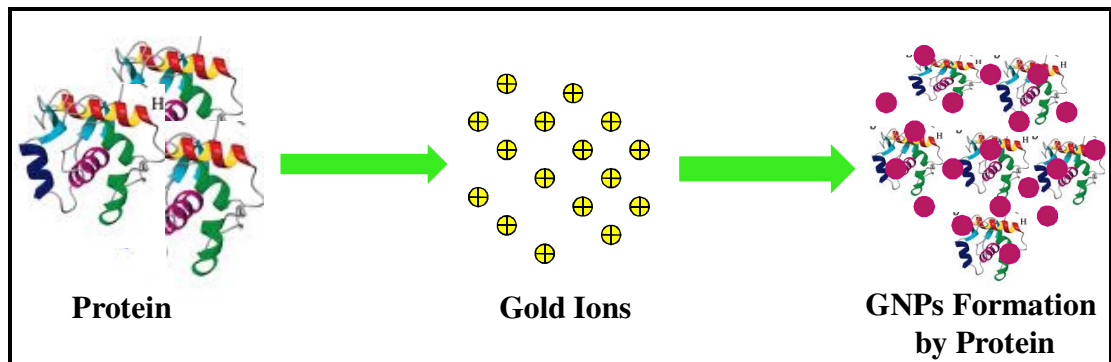
Summary:

In this work, we have fabricated crystalline gold nanoparticles by treating an aqueous solution of 10^{-4}M HAuCl$_4$ with the proteins extracted from roots of *in vitro* raised peanut seedling and purified them by FPLC at room temperature and identified as Mannose glucose binding lectin and Ara h 8 allergen isoforms by ESI MS/MS. These proteins tested positive for the reduction of 10^{-4}M HAuCl$_4$. The results suggest that proteins are the primary biomolecules involved in the reduction of Au (III) to Au (0). We could isolate different protein of molecular weight 16.4, 28.3 and 30 kDa involved in the formation of nanoparticles. The protein with molecular weight 16.4 kDa yielded NPs of 25-60 nm whereas, the protein with molecular weight 28.3 and 30 kDa yielded NPs of 5-20 nm in size. The particles synthesized by 28.3 kDa and 30 kDa were highly monodispersed. These results clearly indicate that the sizes of the nanoparticles can be controlled by different proteins.

4.1 Introduction

Nanoparticle synthesis in the past has been carried out mainly by chemical processes, which may involve the use of toxic chemicals, reducing agents such as sodium borohydride, hydroxylamine [1, 2, 3] a capping agent such as trioctyl phosphine oxide [4, 5] and sometimes organic solvents like toluene or chloroform [6, 7, 9], for improved results. The environmental cost of production can be relatively high. There is a need to develop environmentally sustainable green synthesis alternatives to the existing methods [10]. The selection of an environmentally acceptable solvent system and eco-friendly reducing agent for the formation of nanoparticles is solicited.

Biological approaches for the biosynthesis of intra or extracellular metal nanoparticles using microorganisms such as fungi [11], bacteria [12], algae [13] and yeast [14] by using plants extracts [15-16] and living plants [17]. Although a number of biological species have been found to be capable of synthesizing gold nanoparticles, the control of the size and shape of the particles and the understanding of the mechanism involved for the formation of nanoparticles is not clearly solved.

Gold nanoparticles have many applications and can be produced in a number of shapes like spheres, [18] rods, [19, 20] cubes [21, 22] branched structures, [23, 24] and mixtures of triangular/hexagonal/spherical particles. There are some difficulties for the synthesis of planar thin nanoparticles or nanoplates, in high yield and highly controlled size and shape by chemical method [25, 26].

The new proteins of bacteria, having molecular weights between 25 and 66 kDa could be responsible for the reduction of chloroaurate ions [27]. There are reports showing the formation of nanoparticles by protein. A protein with a molecular weight of approximately 28 kDa was isolated and purified by reverse- phase HPLC and this protein tested positive for the reduction of chloroauric acid in aqueous solution [28].

The gold nanoplates synthesized by using Bovine serum albumin (BSA) were reported [29]. The formation of silver nanoparticles for the first time with nitrate reductase was studied [30]. Au NPs synthesized with α-amylase act as both the reductive reagent and the stabilizer, as reported by Rangnekar *et al.* (2007) [31].

Biomolecules such as amino acids e.g. lysine have also been used as the protective agents for the formation of Au NPs [32].

The developed single step method to prepare lysozyme monolayer-stabilized Au NPs of 2 nm narrow size distribution, which shows high stability and excellent solubility in both aqueous solution and various organic solvents. The use of protein lysozyme as the capping agent gives the particles a biocompatible and hydrophilic surface, which allows their potential applications in biological and medical fields [33]. Intact single crystals of lysozyme were studied for time-dependent, protein-directed growth of gold nanoparticles. The formations of GNPs in crystals were observed after a period of 24 hr [34].

Here we report the isolation of proteins from the peanut roots and their purification by FPLC which are responsible for the synthesis of GNPs. Isolation of protein from the plant sources has not been much studied. The purification of protein was carried out by using FPLC. Different fractions collected were used to check the formation of gold nanoparticles .The active fractions were electrophoresed for confirmation of proteins. The synthesised nanoparticles were characterized by UV-vis, TEM and SAED.

4.2 Experimental Details

The procedure for seedling germination and synthesis of GNPs has been explained in Chapter 3 Section 2.

4.2.1 Preparation of SDS PAGE Chemicals:

1. Acrylamide (Hi-media) and Bisacrylamide (Qualigens): 29.2 gm of acrylamide and 800 mg of bisacrylamide were dissolved in 100 mL of distilled water.

2. 1.5 M Tris HCl (pH 8.8): 18 g of Tris base (Qualigens) was dissolved in 100 mL distilled water and pH was adjusted to 8.8.

3. 0.5 M Tris HCl (pH 6.8): 6.05 gm of Tris base (Qualigens) was dissolved in 100 mL distilled water and pH was adjusted to 6.8.

4. 10% SDS (Hi-media)

5. TEMED (Sigma)

6. 10% APS

10X Running buffer (100 mL):

196 mM Glycine (Merck) + 1% SDS + 50 mM Tris-Base (pH-8.3).

Sample buffer (10 mL):

125 mM Tris HCL + 10% 2-mercaptoethanol (Sigma) + 10% SDS + 10% Glycerol (Qualigens).

Extraction buffer:

100 mM Tris buffer + 1 mM EDTA and 10 mM DDT.

Gel composition:

Table 4.1 Resolving gel

Chemical	*Volume*
Acrylamide + Bisacrylamide	6.7 mL
Tris HCl (pH 8.8)	5 mL
Distilled Water (DW)	7.9 mL
10% SDS	200 μL
10% APS	200 μL
TEMED	23 μL

Table 4.2 Stacking gel

Chemical	*Volume*
Acrylamide + Bisacrylamide	0.75 mL
Tris HCl (pH 6.8)	1.25 mL
DW	2.8 mL
10% SDS	50 μL
10% APS	55 μL
TEMED	6 μL

4.2.2 Silver Staining Preparation

*Fixer Preparation***:**

40 mL of methanol was mixed with 12 mL of glacial acetic acid and final volume is made up to 100 mL with distilled water.

*Silver Stain***:**

200 mg of silver nitrate was dissolved in 100 mL of deionised water to which 75 μL of formaldehyde solution was added.

Sodium thiosulphate stock solution (20 mg mL^{-1}):

200 mg of sodium thiosulphate was dissolved in 10 mL of distilled water.

Sodium thiosulphate working solution:

1 mL of stock solution of Sodium thiosulphate was mixed in 99 mL of distilled water to make 0.02% working solution of sodium thiosulphate.

Developer:

6 gm of sodium carbonate was dissolved in 80 mL of distilled water to which 20 μL of stock solution of sodium thiosulphate and 50 μL of formaldehyde solution was added and the final volume made-up to 100 mL with distilled water.

4.2.3 *Preparation of the separating gel:*

A vertical slab gel (Bioera) was assembled using 1.0 mm spacers. 10% separating gel solution was made according to Table 4.1. After the addition of TEMED and ammonium persulfate, the solution was mixed gently without generating bubbles. The solution was pipetted into the gel cassette leaving 1.5 cm from the top unfilled. The gel solution was overlaid with water to remove trapped air bubbles. A sharp liquid-gel inter-surface was observed when the gel was polymerized.

4.2.4 *Preparation of the stacking gel:*

Stacking gel solution was prepared according to Table 4.2. After the addition of TEMED and ammonium per sulfate the solution was mixed and overlaid on the separating gel. A comb was inserted and due care was taken to removed trapped air bubbles beneath the comb teeth. The gel was left to polymerize.

4.2.5 *Preparation of the sample:*

Equal parts of the protein sample and the loading buffer were mixed in a micro centrifuge tube and kept in a boiling water bath for 3-5 min for SDS-PAGE. Gel was run at room temperature at 40mA.

4.2.6 *Loading and running the polyacrylamide gel:*

Appropriate level of tank buffer was maintained in the lower and upper and buffer chambers. Samples were precisely loaded in side the wells with the help of micropipette. Voltage was set at 40 mA. The run was stopped when the dye reached the bottom of the polyacrylamide gel.

4.2.7 Silver staining of the gel:

The gel was transferred to the fixer solution and kept overnight on dancing shaker. This was followed by 3 x 20 min washes in 50% ethanol. The gel was transferred to sodium thiosulfate solution for 1 min and rinsed thrice with deionized water (20 s each). The gel was kept for silver staining. Formaldehyde was added to the silver stain solution just before use and kept for 20 min with intermittent shaking in dark. The gel was then rinsed thrice with deionized water 20 s each and transferred to the developer till the bands developed. The gel was washed with deionized water and stored in fixer.

4.2.8 Protein Extraction:

The protein extraction was done by taking 2 gm of peanut roots after exposure to 10^{-4}M $HAuCl_4$ for 72 hr, and ground in mortar and pestle with extraction buffer. Then it was centrifuged at 10,000 rpm for 15 min at 4°C. The supernatant containing protein was taken. The extracted protein was dialyzed with 3 kDa dialysis membrane using 20 mM Tris buffer (pH 8.0). Protein was estimated by Bradford's method (Bradford reagent, Sigma).

4.2.9 Protein purification by Fast protein liquid chromatography (FPLC):

Anion Exchange Chromatography

Ion-Exchange (IEX) chromatography separates molecules on the basis of differences in their net surface charge. Molecules vary considerably in their charge properties and exhibit different degrees of interaction with charged chromatography media according to differences in their overall charge, charge density and surface charge distribution. Since all molecules with ionizable groups can be titrated, their net surface charge is highly pH dependent. Proteins, which are built up of many different amino acids containing weak acidic and basic groups, their net surface charge will change gradually as the pH of the environment changes. Each protein has its own unique net charge versus pH relationship which can be visualized as a titration curve. This curve reflects how the overall net charge of the protein changes according to the pH of the surroundings.

IEX chromatography takes advantage of the fact that the relationship between net surface charge and pH is unique for a specific protein. In an IEX separation, reversible interactions between charged molecules and oppositely charged IEX media are controlled in order to favor binding or elution of specific molecules and achieve separation. A protein that has no net charge at a pH equivalent to its isoelectric point (pI) will not interact with a charged medium. However, at a pH above its isoelectric point, a protein will bind to a positively charged medium or anion exchanger and, at a pH below its pI, a protein will bind to a negatively charged medium or cation exchanger.

A simple method, comprising of binding the negatively charged protein to the surface of DEAE-sepharose Anion Exchanger column, followed by washing to remove all the unbound proteins, and subsequent elution of the bound protein by setting up a NaCl gradient was devised by using the following buffers.

***Binding/Equilibration buffer*:** 20 mM Tris-HCl, pH. 8.0

***Elution Buffer*:** 20 mM Tris-HCl, 1M NaCl, pH. 8.0

The column was pre-equilibrated with Equilibration Buffer at a flow rate of 1.0 mL min^{-1} until a stable baseline for A_{280}, pH and conductivity were obtained. Sample was loaded onto the column with a flow-rate of 0.5 mL min^{-1}. The column was washed with equilibration buffer at same flow-rate until A_{280} fell below 1.0 m A.U. The bound protein was eluted by applying a gradient elution against Elution Buffer with 1M NaCl. The gradient was set up for 100% of Elution Buffer over a period of one hr at a constant flow rate of 0.5 mL min^{-1}.

Fractions of 0.5 mL were collected in Eppendorf tubes. Alternate fraction of 100 μL was added to 10^{-4}M $HAuCl_4$ to check the activity of protein for nanoparticles formation. The fractions which were showing high activity were checked on gel electrophoresis.

The characterization of nanoparticles formed by the protein fractions were characterized by UV-vis, TEM and SAED which were discussed in Chapter 2 Section 2.2 and 2.4.

Electrospray Ionization Mass Spectrometry (ESI-MS) Analysis:

After SDS-PAGE, the gel was stained with coomassie blue. The protein bands of 28.3 kDa and 16.4 kDa were excised from the gel. The gel pieces were then destained by destaining solution (50% acetonitrile / 50% 50 mM NH_4HCO_3). The gel was then dehydrated by treating with 100% acetonitrile. After dehydration, acetonitrile was completely removed by evaporating briefly in speedvac till it appears noticeably shrunken and white. Then gel pieces were dissolved in 10 mM DTT in 100 mM NH_4HCO_3 (Ammonium bicarbonate), the proteins were reduced for 45-50 min at 56^OC and allowed to cool at room temperature. DTT (Dithiothreitol) solution was then removed and 55 mM iodoacetate in 100 mM NH_4HCO_3 was added. This mixture was vortexed, spun briefly and incubated for 45 min in dark at room temperature. This was followed by iodoacetamide removal and gel pieces were washed with 100 mM NH_4HCO_3 for 5 min. The gel pieces were again washed twice with 50% acetonitrile, 50% 50 mM NH_4HCO_3 and dehydrated with 100% acetonitrile as mentioned above. Enough trypsin solution was then added to cover the gel pieces (usually around 20 µL) which were then rehydrated at 4^OC for 30 min in buffer containing 50 mM NH_4HCO_3 and trypsin, spun briefly and more NH_4HCO_3 was added to cover the gel pieces (typically another 25 µL). This was followed by overnight digestion at 37^OC. The digested solution (supernatant) was transferred into clean 1.5 mL Eppendorf tube. 50% acetonitrile containing 5% formic acid solution was added to the gel pieces which were incubated and vortexed for 20 min. This was spun and sonicated for 5 mins in a water bath with no heat. Supernatant was removed and combined with initial digested solution (supernatant). Extracted digests was then vortexed, evaporated to reduce to 5-10 µL. The remaining 5-10 µL was spun at 14,000 rpm for at least 10 min. to remove any microparticulates. The supernatant was carefully transferred to a fresh 1.5 mL Eppendorf tube. The sample was then ready for loading onto ESI-MS. Analysis was done using different software's like Protein Lynx Global Server (PLGS) and by searching the databank sequences in UniProt.

4.3 Results and Discussion

4.3.1 Gel electrophoresis:

After the formation of nanoparticles at different time intervals of 24, 48 and 72 hr, the formed nanoparticles solution was concentrated from 100 mL to 10 mL. An aliquot of 50 μL of each solution was loaded on 10% SDS gel electrophoresis to observe the presence of protein bands (Fig. 4.1). Lane P contains deionized water in which plant was grown for 15 days. In this 7-8 protein bands were seen which shows that the protein are released in deionized water during the germination period for 15 days. Four bands of protein were noted when the plant was exposed to 10^{-4}M HAuCl$_4$ solution for a period of 24 hr. Twenty five to thirty bands having similar protein profile were noted in 48 and 72 hr. The number of protein bands increased after a period of 24 hr which could be due to stress of 10^{-4} M HAuCl$_4$ solution. Increased intensity of na0noparticles was observed as the time prolongs which was also shown in UV-vis analysis of Chapter 3 Section 3.2.3.1.1.
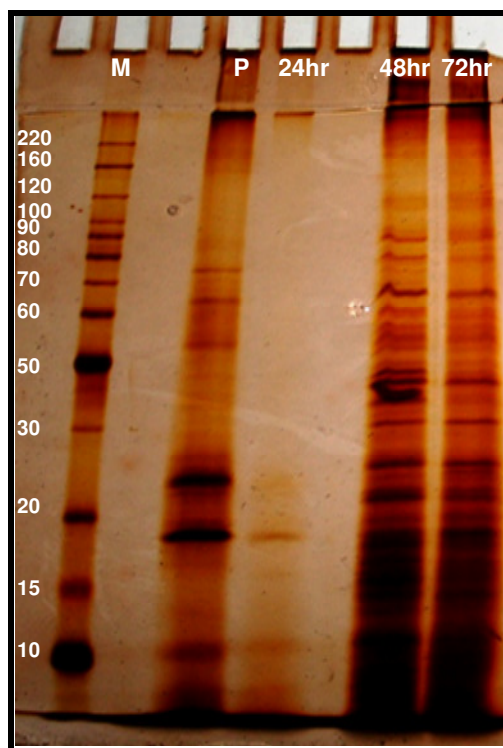
Figure 4.1: PAGE gel electrophoresis of peanut seedling exposed to10^{-4}M HAuCl$_4$ solution for a period of **24**, **48** and **72** hr. **(M)** Marker, **(P)** Plant grown in deionized water for 15 days.

4.3.2 FPLC analysis:

The protein was estimated by Bradford method. 2 mg of protein was loaded for FPLC analysis. The chromatogram of FPLC (Fig. 4.2) shows three peaks at 43, 57 and 63 which indicate the presence of protein. 85 fractions were collected each of 0.5 mL volume. Alternate fraction of 100 μL was used to check the formation of nanoparticles. No activity was observed upto 40th fraction. After the 40th fraction weak intense peak at 530-540 nm was observed in most of the fractions. There were 7 fractions (51, 55, 59, 36, 70, 75 and 84) showing intense peak at 530-540 nm. These fractions were further characterized.
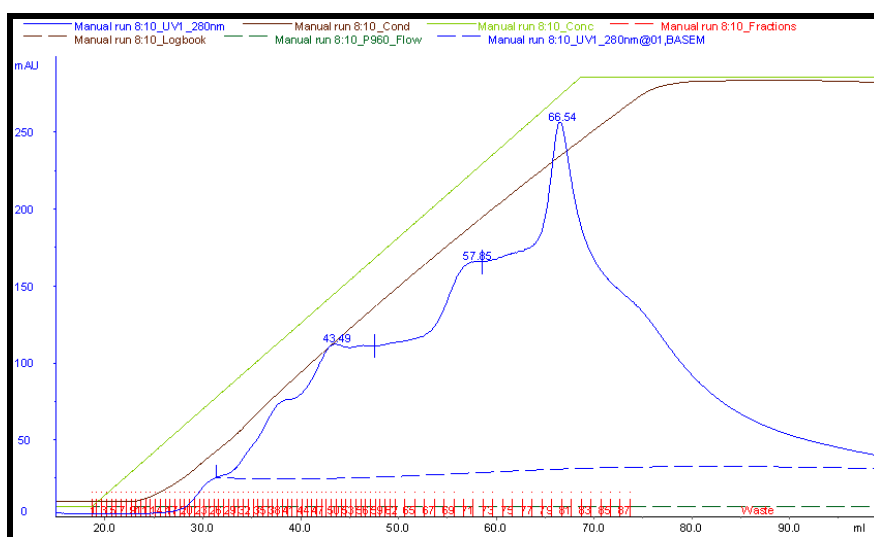

Figure 4.2: Peanut root proteins eluted by FPLC shows the presence of protein peaks

4.3.3 Characterization of nanoparticles formed by protein of 51st fraction:
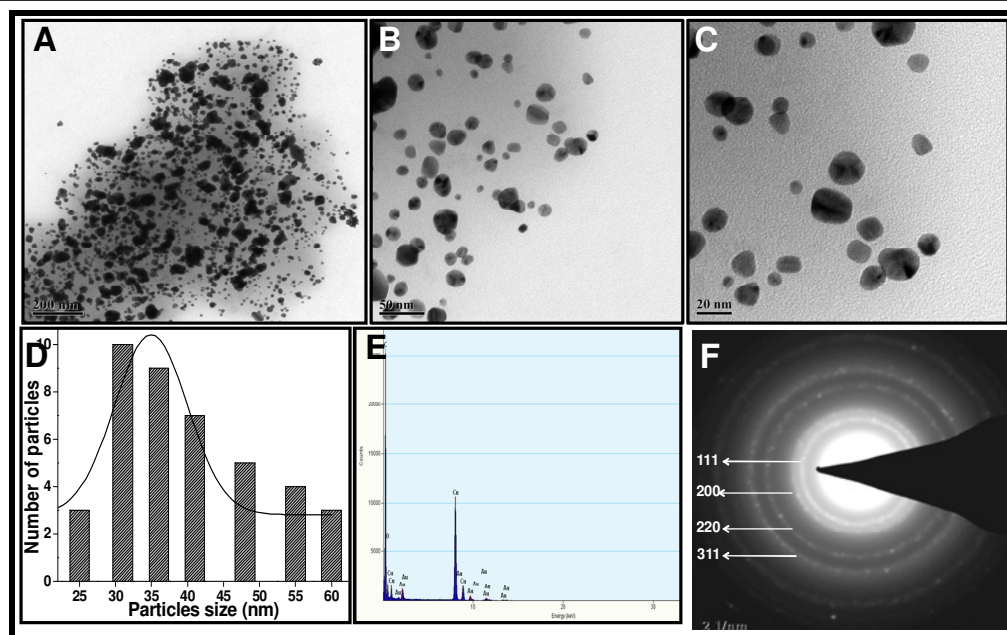
4.3.3.1 UV-vis analysis:

The 100 μL of the 51st fraction was added to the 3 mL of 10^{-4}M $HAuCl_4$. After a period of 12 hr there was a change in the color of solution to light purple. The solution was subjected to UV-vis visible spectroscopy which showed a peak at 530-540 nm indicating the formation of GNPs (Fig. 4.3A). In the control solution containing Tris HCl + NaCl buffer and 10^{-4}M $HAuCl_4$ there was no change in the colour of the solution and the absence of peak at 530 to 540 nm (Fig. 4.3B) indicates no nanoparticles formation in control solution.
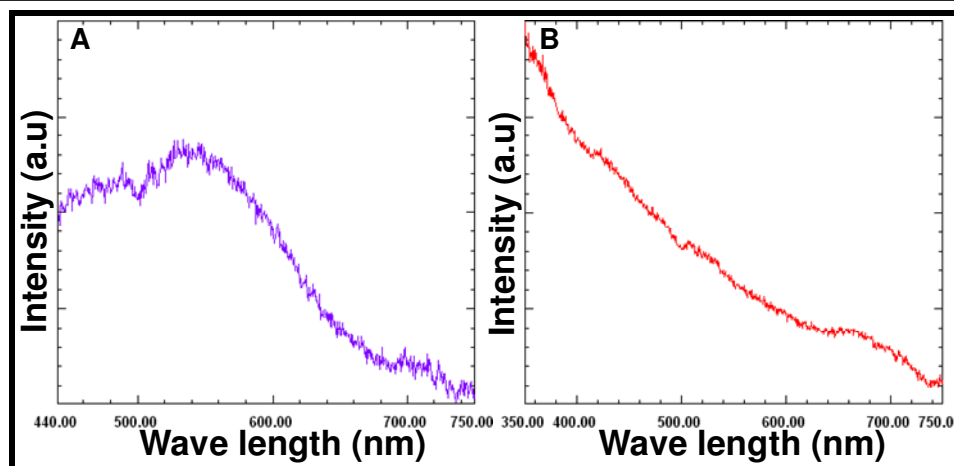
Figure 4.3: **(A)** UV-vis analysis of nanoparticles formed by the protein of 51st fraction and **(B)** the control sample showing absence of peak at 530-540 nm.

4.3.3.2 Characterization of nanoparticles by TEM, EDS and SAED:

The nanoparticles formed by the 51st fraction of protein at different magnifications (Fig. 4.4A-C) showed that they were of different shapes and sizes of NPs. The particles were well separated with no agglomeration. In Fig. 4.4A a white layer of protein around the particles is clearly seen. There was no nanoparticles formation was observed where the protein is absent. This clearly indicates the formation of nanoparticles is due to protein. The particles size distribution (Fig. 4.4D) indicates the particle sizes ranged from 25 to 60 nm in which most of the particles were 30 nm in size. The EDS analysis was also performed to confirm that the formed nanoparticles were of gold. The other peaks oxygen, carbon and copper were also observed. Oxygen could be from the air present in the chamber and carbon from the biomolecules present on the surface of the nanoparticles. The copper is from the grid used for analysis (Fig. 4.4E). SAED was also performed to confirm whether the nanoparticles are crystalline in nature (Fig 4.4.F).
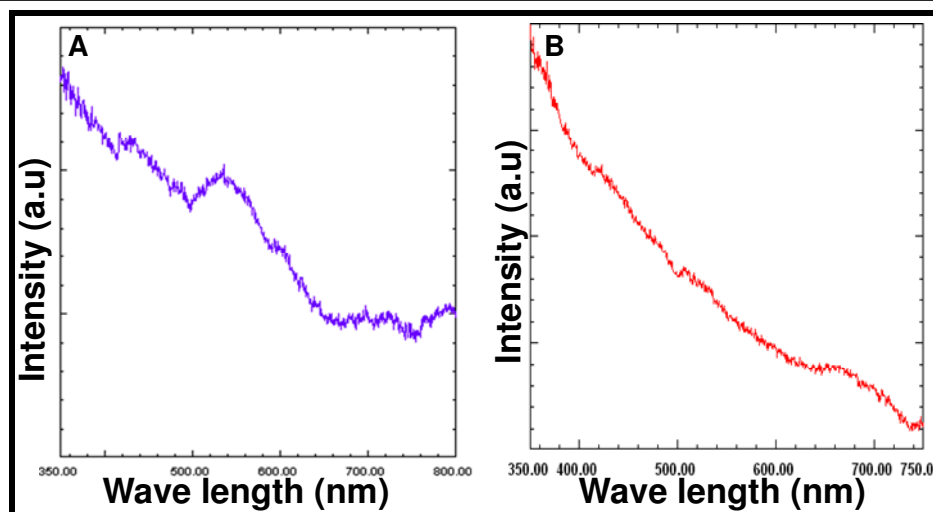
Figure 4.4: TEM Characterization of nanoparticles formed by 51st fraction, **(A-C)** at different magnifications, **(D)** Particle size distribution, **(E)** EDS analysis, **(F)** SAED pattern.

4.3.4 Characterization of nanoparticles formed by protein of 70th fraction:

4.3.4.1 UV-vis analysis:

The FPLC purified fraction of 100 μL was added to the 3 mL of 10^{-4}M HAuCl$_4$. After a period of 12 hr there was a change in color of solution to light purple colour. The solution was subjected to UV visible spectroscopy showing a peak at 520-530 nm indicating the formation of GNPs (Fig. 4.5A). In the control solution containing Tris HCL + NaCl buffer and 10^{-4}M HAuCl$_4$ there was no change in the colour of the solution and also the absence of peak at 530 to 540 nm (Fig. 4.5B) indicates that no nanoparticles were formed in control solution.
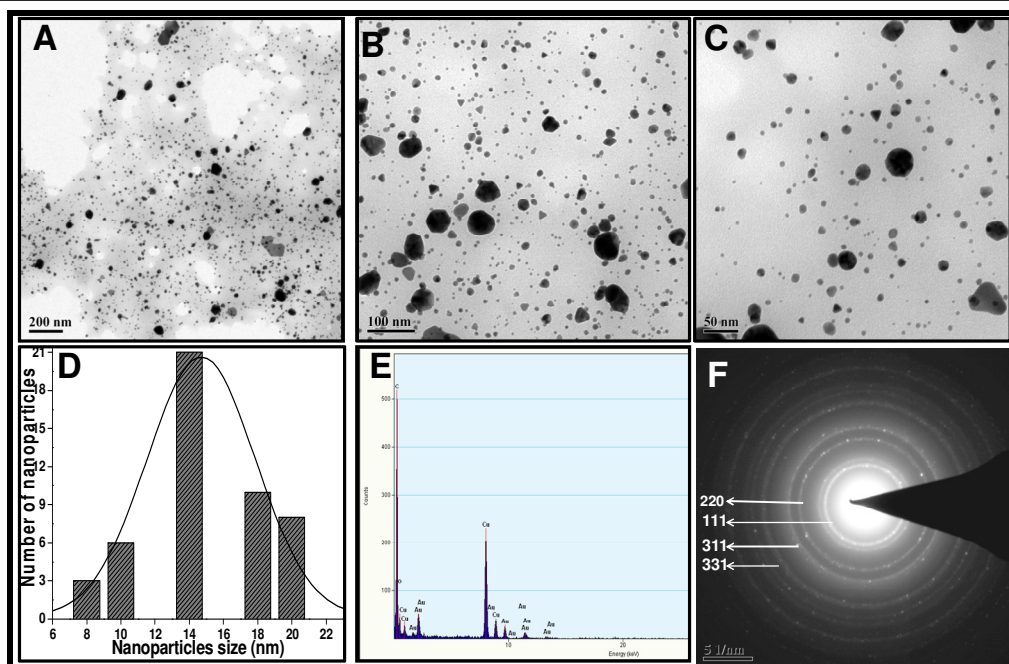
Figure 4.5: **(A)** UV analysis of nanoparticles formed by the 70th fraction and **(B)** is the control showing absence of peak at 530-540 nm.

4.3.4.2 Characterization of nanoparticles by TEM, EDS and SAED:

The nanoparticles formed by the 70th protein fraction shown at different magnifications (Fig. 4.6A-C) were of different shapes and sizes. The particles are well separated with no agglomeration. Particles of circular, octahedral and prism shape were observed. Fig. 6A clearly indicates a white layer of protein around the particles. There were no nanoparticles observed where the protein was absent. This clearly indicates that the formation of nanoparticles is due to protein of molecular weights 29 and 30 kDa. The particles size distribution seen in Fig. 4.6D indicates the particles sizes ranged from 8 to 20 nm in which most of the particles were of 14 nm size. The EDS analysis was also performed to confirm that the formed nanoparticles were of gold. The peak of Au clearly indicates the formation of gold nanoparticles. The other peaks oxygen, carbon and copper were also observed. Oxygen could be from the air present in the chamber and carbon from the biomolecules present on the surface of the nanoparticles. Copper is from the grid used for analysis (Fig. 4.6E). The SAED was also performed to confirm the crystalline nature of nanoparticles. The SAED shows the particles are highly crystalline in nature (Fig. 4.6F).

Figure 4.6: **(A-C)** Characterization of nanoparticles formed by protein of 70th fraction by TEM at different magnifications. **(D)**. Particle size distribution, **(E)**. EDS analysis, **(F)**. SAED pattern.

4.3.5 Characterization of nanoparticles formed by protein of 84th fraction:

4.3.5.1 UV-vis analysis:

The FPLC purified 84th fraction showed the formation of GNPs after addition of 100 µL to the $HAuCl_4$ solution. The colour of the solution changed to light pinkish indicating formation of nanoparticles. The particles were scanned from 400 to 750 nm, showing peak at 520-530 nm (Fig. 4.7A) indicating the formation of nanoparticles. There was no peak observed in the control solution (buffer used for FPLC and $HAuCl_4$ solution) (Fig. 4.7B).
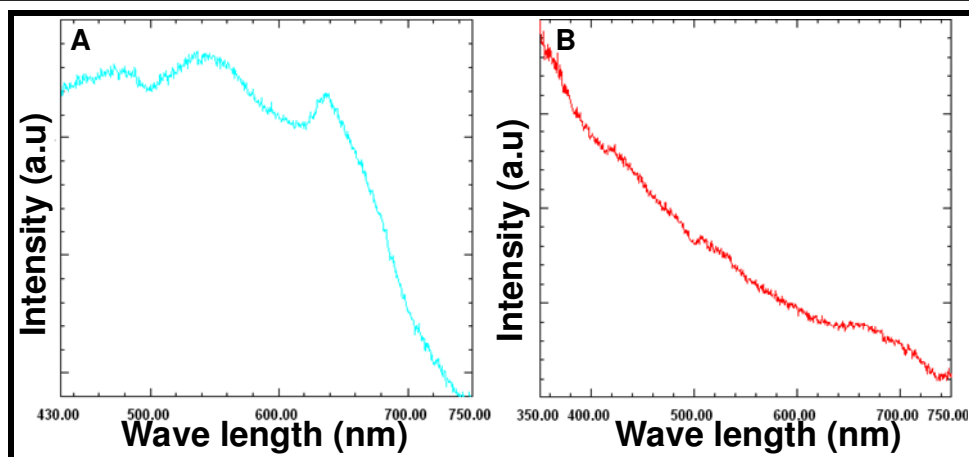
Figure 4.7: (A) UV analysis of nanoparticles formed by the 84th fraction and **(B)** is the control with absence of peak at 530-540 nm.

4.3.5.2 TEM analysis:

The nanoparticles formed by the 84th fraction of protein shown at different magnifications (Fig. 4.8A-C) were of different shapes and sizes. The particles are well separated with no agglomeration. Particles of circular and highly monodisperse nature were observed. Fig. 4.8C shows a white layer of protein around the particles. This clearly indicates that the formation of nanoparticles is due to protein of molecular weights 29 and 30 kDa. The particle size distribution (Fig. 4.8D) indicates that the particle sizes ranged from 5 to 8 nm in which most of the particles were 7 nm in size. The EDS analysis was also performed to confirm that the formed nanoparticles were of gold. The peak of Au clearly indicates the formation of gold nanoparticles. The other peaks oxygen, carbon and copper were also observed. Oxygen could be from the air present in the chamber and carbon from the biomolecules present on the surface of the nanoparticles. The copper is from the grid used for analysis (Fig 4.8E). The SAED was also performed to confirm that the nanoparticles are of crystalline nature. The SAED shows that the particles are highly crystalline in nature (Fig. 4.8F).
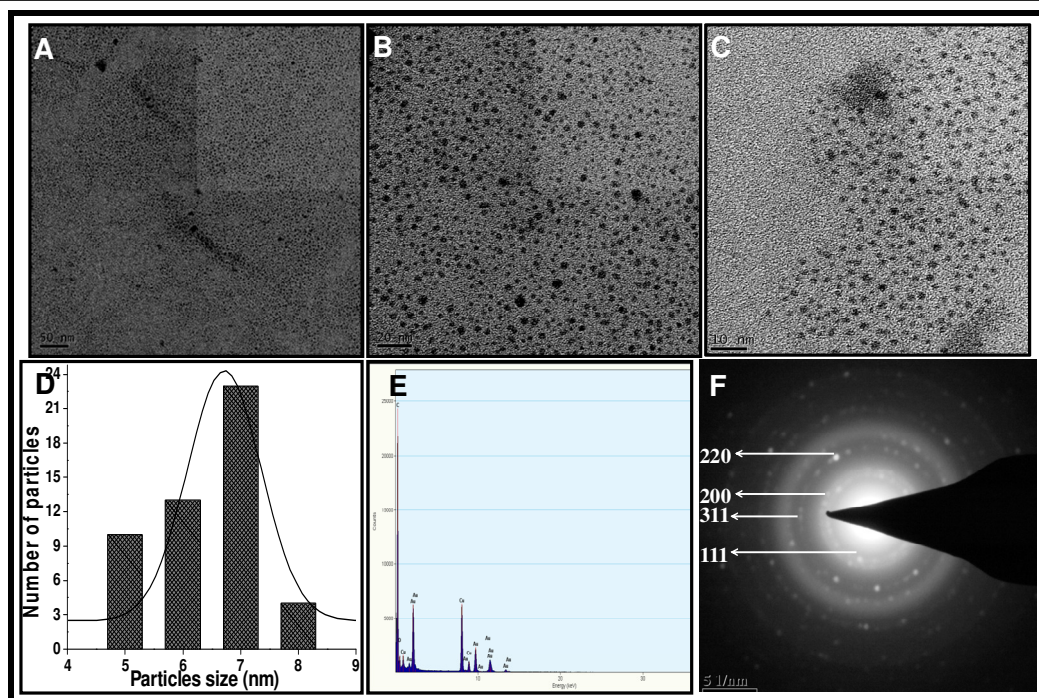
Figure 4.8: (A-C) Characterization of nanoparticles formed by 84th protein by TEM at different magnifications, **(D)** particle size distribution, **(E)** EDS analysis, **(F)** SAED of the nanoparticles.

*4.3.5.3 SDS PAGE gel electrophoresis***:**

The fractions which were showing high activity and one of the fractions which was not showing any activity were loaded on to the 10% SDS PAGE gel to confirm the presence of protein. There was absence of protein band observed in 37th fractions which showed there was no nanoparticle formation, whereas in the fractions 51-55 the presence of a protein band was observed, the molecular weight of the protein is approximately around 21 kDa. The fractions 59-84 showed presence of two protein bands of molecular weight approximately 29 and 30 kDa (Fig. 4.9). These proteins helped in the formation of nanoparticles.

Figure 4.9: SDS PAGE gel electrophoresis of fractions collected from FPLC which were showing high activity in formation of nanoparticles. Fraction 37 showing no protein band, where the activity was absent, 51 and 55 fractions showing 21kDa proteins. Fractions 59 to 84 showed 29 and 30kDa protein.

An interesting result which we observe here is that the protein of molecular weight 21 kDa is helping in the synthesis of 25 to 60 nm size nanoparticles, while the 29 and 30 kDa proteins are helping in the formation of nanoparticles of 5 to 20 nm in size. With the 70th fraction, the particles were of 8-20 nm whereas with 84th fraction, the particles were of 5-8 nm size. The slight variation in size of the particles was of 5 to 10 nm with different fractions of the same protein, which could be due to the variation of protein concentration added to the HAuCl$_4$ solution.

Recent reports have shown the synthesis of nanoparticles by using proteins of various kinds of sources, nitrate reductase in fungus [30], the formation of gold nanoparticles by the proteins of molecular weight 19 and 25 kDa by fungus [35]. The 28 kDa protein was purified by reverse phase HPLC and the purified protein was used as a source of nanoparticles formation by algal cells [28]. The cellular oxido-reductive proteins of *Chlamydomonas reinhardtii* was reported in the formation of silver nanoparticles [36]. The time dependent formation of gold nanoparticles by protein crystals of lysozyme was also studied recently [34].

In recent study on the synthesis of Au microplates using BSA, this protein has both the reducing and stabilizing agents. The hydroxyl groups present in BSA served as a

weak reducing agent. The cysteine residues provides a chemical method of adhering BSA onto the Au surface to function as a stabilizing agent [29]

The recent reports support the formation of nanoparticles by using protein/enzyme. The formation of nanoparticles with the proteins/enzymes of microorganisms is studied. The proteins of plant have not yet been explored for the synthesis of nanoparticles which is complex system unlike microorganisms. In the present study, it has been found that the proteins of peanut root isolated and purified as 21, 29 and 30 kDa molecular weight were helping in the formation of gold nanoparticles.

ESI-MS Analysis:

The protein of molecular weight approximately 29 kDa on SDS gel electrophoresis showed positive result in formation of nanoparticles. The peptides formed by trypsin digestion of the 29 kDa band were further analyzed by ESI MS/MS. The ESI MS/MS data was compared with the available data bank (NCBI and Uniprot). The data shows mannose glucose binding lectin fragment OS *Arachis hypogaea* protein (accession no **Q43377**). The accurate molecular weight of the protein is 28.3 kDa. The protein has coverage % of 62.99 and the pI of protein is 5.22 as shown in Table 1. We have also purified and identified another protein of molecular weight 21 kDa from SDS gel electrophoresis which was analyzed by ESI MS/MS. The protein found to be Ara h 8 allergen isoform OS *Arachis hypogaea* when compared with the data base (accession no is **B0YIU5**). The accurate molecular weight of the protein is 16.4 kDa, pI of the protein is 4.89 and the coverage (%) is 75.82. The sequence of both proteins is shown in Table 4.1. The obtained proteins could possibly be due to gold not being an essential nutrient for the plants. When the plant is exposed to gold solution it undergoes stress and releases stress defence proteins such as lectins. These proteins are secreted by the peanut roots into the gold solution where they reduce the ionic form of gold present in the solution and convert it in to metallic form. The use of lectins has been reported for glycoanalysis method in which lectins are used to probe the glycans of therapeutic glycol proteins that are adsorbed onto gold nanoparticles [37].

Table 4.1 The ESI MS/MS analysis of the matched proteins with available data base.

No	Accession No	Protein Name	PI	Mw (Da)	MW Coverage (%)	proteins Sequence
1	**Q43377**	Mannose glucose binding lectin Fragment OS Arachis hypogaea	5.22	28.3	62.99	ldslsfsynn feqddernli lqgdakfsas kgiqltkvdd ngtpakstvg rvlhstqvrl wekstnrltn fqaqfsfvik spidngadgi affiaapdse ipknsaggtl glfdpqtaqn psanqvlav efdtfyaqdsn gwdpnyqhig idvnsiksaa ttkwerrdgq tlnvlvtyda nsknlqvtas ypdgqryqls yrvdlrdylp ewgrvgfsa asgqqyqshel qswsftstll ytsphylklg rfmi
2	**B0YIU5**	Ara h 8 allergen isoform OS Arachis hypogaea	4.89	16.4	75.82	mgvhtfee esspvpppak lfk atvvdgdel tpklipaiqs ieivegnggp gtvkkvtave dgktsyvlhk idaideatyt ydytisggtg fqeilekvsf ktkleaadgg skikvsvtfh

The Fig. 4.10 shows the coverage map of the whole protein sequence. Sequences which are highlighted in blue are the peptides of protein which matched with the available data base. Both the proteins show high coverage percent of 62.99 (accession no: **Q43377**) and 75.82 (accession no: **B0YIU5**).

```
Q43377_ARAHY Coverage Map
 A
1      LDSLSFSYNN    FEQDDERNLI    LQGDAKFSAS    KGIQLTKVDD    NGTPAKSTVG
51     RVLHSTQVRL    WEKSTNRLTN    FQAQFSFVIK    SPIDNGADGI    AFFIAAPDSE
101    IPKNSAGGTL    GLFDPQTAQN    PSANQVLAVE    FDTFYAQDSN    GWDPNYQHIG
151    IDVNSIKSAA    TTKWERRDGQ    TLNVLVTYDA    NSKNLQVTAS    YPDGQRYQLS
201    YRVDLRDYLP    EWGRVGFSAA    SGQQYQSHEL    QSWSFTSTLL    YTSPHYLKLG
251    RFMI
```

```
B0YIU5_ARAHY Coverage Map
 B
1      MGVHTFEEES    TSPVPPAKLF    KATVVDGDEL    TPKLIPAIQS    IEIVEGNGGP
51     GIVKKVIAVE    DGKTSYVLHK    IDAIDEATYT    YDYTISGGTG    FQEILEKVSF
101    KTKLEAADGG    SKIKVSVTFH    TKGDAPLPDE    VHQDVKQKSQ    GIFKAIEGYV
151    LSN
```

Figure 4.10: ESI-MS analysis shows the sequence of matched peptide of proteins. **(A)** Mannose glucose binding lectin of MW 21 kDa. **(B)** Ara h 8 allergen isoform OS of protein of MW 16.4 kDa.

4.4 Conclusions

Nanobiotechnology is an important research area which deals with environment friendly methods for the controlled synthesis of nanoparticles of desired shape and sizes. As a result, researchers in the field of nanoparticles synthesis use biological systems to achieve desired qualities in synthesizing nanoparticles in a "green" way without using any hazardous chemicals. Many organisms are able to produce nanomaterials either intra- or extra-cellularly. Our work confirms the formation of gold nanoparticles with lectin group proteins. To the best of our knowledge, this is the first report on using the proteins isolated from the plant source for the formation of gold nanoparticles. Further work has to be carried out to confirm the interactions of gold ions with the proteins during the synthesis of gold nanoparticles.

Biological synthesis of gold nanoparticles could have many applications in various fields but the uncontrolled synthesis of size and shape of nanoparticles is major drawback. The mechanism of biosynthesis for the formation of nanoparticles is an importance aspect to understand biosynthesis of nanoparticles for the commercial

production and the complete conversion of ionic gold to metallic gold. The synthesis of nanoparticles by purified biomolecules will be much easy than using the whole system (plants and microorganisms) and consume less time in preparation of nanoparticles on large scale.

References

[1] Gole, A., Murphy, C. J. Seed-mediated synthesis of gold nanorods, role of the size and nature of the seed. *Chem. Mater*. 2004, 16, 3633–3640.

[2] Meltzer, S., Resch, R., Koel, B. E., Thompson, M. E., Madhukar, A., Requicha, A. A. G., Will, P. Fabrication of nanostructures by hydroxylamine seeding of gold nanoparticle templates. *Langmuir*, 2001, 17, 1713–1718.

[3] Westcott, S. L., Oldenburg, S. J., Lee, T. R., Halas, N. J. Formation and adsorption of clusters of gold nanoparticles onto functionalized silica nanoparticle surfaces *Langmuir,* 1998, 14, 5396–5401.

[4] Puntes, V. F., Krishnan K. M., Alivisatos, A. P. Colloidal nanocrystal shapes and size control: The case study of cobalt. *Science*, 2001, 291, 2115–2117.

[5] Peng, Z. A., Peng, X. G. Nearly Monodisperse and shape-controlled CdSe nanocrystals via alternative routes: nucleation and growth. *Am. Chem. Soc*. 2002, 124, 3343–3353.

[6] Brust, M., Walker, M., Bethell, D., Schiffrin, D. J., Whyman, R. J. Synthesis of thiol derivatised gold nanoparticles in a two phase liquid/liquid system. *Chem. Soc. Chem. Commun*. 1994, 801–802.

[7] Gittins, D. I., Caruso, F. Spontaneous phase transfer of nanoparticulate metals from organic to aqueous media. *Angew. Chem. Int. Ed*. 2001, 40, 3001–3004.

[8] Gittins, D. I., Caruso, F. Biological and physical applications of water-based metal nanoparticles synthesized in organic solution *Chem- Phys Chem.* 2002, 3, 110–113.

[9] Selvakannan, P. R., Mandal, S., Pasricha, R., Adyanthaya, S. D., Sastry, M. One-step synthesis of hydrophobized gold nanoparticles of controllable size by the reduction of aqueous chloroaurate ions by hexadecylaniline at the liquid- liquid interface. *Chem. Commun.* 2002, 13, 1334–1335.

[10] Raveendran, P., Fu, J., Wallen, S. L. Completely "green" synthesis and stabilization of metal nanoparticles. *J. Am. Chem. Soc*. 2003, 125, 13940–13941.

[11] Ahmad, A., Senapati, S., Khan, M. I., Kumar, R., Sastry, M. Extra-cellular biosynthesis of monodisperse gold nanoparticles by a novel extremophilic actinomycete, *Thermomonospora* sp. *Langmuir,* 2003, 19, 3550–3553.

[12] Klaus, T., Joerger, R., Olsson, E., Granqvist, C.G., Silver-based crystalline nanoparticles, microbially fabricated. *Proc. Natl. Acad. Sci.* U.S.A. 1999, 96, 13611–13614.

[13] Singaravelu, G., Arockiamary, J., Ganesh, K., Govindaraju, K. A novel extracellular synthesis of monodisperse gold nanoparticles using marine alga, *Sargassum wightii* Greville. *Colloids Surf. B*, 2007, 57, 97-101.

[14] Mourato, A., Gadanho, M., Lino, A. R., Tenreiro, R. Biosynthesis of crystalline silver and gold nanoparticles by extremophilic yeasts. *Bioinorg. Chem. Appl.* 2011, 546074-546082.

[15] Shankar, S. S., Rai, A., Ahmad, A., Sastry, M. Rapid synthesis of Au, Ag, and bimetallic Au core–Ag shell nanoparticles using Neem (*Azadirachta indica*) leaf broth. *Colloids Surf. B,* 2004, 275, 496–502.

[16] Raju, D., Mehta, U. J., Hazra, S. Synthesis of gold nanoparticles by various leaf fractions of *Semecarpus anacardium* L. tree. *Trees- Struc. Funct*. 2011, 25, 145–151.

[17] Gardea-Torresdey, J. L., Parsons, J. G., Gomez, E., Peralta-Videa J. R, Troiani, H. E, Santiago, P., Jose-Yacaman, M. Formation and growth of Au nanoparticle inside live *alfalfa* plants. *Nano Lett*. 2002, 2, 397–401.

[18] Daniel, M. C., Astruc, D. Gold nanoparticles assembly, supramolecular chemistry, quantum-size-related properties, and applications toward biology, catalysis, and nanotechnology. *Chem. Rev*. 2004, 104, 293–346.

[19] Sau, T. K., Murphy, C. J. Seeded high yield synthesis of short Au nanorods in aqueous solution. *Langmuir*, 2004, 20, 6414–6420.

[20] Kim, F., Song, J. H., Yang, P. D. Photochemical synthesis of gold nanorods. *J. Am. Chem. Soc*. 2002, 124, 14316–14317.

[21] Sun, Y. G., Xia, Y. N. Shape-controlled synthesis of gold and silver nanoparticles. *Science*, 2002, 298, 2176–2179.

[22] Jin, R. C., Egusa, S. J., Scherer, N. F. Thermally-induced formation of atomic Au clusters and conversion into nanocubes. *J. Am. Chem. Soc.* 2004, 126, 9900–9901.

[23] Chen, S. H., Wang, Z. L., Ballato, J., Foulger, S. H., Carroll, D. L. Monopod, bipod, tripod, and tetrapod gold nanocrystals. *J. Am. Chem. Soc.* 2003, 125, 16186 - 16187.

[24] Yamamoto, M., Kashiwagi, Y., Sakata, T., Mori, H., Nakamoto, M. Synthesis and morphology of star-shaped gold nanoplates protected by Poly (*N*-vinyl-2-pyrrolidone) *Chem. Mater.* 2005, 17, 5391–5393.

[25] Chu, H. C., Kuo, C. H., Huang, M. H. Thermal aqueous solution approach for the synthesis of triangular and hexagonal gold nanoplates with three different size ranges. *Inorg. Chem.* 2006, 45, 808 – 813.

[26] Tsuji, M., Hashimoto, M., Nishizawa, Y., Kubokawa, M., Tsuji, T., Microwave assisted synthesis of metallic nanostructures in solution. *Chem. Eur. J.* 2005, 11, 440–452.

[27] Reddy, A. S., Chen, C. Y., Chen, C. C, Jean, J. S., Chen, H. R., Tseng, M. J., Fan, C. W., Wang J. C. Biological synthesis of gold and silver nanoparticles mediated by the bacteria *Bacillus subtilis*. *J. Nanosci. Nanotechnol.* 2010, 10, 6567–6574.

[28] Xie, J., Lee, J .Y., Wang, D. I. C., Ting, Y. P. Identification of active biomolecules in the high-yield synthesis of single-crystalline gold nanoplates in algal solutions. *Small*, 2007, 3, 4: 672 – 682.

[29] Au, L., Lim. B., Colletti, P., Jun, Y., Xia, Y. Synthesis of gold microplates using Bovine Serum Albumin as a reductant and a stabilizer. *Chem. Asian J*. 2010, 51, 123–129.

[30] Kumar, S. A., Abyaneh, M. K., Gosavi, S. W., Kulkarni, S. K., Pasricha, R., Ahmad, A., Khan, M. I. Nitrate reductase-mediated synthesis of silver nanoparticles from AgNO$_3$. *Biotechnol. Lett.* 2007, 29, 439–445.

[31] Rangnekar, A., Sarma, T. K., Singh, A. K., Deka, J., Ramesh, A., Chattopadhyay, A. Retention of enzymatic activity of α-Amylase in the reductive synthesis of gold nanoparticles. *Langmuir,* 2007, 23, 5700-5706.

[32] Zhong, Z., Luo, J., Ang, T. P. Highfield, J. Lin, J, Gedanken, A. Controlled organization of Au colloids into linear assemblies. *J. Phys. Chem. B.* 2004, *108*, 18119-18123.

[33] Yang, T., Li, Z., Wang, L., Guo, C., Sun, Y. Synthesis, characterization, and self-assembly of protein lysozyme monolayer-stabilized Gold nanoparticles *Langmuir,* 2007, 23*,* 10533-10538.

[34] Wei, W., Wang, Z., Zhang, J., House, S., Gao, Y., Yang, Y., Robinson, H., Tan, L. H., Xing, H., Hou, C., Robertson, I. M., Zuo, J., Lu, Y. Time-dependent, protein-directed growth of gold nanoparticles within a single crystal of lysozyme. *Nat. Nanotechnol.* 2011, 6, 93-97.

[35] Xiao-rong, Z., Xiao-xiao, H.E., Ke-min, W., Xiao-hai, Y. Different active biomolecules involved in biosynthesis of gold nanoparticles by three fungus species. *Plant Resourc. Conserv. Utilization. Res.* 2011, 2, 1, 53-64.

[36] Barwal, I., Ranjan, P., Kateriya, S., Yadav, S. C. Cellular oxido-reductive proteins of *Chlamydomonas reinhardtii* control the biosynthesis of silver nanoparticles. *J. Nanobiotechnol.* 2011, 9, 56, doi: 10.1186/1477-3155-9-56.

[37] Sanchez-Pomales, G., Morris**, T. A.**, Falabella**, J. B.**, Tarlov**, M. J.**, Zangmeister**, R. A.** Lectin-based gold nanoparticle assay for probing glycosylation of lycoproteins. *Biotechnol. Bioeng.* 2012, DOI 10.1002/bit.24513.

Chapter 5

Applications of nanoparticles.
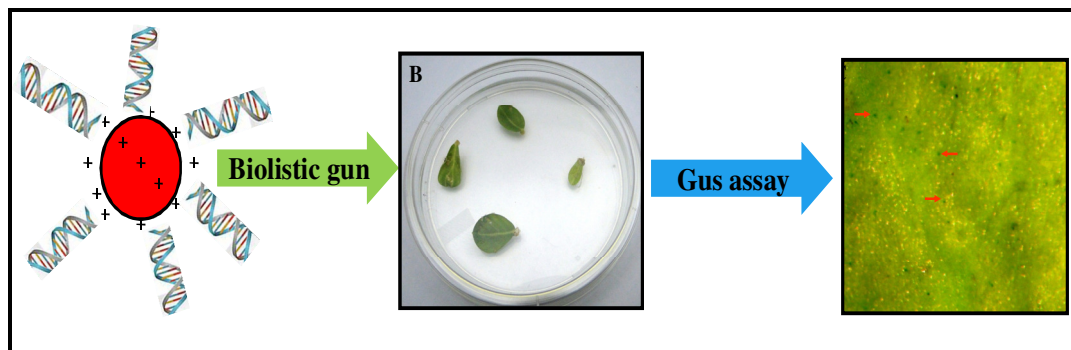
Summary:

In this chapter, we report for the first time biosynthesis of cationic gold nanoparticles (C-GNPs) by using peanut leaf extract. The formed particles were characterized by UV-vis, TEM, EDS and SAED. The surface charge of the particles was confirmed by dynamic light scattering (DLS) and binding of DNA onto the cationic nanoparticles was checked on agarose gel electrophoresis. As these particles were not stable for longer time, we synthesized the cationic nanoparticles by using chemical method which was stable for longer period. The particles were characterized by UV-vis, TEM, EDS and SAED. The time and volume dependent DNA binding efficiency with cationic nanoparticles was studied. The successful gene delivery into peanut leaves was carried out by using cationic nanoparticles and the transformation was confirmed by GUS (β-glucuronidase) assay method.

5.1 Introduction

Nanoparticles are materials that are small enough to fall within the nanometeric range, with at least one of their dimensions being less than a few hundred nanometers. This reduction in size brings about significant changes in their physical properties with respect to those observed in bulk materials. The upcoming area of nanotechnology for development of nanodevices and nanomaterials [1, 2] opens up potential applications in agriculture and biotechnology. Nanoparticles are currently being widely used for targeted delivery of drugs in cancer treatments [3, 4].

Application of nanotechnology in agriculture at global level is in developing stage. Nanoscience helps the development of a range of inexpensive nanotech applications for enhanced plant growth. Nanoparticles and nanocapsules provide an efficient means to distribute pesticides and fertilizers in a controlled fashion with high site specificity thus reducing damage [5].

The nanoparticle formation and encapsulation of a model pDNA (plasmid DNA) with chitosan was studied. A series of chitosan nanoparticles with various molecular parameters were prepared, and the effect of molecular weight and deacetylation degree of chitosan on encapsulation efficiency was also studied. The formed chitosan nanoparticles effectively condense pDNA, protecting it from DNase degradation [6].

The high transformation efficiency of *E. coli* cells with plasmid by adding amino modified silica nanoparticles than chemical method (calcium chloride) for the improvement of transformation of DNA was studied in bacteria [7]. The successful penetration of DNA bound with the cationic gold nanoparticles (C-GNPs) to HePG2 (Human hepatocellular liver carcinoma cell line) cells were studied [8].

There is a huge scope for applying nanoparticles and nanocapsules to plants for agricultural use [9-15]. The transfer of gene by bombardment of DNA absorbed gold particles has been successfully used to generate transgenic plants in a species-independent manner [16].

The efficiency of DNA delivery into plants by gold nanoparticles embedded in sharp carbonaceous carriers is demonstrated. The nanogold embedded carbon matrices are prepared by heat treatment of biogenic intracellular gold nanoparticles. The DNA delivery efficiency is tested on different plants such as *Nicotiana tabacum*, *Oryza sativa* and *Leucaena leucocephala* [17].

The efficient delivery of DNA and chemicals through silica nanoparticles in plant cells, without use of specialized equipment has been reported recently [18]. The ability of surface functionalized mesoporous silica nanoparticles (MSNs) to penetrate plant cell walls also opens up new ways to precisely manipulate gene expression at single cell level by delivering DNA.

The use of fluorescent labeled starch-nanoparticles used as plant transgenic vehicle was reported in which the nanoparticle biomaterial were designed in such a way that it binds the pDNA and transport genes across the plant cell wall by inducing instantaneous pore channels in cell wall, cell membrane and nuclear membrane with the help of ultrasound [19].

Here in this chapter, we demonstrate for the first time the biosynthesis of cationic gold nanoparticles and its binding with pDNA. The formation of cationic nanoparticles was noted and confirmed the charge on the surface of nanoparticles. As these particles were not stable for a longer time, the chemical mediated synthesis of cationic gold nanoparticles was carried out. Time dependent binding efficiency of pDNA to the particles was done by using nanodrop. Characterization of these nanoparticles by UV-vis, TEM and EDS analysis was done. The pDNA bound to these nanoparticles was used as carriers for transformation of pDNA into plant tissue.

5.2 Experimental details

5.2.1 Preparation of peanut extract:

An amount of 2 gm leaves of peanut seedlings which were grown on deionized water were taken, added to 10 mL of deionized water, crushed in mortar and pestle and centrifuged at 10,000 rpm at 4°C for 10 min to separate the biomass and supernatant. The supernatant was taken and used as reducing agent.

5.2.2 Synthesis of positively charged gold nanoparticle:

The biosynthesis of cationic gold nanoparticles was done by adding 100 μL of 213 mM cysteamine (Sigma-Aldrich) to 10 mL of 1.42 mM $HAuCl_4$ (Sigma-Aldrich). It formed a yellow coloured solution. After stirring for 20 min at room temperature, 100 μL of peanut leaf extract supernatant was added to the mixture solution while stirring for 10 min in dark condition. The color of mixture solution changed from yellow to purple. After further mild stirring, the gold nanoparticle solution was stored in dark at 4°C and further characterization was carried out.

The chemical synthesis was done by the same procedure mentioned above, except that instead of peanut leaf extract, 2 μL of 10 mM sodium borohydride was used as reducing agent.

5.2.3 Dynamic light scattering (DLS):

Dynamic light scattering and zeta potential measurements for the nanoparticles samples were performed on a Brookhaven 90 Plus/BI-MAS Instrument (Brookhaven Instruments, New York), equipped with a 15 mW solid state laser at a wavelength of 657 nm and scattering signals were collected at 90°, placed in the measurement cell in a 1 cm path cuvette at an average of 6 runs per scan.

5.2.4 Plasmid DNA isolation:

The *Escherichia coli* bacterial cultures were grown overnight on shaker (200 rpm) at 37°C in LB (Luria Broth) broth, with appropriate antibiotics. About 1.5 to 3 mL culture was centrifuged for 1 min at 7,000 rpm to pellet the bacterial cells. The pellet was re-suspended in 200 μL of solution-I (Table 5.1) by vigorous pipetting, 400 μL of solution II (Table 5.1) was added, mixed by inversion till the solution becomes clear,

normally for 2-3 min. The cell lysate was neutralized by addition of 300 μL of solution III (Table 5.1) mixed well and incubated on ice for 5 min. The cell debris was removed by centrifugation for 10 min at 10,000 rpm at 4ºC. The supernatant was transferred to another microfuge tube, RNase A was added to a final concentration of 20 μg mL^{-1} [20] and incubated at 55ºC for 20 min. To the above solution 400 μL of chloroform was added, vortexed for 2 min and centrifuged for 10 min at 10,000 rpm at room temperature. The upper aqueous layer was transferred to a clean tube, 1/10th volume sodium acetate and one volume absolute ethanol were added with gentle mixing and kept at -20ºC for 1-2 hr. The sample was centrifuged at 13,000 rpm for 15 min at 4ºC. The pellet was washed twice with 70% ethanol and dried under vacuum. The dried pellet was dissolved in 40 μL of deionized water and 40 μL of PEG/NaCl solution (20% PEG 8000 in 2.5 M NaCl) was added. The mixture was incubated on ice for 20 min and the pDNA was pelleted out by centrifugation at 13,000 rpm for 15 min at 4ºC. The supernatant was aspirated carefully; the pellet was washed with 70% ethanol and air-dried. The dried pellet was re-suspended in 20 μL deionized water and stored at -20ºC.

Table 5.1: Chemicals used for plasmid DNA isolation

Name	Components
Solution I or Resuspension buffer	50 mM Glucose, 25 mM Tris-HCl (pH 8.0), 10 mM EDTA (pH 8.0).
Solution II or Lysis buffer	0.2 N NaOH and 1% SDS
Solution III or Neutralisation buffer	3 M Potassium acetate (pH 4.8)
RNase A	10 mg L^{-1}
Other solutions or Reagents	Chloroform, Absolute ethanol, 3.0 M Sodium acetate, 70% ethanol & Deionized sterile water

5.2.5 Binding of plasmid DNA:

10 μL of cationic gold nanoparticles and 10 μL of 12kb pDNA (pCAMBIA-1301 with 1.1kb insert) were mixed together in an Eppendorf tube and kept at room temperature for 20 min and later checked on 0.7% agarose gel for binding of DNA. The cationic gold nanoparticles were characterized by TEM, EDS and SAED.

5.2.6 Quantification of Plasmid DNA by Nanodrop:

The time dependent binding efficiency of pDNA to C-GNPs was carried out. 20 µL of C-GNPs and 1 µL of pDNA containing 130 ng was taken and incubated at room temperature at different time intervals and different volume of C-GNPs. The particles which were incubated with pDNA and C-GNPs were centrifuged at 15,000 rpm for 30 min. The supernatant containing the unbound pDNA was quantified using nanodrop.

5.2.7 Biolistic transformation using PDS-1000/He Biolistic particle delivery system:

The pDNA bound to the cationic gold nanoparticles was coated on the micro carrier and allowed to dry under laminar. The leaf explants of peanut were bombarded after arranging at the centre of a 90 mm diameter petri-plate using rupture discs with 650 pounds per square inch (psi) specification with 25 inches of Hg vacuum. For callus induction, explants were incubated in dark on media containing basal MS medium, B5 vitamins, 1 mg L^{-1} BAP, 1 mg L^{-1} NAA, 30 g L^{-1} sucrose and 7 g L^{-1} agar for a week. The medium also contained plant selection marker Hygromycine at 50 mg L^{-1} concentration. After a period of one week, the explants that were bombarded were subjected to GUS assay.

5.2.8 GUS histochemical assay:

The GUS staining solution was prepared by taking 1 mM X-Gluc (5-bromo, 4chloro, 3- indolyl-β-D-glucuronide: Cyclohexylammonium salt (X-GlcA) from a 20 mM stock made in dimethylformamide, 100 mM sodium dihydrogen phosphate dihydrate and 0.5% Tween-20. The pH of the solution was adjusted to 7.0 with 1N NaOH. The histochemical GUS assay was performed as described by [21] to monitor GUS gene expression in peanut leaf. The GUS assay was carried out on explants grown on selection medium for a period of week. The leaf explants were immersed in GUS assay solution and incubated at 28ºC overnight. *GUS* gene expression was observed and photographed by using Carl Zeiss microscope.

## 5.3 Results and Discussion

5.3.1 Visible analysis:

The formation of nanoparticles was observed after addition of 100 µL of peanut leaf extract to 213 mM Cysteamine and 1.42 mM in $HAuCl_4$. There was no change in colour of the solution in control (Fig. 5.1A). After a period of 20 min of stirring under dark condition there was change in the colour of the solution from yellow to purple at room temperature which indicates the formation of nanoparticles (Fig. 5.1B).
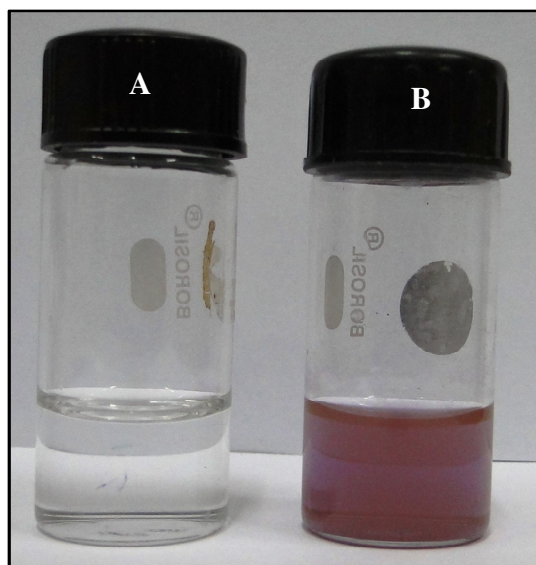
Figure 5.1: Biosynthesis of cationic gold nanoparticles by peanut leaf extract **(A)** Control, **(B)** Cationic gold nanoparticles.

5.3.2 UV-vis analysis:

The UV-vis spectroscopy of C-GNPs were scanned from 300 to 900 nm wavelength showing maximum intensity of peak at 550 to 560 nm (Fig. 5.2) indicating the formation of C-GNPs. The UV shift which is towards higher wavelength could be due to the bigger size of nanoparticles.
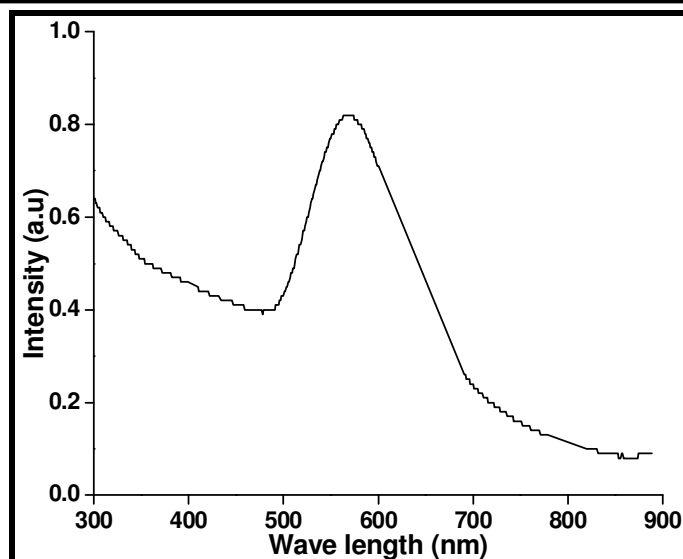
Figure 5.2: UV-vis analysis of cationic gold nanoparticles synthesized by peanut leaf extract.

5.3.3 TEM analysis:

The C-GNPs which were formed by peanut leaf extract are shown at different magnifications (Fig. 5.3A-B). The particles are of different shapes, bigger in size and well separated. The Fig. 5.3C indicates that the particles are crystalline in nature. The particles size ranged from 110 to 130 nm in which most of the particles were of 120 nm (Fig. 5.3D). The charge of the particles was also calculated by dynamic light scattering (DLS) which shows 23.06 mV. This indicates that the formed nanoparticles surface had positive charge. The charge on the nanoparticles is due to the addition of Cysteamine during the process of reduction. In previous reports, [22] researchers have shown that Cysteamine helps in giving positive charge on to the nanoparticles.
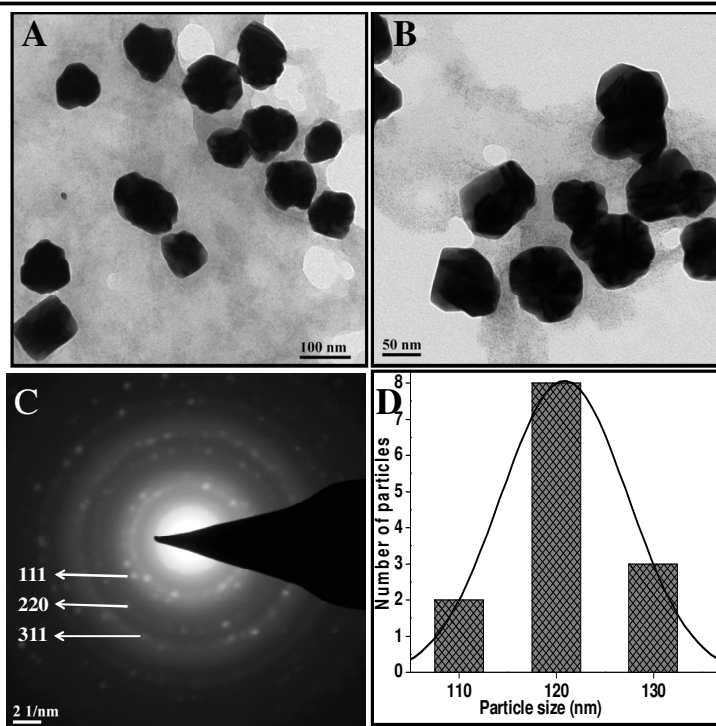
Figure 5.3: Characterization of cationic gold nanoparticles synthesized by peanut leaf extract. **(A, B)** TEM images at different magnifications, **(C)** SAED, **(E)** Particle size distribution.

5.3.4 Binding of plasmid DNA onto C-GNPs:

An experiment was performed to confirm the binding of pDNA to C-GNPs. The p DNA 20 μL and C-GNPs 20 μL were added to the Eppendorf tube and kept at room temperature for a period of 20 min. Then pDNA with C-GNPs and pDNA alone was loaded on to 0.7% agarose gel and gel was run. The Fig. 5.4A shows the pDNA with C-GNPs has not moved from the agarose gel which indicates the plasmid has been bound to the C-GNPs. In control with only pDNA it was observed that the plasmid had moved out from the gel (Fig. 5.4B). The binding of pDNA to C-GNPs is because of the negatively charged DNA which binds to the positively charged nanoparticles. Usually DNA moves from the negative charge to positive charge, whereas, the DNA bound to positive charged particles did not move from the well of the gel. These particles are not stable for more than 24 hr which get agglomerated and settle down. Hence, we carried out chemical synthesis of cationic nanoparticles for our further experiments.
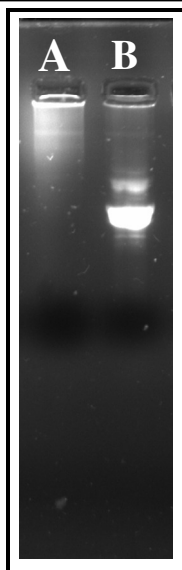
Figure 5.4 Agarose gel showing the binding of pDNA **(A)** pDNA with cationic gold nanoparticles, **(B)** only pDNA

Chemical synthesis of cationic GNPs

5.3.5 Visible analysis:

There was no change in colour of the solution in control (Fig. 5.5A). The formation of nanoparticles was observed after addition of 2 µL of 10 mM sodium borohydride. After a period of 20 min of stirring under dark condition there was change in the colour of the solution to purple colour at room temperature which indicates the formation of nanoparticles (Fig. 5.5B).
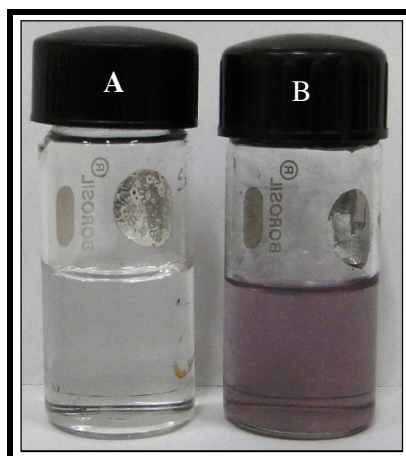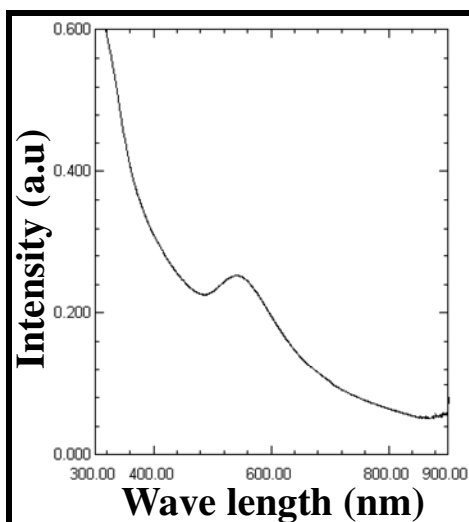

Figure 5.5 Synthesis of cationic gold nanoparticles by sodium borohydride **(A)** Control, **(B)** Cationic gold nanoparticles.

5.3.6 UV-vis analysis:

The UV-vis spectroscopy of C-GNPs were scanned from 300 to 900 nm wavelength shows maximum intensity of peak observed at 520 to 530 nm (Fig. 5.6) indicating the formation of GNPs. The UV shift which is toward lower wavelength could be due to the smaller size of nanoparticles. In case of biosynthesis of the C-GNPs by peanut leaf extract, the UV shift to higher wavelength showed that the particles are bigger in size as observed in TEM.

Figure 5.6: UV of cationic gold nanoparticles synthesized by sodium borohydride

### 5.3.7 Binding of plasmid DNA to C-GNPs:

The binding of pDNA to C-GNPs was confirmed by agarose gel electrophoresis. Aliquots of 20 μL pDNA and 20 μL of C-GNPs were added to the Eppendorf and kept in room temperature for a period of 20 min. Then pDNA with C-GNPs and pDNA alone was loaded on to 0.7% agarose gel and the gel was run. In control, with only pDNA, the plasmid had moved out from the gel (Fig. 5.7A). The pDNA with C-GNPs did not move from the agarose gel which indicates that the plasmid has bound to the C-GNPs (Fig. 5.7B). The possible reasons are explained in Section 3.4 of this Chapter.
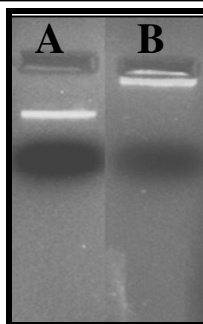
Figure 5.7: Gel showing the binding of pDNA (**A**) only pDNA (**B**) pDNA with chemically synthesized cationic gold nanoparticles

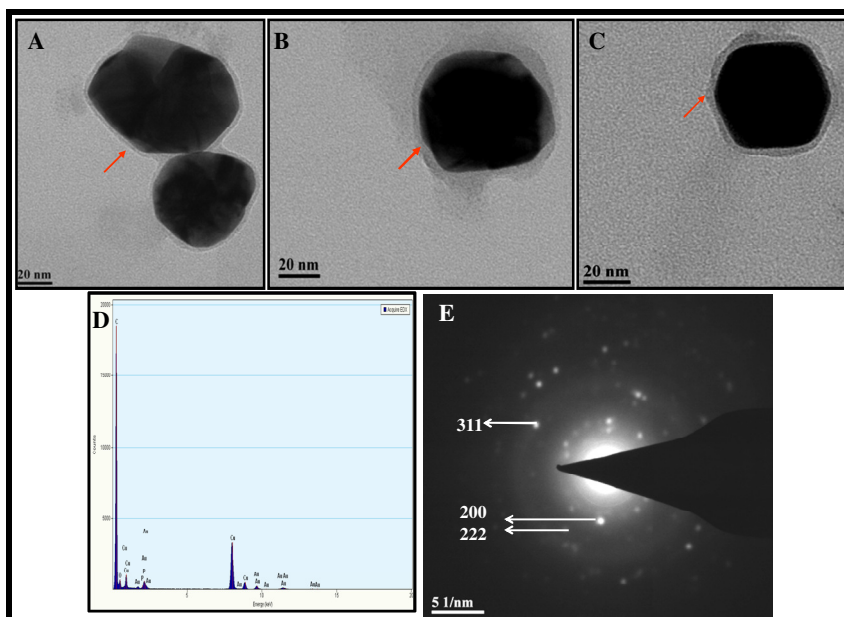### 5.3.8 Characterization of C- GNPs:

The C-GNPs which were formed by chemical method are shown in Fig. 5.8A-B. The TEM images show the particles are of different shapes, the particles were well separated. The SAED (Fig. 5.8C) indicates the particles are crystalline in nature. The particle size ranged from 60 to 74 nm in which most of the particles were of 68 nm size (Fig. 5.8D).
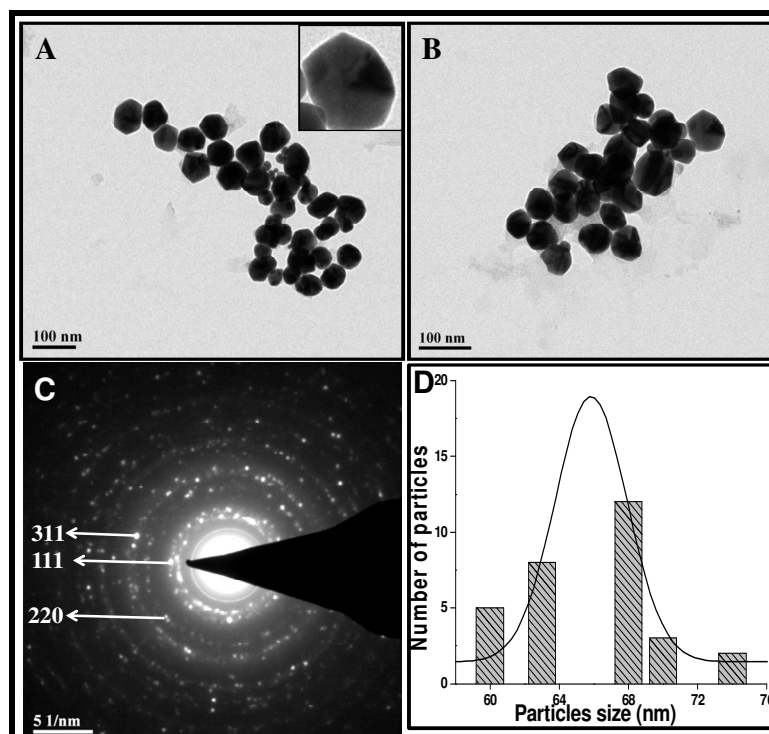
Figure 5.8: Characterization of chemically synthesized cationic nanoparticles synthesized extract (**A, B**) TEM images, (**C**) SAED, (**E**) Particle size distribution.

### 5.3.9 TEM Characterization of C- GNPs bound to DNA:

The C-GNPs formed by chemical method were bound to the pDNA (Fig. 5.9A-C). The particles were well separated after binding of DNA where no aggregation was observed. There is a clear layer of DNA bound around the nanoparticles which confirms the binding of DNA to nanoparticles. The layer bound around the particles could be possibly due to the attraction of more amount of pDNA which is negatively charged to the positively charged particles. An attempt of EDS analysis to know the chemical composition after binding of pDNA to nanoparticles was made. The element peaks of oxygen, copper, carbon, gold and phosphate were observed. The oxygen is from the biomolecules or air present in the chamber, copper from the grid used for the TEM analysis, carbon from the biomolecules bound to the nanoparticles. Gold is from the particles which were formed after the reduction of $HAuCl_4$ ions. The phosphate is from the DNA which acts as a backbone of DNA, which is attached to the sugar molecule of DNA. This shows that the phosphate peak comes from the DNA (Fig. 5.9D) This EDS analysis confirms the layer bound to the particles is DNA. The SAED (Fig. 5.9E) indicates the particles are crystalline in nature. The SAED is slightly diffused could be due to binding of DNA, while in C-GNPs without pDNA the SAED pattern is clear.

Figure 5.9: Characterization of cationic nanoparticles bound to pDNA (**A -C**) TEM images (**D**) EDS analysis (**E**) SAED.

5.3.10 Time and volume dependent binding of plasmid DNA to C-GNPs:

An experiment was conducted to know the binding efficiency of pDNA to C-GNPs. An amount of 1 μL containing 130 ng of pDNA and 20 μL of C-GNPs were taken and incubated at different time from 10 min to 40 min. The bound and unbound pDNA was separated by centrifugation. The supernatant containing unbound pDNA was taken and quantified. As the incubation time increases, the decrease in the unbound DNA was observed (Fig. 5.10A). This shows the binding of DNA increases with increase in time indirectly. After a period of 30 to 40 min, there was same amount of unbound DNA observed. This shows the saturation of binding of pDNA to C-GNPs in the solution after a period of 30 min. Keeping the concentration of pDNA constant, variation of volume dependent C-GNPs was studied. The binding efficiency from 5 to 20 μL of C-GNPs was studied. It was noticed that as the volume increases, unbound pDNA decreases (Fig. 5.10B), thus implying increase in binding. The binding efficiency after 15 and 20 min was approximately the same, where much variation was not observed.
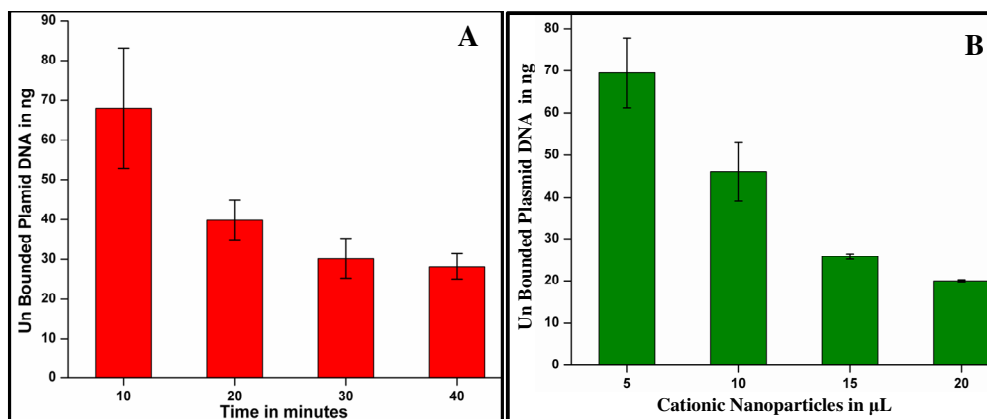

Figure 5.10: Binding efficiency of pDNA to cationic nanoparticles (**A**) Time dependent binding (**B**) Different volumes of cationic nanoparticle dependent binding to pDNA.

5.3.11 pDNA delivery into peanut leaf by C-GNPs:

The C-GNPs which were bound to the plasmid were used as carrier of DNA into peanut leaf. The bound particles were coated onto the macro carrier and allowed to dry. After the particles were bombarded with 650 psi onto peanut leaves, they were allowed to grow in the basal MS medium containing B5 vitamins, 1 mg L^{-1} BAP and 1 mg L^{-1} NAA and Hygromycine 50 mg L^{-1}. Browning of control leaves was observed after a period of 1 week (Fig. 5.11A), whereas the leaves bombarded with the biolistic

gun were green in colour and the induction of callus from the injured part of leaves could be observed (Fig. 5.11B and C). This showed the leaves growing in Hygromycin containing medium indicating the integration of pDNA. The transformation was confirmed by GUS assay. In previous report, the gene delivery with mesoporous silica nanoparticles tagged with the gold nanoparticles has been demonstrated [18]. Fungus-mediated synthesized intercellular gold nanoparticles used for the transformation showed that the efficiency has increased more than the conventional methods of gene transformation in *Nicotiana tabacum, Oryza sativa and Leucaena leucocephala* [17]. There are reports on successful transformation of gene in HepG2 cells by using C-GNPs [8]. A recent study showed the gold nanoparticles of 50 nm in diameter significantly improved plasmid transformation efficiency by 5–7 fold compared with that obtained using naked plasmid [23].
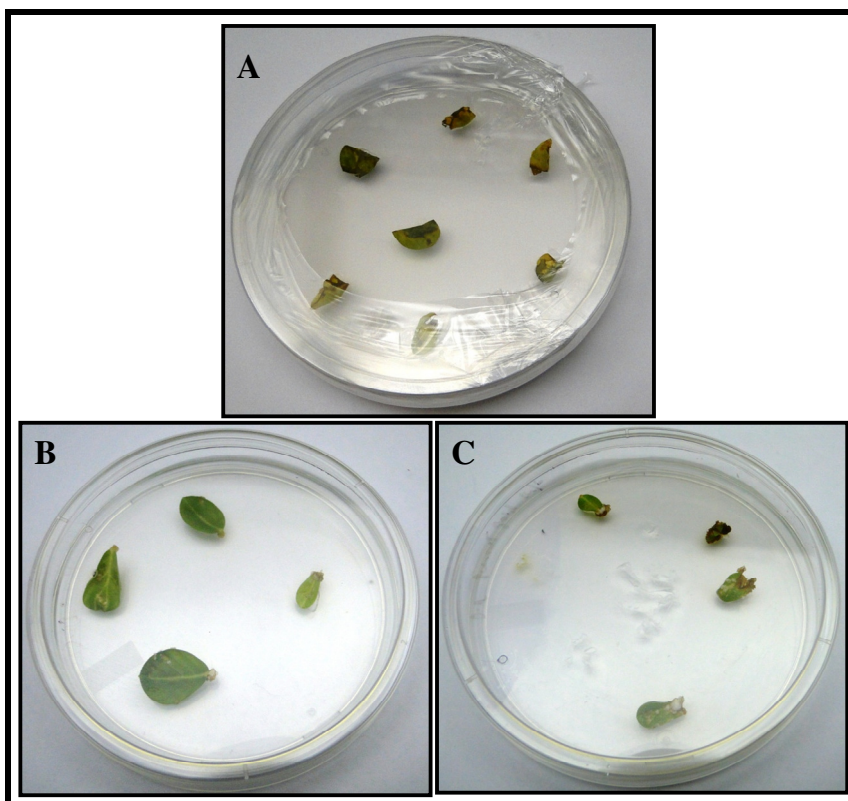
Figure 5.11: Peanut leaves growing on Hygromycin containing medium (**A**) Control (**B and C**) leaves inducing callus on hygromycine medium.

5.3.12 GUS Assay:

The transgenic leaves which were growing on Hygromycine medium were taken for GUS assay. In control leaves, no GUS expression was observed after overnight (12 hr) exposure in GUS buffer (Fig. 5.12A,B) whereas in peanut leaves which were used for bombardment grown in Hygromycine medium showed GUS expression indicated by arrows (Fig. 5.12C,D) which confirms the integration of pDNA into peanut leaves.
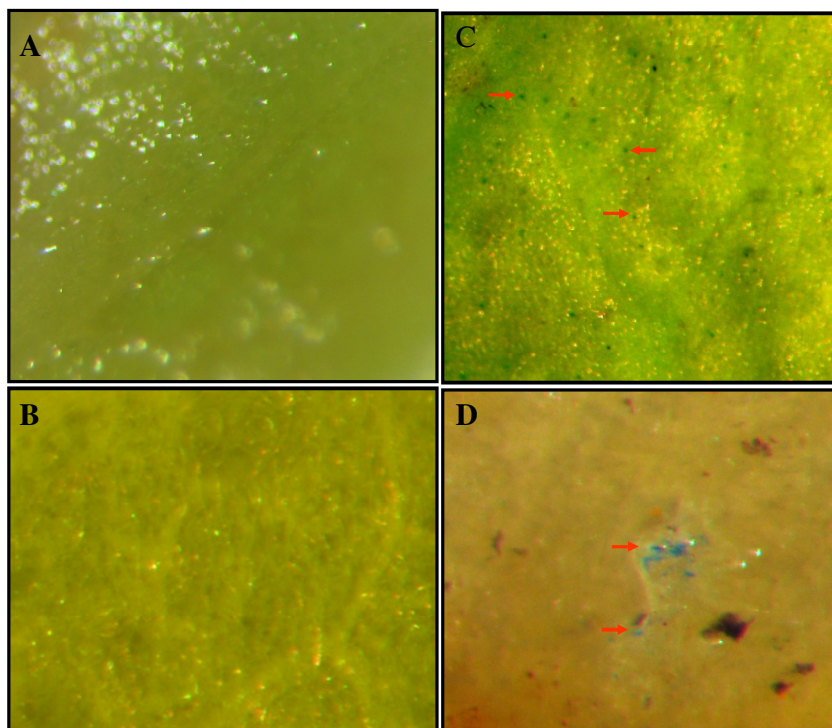
Figure 5.12: GUS assay of peanut leaves **(A, B)** In control leaves no GUS spots observed **(C, D)** Leaves bombarded with cationic gold nanoparticles showing GUS spots.

5.4 Conclusions

Here we report the use of synthesized C-GNPs for the successful binding of pDNA to C-GNPs and gene delivery in peanut leaves by using biolistic gene gun. The GUS assay confirms the successful transformation of peanut leaves. Now-a-days, applications of nanotechnology are mainly focused on animal science and medical research. Here, we have demonstrated that the gold nanoparticles can also be used in plant science. Further investigation need to be done for the efficiency of gene delivery with C-GNPs and available methods for gene transformation.

References

[1] Scott, N., Chen, H. 2003. Nanoscale science and engineering for agriculture and food systems. Washington, DC: Cooperative State Research, Education and Extension Service, United States Department of Agriculture.

[2] Joseph, T., Morrison, M. 2006. Nanotechnology in agriculture and food *www.nanoforum.org.*

[3] Alexiou, C., Wolfgang, A., Klein, R. J., Parak, F. G., Hulin, P. Bergemann, C. Locoregional cancer treatment with magnetic drug targeting. *Cancer Res.* 2000, 60, 6641–6648.

[4] Alexiou, C., Jurgons, R., Schmid, R., Hilpert, A., Bergemann, C., Parak, F. *In vitro* and *in vivo* investigation of targeted chemotherapy with magnetic nanoparticle. *.J. Magn. Magn. Mater.* 2005, 293, 1, 389–393.

[5] Nair, R., Varghese, S. H, Baiju G., Nair, T., Maekawa, Y., Yoshida, D., Kumar, S. Nanoparticulate material delivery to plants. *Plant Sci.* 2010, 179, 154–163.

[6] Bozkir, A., Saka O. M. Chitosan nanoparticles for plasmid DNA delivery: effect of chitosan molecular structure on formulation and release characteristics. *Drug Delivery.* 2004, 11, 107–112.

[7] Zeng, W., Deng, Y., Yang Z., Yuan, W., Huang, W., Zhu, Y., Bai, Y., Li, Y., Peng, Z., Wang, Y., Zhu, Y., Liu, M., Wu, X. High transformation efficiency of *Escherichia coli* with plasmid by adding amino modified silica nanoparticles. *Biotechnology*, 2006, 5, 3, 341-343.

[8] Zhang, Y., Liu, G., Hou, C., Chen, J., Wang, J., Pan, Y. Preparation of cationic gold nanoparticles and their transfection ability into cultivated cells. *Nanosci.* 2007, 12, 49-53.

[9] Liu, Y., Laks, P., Heiden, P. Controlled release of biocides in solid wood. I. Efficacy against brown rot wood decay fungus (*Gloeophyllum trabeum*). *J. Appl. Polym. Sci.* 2002, 86, 596–607.

[10] Liu, Y., Laks, P., Heiden, P. Controlled release of biocides in solid wood. II. Efficacy against *Trametes versicolor* and *Gloeophyllum trabeum* wood decay fungi. *J. Appl. Polym. Sci.* 2002, 86, 608–614.

[11] Liu, Y., Laks, P., Heiden, P. Controlled release of biocides in solid wood. III. Preparation and characterization of surfactant-free nanoparticles. *J. Appl. Polym. Sci.* 2002, 86: 615–621.

[12] Pavel, A., Trifan, M., Bara I. I., Creanga, D. E., Cotae, C. Accumulation dynamics and some cytogenetical tests at *Chelidonium majus* and *Papaver somniferum* callus under the magnetic liquid effect. *J. Magn. Magn. Mater.* 1999, 201, 443–445.

[13] Cotae, V., Creanga, I. LHC II system sensitivity to magnetic fluids. *J. Magn. Magn. Mater.* 2005, 289, 459–462.

[14] Pavel, A., Creanga, D. E. Chromosomal aberrations in plants under magnetic fluid influence. *J. Magn. Magn. Mater*. 2005, 289, 469–472.

[15] Joseph, T., Morrison, M. Nanotechnology in agriculture and food. 2006, www.nanoforum.org.

[16] Christou, P., McCabe, D. E., Swain, W. F. Stable transformation of soybean callus by DNA-coated gold particles. *Plant Physiol*. 1988, 87, 671–674.

[17] Vijayakumar, P. S., Abhilash, O. U., Khan, B. M., Prasad, B. L. V. Nanogold-loaded sharp-edged carbon bullets as plant-gene carriers. *Adv. Funct. Mater*. 2010, 20, 2416–2423.

[18] Torney, F., Trewyn, B. G., Lin, S-Y., Wang, K. Mesoporous silica nanoparticles deliver DNA and chemicals into plants, *Nat. Nanotechnol*. 2007, 2, 295–300.

[19] Jun, L., Feng-hua, W., Ling-ling, W., Su-yao, X., Chun-yi,. Dong-Ying,T., Xuan-ming, L. Preparation of fluorescence starch-nanoparticle and its application as plant transgenic vehicle, *J. Cent. South Univ. Technol.* 2008, 15, 768–773.

[20] Sambrook, J., Fritsch, E. F., Maniatis, T. Molecular cloning; A Laboratory Manual, 2nd ed., 1989. New York: Cold Spring Harbor Laboratory Press, Cold Spring Harbor.

[21] Jefferson, R. A., Burgess, S. M., Hirsh, D. ß-glucuronidase from *Escherichia coli* as a gene-fusion marker. *Proc. Natl. Acad. Sci. USA*. 1986, 83, 8447-8451.

[22] Kim, J. W., Kim J. H., Chung S. J., Chung, B. H. An operationally simple colorimetric assay of hyaluronidase activity using cationic gold nanoparticles. *Analyst,* 2009, 134, 1291-1293.

[23] Lee, Y. H., Wu, B., Zhuang, W. Q., Chen, D. R., Tang, Y. J. Nanoparticles facilitate gene delivery to microorganisms via an electrospray process. *J. Microbiol. Methods*, 2011, 84, 228-233.

Chapter 6

General discussion and conclusions

$\mathbf{T}$he work carried out in this thesis is mainly concentrated on studies of copper and manganese accumulation by plants growing on mining areas, selective leaching of above metals using microbes and their conversion to technologically challenging materials like copper oxide and manganese oxides. Study on metal tolerance and accumulation by plants growing in mining area will be an easy way to identify the metal accumulating and hyperaccumulator plants. In addition to this, biosynthesis of highly monodispersed gold nanoparticles from the plant *Arachis hypogea*, alongwith formation of cationic gold nanoparticles and using them in gene delivery was also conducted.

A study was carried out in copper mining area in which *Prosopis juliflora* and *Ailanthus excelsa* plants were growing in different locations of mining sites. The results showed that Cu accumulation was higher in leaves of both the plants, of which *Prosopis juliflora* accumulated at a higher-fold than *Ailanthus*. The amount of metal accumulated was 775.29 $\mu g\ g^{-1}$ which is close to hyperaccumulation value. The metal content was 42 times more than its control plants which are growing in metal contamination free soil. This reveals that these plants could be potential hyperaccumulators.

We also carried out the metal accumulation of Mn by three naturally growing tree species viz., *Cassia siamea*, *Azadirachta indica* and *Holoptelia integrifolia* identified on a manganese mine dump. The information was generated on Mn accumulation and distribution in different parts of these trees. Of all these plants, *Holoptelia* accumulated higher amount of metal than other plants. The amount of metal accumulated was 2682.19 $\mu g\ g^{-1}$. Mn content was 19 times more than its control plants which are growing in soil free of metal contamination.

We bioleached both the metals (Cu and Mn) from the plant by using *Fusarium oxysporum* and successfully converted them to nanoparticles. The recovery of metals and their conversion to nanomaterials using microorganisms from waste of leaves containing high amount of metals is an exciting possibility and could lead to recovery of metals from plants and can be developed as an economically viable green approach toward the large-scale synthesis of oxide nanomaterials.

The fabrication of nanomaterials via chemical and physical routes occurs under harsh environments like extremes of temperature, pressure and pH. Moreover, these methods are non eco-unfriendly, cumbersome and yield bigger particles which agglomerate due to not being capped by capping agents. In contrast, biological synthesis of inorganic nanomaterials occurs under ambient conditions viz. room temperature, atmospheric pressure and physiological pH. These methods are reliable, eco-friendly and cost effective.

In the present thesis, we have explored plants extracts, living plant and callus cell-mediated biological approach toward the synthesis of gold nanoparticles and an attempt has been made for recovery of intracellularly synthesized nanoparticles from roots.

A range of aqueous boiled plant extracts have been used for the synthesis of gold and silver nanoparticles initially by our group at NCL, Pune, and later by other groups too. This process is energy intensive as boiling is required. In order to synthesize gold nanoparticles completely at room temperature without the requirement of any external thermal energy, we screened a range of aqueous plants extracts made at room temperature and screened them for extracellular gold nanoparticles. Out of the several plant extracts screened by us, only *Semecarpus anacardium* leaf extract produced considerable amounts of extracellular, water dispersible and stable gold nanoparticles in the range of 21-25 nm at room temperature.

Our group and others have already synthesized gold-silver (Au-Ag) alloy nanoparticles of different sizes and shapes using boiled plant extracts. This led us into thinking towards the possibility of the synthesis of highly monodispersed, water dispersible and stable gold nanoparticles using plant extracts. We screened a range of living plants, where it was found that only the whole roots of *Arachis hypogea* produced highly monodispersed gold nanoparticles.

The extracellular nanoparticles were monodispersed and of 5-9 nm size whereas the intracellular nanoparticles were spherical particles of 5-8 nm in size and oval shape. We report, for the first time, both intra and extracellular synthesis of gold nanoparticles by using living peanut seedlings without any interference of other metal

ions and successful recovery of nanoparticles from the peanut roots was also studied along with its characterization.

The study was done to confirm the synthesis of intra and extra-cellular gold nanoparticles by peanut callus cells like the bacteria, fungus, yeast, etc. The nanoparticles formed by reaction of aqueous $HAuCl_4$ ions with the peanut callus cells were studied. The extracellular nanoparticles formed are of different shapes and sizes whereas the intracellular nanoparticles are highly monodispersed. In the case of extracellular synthesis, reduction of gold ions and subsequent formation of highly stable GNPs was noted.

In order to know the exact mechanism of formation, we decided on further investigation and finally identified the protein responsible for monodispersed gold nanoparticles synthesis. The mechanism of biosynthesis for the formation of nanoparticles is an important aspect to understand biosynthesis of nanoparticles for the commercial production and the complete conversion of ionic gold to metallic gold.

The synthesis of nanoparticles by purified biomolecules will be much easy than using the whole system (plants and microorganisms) and will consume less time in preparation of nanoparticles in large scale. The isolation of protein from the peanut root and purification of protein was done by FPLC and the purified fractions were tested for the formation of nanoparticles. The fractions which showed high activity in nanoparticles formation were checked on gel electrophoresis to confirm the presence of protein. The synthesis of nanoparticles by isolated protein from the plant sources has not been studied yet. We observed interesting result that the protein of molecular weight 21 kDa is helping in the synthesis of 25 to 60 nm size nanoparticles, while the 29 and 30 kDa proteins are helping in the formation of nanoparticles of 5 to 20 nm in size.

For the application of nanoparticles, biosynthesis of cationic gold nanoparticles and its binding with p-DNA was studied. The formation of cationic nanoparticles was noted and the charge on the surface of nanoparticles was confirmed. As these particles were not stable for a longer time, the chemical mediated synthesis of cationic gold nanoparticles was carried out. The binding of plasmid DNA onto the C-GNPs was

confirmed on agarose gel electrophoresis. We report the use of synthesized C-GNPs for the successful binding of p-DNA to C-GNPs and gene delivery in peanut leaves by using biolistic gene gun. The transformation was confirmed by GUS assay.

This study suggests that the metal accumulation and recovery of metal and conversion to nanoparticles which is reliable and eco-friendly processes for the recovery and formation of nanoparticles. Biosynthesis of nanoparticles by using plants will be easy over other synthesis processes in terms of low energy intake, non-polluting environment and reduction in cost. Also, the biosynthesis of inorganic nanoparticles using plants is a highly efficient process. Plants have been used to reduce the metal ions and subsequent formation of nanoparticles extracellularly as fast as the chemical methods. Plant based methods are also much faster (few minutes) and safer than the fungal methods which take around 6-7 days to complete the synthesis process.

Scope and future prospects

➢ We have identified the fungus *Fusarium oxysporum* for the bioleaching of copper and manganese and their conversion to oxide nanoparticles from the leaves of *Prosopis juliflora* and *Holoptelia integriflora* respectively. Thus, environment friendly protocols for the synthesis of inorganic nanoparticles have been demonstrated which can ensure abundant supply of nanomaterials which will be inexpensive and easy to fabricate, eliminating the requirement of any extremes of temperature or pressure, and will find tremendous number of applications in medicine, agriculture, engineering, biotechnology, etc.

➢ Understanding the mechanism of bioleaching of copper and manganese and applying them to the controlled and scalable synthesis of oxide nanoparticles of the above mentioned materials.

➢ We have biologically synthesized monodispersed gold nanoparticles intra- and extra-cellularly using the plant. The nanoparticles thus obtained are water dispersible, naturally protein capped and highly stable at room temperature. As these inorganic nanoparticles are in the size range of 10-50 nm, these may find various applications in targeted drug delivery systems without chances of toxicity as owing to their small size and these may easily pass through the kidneys and will be excreted through urine. Since these nanoparticles are

capped by natural proteins, they may directly bind to multiple-receptors such as LHRH (luteinizing hormone-releasing hormone), EGFR (Epidermal growth factor receptor) and EpCAM (Epithelial cell adhesion molecule), without the involvement of any targeting agents. Also, our nanoparticles may bind to integrins and VEGFs (Vascular endothelial growth factors) and help in the development of a novel anti-angiogenesis strategy for the treatment of a wide range of solid tumors. These nanoparticles may fulfill the emerging need for cheaper drugs in abundant amounts with no side effects to the patients and non-hazardous to the environment.

List of Publications

1) **D. Raju**, Sunil Kumar, Urmil J. Mehta, Sulekha Hazra*. Differential Accumulation of Manganese in Three Mature Tree species (*Holoptelia*, Cassia, Neem) growing on a mine Dump**. *Current Science*, 2008, 94, 639-643.

2) **D. Raju**, Urmil J. Mehta*. Synthesis of gold nanoparticles by various leaf fractions of *Semecarpus anacardium* L. tree. *Trees - Structure and Function*, 2011, 25, 145 – 151.

3) **D. Raju**, Urmil J. Mehta†* and Absar Ahmad*. Phytosynthesis of Intra- and Extracellular Gold Nanoparticles by living Peanut Plant (*Arachis hypogaea* L.) (*Communicated*).

4) Poonam Lapalikar, **D. Raju**, Urmil J. Mehta*. *In vitro* studies on Zinc, Copper and Cadmium accumulation potential of *Jatropha curcas* L. seedlings (*Communicated*).

5) Poonam Lapalikar, **D. Raju**, Urmil J. Mehta*. Evaluation of growth and accumulation of Copper by plants grown on Copper tailing dam soil. (*Communicated*).

6) **D. Raju**, Urmil J. Mehta†* and Absar Ahmad*. Biosynthesis of highly stable intra and extracellular gold nanoparticles by using live peanut *(Arachis hypogaea)* callus cells. (*Communicated*).

7) **D. Raju**, Urmil J. Mehta†* and Absar Ahmad*. Protein isolation and purification from the peanut roots and its role in synthesis of gold nanoparticles. (*Manuscript under preparation*).

8) **D. Raju**, Urmil J. Mehta†* and Absar Ahmad*. Bio recovery of intracellular gold nanoparticles from peanut roots and its characterization (*Manuscript under preparation*).

9) **D. Raju**, Urmil J. Mehta†* and Absar Ahmad*. Gene delivery by using cationic gold nanoparticles in peanut leaves. (*Manuscript under preparation*).

Poster presentations

D. Raju, Sunil Kumar., Urmil J. Mehta, Sulekha Hazra* Accumulation of Mn in Three Tree Species Growing on Manganese Mine Dump. National Environmental Engineering Research Institute, Nagpur, Jan. 10-11, 2008.

D. Raju, Anuya Nisal, Sulekha Hazra*. Synthesis of silver nanoparticles in living *Alfalfa* plants. Science Day, National Chemical Laboratory, Pune, Feb., 2009.

D. Raju, Anuya Nishal, Urmil J. Mehta and Sulekha Hazra* Studies on the leaf surface of the Ag Nanoparticles Synthesizing *Alfalfa* plants using Environmental Scanning Electron Microscopy. Institute of Himalayan Bioresource Technology, Palampur, April 3-4, 2009.